ACKNOWLEDGEMENTS

IN THE NAME OF ALMIGHTY ALLAH, THE MERCIFUL, THE COMPASSIONATE. I GLORIFY ALMIGHTY ALLAH AND ASK BLESSINGS AND SEND SALUTATION UPON SAYDINA MUHAMMAD (PEACE BE UPON HIM), THE MOST NOBLE, THE MOST KIND, THE MOST GENEROUS, HAVING THE HIGHEST LEVEL OF EXEMPLARY AND THE BEST IKHLAQ. MAY ALLAH SHOWER HIS RAIN OF RAHMAT UPON THE FAMILY AND COMPANIONS OF HIS MOST BELOVED PROPHET (PEACE BE UPON HIM).

I am thankful to my Advisor Professor M. Sakhawat Hussain for his considerate and conscious guidance for the completion of this research work. I am thankful to my co-advisor Dr. Muhammad Aslam Khan, who gave his time and expertise to not only accomplish this work but also for careful reading this draft. I wish to thank my Committee Members Prof. Shaikh Ashrof Ali, Prof. Abdur Rahman Al-Arfaj and Prof. Anverhussein A. Isab for unstinting assistance they have provided at all stages of this intricate work. I express my gratitude to Dr. Assad Ahmed Thukair, Chairman of Chemistry Department, KFUPM for his support without which I would not be able to successfully complete this research work.

A great help was received from Research Institute (KFUPM) and OTS Lab (Chemistry Department KFUPM) for the analysis of polymer samples. In this regard, co-operation by Dr. Haleem Hamid and Mr. Aal –e- Ali is gratefully acknowledged. I wish to express my appreciation of the considerable assistance received for Laser Facilities from the Center For Applied Physical Sciences, KFUPM.

I am thankful to my prestigious organization PAEC for allowing me for Ph.D. studies. In this regard I am especially grateful to Mr. Manzoor Ahmad (M-1 KCP-I), Mr. Rana Akhtar (CSO), Dr. Muhammad Imran (Manager A. Labs) KCP-I, Hafiz Khizar Hayat, Mr. Gyassuddin (PSO) and Dr. N. A. Javed (ex G. M. KCP-I). I am also grateful to my colleagues (scientists, engineers and lab technicians in addition to administration) at KCP-I for their encouragement and prays.

I am grateful to Dr. Fettouhi for Arabic translation of the abstract. I am highly indebted to all lab technicians and chemists working in the Labs of the Chemistry Department, for their help to accomplish this task. I am grateful to all my friends, Mr. Abdul Hameed, Dr. Saeed Ahmad, Dr. Ali Er Reyyes, Dr. Waqar Ashraf, Mr. Younis, Mr. Tejani, Mr. Bashir, Mr. Ameen, Mr. Abu Jafar, Mr. Shamsee, Mr. I. W. Qazi, Prof. Majid (Pakistan), for their support and encouragement in connection with whole of my educational career.

I am grateful (with many thanks) to Mr. Zahid Qamar and his family, Mr. Abdul Hameed Awan (my cousin), Shaikh Feyyaz Skindar, Prof. Aftab, Dr. Kaleem and his family, Mr. Waseem (Gujranwala) and his family and Mammoo Jameel Hussain for their fabulous support during this period. May Allah Pak reward them for their generous help. Additionally, I am indebted to all my well wishers who prayed and helped for my success. May Almighty Allah reward them with great honor in Dunia and Akharat (Aameen).

I am highly thankful to my parents, brothers, sisters and all other family members, especially to my beloved Late Uncles Manzoor Ahmad Awan and Talib Hussain Awan for their great concern and generous support and prays for my success.

At last but not the least I am grateful to my dedicated wife and children, Haleema, Hajrah, Sarah and Khadeeja for their patience, prays and love and affection.

Finally, I have no words to thank my pious Shaykh Pir Ghulam Raza Alvi, Shadhli, Qadri for his great concern for me. I have not seen any person more Aabid, Zahid and Aalim like him. I pray to Almighty Allah to raise his Honor in Dunia and Akharat (Aamen). I pray to Almighty Allah to bring the prosperity for the Muslims in general and People of Saudi Arabia in Particular. May Allah Karim shower His BURKA in the work of all the employees of KFUPM. (Aameen).

FINALLY, COUNTLESS DAROOD WA SALAM ON SAYED UL MURSALEEN AND IMAM UL MUTAQEEN SAYDINA WA HABEEBANA MUHAMMAD (PEACE BE UPON HIM). I SEEK HIS SHAFAH FROM ALMIGHTY ALLAH ON THE DAY OF JUDGEMENT (AAMEEN).

TABLES OF CONTENTS

CONTENTS		PAGE
List of Figures		xiii
List of Schemes		xvii
List of Tables		xviii
Abstract (English)		xxii
Abstract (Arabic)		xxiii
CHAPTER 1	**INTRODUCTION**	**1**
1.1	Free-radical Polymerization	1
1.2	Catalytic Chain Transfer Polymerization	2
1.3	Aims of the investigations	4
1.4	Outline of This Thesis	7
CHAPTER 2	**A REVIEW ON CATALYTIC CHAIN TRANSFER**	**8**
2.1.	Non-catalytic Chain Transfer Agents	8
	2.1.1 Thiols and Mercaptans	8
	2.1.2 Other Non-Catalytic Chain Transfer Agents	10

2.2. Catalytic Chain Transfer Agents 12

2.2.1 The Initial Discovery 12

2.2.2 Different Chain Transfer Agents 20
2.2.3 Chain Transfer Mechanism 27

2.2.3.1 Chain Transfer Phenomenon 27

2.2.3.2 Mechanistic Aspects of Catalytic Chain Transfer 30
Polymerization

2.3 Copolymerization 34

CHAPTER 3 PULSED LASER POLYMERIZATION 39

3.1 Literature Review 39

3.2. Propagation Rate Calculation from GPC 40

3.2.1 Consistency Tests 42

3.2.2 Understanding why k_p is given by the point of inflection 44

CHAPTER 4 EXPERIMENTAL PROCEDURES 46

4.1. Material and Analytical Techniques 46

4.1.1 Gel permeation Chromatograph (GPC) 46

4.1.2 NMR Spectroscopy 47

4.1.2.1 ^{1}H NMR 47

4.1.2.2 ^{13} NMR 47

4.1.2.3 DEPT 135 47

4.1.3 FTIR and UV/Visible Spectroscopy 48

4.1.4 UV Excimer Laser 48

4.2. Preparation of Catalysts used as Chain Transfer Agent (CTA) 48

4.2.1 Preparation of BF_3-briged bis(dimethylglyoxime)cobalt(II) Complex 48

4.2.2 Preparation of BF_3-briged bis(α-furilglyoxime)cobalt(II) Complex 49

4.2.3 Preparation of $[Co(dmg\text{-}H.H_2O)_2]$ Catalyst 55

4.2.4 Preparation of $Rh(afdo\text{-}2H.BF_2)_2]\,CH_3COO^-$ Complex 55

4.3. Polymerization Reactions 57

4.3.1 Purification of Monomers 58

4.3.2 Degassing The Monomer Solution 59

4.3.3 Thermal Polymerization 61

4.3.3.1 Polymerization in the Absence of Chain Transfer Agent at 70 and 80 °C using Benzoyl peroxide as an Initiator 61

4.3.3.2 Polymerization in the pesence of Chain Transfer Agent 62

4.3.3.2.1 Polymerization of Styrene at 60, 70, and 80 °C 62

4.3.3.2.2 Polymerization of Methyl methacrylate at 50 °C 63

4.3.3.2.3 Polymerization of Methyl methacrylate at 60 °C 63

4.3.3.2.4 Polymerization of Methyl methacrylate at 70 °C 64

4.3.3.2.5 Polymerization of Methyl methacrylate at 80 °C 64

4.3.3.2.6 Polymerization of Butyl methacrylate at 60 °C 64

4.3.3.2.7 Polymerization of Butyl methacrylate at 70 and 80 °C 65

4.3.3.2.8 Copolymerization of MA with Styrene 65

4.3.3.2.9 Polymerization of MMA and Styrene at 60 °C in the 66

the presence of [Rh(afdo-2H.BF_2)$_2$]Cl 66

4.4. Solution Preparation for the Pulsed Laser Polymerization (PLP) 66

4.4.1 Samples Preparation for the PLP of MMA and Styrene in the 66

absence of Chain Transfer Agent (CTA)

4.4.2 Samples Preparation for the PLP in the presence of Chain 67

Transfer Agent (CTA)

4.4.2.1 Polymerization of MMA in the presence of [Co(dmg-2H. 67

BF_2)$_2$] CTA

4.4.2.2 Polymerization of MMA in the presence of [Co(afdo-2H. 69

BF_2)$_2$]CTA

4.4.2.3 Polymerization of styrene in the presence 69

of [Co(dmg-2H.BF_2)$_2$] as CTA

4.4.2.4 Polymerization of Butyl methacrylate (BMA) in the 70

presence of [Co(dmg-2H.BF_2)$_2$] CTA

4.4.2.5 Polymerization of Butyl methacrylate (BMA) in the 70

presence of [Co(afdo-2H.BF_2)$_2$] CTA

4.5 Polymerization of Methyl methacrylate (MMA) in the presence of Wilkinson's Catalyst 71

4.6. Polymer Characterization 72

4.6.1 Electronic Spectroscopy of Polymer Samples 72

4.6.2 ^{1}H NMR and ^{13}C NMR of Polymer Samples 73

4.6.3 Dilute Solution Viscometry (DSV) 73

4.7. Molecular Weight and Molecular Weight Distribution (MWD) 74

4.7.1 Gel Permeation Chromatography (GPC) 74

4.7.2 Viscosity Measurements 76

4.7.2.1 Viscosity Definitions 76

4.7.2.2 Viscosity-average Molecular Weight (M_v) 76

4.7.2.3 Complications with Viscosity-average Molecular Weight 78

4.8 Determination of Chain Transfer Constant (C_s) 80

CHAPTER 5 RESULTS AND DISCUSSION 82

5.1.1 Characterization of the Ligands 82

5.1.2 Characterization of the complexes 98

5.2. Polymerization with Heat 101

5.2.1 Polymerization of MMA using Benzoyl Peroxide (BPO) as an Initiator at 70.0 °C and 80.0 °C 101

5.2.2 Copolymerization of Methyl acrylate and Styrene for 90 minutes at 70 ^{0}C 112

5.2.3 Copolymerization of Methyl methacrylate and Methyl acrylate in 115

the presence of [Rh(afdo-2H.BF_2)$_2$]Cl

5.2.4 Polymerization of MMA at 60 °C in the presence of Rh(afdo-2H.BF_2)$_2$]Cl catalyst using AIBN as an Initiator 119

5.2.5 Polymerization of MMA using Wilkinson's catalyst 119

5.2.6 Polymerization of Styrene at 60 °C in presence of [Co(dmg-2H.BF_2)$_2$] Chain Transfer agent 124

5.2.7 Polymerization of Styrene at Higher Temperature using [Co(afdo-2H.BF_2)$_2$] as Chain Transfer Agent 128

5.2.8 Polymerization of Methyl methacrylate at 50, 60, 70 and 80 °C using [Co(afdo-2H.BF_2)$_2$] as a Chain Transfer Agent 139

5.2.9 Polymerization of Butyl methacrylate at 60, 70 and 80 °C using [Co(afdo-2H.BF_2)$_2$] as a Chain Transfer Agent 154

5.3. Pulsed Laser Polymerization (PLP) 166

5.3.1 PLP of MMA without using Chain Transfer Agent 166

5.3.2 Pulsed Laser Polymerization of Methyl methacrylate in the presence of Wilkinson's Catalyst 173

5.3.3 Pulsed Laser Polymerization of Methyl methacrylate in the presence of [Co(afdo-2H.BF_2)$_2$] Chain Transfer Agent 184

5.3.4 Pulsed Laser Polymerization of Methyl methacrylate in the presence of [Co(afdo-2H.BF_2)$_2$] and [Co(dmg-2H.BF_2)$_2$] Chain Transfer Agents 176

5.3.5 Pulsed Laser Polymerization of Butyl methacrylate in the presence of [Co(dmg-2H.BF_2)$_2$] Chain Transfer Agent 206

5.3.6 Pulsed Laser Polymerization of Butyl methacrylate in the presence of [Co(afdo-2H.BF_2)$_2$] Chain Transfer Agent 208

Conclusions **214**

Future Prospects **216**

References **217**

Appendix **228**

Curriculum Vitae **231**

LIST OF FIGURES

FIGURE		PAGE
Figure 1.1	Different Catalysts used as Chain Transfer Agents	6
Figure 2.1	The structure of coenzyme B_{12}	13
Figure 2.2	The structure of cobalt porphyrin	13
Figure 2.3	The structure of cobalt phtalocyanine	15
Figure 2.4	The structure of soluble cobalt phtalocyanine	15
Figure 2.5	The structure of cobaloxime	15
Figure 3.1	Sequence of events in Pulsed Laser Polymerization	41
Figure 3.2	Chromatogram used to determine degree of Polymerization	43
Figure 3.3	Spike distribution of chain lengths	45
Figure 3.4	Termination in PLP not instantaneous	45
Figure 3.5	Stochastic broadening	45
Figure 4.1	UV/Vis absorption spectrum of $[Co(dmg\text{-}2H.BF_2)_2]$	51
Figure 4.2	UV/Vis absorption spectrum of $[Co(afdo\text{-}2H.BF_2)_2]$	52
Figure 4.3	UV/Vis absorption spectrum of alpha furilglyoxime ligand	53
Figure 4.4	UV/Vis absorption spectrum of dimethyl glyoxime ligand	54
Figure 4.5	UV/Vis absorption spectrum of $[Co(dmg\text{-}H)_2 (H_2O)_2]$	56
Figure 4.6	Test Tube used for removal of dissolved oxygen from the sample	60
Figure 4.7	Experimental setup for Pulsed Laser Polymerization of MMA	68

Figure 5.1	^{15}N, ^{13}C and ^{1}H NMR spectra of dimethylglyoxime	85
Figure 5.2	IR spectrum of dimethlyglyoxime	86
Figure 5.3	IR spectrum of α-furilglyoxime	87
Figure 5.4	^{1}H NMR of α-furilglyoximes	88
Figure 5.5	^{13}C and ^{15}N NMR of α-furiglyoxime	89
Figure 5.6	Isomers for α-furilglyoxime ligand	90
Figure 5.7	COSY spectra for α-furilglyoxime	92
Figure 5.8	HMBC of α-furilglyoxime	96
Figure 5.9	HMQC of α-furilglyoxime	97
Figure 5.10	Polymerization of MMA at 70 °C using BPO as an initiator	104
Figure 5.11	Polymerization of MMA at 80 °C using BPO as an initiator	107
Figure 5.12	Comparison of M_w Values at 70 and 80 °C using BPO as Initiator	111
Figure 5.13	Graph between Molar Ratio of MA/MMA and Peak Molecular Weight for copolymerization of MA and MMA at 60 °C	118
Figure 5.14	Graph between percent conversion and molecular weight for the Polymerization of MMA using Wilkinson's Catalyst at 60 ^{o}C	123
Figure 5.15	Dependence of percent conversion on catalyst concentration for Polymerization of styrene using [Co(dmg-2H.BF_2)$_2$] as CTA	126
Figure 5.16	Mayo plot for the Polymerization of Styrene at 60 °C using [Co(dmg-2H.BF_2)$_2$] as a Chain Transfer Agent	129
Figure 5.17	Mayo Plot for the Polymerization of Styrene at 60 and 70 °C using [Co(afdo-2H.BF_2)$_2$] as Chain Transfer Agent	135

Figure 5.18	Mayo plot for the calculation of C_s value from M_w values at 60 °C	136
Figure 5.19	Dependence of percent conversion on the concentration of [Co(afdo-2H.BF_2)$_2$] CTA for Polymerization of MMA at 60 ^oC	144
Figure 5.20	Dependence of percent conversion on the concentration of [Co(afdo-2H.BF_2)$_2$] CTA for Polymerization of MMA at 50 ^oC	145
Figure 5.21	Mayo plots for the Polymerization of MMA at 50 and 60 °C using [Co(afdo-2H.BF_2)$_2$] as CTA	147
Figure 5.22	Mayo plots for polymerization of MMA at 70 and 80 °C	148
Figure 5.23	Compos. Activa. Energy for Degree of Polymerization of MMA	153
Figure 5.24	Mayo plots for the Polymerization of Butyl methacrylate (BMA) at 60 and 70 ºC using [Co(afdo-2H.BF_2)$_2$] as CTA	159
Figure 5.25	Mayo plot for Polymerization of BMA at 80 °C	160
Figure 5.26	Comparasion of PDI values for Polymerization of MMA and BMA	164
Figure 5.27	A representative GPC chromatogram	172
Figure 5.28	Molecular Weight Distribution Curves	176
Figure 5.29	220 MHz ^{1}H NMR spectra of PMMA samples of different tacticities in o-dicholorobenzene at 100 °C	181
Figure 5.30	500 MHz ^{1}H NMR spectra of PMMA samples in $CDCl_3$ at 298 K	182
Figure 5.31	The conformation indicating non-equivalent methylene protons Diagram also indicating diads and triads	183
Figure 5.32	Effect of CTAs on percent conversion for PLP of MMA	190
Figure 5.33	Mayo plot for PLP of MMA using [Co(afdo-2H.BF_2)$_2$] as CTA	194
Figure 5.34	Mayo plot (^{1}H NMR) for PLP of MMA using [Co(dmg-2H.BF_2)$_2$]	195

Figure 5.35	Mayo plot (GPC) for PLP of MMA [$Co(dmg\text{-}2H.BF_2)_2$] as CTA	196
Figure 5.36	Dependece of PDI values on CTA for PLP of MMA	199
Figure 5.37	Dependence of PDI on [$Co(afdo\text{-}2H.BF_2)_2$]	200
Figure 5.38	A qualitative molecular orbital scheme for the energy levels	202
Figure 5.39	^{I}H NMR spectrum of PMMA	203
Figure 5.40	^{13}C with DEPT 45 and 135 spectra of PMMA	204
Figure 5.41	Graph between PDI and CTA for PLP of BMA at 25 ºC	211

LIST OF SCHEMES

Scheme		Page
Scheme 2.1	Two-step Hydrogen Abstraction mechanism	31
Scheme 2.2	Catalytic Chain Transfer mechanism by β-hydrogen elimination Mechanism	32
Scheme 2.3	β-elimination of Hydrogen with the formation of dead polymer chain with terminal double bond in Catalytic Chain Transfer Mechanism	35
Scheme 2.4	Insertion of monomer (MMA) in LCo(III)H intermediate in Catalytic Chain Transfer Mechanism	36
Scheme 2.5	Resonance structures of cobaloximes showing ring current	37
Scheme 2.6	Propagation Reactions for Copolymerization	38
Scheme 5.1	Mechanism for Self-initiated polymerization in MMA	113
Scheme 5.2	Proposed Living Free-radical Polymerization of MMA at 60 °C in the presence of Wilkinson's Catalyst	125
Scheme 5.3	Comparative Mechanism of Hydride ion abstraction by Styrene and MMA	138
Scheme 5.4	Dissociation of Wilkinson's Catalyst in the presence of Ultra violet light	179

LIST OF TABLES

Table		Page
Table 2.1	Chain Transfer Constant values for Mercaptans	11
Table 2.2	Effect of different substituents on chain transfer constant value	17
Table 2.3	Chain Transfer Constant (CTA) "C_s" values	19
Table 2.4	Chain Transfer Constant value for different Monomers using cobalt complex of hematoporphyrin tetramethyl ether	21
Table 2.5	"C_s" value for different Cobalt complexes used as CTA	22
Table 4.1	Elemental Analysis for complexes used as Chain Transfer Agents	50
Table 4.2	Definitions of Molecular weights obtained from GPC	75
Table 4.3	Definitions of different types of Viscosity	77
Table 5.1	^{1}H NMR peak assignments for α-furilglyoxime in d_6-DMSO	93
Table 5.2	^{13}C NMR of ∝-furilglyoxime in d_6-DMSO	94
Table 5.3	Infrared spectra of ligands and catalyst	99
Table 5.4	Comparison of UV/Vis absorption spectra of [Co(dmg-2H. $BF_2)_2$] and [Co(dmg-2H.$BF_2)_2$]	100
Table 5.5	Polymerization of MMA at 70.0 °C (Run #1)	102
Table 5.6	Polymerization of MMA at 70.0 °C (Run #2)	103
Table 5.7	Results for Polymerization of MMA with BPO at 80.0 °C	106
Table 5.8	Results for the Copolymerization of Styrene and Methyl acrylate	114
Table 5.9	Different molar ratios of Monomers for the Copolymerization of	116

	Methyl methacrylate and Methyl acrylate at 60 °C	
Table 5.10	Molecular weight distribution (MWD) for the Copolymerization of Methyl methacrylate and Methyl acrylate at 60 °C	117
Table 5.11	Results for the Polymerization of MMA in the presence of [Rh(afdo-2H.BF_2)$_2$] Cl catalyst	120
Table 5.12	Polymerization of MMA in the presence of Wilkinson's Catalyst using AIBN as an initiator at 60 °C for a total duration of 90 min.	122
Table 5.13	Different parameters used to calculate the value of Chain Transfer Constant from Mayo plot using M_v values	127
Table 5.14	Polymerization of Styrene at 60 ^oC using [Co(afdo-2H.BF_2)$_2$] CTA	130
Table 5.15	Polymerization of Styrene in the presence of [Co(afdo-2H.BF_2)$_2$] at 70 and 80 ºC using AIBN (6.1x10^{-3} M) as Initiator	131
Table 5.16	The percent difference among the Molecular weights for the Polymerization of Styrene using [Co(afdo-2H.BF_2)$_2$] as CTA	133
Table 5.17	Point to point C_s value for the Polymerization of Styrene using AIBN as initiator and [Co(afdo-2H.BF_2)$_2$] as CTA	134
Table 5.18	MWD for the Polymerization of MMA at 50 ^0C	140
Table 5.19	MWD for the Polymerization of MMA at 60 ^0C	141
Table 5.20	MWD for the Polymerization of MMA at 70 ^0C	142
Table 5.21	MWD for the Polymerization of MMA at 80 ^0C	143
Table 5.22	Viscosity data for the Polymerization of MMA at 80 °C	149
Table 5.23	Viscosity-average molecular weight data to construct Mayo plot	150

Table 5.24	Comparison of C_s value for the Polymerization of MMA using [Co(afdo-2H.BF_2)$_2$] as Chain Transfer Agent	151
Table 5.25	MWD of PBMA at 60 °C using [Co(afdo-2H.BF_2)$_2$] as CTA	155
Table 5.26	MWD of PBMA at 70 °C using [Co(afdo-2H.BF_2)$_2$] as CTA	156
Table 5.27	MWD of PBMA at 80 °C using [Co(afdo-2H.BF_2)$_2$] as CTA	157
Table 5.28	Comparison of C_s value for the Polymerization of BMA using [Co(afdo-2H.BF_2)$_2$] as CTA	162
Table 5.29	Absolute viscosity of MMA and BMA at Higher Temperatures	163
Table 5.30	Homopolymerization of MMA without using AIBN	167
Table 5.31	Homopolymerization of MMA using Excimer Laser159	168
Table 5.32	Homopolymerization of styrene using Excimer Laser	168
Table 5.33	Molecular weight distribution for the PLP of Styrene	170
Table 5.34	Values of k_p for the PLP of Styrene	171
Table 5.35	Effect of Wilkinson's Catalyst on MWD for PLP of MMA	174
Table 5.36	Effect of the irradiation time on PLP of MMA at constant concentration (1.3mM) of Wilkinson's Catalyst	177
Table 5.37	Intensity ratios of syndiotactic to isotactic C-CH_3 groups in ^{1}H NMR of atactic PMMA	185
Table 5.38	PLP of MMA using [Co(afdo-2H.BF_2)$_2$] as CTA	185
Table 5.39	MWD for the PLP of MMA using [Co(afdo-2H.BF_2)$_2$] as CTA	186
Table 5.40	PLP of MMA in presence of [Co(dmg-2H.BF_2)$_2$] CTA	188
Table 5.41	PLP of MMA in presence of [Co(afdo-2H.BF_2)$_2$] CTA	189
Table 5.42	C_s calculation for PLP of MMA using [Co(dmg-2H.BF_2)$_2$] CTA	191

Table 5.43	C_s calculation (GPC) for PLP of MMA using [Co(dmg-2H.BF_2)$_2$]	193
Table 5.44	Eexperimental results for C_s calculation	193
Table 5.45	Results from ^{13}C NMR spectra of PMMA samples	205
Table 5.46	Data for PLP of BMA using [Co(dmg-2H.BF_2)$_2$] as CTA	207
Table 5.47	Data for Mayo Plot for PLP of BMA	209
Table 5.48	Data for PLP of BMA using [Co(dmg-2H.BF_2)$_2$] as CTA	210
Table 5.49	Data for PLP of BMA using [Co(afdo-2H.BF_2)$_2$] as CTA	213

Abstract

NAME: SHAFIQUE AHMAD
TITLE OF STUDY: CHAIN TRANSFER AGENTS: CHARACTERIZATION AND THEIR USE IN POLYMERIZATION REACTIONS
MAJOR FIELD: CHEMISTRY
DATE OF GEGREE: MAY 2003

The primary aim of this dissertation was to prepare catalysts of Co(II) and their use in polymerization reactions. For this purpose, dioxime complexes of Co(II) have been synthesized and characterized by elemental and spectroscopic techniques. This new class of metal-chelates was found to act as Chain Transfer Agent (CTA) for controlled polymerization of Methyl methacrylate (MMA), Butyl methacrylate (BMA) and Styrene. By using $[Co(afdo\text{-}2H.BF_2)_2]$ and $[Co(dmg\text{-}2H.BF_2)_2]$, (afdo = α-furil glyoxime and dmg = dimethyl glyoxime) complexes as Chain Transfer Agents low molecular weight of the PMMA, PBMA and PSTY were obtained. It has been noted that $[Co(afdo\text{-}2H.BF_2)_2]$ catalyst acts as less efficient CTA as compared to $[Co(dmg\text{-}2H.BF_2)_2]$ catalyst for the polymerization of Methyl methacrylate. However, this is more efficient for polymerization of BMA. We have also investigated the effect of $[Co(afdo\text{-}2H.BF_2)_2]$ catalyst at 60, 70 and 80 °C for polymerization of styrene and it was noted that efficiency of the catalyst decreased at higher temperature. The efficiency of a chain transfer agent is reflected by chain transfer constant (C_s) value, which was calculated from the slope of Mayo plot. The C_s value for Pulsed Laser Polymerization (PLP) of MMA using $[Co(afdo\text{-}2H.BF_2)_2]$ as CTA was found to be around 2500, while for PLP of MMA, with $[Co(dmg\text{-}2H.BF_2)_2]$ catalyst was about 13,400. We believe that for PLP of MMA electronic factors are dominant and for the PLP of BMA probably steric effects are dominant. It has been noted that polydispersity index (PDI) value for PLP of MMA with $[Co(afdo\text{-}2H.BF_2)_2]$ catalyst is less than 1.5, which probably indicates living free-radical polymerization. We have also successfully determined various kinetic parameters such as activation energy for degree of polymerization (E_{xn}), activation energy for propagation reactions (E_p) and transfer rate constant ($k_{tr's}$) for polymerization of Styrene and MMA at higher temperatures.

We have also investigated the effect of $[Rh(afdo\text{-}2H.BF_2)_2]Cl$ and Wilkinson's catalyst $[RhP(Ph)_3Cl]$ on the polymerization MMA. Both these catalysts were found to promote the polymerization process. For all the polymerization studies either Benzoyl Peroxide or 2,2'-Azobis-(2-methylpropionitrile) [AIBN] were used as initiators. Excimer Laser (308 nm input at 10 Hz) was used as a laser source for Pulsed Laser Polymerization.

DOCTOR OF PHILOSOPHY DEGREE
KING FAHD UNIVERSITY OF PETROLEUM & MINERALS
DHAHRAN, SAUDI ARABIA

الرسالة

الاسم: شفيق احمد
عنوان البحث: عوامل نقل السلاسل في تفاعلات البلمرة: توصيف وتطبيقات
التخصص: الكيمياء
تاريخ الشهادة: محرم 1424

الهدف الرئيسي لموضوع بحث هذه الرسالة هو تصنيع حفازات تحتوي على الكوبالت الثنائي واستعمالها في تفاعلات البلمرة. لهذا الغرض تم تصنيع بعض أكزيمات الكوبالت الثنائي و توصيفها بتقنيات التحليل الذري وتقنيات الأطياف. لقد وجد أن هذه المجموعة الجديدة من المركبات التناسقية تؤدي دور عامل نقل للسلاسل (CTA) في تفاعلات بلمرة الميثل ميثكرليت, البيوتايل ميثكرليت و كذلك الستايرين. وتم الحصول على مبلمرات البوليميثل ميثكرليت و البولي بيوتايل ميثكرليت وكذلك البوليستايرين ذات كتل جزيئية منخفضة بواسطة المركبات الناقلة للسلاسل من نوع $[Co(afdo\text{-}2H.BF_2)_2]$ و $[Co(dmg\text{-}2H.BF_2)_2]$. وقد وجد أن هذا الأخير أكثر فعالية من الأول في تفاعلات بلمرة الميثل ميثكرليت, فيحين وجد أن الأول أكثر فعالية فيما يخص بلمرة البيوتايل ميثكرليت. وقد تمت دراسة فاعلية المركب $[Co(afdo\text{-}2H.BF_2)_2]$ على درجات الحرارة : 60, 70 و 80 درجة مئوية بالنسبة لبلمرة الستايرين و تمت ملاحظة انخفاض فاعلية الحفاز مع ارتفاع درجات الحرارة. و تم تقدير قيم ثابت النقل للسلسلة (C_s), الذي يعكس مدى فاعلية عامل النقل, باستخدام معادلة مايو. وقد وجد أن قيمة ثابت النقل في تفاعلات البلمرة القائمة على نبض الليزر بالنسبة لتفاعل الميثل ميثكرليت المحفز بالمركب $[Co(afdo\text{-}2H.BF_2)_2]$ تساوي 2500. فيحين تبلغ قيمة الثابت 13400 بالنسبة للتفاعل المحفز بالمركب $[Co(dmg\text{-}2H.BF_2)_2]$. ونعتقد أن العامل الإلكتروني هو المسيطر في الحالة الأولى بينما يحتمل أن يكون عامل الحجم هو المسيطر في الحالة الأخيرة. وقد لوحظ أن قيمة دليل التشتت المتعدد(PDI) هي أقل من 1.5 بالنسبة لتفاعلات بلمرة الميثل ميثكرليت القائمة على نبض الليزر والمحفزة بالمركب $[Co(afdo\text{-}2H.BF_2)_2]$, مما يشير إلى احتمال حصول عملية بلمرة قائمة على جدور حية و حرة. وقد استطعنا الحصول بنجاح على معطيات حركية التفاعل مثل طاقة التنشيط لدرجة البلمرة (E_{xn}), و طاقة التنشيط لتفاعلات التمدد (E_p) و كذلك ثابت سرعة النقل ($k_{tr's}$) لتفاعلات الستايرين و الميثل ميثكرليت على درجات حرارة عالية. تمت كذلك دراسة تأثير مركبات $[CH_3COO^-Rh(afdo\text{-}2H.BF_2)_2]$ و $[RhP(Ph)_3]Cl$ (حفاز ويلكنسون) على بلمرة الميثل ميثكرليت. و قد وجد أن كليهما يحسن عملية البلمرة. وقد تم استعمال كل من بيروكساید البنزويل أو 2ر2-ازوبس-(2-ميثايل بروبيونايترايل) كعاملي بدء و ليزر اللإكسايمر (308 نانومتر – 10 هرتز) كمصدر ليزر لعمليات البلمرة القائمة على نبض الليزر.

CHAPTER 1

INTRODUCTION

Synopsis: This chapter starts with a brief introduction in free-radical polymerization. Then catalytic chain transfer polymerization (CCTP) has been discussed including some advantages of CCTP. Next, the aims of the present investigation are discussed with structures of the chain transfer agents being used in the polymerization reactions. Finally, a short outline of all chapters in this dissertation is given.

1.1 Free-radical Polymerization

Free-radical polymerization is a very versatile polymerization mechanism that can be applied to a wide variety of vinyl monomers. The resulting polymeric materials can be used in applications ranging from packaging materials to coatings as well as automotive parts. These different applications require different material properties, which are determined amongst others by the microstructure of the polymer chain, the interactions between the chains and the types of additives. When we focus on the microstructure, we can distinguish polymers that differ in the structure of the backbone, in molecular weight, in composition and in end groups. When a polymer consists of more than one monomer, it is called a copolymer. In this class of polymers several variations are known as well. Two linear copolymers with the same overall composition can have a different distribution of the monomers over the polymer chain resulting in random, gradient or even block copolymers. Thus, it is clear that in principle several different microstructures

can be obtained. However, in free-radical polymerization it is impossible to obtain a polymer in which all chains have exactly the same structure. They will differ in length, composition, end groups and backbone structure, even when all chains are initiated at exactly the same moment and in the same way. During the polymerization these structural differences will usually become larger as the ratios of the different components in the reaction mixture change. So it is not easy to control the polymerization and thus to obtain polymers with a predefined structure. In the past two decades, several techniques were developed to control one or more aspects of the chain structure. Many of these are aimed at producing homopolymers with narrow molecular weight distributions and eventually block copolymers. Otsu *et al* [1] first used to work disulfides that were capable of both initiating and, after dissociation, reversibly terminating the free-radical polymerization. Since then many other techniques were developed that were based on reversibly terminating the growing polymeric radicals, like nitroxide mediated polymerization (NMP) [2], atom transfer radical polymerization (ATRP) [3,4] and reversible addition fragmentation chain transfer (RAFT) polymerization [5]. Together, these form the field of controlled radical polymerization.

1.2 Catalytic Chain Transfer Polymerization

The terms controlled polymerization, living, living/controlled, pseudo-living, living polymerization with reversible deactivation and others are scattered through the literature. A search of Chemical abstract (CAPLUS; accessed February 8, 1999) revealed 484 articles [6] with the term living (free) radical (this group includes 11 articles with quasi-living, 13 with pseudo-living) and 149 articles with the controlled (free) radical (28 of these were also indexed under living (free) radical; 20 articles on diffusion controlled

polymerization have been excluded from this number. The term controlled or control is also used in connection with other mechanisms for controlling polymerization [7-8]. These include chain transfer (which controls radicals polymerization no less efficiently, but in different sense), catalytic termination, template polymerization, and number of other methods that control different features of free radical polymerization. The art of radical polymer science is to control the polymerization to achieve particular results and this can be achieved by catalytic chain transfer polymerization.

In catalytic chain transfer (CCT) polymerization small quantities of generally an organocobalt complex are used to catalyze chain transfer for methacrylates, styrene and α-methylstyrene. In this way, polymer chain length can be varied practically independently of initiator concentration and therefore of the rate of polymerization. In the polymerization of other monomers like acrylates and vinyl acetate the same catalysts inhibit the polymerization reaction. This catalytic chain transfer behavior was first described by a Russian research group in the early eighties [9-10]. Since it was developed in the same period of time as NMP and ATRP, catalytic chain transfer polymerization is often included in the field of controlled radical polymerization as well, although the basic principle is different. The main difference is that in NMP and ATRP in an ideal situation, the growth-time of a single chain equals reaction time due to reversible termination of the growing chains, whereas in CCT a chain is formed within *e.g.* one second and cannot grow further.

CCT has several advantages over more traditional ways of controlling molecular weight. In order to obtain low molecular weight polymers, neither large amounts of chain transfer agents like mercaptans, which can add color and odor to polymer product, are

required and nor large amounts of initiator is needed. In addition, the process can be carried out at lower temperatures. Another advantage of CCT is that, under well-controlled experimental conditions, nearly all polymer chains will have an unsaturated bond at the chain end, which remains available for post-reactions. These advantages make CCT process a very promising technique for example in the coatings industry, which due to more strict environmental requirements is forced to look for ways to produce coatings with a lower solvent content (the so-called high-solid coatings), requiring low molecular weights polymers. Also in the production of water-borne systems via emulsion polymerization CCT can be readily applied. The attractiveness of CCT towards industry is also reflected by the fact that the majority of the early literature on CCT is found in patents [11-12].

1.3 Objectives of the investigations

CCT has been mostly applied in homopolymerizations of Methyl methacrylate (MMA) and styrene. For MMA a general mechanism has been suggested that is now widely accepted. The focus, however, of the majority of the mostly industry driven research on CCT has been on novel catalysts and on the application of the macromonomers produced by CCT. That is why, many aspects of the mechanism and of the interaction of the catalyst with other compounds are still matters of discussion, although CCT was discovered more than twenty five years ago. As discussed before, one of the main fields of application for CCT is in the coatings industry. For the production of polymers for coatings, usually a mixture of various types of monomers is used containing *e.g.* both functional and non-functional acrylates and methacrylates and

styrene. In oreder to understand and control these complex systems containing CCT active monomers like methacrylates, and CCT inactive monomers like acrylates in solution or even emulsion, will be necessary to first thoroughly investigate the homopolymerizations of these monomers with heat and then with Laser. The main advantage of Pulsed laser Polymerization (PLP) is that all aspects of polymerization can be studied at room temperature. The main objectives of this investigation specified were,

1. Synthesis of the catalysts 1 and 2 using Cobalt(II) and Rhodium(II) as the central metal atom.
2. Characterization of the catalysts using spectroscopic methods such as FTIR, UV-Vis and ^{1}H and ^{13}C NMR studies.
3. Investigation about trends in molecular weight of the polymers by bulk homopolymerization of suitable monomers with and without these catalysts using AIBN as an initiator.
4. Investigation about the effect of laser radiation with/without initiator and catalysts on the rate of polymerization. This is significant because there are several aspects in the use of PLP that still require considerable research.
5. Comparative study of Wilkinson's catalyst with other catalysts of Co(II) and Rh(II) for regulating the molecular weight of the polymers.
6. Investigating the influence of laser generated ultrasound on polymerization reactions.

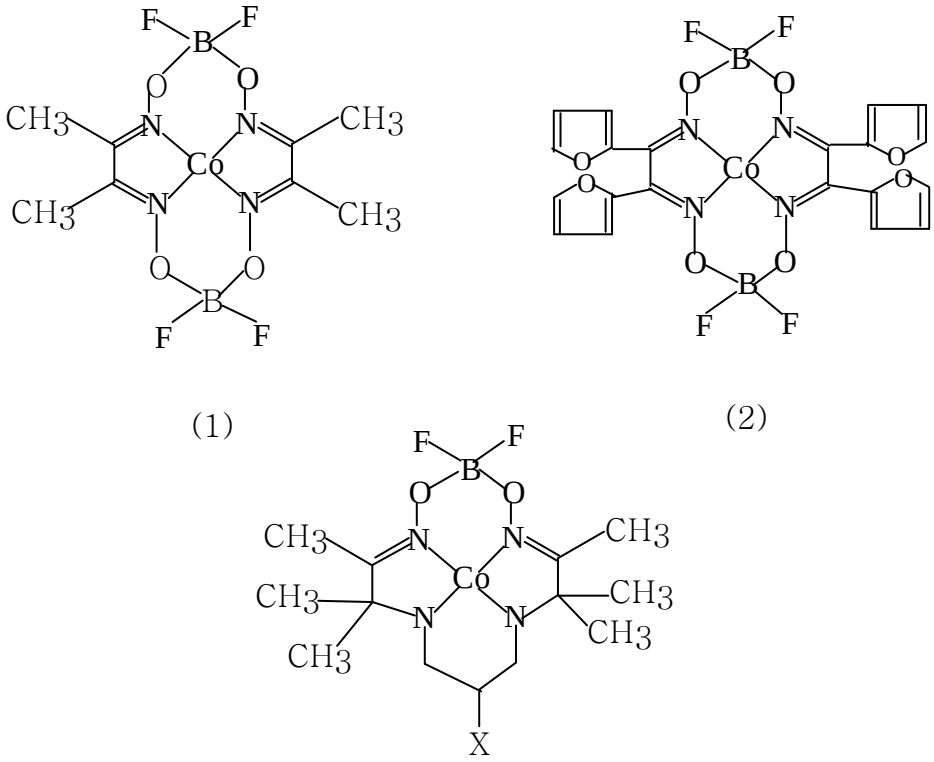

Figure 3.1 Different Catalysts used as Chain Transfer Agents for Polymerization Reactions: catalyst 1= $[Co(dmg\text{-}2H.BF_2)_2]$, catalyst 2 = $[Co(afdo\text{-}2H.BF_2)_2]$

7. Determination of molecular weight of the polymer using dilute solution viscosity and Gel Permeation Chromatography (GPC).
8. Determination of the catalytic chain transfer constant (C_s) values for all the catalysts used.

1.4 Outline of Thesis

A short overview is given in chapter 2 dealing with the research on catalytic chain transfer of the past two decades. Different types of Chain Transfer Agents used to date in literature are presented. This has been mainly divided into two portions viz: catalytic chain transfer agents and non catalytic chain transfer agents. The chapter also deals with chain transfer phenomenon and include discussion on mechanistic aspects of CTA and some features of co-polymerization are also included. Chapter 3 gives brief description about Pulsed Laser Polymerization. Chapter 4 includes experimental part, and consists of mainly synthesis of catalysts and preparations of samples for polymerization. Chapter 5 is about results and discussion. It initially focuses on characterization of ligands and catalysts used in polymerization. Next, results for polymerization with heat are discussed and that is followed by results for Pulsed Laser Polymerization. Finally, some conclusive remarks about all the work performed are given. The significance of this research and suggestions for further work are also included in this chapter.

CHAPTER 2

REVIEW ON CATALYTIC CHAIN TRANSFER

Synopsis: Initially role of non-catalytic chain transfer agents in polymerization reactions will be given. This will be followed by a short introduction into cobalt chemistry in general. Starting from the initial discovery, different types of chain transfer agents along with chain transfer constant values will be discussed.

2.1. Non-catalytic Chain Transfer Agents

2.1.1 Thiols and Mercaptans

Thiols and mercaptans are an important class of compounds widely used in industry to control the molecular weight of polymers. Commercial Thiols used for this purpose are usually sold as mixtures containing a wide range of carbon chain lengths. The effectiveness as chain regulators depends on the type of polymerization (*e.g.* bulk, suspension, emulsion etc) and the reaction conditions. Their presence in the reaction mixture introduces certain modifications in the kinetics of the reaction, mechanism of de-sorption and re-absorption, and particle nucleation [13]. Mercaptans such as tertiary dodecyl (TDM) and normal-dodecyl mercaptan (NDM) have long been used as chain transfer agents to modify free radical polymerization in polystyrene, SBR rubber, ABS and other polymers. Chain transfer agents are necessary to control the molecular size and weight so that the resulting polymers have good processability and other properties

required for their use. A decrease in the rate of polymerization with increasing concentration of the CTA is generally observed in all polymerization systems [14-15]. The decrease is however more prominent with the short chain compounds like butanethiol or 2-mercaptoethanol, because they are usually more soluble and diffusion is less hindered. The chain transfer efficiency of the mercaptans and their effect on the rate of polymerization decreases with increasing chain length. For example, n-dodecyl mercaptan was found to have little or no effect on the rate of polymerization of styrene [16-17], or on its rate of co-polymerization with Butyl acrylate [13]. In addition to chain transfer, some mercaptans have been found to act as initiators as well. This is the case with t-dodecanethiol in the co-polymerization of MMA with styrene [18]. Chain transfer activity is not restricted only to thiols.

The use of functionalized thiols (mercaptans) in the synthesis of low molecular weight polymers for various applications has also been reported [19]. 2-mercaptoethanol was used to obtain oligomers applicable in reactive injection molding (RIM) and in 'high solids' surface coatings formulations. An average chain transfer constant (C_s) value of 2.44±0.1, was quoted for MMA in suspension polymerization, and was found to be independent of the concentration of the chain transfer agent. Similarly, butanethiol was used in the synthesis of poly(vinyl acetate) and poly(vinyl alcohol) [20]. Low molecular weight poly(methyl Methacylate-co-n-Butyl methacrylate) was studied in emulsion, using iso-octyl-3-mercaptopropionate [21]. These polymers were developed for use as fugitive binders of high temperature powders to be applied in a rapid photocopying method known as selective laser sintering (SLS). The polymerization of MMA, methyl acylate (MA), Vinyl acetate (VA) and Styrene was studied in the presence of N-

hydroxypyridine-2-thione and N-hydroxy-4-methlthiazole-2(3H)-thione in bulk, at 60 °C [22]. In all cases, C_s values in the range 0.32-20 were reported except with vinyl acetate where a value of 80 was reported. The C_s values of some of the common mercaptans [23-31] used in the polymerization are shown in Table 2.1.

2.1.2 Other Non-Catalytic Chain Transfer Agents

The use of halogenated hydrocarbons to regulate the molecular weight of polymeric products has for long been established. The presence of carbon tetrabromide (CBr_4) [17] and carbon bromotrichloride ($CBrCl_3$) [32] in the emulsion polymerization of styrene was found to promote the production of low molecular weight free radicals in the latex particle. The active species suspected to be tribromomethyl radical ($\cdot CBr_3$) or its adduct with monomer, was able to escape from the latex particles. Their escape results in a decrease in the total number of free radical in the system compared to the number observed in the absence of the CTA. A consequence of this is a decrease in the rate of polymerization. Carbon tetrabromide has similarly been used in acrylic latex paints formulations. Molecular weight control in poly(Methyl methacrylate-co-Butyl acrylate) was achieved in this manner [33].

Table 2.1 Chain Transfer Constant Values for Mercaptans

Chain Transfer Agent	Temperature (°C)	Monomer	C_s	Reference
Ethyl Mercaptan	50	Methyl acrylate	1.57	23-24
n-Butyl Mercaptan	60	Methyl acrylate	1.69	24-25
Isopropyl Mercaptan	60	Methyl Methacrylate	0.38	24,26
n-Butyl Mercaptan	60	Methyl Methacrylate	0.68	24-25
t-Butyl Mercaptan	60	Methyl Methacrylate	0.18	24,26
n-Amyl Mercaptan	50	Methyl Methacrylate	0.72	27
Ethyl Mercaptan	50	Styrene	17.1	24,28
n-Butyl Mercaptan	60	Styrene	21	24,29
t-Butyl Mercaptan	50	Styrene	15.4	24,30
n-Amyl Mercaptan	40	Styrene	21	27
n-Hexyl Mercaptan	99	Styrene	15.3	24,30
n-Octyl Mercaptan	50	Styrene	19	24,31
sec-Octyl Mercaptan	99	Styrene	3.2	27,30
t-Octyl Mercaptan	50	Styrene	4.3	31
n-Dodecyl Mercaptan	60	Styrene	18.7	31
n-Tetradecyl Mercaptan	50	Styrene	19	24,31
n-Octadecyl Mercaptan	99	Styrene	14.7	24,30

The greater transfer constant for carbon tetrabromide [34] compared to the tetrachloride is due to the weaker C-Br bond. The low C_s value for chloroform compared to carbon tetrachloride is explained by C-H bond breakage in the former. The thiols have the largest transfer constants of most non-catalytic known compounds due to the weak S-H bond. The weak S-S bond leads to high transfer constants for disulfides. Poly(styrene disulfide) and poly(styrene tetrasulfide) have been found to be potential chain transfer agents in styrene polymerization [35].

2.2. Catalytic Chain Transfer Agents

2.2.1 The Initial Discovery

Coenzyme B_{12} [36], (Figure 2.1), has played an important role in the development of cobalt chemistry. It serves as a cofactor in various enzymatic reactions that proceed via radical intermediates, in which Co is d^7 [37]. Under this background, in 1975, Boris Smirnov and Alexander Marchenko [9] discovered catalytic chain transfer (CCT) to a monomer in radical polymerization. They had set out to test cobalt porphyrin (Figure 2.2) as catalysts for radical polymerization of MMA. The very first experiments with cobalt porphyrin (Figure 2.2) gave quite odd results. According to Calorimetric results, the polymerization was complete, but the contents of the reaction ampoule remained liquid [9]. Although porphyrins were found to be excellent catalysts for kinetic studies, their cost was always a problem. Despite the wide presence of porphyrins in nature, their low concentrations in natural raw materials inevitably makes the cost of porphyrin isolation and purification too high for common polymeric applications.

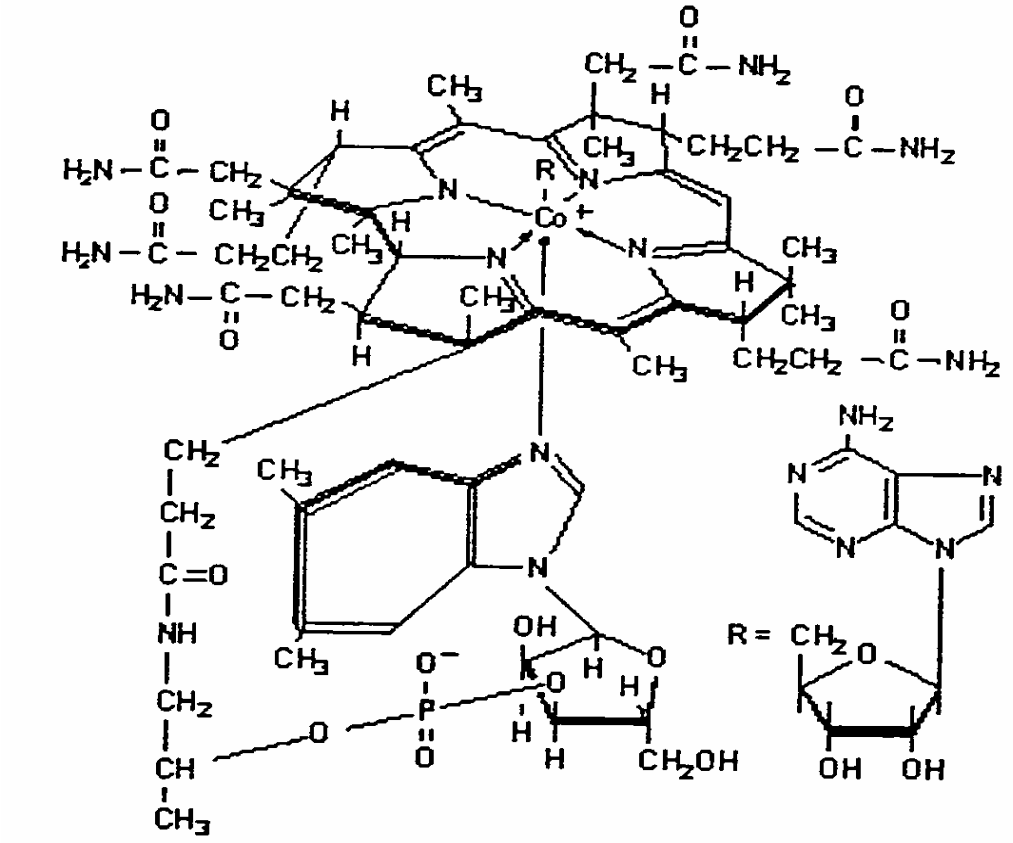

Figure 4.1 The structure of coenzyme B_{12}

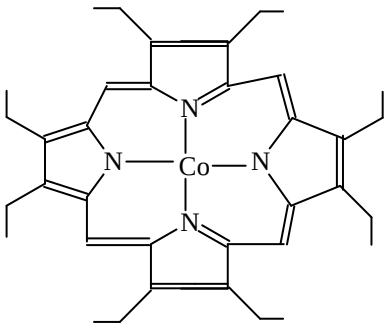

Figure 2.2 Cobalt porphyrin

Catalyst removal was another CCT problem recognized early on. Therefore, various researchers tested alumina, silica, and macroporous crosslinked polymetrhacrylate. Several different porphyrins were attached to the surfaces of these sorbents via different means, but none of supported catalysts worked. Bel'goviskii and co-workers [39-40] showed that the failure of supported catalysts was caused by the pacers between the porphyrin and surface of the solid support being too short. Other cobalt-chelate complexes, like acetoacetones, naphthenates, and even vitamin B_{12} were found to be inert in radical polymerizations.

In an attempt to extend CCT to other metals, it was found that porphyrin complexes of metals other than cobalt were completely inert in radical polymerization. Cobalt phthalocyanine (Figure 2.3), the closest analogue of porphyrins, was found to catalytically inhibit radical polymerization [41] instead of causing CCT. This strange difference in cobalt complex of unsubstituted phthalocyanine was soon explained. The cobalt complex of unsubstituted phthalocyanine is not soluble in most organic solvents, except, dimethylforamide (DMF) and dimethylsulfoxide, so the testing of cobalt phthalocyanine activity was studied in DMF. Subsequently, cobalt tetra-tert-butylphthalocyanine (Figure 2.4), which is soluble in a wide range of solvents, was tested in bulk MMA, and a normal CCT behavior was observed. In a search for a commercially viable CCT catalyst in 1979, Gridnev [42-43] and coworkers discovered cobaloximes (Figure 2.5) to be extremely active CCT catalysts. These complexes were an order of magnitude more active than porphyrins and were an order of magnitude less expensive than porphyrins.

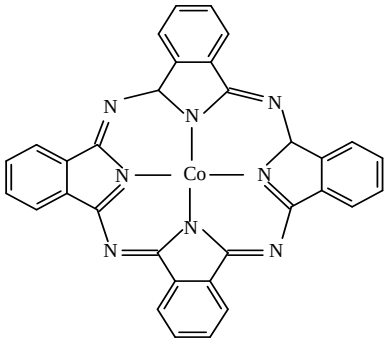

Figure 2.3 Cobalt phthalocyanine

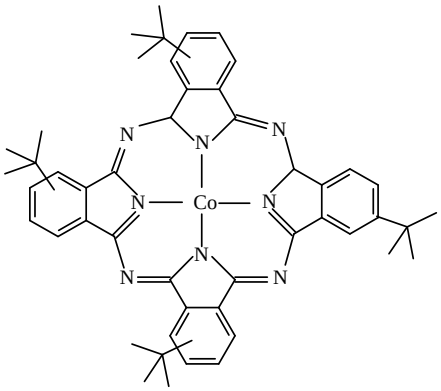

Figure 2.4 Soluble cobalt phthalocyanine

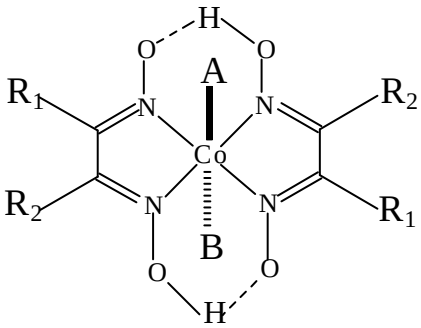

Figure 2.5 Cobaloxime

Among the other positive features of cobaloximes are low color, good solubility, and ease of tuning properties by the ligand structure being changed, as shown in the Table 2.2. The contents of the Table 2.2 may be separated into three groups. The top group (entries 1-7) show the effect of variation in the A group. This type of ligand works as an on/off switch for the catalysis. Strong anionic ligands, such as CN, NO_2, and primary radicals, prevent CCT by locking the cobalt into oxidation state three, whereas Co(II) species are required to abstract hydrogen atoms from a growing radical chain.

The cobalt-carbon bond in cobaloximes with secondary radicals as A-ligands is less stable than that with primary radicals; it is easily cleaved upon heating to release catalytically active Co(II) chelate. Such cobaloximes could be called self-activated. In this connection, the behavior of halogens and pseudohalogens is interesting. They do not block the catalysis like CN does, but they also do not produce fully active cobaloxime (II). This intermediate reactivity of cobaloximes with halogens as A-ligands reflects relatively complex chemistry. It was suggested that propagating radicals or other carbon-centred radicals reduce the Co(III) to Co(II), but hydrohalogenic acid (HA) partly hydrolyzes the OHO hydrogen-bonded bridge in the cobaloxime. Later it was shown that even small changes in the structure of the equatorial ligand of the CCT catalysts can cause a dramatic decrease in the catalytic properties of the cobalt. The second group of catalysts in Table 2.2 (entries 9-12) describes how the catalytic properties depend on the substituents in the glyoxime moiety in contrast to porphyrins, which are relatively insensitive to changes in the substituents on the macrocycle, glyoximes can change the rate constant of the hydrogen transfer by as much as a factor of five.

Table 2.2 Effect of different substituents on chain transfer constant value

Entry	R_1	R_2	A(Acid)	B(Base)	C_s
1	CH_3	CH_3	CH_3	H_2O	<50
2	$-(CH_2)_4-$		Ethyl	H_2O	<50
3	CH_3	CH_3	CN	Py	<50
4	CH_3	CH_3	NO_2	Py	<50
5	CH_3	CH_3	Cl	Py	5000
6	CH_3	CH_3	I	Py	1000
7	CH_3	CH_3	Sec-Butyl	H_2O	13,000
8	CH_3	CH_3	Cl	Py	5000
9	CH_3	CH_3	Cl	Py	4000
10	CH_3	$COOC_2H_5$	Cl	Py	12,000
11	CH_3	$COCH_3$	Cl	Py	25,000
12	$-(CH_2)_4-$		Cl	Py	4000
13	Ph	Ph	Cl	H_2O	25,000
14	Ph	Ph	Cl	Py	30,000
15	Ph	Ph	Cl	$P(Ph)_3$	100,000

It looks that electron-withdrawing groups increase the reactivity. The third group is devoted to the role of B-ligands (lewis bases). They may change the rate constant several times. Together with the R-substituents, B-ligands allow the researchers to vary the reactivity of a CCT catalyst by many orders of magnitude.

Cobalt(II) porphyrins generally do not form stable coordination bonds with B-ligands for some reason. In 1984 Burczyk and co-workers [44] introduced cobaloximes (as already discussed), which proved to be an order of magnitude more active than the porphyrins that had been used before. A few years later a modified cobaloxime was reported [45], in which the hydrogen bridges were replaced by difluoroboron groups, which makes the complex hydrolytically more stable. Additional advantages are that the synthesis is quite straightforward and relatively cheap.

A short overview of a selection of conventional and catalytic chain transfer agents and their chain transfer coefficients, C_s, for Methyl methacrylate is given in Table 2.3. For comparison C_s for uncatalyzed chain transfer to monomer is shown as well. Although it is realized that the transfer and reinitiation steps in catalyzed and uncatalyzed chain transfer to monomer are not equivalent, these data are used to calculate the efficiency of the catalysts, *i.e.* the ratio of C_s with and C_s without catalyst. This ratio is found to be around 10^9, close to the range for enzymatic catalysis [45]. In a review Davis *et al* [46] gave some valuable rules of thumb to predict whether a cobalt complex will be active or inactive in CCT. First of all the Co(II) complex should exist in a *low spin* state. Most Co(II) complexes surrounded by two oxygen and two nitrogen atoms for example are in a high spin state and therefore inactive. In most active complexes four nitrogen atoms are directly bonded to cobalt. Secondly, when electrons in the macrocyclic ligand are only

Table 2.3 Chain Transfer Constant "C_s" value for some catalytic (entries 5-8) and non catalytic Chain Transfer Agents (entries 1-4)

Compound	C_s	References
1. Methyl methacrylate	1×10^{-5}	47
2. Dibenzyl disulfide	$6. \times 10^{-3}$	48
3. CBr_4	0.27	47
4. n-dodecanethiol	1.2	49
5. Cobalt(II)-hemtoporphyrinIX,tetramethyl ether	2.4×10^{3}	10
6. Cobalt phthalocyanine	2.9×10^{3}	50
7. Bis[(difluoroboryl)diphenylglyoximato]Co(II)	2.5×10^{4}	51
8. Cobaloxime boron fluoride	2.8×10^{4}-4.0×10^{4}	52-53

partially delocalized, the complex will be less colored. This can be an important consideration for industrial applications.

2.2.2 Different Chain Transfer Agents

Chain Transfer Constant values for different chain transfer agents have already been presented in Table 2.2 and 2.3. Enikolopyan and co-workers [9-10] used cobalt complex of hematoporphyrin (Co-Por) for polymerization of MMA. They found that Co-Por is a catalyst of at least chain 2000 acts of the chain transfer. They further reported that magnitude of the catalytic constant C_{por} does not depend on temperature within 40-70 °C range, and reported an average value of $C_{por} = (2.4 \pm 0.1) \times 10^3$. The absence of the temperature dependence of C_{por} testifies to the fact that activation energy of the chain propagation reaction and that of the limiting stage of the catalytic process are close and within the range of 4-5 K.cal/mole. The catalytic chain transfer values are given in Table 2.4 and Table 2.5 [9-10].

Burczyk et al [44] replaced the porphyrin with a cobalt(II) dimethyl glyoxime known as cobaloximes. Most significant examples of ligands utilized are dimethylglyoxime (dmg) and diphenylglyoxime (dpg). The compounds of these ligands were stabilized with a coordinating base ligand, such as pyridine or triphenylphosphine. They used this cobaloxime for free-radical polymerization of Methyl methacrylate at 60 °C and reported value of C_s between 10^3-10^4. Contrary to Smirnov observation [9-10] for chain length dependence only up to 8 monomer units, Burczyk observed a large inverse dependence of chain lengths for cobaloxime.

Table 2.4 Chain Transfer Constant value for different Monomers using cobalt complex of hematoporphyrin tetramethyl ether

Monomer	C_s	Monomer	C_s
Methyl methacrylate	2.4×10^3	Glycidil methacrylate	4.5×10^2
n-butyl methacrylate	1.2×10^3	Styrene	2×10^2
n-nonyl methacrylate	1.05×10^3	Styrene +10%MMA	2×10^2
n-dodecyl methacrylate	8×10^3	MMA + 10% acetic acid	2×10^2

Table 2.5 "C_s" value for different Cobalt complexes used as Chain Transfer Agent for the Polymerization of MMA

Metal Complex	C_s at 10^{-5} M of Complex
Co^{2+}-meso-tetraphenylporphyrin	4.1×10^3
Co^{2+}-mesoporphyrin, dimethyl ether	2.1×10^3
Co^{2+}-protoporphyrin, dimethyl ether	1.2×10^3
Co^{2+}-naphthenate	inert
Co^{2+}-phythalocyanin	>>70
Vitamin B_{12}	inert
$Rh^{3+}Br$- etioporphyrin	inert

This improved the oxygen sensitivity of the cobaloxime, allowing ease of use. Gridnev [43] reported on the use of cobaloximes for a number of methacrylates and styrene. Sanayei and O'Driscoll [54] investigated the effect of cobaloxime boron fluoride (COBF) at different temperatures for polymerization of MMA using AIBN as initiator. The C_s value was found to be between 2.8 x 10^4 to 6.6 x 10^4 and depending on chain length and temperature, they concluded that the chain transfer constant value decreases with increase in chain length but reaches a limiting value for chains more than 8 units in length. With temperature increase the C_s value decreases. They found activation energy for the chain transfer coeffecient is –10.1 KJ/mol. Suddaby and co-workers [55] reported C_s value of 36,000 for COBF in bulk polymerization of MMA, 25,000 for MMA in Toluene solution and 1500 for bulk styrene. Actually, a wide range of C_s values are reported by several groups for COBF catalyst [52-53].

Values varying from 20,000 to 2280 over the molecular weight range of 500 to 186,000 have been reported for bulk polymerization of MMA at 60 °C [55]. This wide range was attributed to the dependence of C_s on chain length. A number of inherent shortcomings were encountered regarding the use of the hydrogen-bonded compound discussed above. The most important of these shortcomings was its instability towards hydrolysis and oxidation by atmospheric oxygen. Therefore, the hydrogen bonds were replaced by a BF_2 moiety [complex 1 Figure 2.6] to enhance stability. A consequence of this increased stability is evident in the C_s values reported for this complex. These values, though generally higher compared to the hydrogen-bonded species, vary over a wide range between 28,000 to 66,000 for MMA in bulk over a temperature range of 60 to 90 °C. In all these reports, the dependence of C_s on chain length was noted.

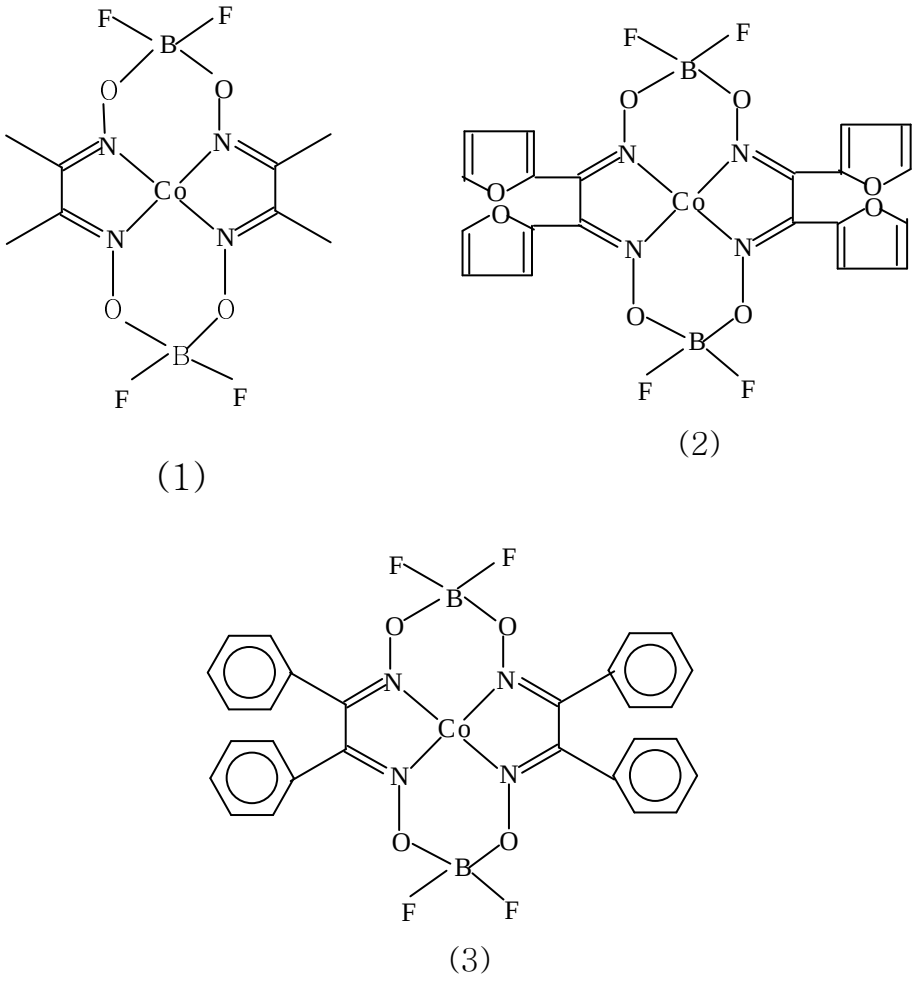

Figure 2.6 Structure of Different Chain Transfer Agents

In solution polymerization of MMA, C_s value was found to be dependent not only on type of solvent but also on impurities in these solvents.

For polymerization of MMA in butanone solvent C_s value in the range 1700-11,000 was recorded. However, when the butanone was distilled a dramatic increase was observed, the range increasing to 12,000-25,000. The reason for the low values observed in unpurified butanone was attributed to catalyst poisoning by traces of acid present in the solvent. When the polymerization was conducted in methanol solvent the C_s value was found to decrease significantly i.e. 9,500-12,000. This may not be unconnected with the fact that the polymer precipitates out in methanol. It is also most likely that there is a strong interaction between the chain transfer agent and methanol. For styrene this catalyst was found to have C_s value lower than 2000.

Chain transfer activity has also been investigated for BF_2-bridged bis(diphenylglyoxime)cobalt(II) [catalyst 3 Figure 2.6]. The values obtained for this are lower than reported for (dimethylglyoxime)cobalt(II). This could possibly be due to catalyst purity or larger surface area compared to (dimethylglyoxime)cobalt(II). Alternatively, the interaction of this catalyst with the polymer may be stronger, resulting in a strong Co-alkyl bond. However, this is not likely from a consideration of steric effect. C_s values reported for styrene fall between 600-700. Forster et al [56] have found C_s value for Tetraphenyl Cobaloxime Boron Floride (COPhBF) [catalyst **3**] to be 2×10^3 for polymerization of 2-phenoxyethyl methacrylate. Both catalysts **4** and **5** [Figure 2.7] have low C_s values of 900-1300 and less than even 100 for polymerization of MMA at 60 °C. To the best of our knowledge no C_s value has been reported for catalyst **2** this far.

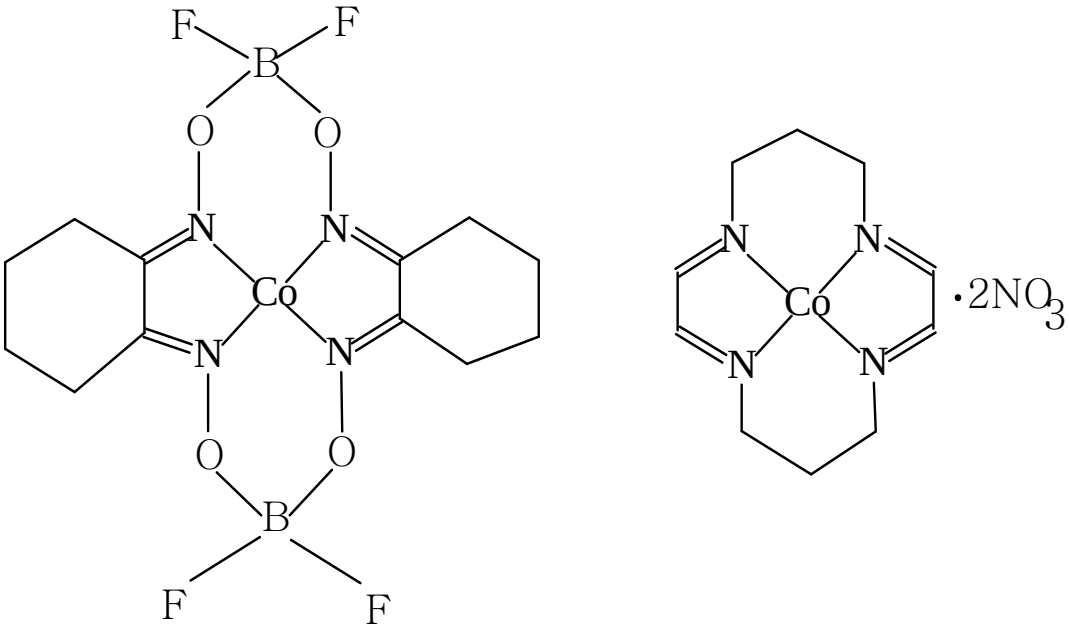

(4) (5)

Figure 2.7 Different structures of catalysts used (not frequently) as Chain Transfer Agents

2.2.3. Chain Transfer Mechanism

2.2.3.1 Chain Transfer Phenomenon

Radical chain polymerization is a chain reaction consisting of a sequence of three steps viz. initiation, propagation, and termination. At some point, the propagating polymer chain stops growing and terminates. Two radicals react with each other by combination (coupling) as shown in equation 2.1, or, more rarely, by disproportionation in which a hydrogen radical that is β to one radical center is transferred to another radical center, as indicated in equation 2.2. Termination can also occur by a combination of coupling and disproportionation. Although experimental data are not available for all monomers, most polymer radicals appear to terminate predominantly or entirely by coupling (except where chain transfer predominates) thus yielding polydispersity index (equation 2.5) value between 1.5 to 2.0.

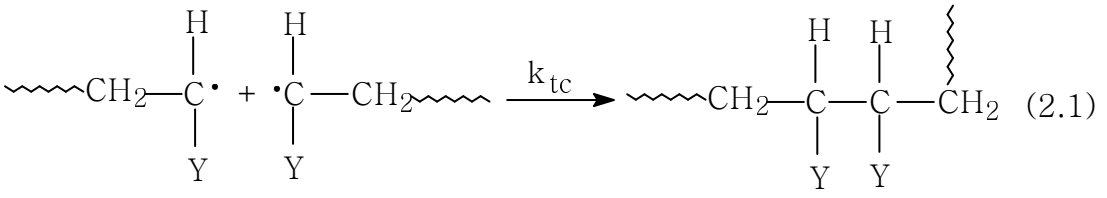

(2.1)

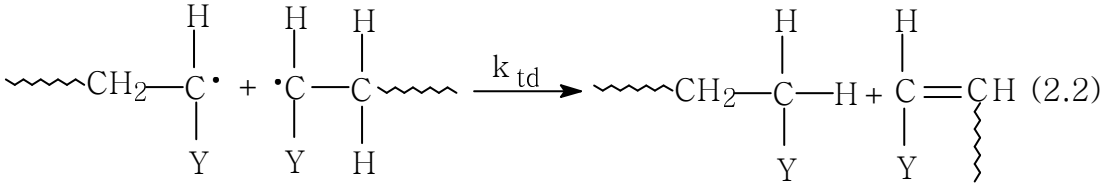

(2.2)

However, varying extents of disproportionation are observed depending on the reaction system. Disproportionation increases when the propagating radical is sterically hindered

or has many β-hydrogens available for transfer. Thus whereas styrene, Methyl acrylate, and acrylonitrile undergo termination almost exclusively by coupling, Methyl methacrylate undergoes termination by a combination of coupling and disproportionation [57-58]. In many polymerization systems the polymer molecular weight is observed to be lower than predicted on the basis of the experimentally observed extents of termination by coupling and disproportionation. This effect is due to the premature termination of a growing polymer by the transfer of a hydrogen or other atom or species to it from some compound present in the system-the monomer, initiator, or solvent, as the case may be. These *radical displacement reactions* are termed as chain transfer reactions and may be depicted by equation 2.3 and 2.4.

$$R_n + LCo \xrightarrow{k_{tr}} \overset{=}{P}_n + LCoH \qquad (2.3)$$

$$LCoH + M \xrightarrow{k_r} LCo + R_1 \qquad (2.4)$$

where, R_n and R_1 are the polymeric and monomeric radicals, respectively. M is the monomer, LCo is cobalt (II) chelate, LCoH is its corresponding Co(III) hydride and $P^{=}_n$ is an oligomer or polymer with a terminal double bond. Chain transfer is a chain-breaking reaction; which results in a decrease in the size of the propagating polymer chain. The effect of chain transfer on the polymerization rate is dependent on whether the rate of reinitiation is comparable to that of the original propagating radical. Chain transfer is important in that it may alter the molecular weight of the polymer (see chapter 5: Results and discussion) product in an undesirable manner. On the other hand, controlled chain transfer may be employed to advantage in the control of molecular weight at a specified level. Re-initiation in CCT takes place with the rate constants

considerably faster than that in mercaptans. The effectiveness of chain transfer agent is reflected by chain-transfer constant C_s value as defined in equation 2.5. Higher C_s value signifies that chain transfer agent is effective and regulates the degree of polymerization (DP_n).

$$C_S = \frac{k_{tr's}}{k_p} \qquad (2.5)$$

Chain-transfer constant to initiator "C_I" is usually negligible, and values for some of commonly used initiators in free-radical polymerization are given in Appendix A. The monomer chain-transfer constants 'C_M" are generally small for most monomers being in the range 10^{-5} - 10^{-4} (Appendix B). Transfer to monomer does not, however, prevent the synthesis of polymers of sufficiently high molecular weight to be of practical importance. C_M is low because the reaction involves breaking the strong vinyl C-H bond. Considerable evidence [59-60] indicates that the experimentally observed C_M for styrene may be due in large part to the Diels-Alder dimer transferring a hydrogen (probably the same hydrogen transferred in the thermal initiation process) to monomer.

Chain transfer to polymer "C_p" results branched polymer. Ignoring chain transfer to polymer does not present a difficulty in obtaining precise values of C_I, C_M, and C_s, since these are determined from data at low conversions. Under these conditions the polymer concentration is low and the extent of transfer to polymer is negligible. However at higher concentration, the effect of chain transfer to polymer plays a very significant role in determining the physical properties and the ultimate applications of a polymer [61]. The chain transfer behavior of non catalytic species can be represented as follows,

$$R_n + RS—SR \longrightarrow R_n—SR + RS^{\bullet} \qquad (2.6)$$

where, R_n as defined previously is growing polymer chain, while RS-SR is disulfide used to terminate the growing polymer chain.

2.2.3.2 Mechanistic Aspects of Catalytic Chain Transfer Polymerization

Gridnev proposed the catalytic cycle mechanism in his Ph.D. thesis in 1983 which was soon published in the first review [41] of CCT. Although to date no conclusive evidence exists regarding the actual mechanism by which CTA takes place, it is generally believed that it involves a two-step process consisting of a hydrogen abstraction (Scheme 2.1) by the cobalt(II) complex and a subsequent reinitiation reaction between a monomer molecule and the cobalt(III) hydride complex [44,62-66] formed. Although the general understanding seems to be that the two steps in Scheme 2.1 are conventional hydrogen transfer reactions, a possible β-elimination of a hydrogen atom from a coordinated radical cannot be ruled out at present (Scheme 2.2).

Scheme 2.1 Two-step Hydrogen Abstraction Mechanism

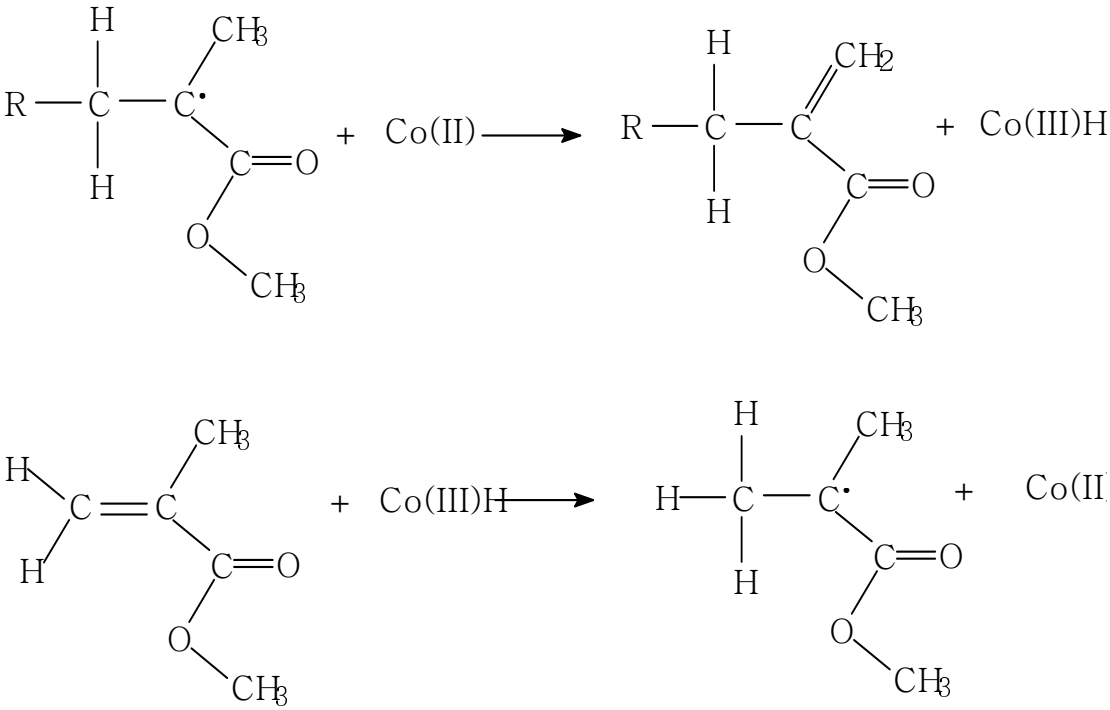

Scheme 2.2 Catalytic Chain Transfer Mechanism by β-hydrogen elimination

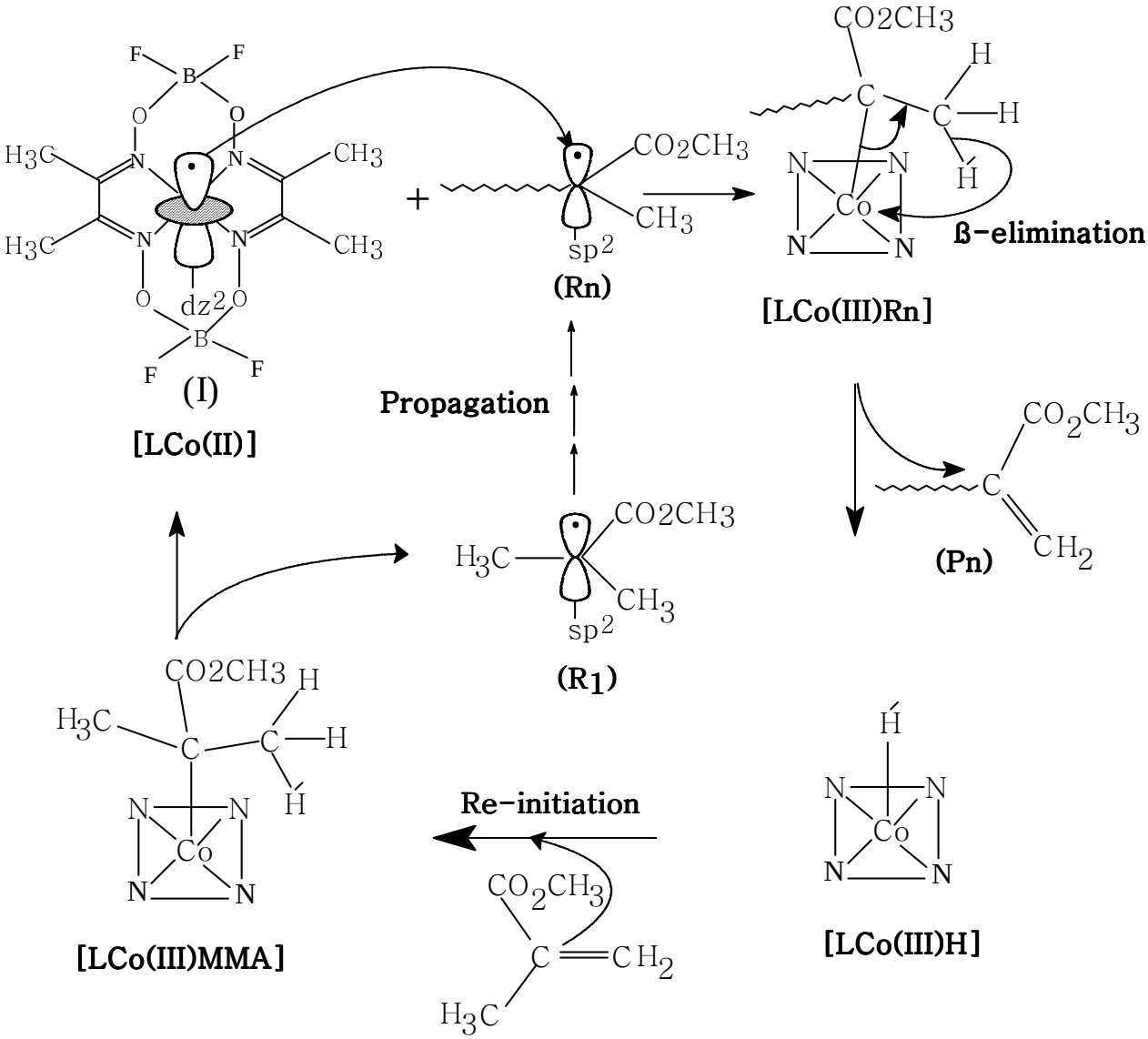

Earlier Enikolopyan and co-workers [10,67] proposed the mechanism for CCT. A simplified catalytic cycle with slight addition for catalytic chain transfer polymerization is represented in Scheme 2.2. In Catalytic Chain Transfer (CCT) initiation, propagation and termination occur as in a normal free-radical polymerization, with the addition of the transfer reaction. The literature data [68] suggest that for Co(II) complexes (we assume the same structure in bulk PLP of MMA) the unpaired electron occupies the dz^2 orbital, which perturbs the growing free radical polymer chain and produces new Co-C bond by interacting with unpaired electron in the sp^2 orbital of the growing oligomer or polymer chain (R_n). From Co(III)-R_n intermediate, β-elimination of hydrogen takes place [Scheme 2.3] and thus producing a dead polymer chain "P_n" and "LCo(III)H" cobalt hydride.

This process is feasible as not only steric interactions are removed but also a strong Co-H bond is formed. It is important to note that both the Co(III) ion and H^{-1} (hydride ion) are soft acid and base, respectively. The overlap of "dz^2" with "s" orbital of hydride ion (which is of comparable size as I^-) is better than the "dz^2" with "sp^2" orbital of growing polymer chain. But steric interaction is, probably the dominant factor than the strength of the Co-H bond.

The monomer can react with LCo(III)H via an insertion mechanism to form LCo(III)R_1. This probably takes place through LHCo(III)-‖ intermediate as shown in Scheme 2.4. CCT can be conducted with the rate constants hundreds and thousands of times faster than the best mercaptans. In fact, the efficiency of CCT measured as a ratio of the rate constant of the catalyzed reaction versus the noncatalyzed one, approaches 10^9. This number indicates that cobaloximes catalyses in CCT are as rapid as enzymatic catalyses that display efficiencies in the range 10^9-10^{11}.

It has been noted [69] that the macrocycle around cobalt is the most important factor responsible for the catalytic properties. It was found that the active CCT catalyst must have cobalt surrounded by a tetradentate, chelating, planar system of conjugated π electrons able to maintain the ring current and containing at least two nitrogen atoms in the coordination plane. The macrocycle does not have to be closed, but the highest activity is observed when the ring is closed. Any deviations from these requirements result in a drastic reduction of the catalytic activity. This is the minimally required structure. It can be incorporated into the bigger system of π electrons or have more Substituents. Cobaloximes have either a hydrogen atom or BF_2 group in the main macrocycle and so may look like an exclusion from the developed rule because of the break in the π conjugation. However, a closer observation of the resonance structures in cobaloximes (Scheme 2.5) indicates that ring current can be maintained in them by hydrogen jumping from one oxygen atom to another.

2.3 Copolymerization

The simultaneous polymerization of two or more different monomers in the same reaction mixture is called copolymerization. The polymerization of a monomer to the backbone of another polymer is known as graft copolymerization. There are four different types of copolymeres [70].

Random:	-ABBAAABAB-
Alternating:	-ABABABABABA-
Block:	-AAAAABBBBB-

Scheme 2.3 β-elimination of Hydrogen with the formation of dead polymer chain with terminal double bond in Catalytic Chain Transfer Mechanism

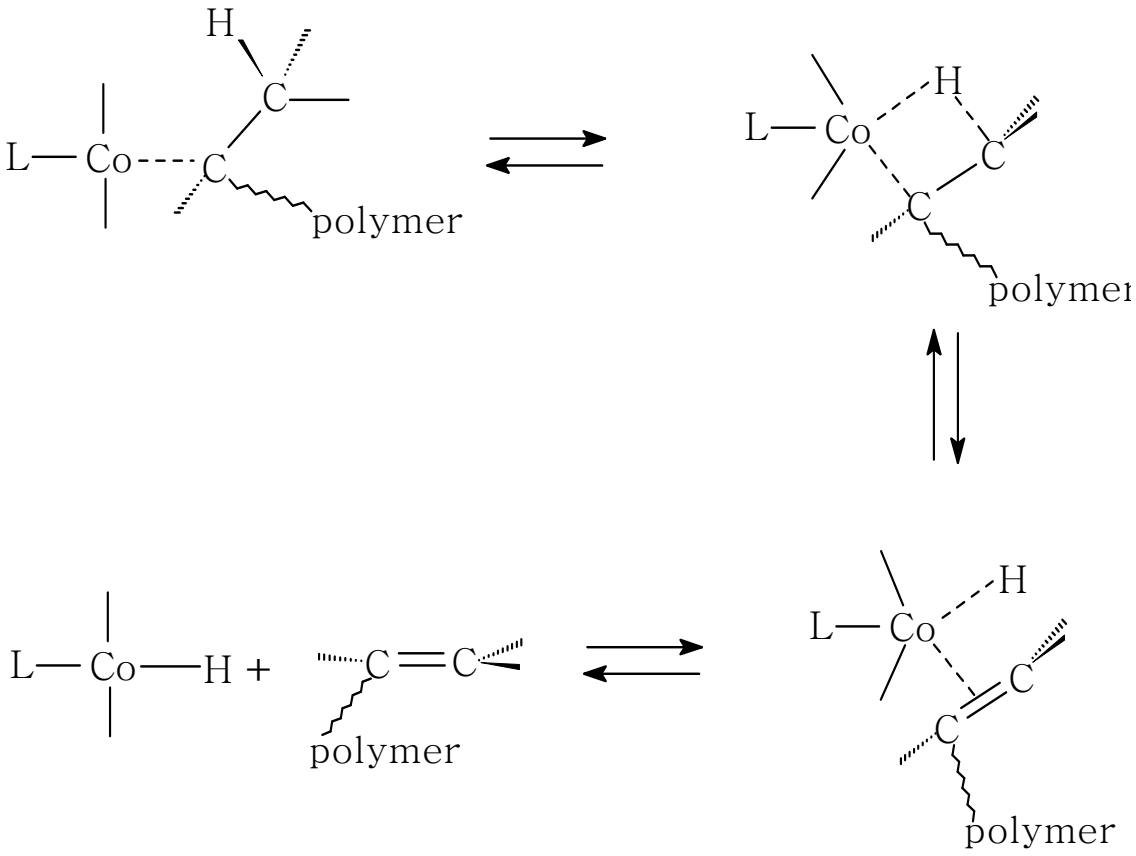

Scheme 2.4 Insertion of monomer (MMA) in LCo(III)H intermediate in Catalytic Chain Transfer Mechanism

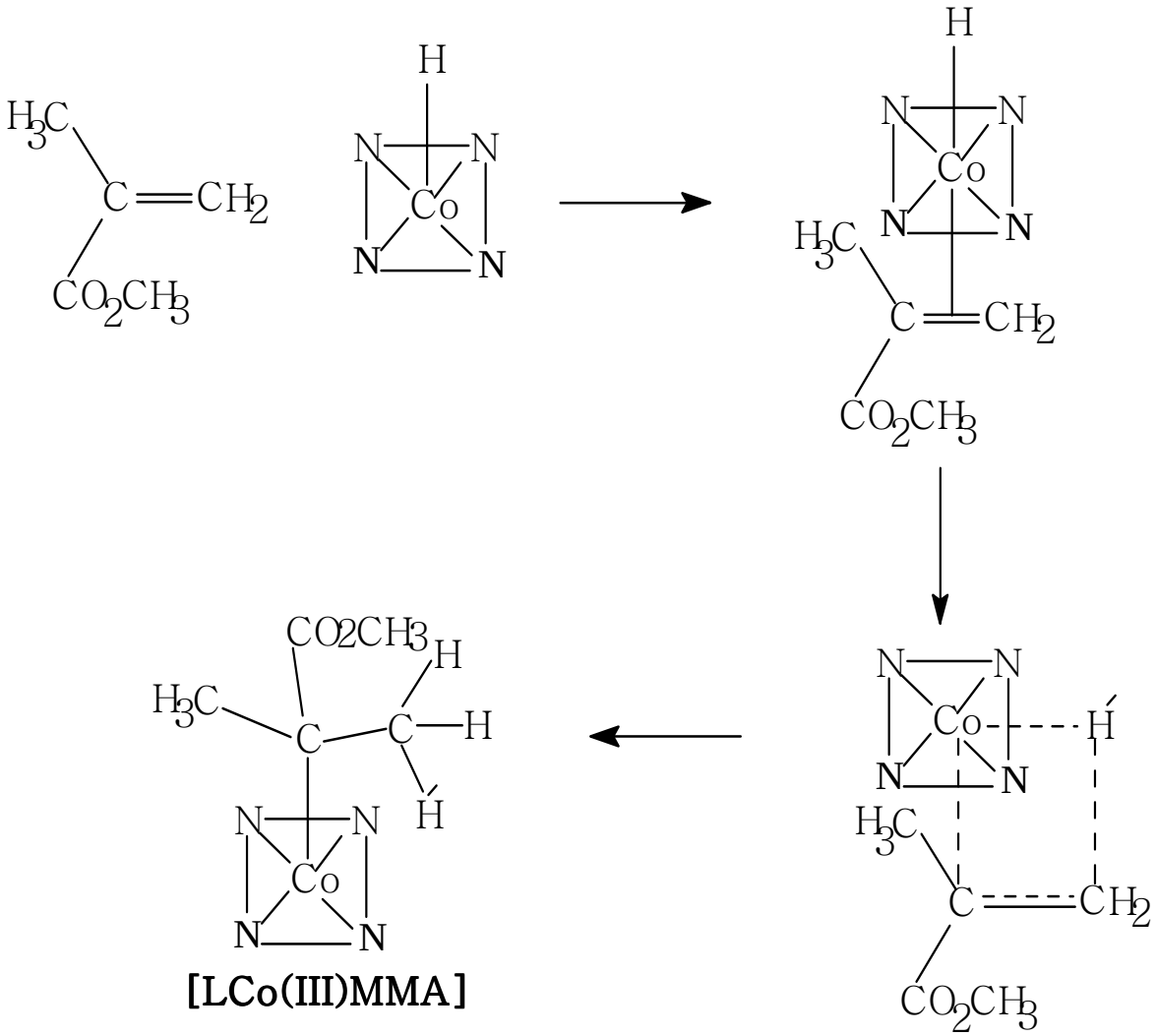

Scheme 2.5 Resonance structures of cobaloximes showing ring current

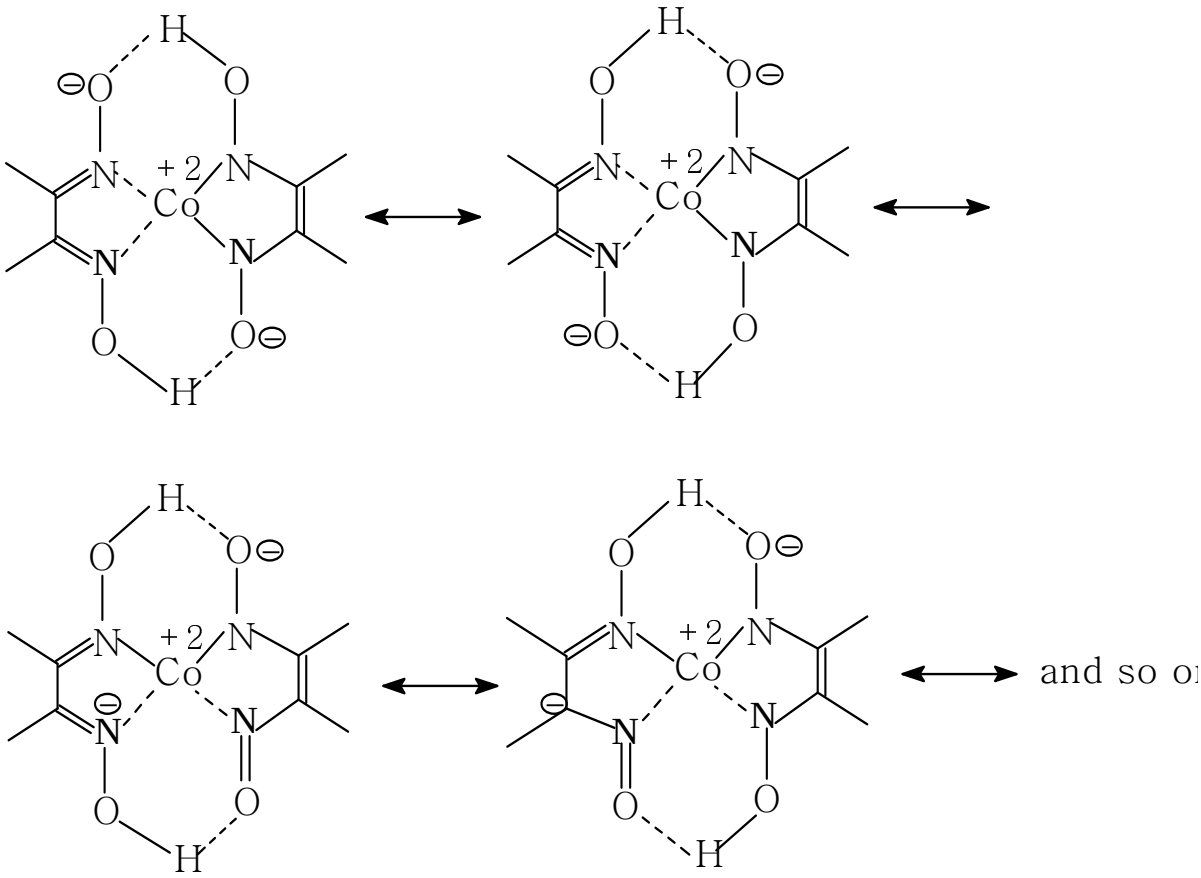

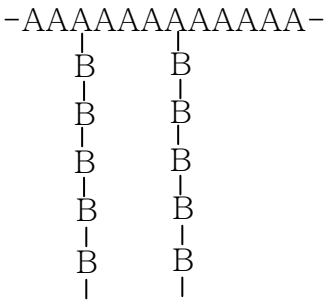

Graft

In the polymerization of a mixture of two or more monomers, the rate at which different monomers add to the growing chain determine the composition and hence the properties of the resulting copolymer. Usually in free-radical copolymerizations two types of radicals and monomers are present. The terminal or Mayo-Lewis model from graft copolymer] for binary copolymerization of styrene (S) and MMA can be summarized by Scheme 2.6. Similar schemes exist for copolymerization of other monomers.

Scheme 2.6 Propagation reactions for copolymerization

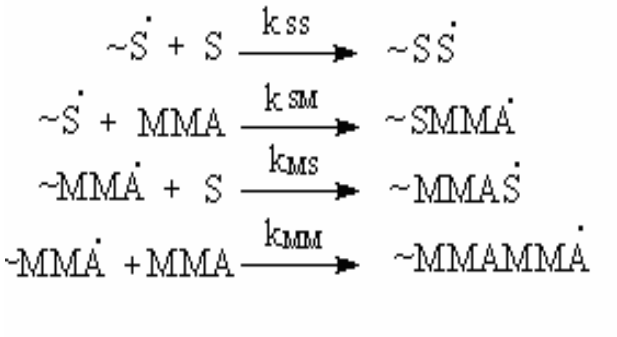

CHAPTER 3

PULSED LASER POLYMERIZATION

Synopsis: This chapter initially presents a brief literature review about Pulsed Laser Polymerization (PLP). Next, the method of extracting the propagation rate constant from GPC chromatogram has been described. Finally, an explanation as to why the k_p is given by the point of inflection has been elaborated.

3.1 Literature Review

Polymerization by photoinitiation has significant practical advantages in the printing and coating industries [71-72]. Photochemical polymerization has found applications in decorative and protective coatings and inks for metal, paper, wood, and plastics; in photolithography for producing integrated and printed circuits; and in curing dental materials. Photopolymerization is of special interest in applications where economic and /or environmental considerations require the use of solvent-free systems. This technique was developed in mid-80's by Olaj and co-workers [73-74]. A wide range of laser wavelengths was used in the experiments reported so far. These lasers include an Excimer Lasers (XeF@ 351nm.), (XeCl@ 308nm, 355 nm) [73-75] and a Nd:YAG laser with a HG—2 harmonic generator [76-77]. Nitrogen laser working at 337 nm should be equally effective, although no reports exist in the literature. Kato *et al* [78] achieved a well-controlled polymerization of MMA with the ternary initiating

system consisting of CCl_4, $RuCl_2(PPh_3)_3$, and $MeAl(ODBP)_2$. In 1997 Sawamoto et al reported two new catalysts for the atom transfer radical polymerization (ATRP) of MMA, i.e. $FeCl_2(PPh_3)_3$ [79] and $NiBr_2(PPh_3)_2$ [80]. Percec [81] et al reported the polymerization of styrene by ATRP using Wilkinson's catalyst. Moineau and co-workers [82] in 1998 reported polymerization of MMA initiated by 2,2'dichloroacetophenone in the presence of Wilkinson's catalyst (plus 7 equivalent PPh_3) in THF at 60 °C. Forster and coworkers [83] have reported photo-polymerization of 2-phenoxyethyl methacrylate by using Co(II) catalyst $[Co(dpgo\text{-}2H)_2(BF_2)_2]$ as a chain transfer agent using Nd:YAG laser (Continuum Surelite I-200) with a harmonic generator to produce 355 nm UV laser radiation at 60 °C.

3.2 Propagation Rate Calculation from GPC

The PLP technique has revolutionized free-radical polymerization kinetics, particularly with regard to obtaining the rate constants for propagation, k_p. Prior to the development of this technique, values for this constant reported, for example, in the Polymer Handbook [24] the values varies by more than an order of magnitude for the same monomer under ostensibly the same conditions. The problems arose, among other reasons, because older techniques such as the rotating sector method make subtle assumptions about termination kinetics, which are not always valid. A system containing monomer and photoinitiator was exposed to laser pulses. Each laser pulse generates a burst of short radicals, which then proceed to initiate polymerization. Some (but by no means all) chains photo-initiated by one laser pulse are terminated "instantly" by short radicals formed from the subsequent one (Figure 3.1). If one can identify the degree of

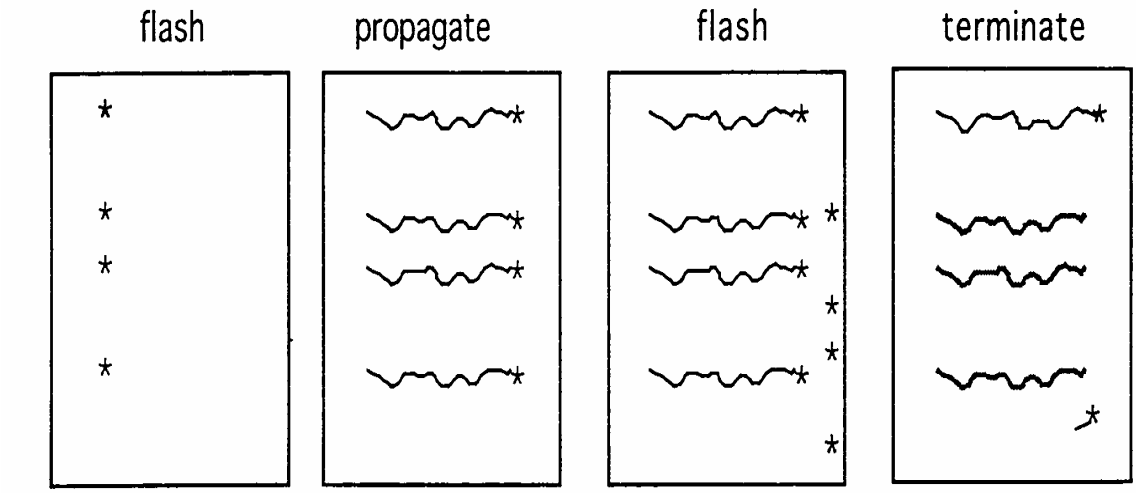

Figure 3.1 Sequence of events in Pulsed Laser Polymerization

polymerization of the chains so terminated, the value of k_p can then be found from a knowledge of the monomer concentration [M], and the time between pulses t_f by using equation 3.1.

degree of polymerization (Lo) = k_p x [M] x time between laser pulses (3.1)

The inspiration of Olaj et al was to show that independent of the occurrence of other kinetics events (e.g., transfer), the chain length L_0 could be identified as the point of inflection on the low molecular weight side of a "fundamental" molecular weight distribution peak. In this way degree of polymerization (L_0) can be measured and k_p determined [75]. Modeling with a wide variety of possible kinetic schemes have also shown that the degree of polymerization corresponds closely to the point of inflection on the molecular weight distribution from GPC [Figure 3.2].

3.2.1 Consistency Tests

The apparent value of k_p must be independent of:

- time between pulses
- laser power
- initiator concentration
- same value of k_p from first and second points of inflection.

Without these consistency tests, the results are not reliable.

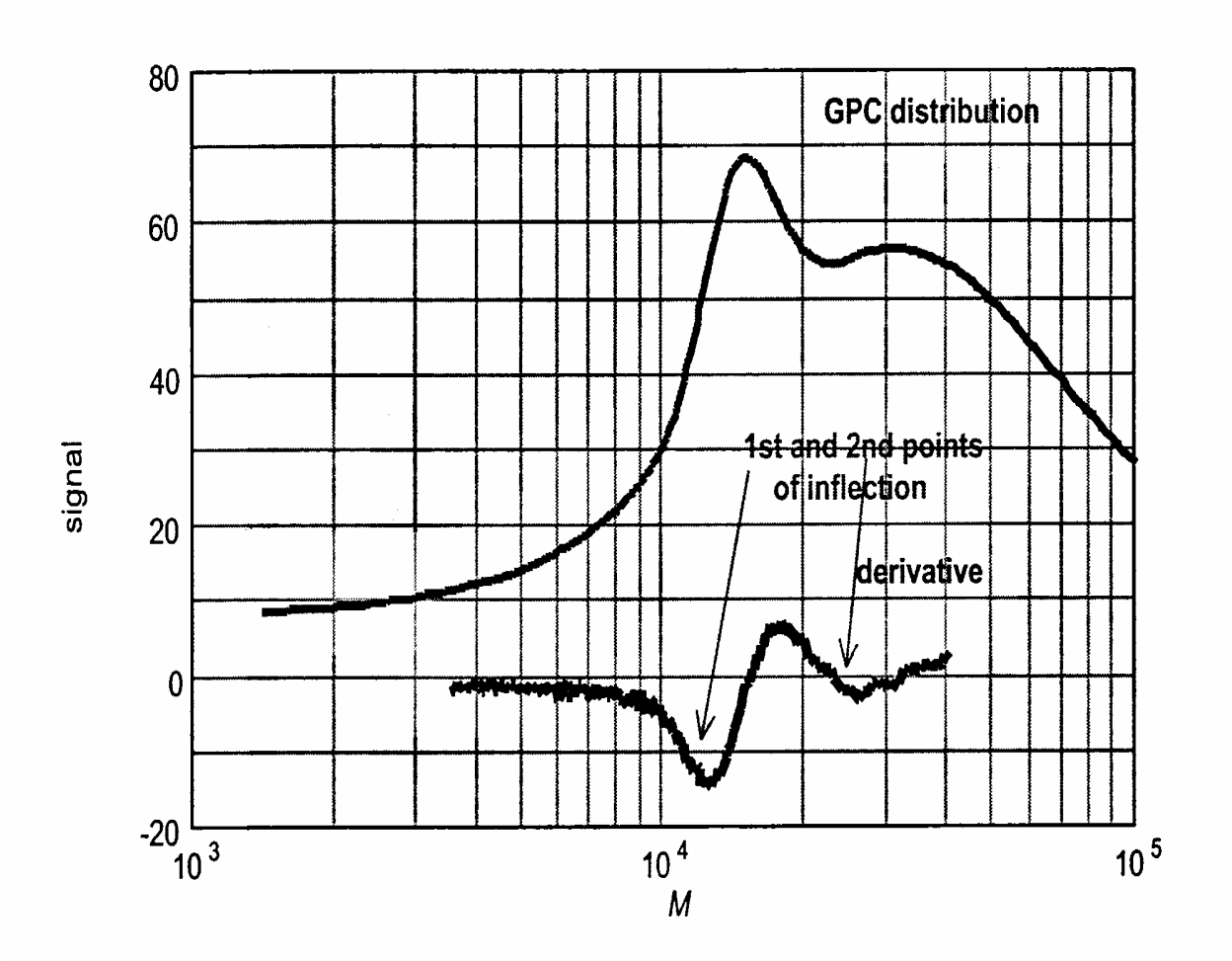

degree of polymerization (L_0) = point of inflection on GPC

Figure 3.2 A typical Chromatogram used to determine degree of polymerization from point of inflection

3.2.2 Understanding as to why k_p is given by the point of inflection

If all the growing radicals are added on new monomer at exactly the same moment, and termination by new short radical occurred instantly, one would have a spike distribution of chain lengths (Figure 3.3). However, termination is not instantaneous, and some chains will be terminated after a short chain has grown a bit, giving the type of distribution shown in (Figure 3.4). Then there is stochastic broadening: adding on a monomer unit is a random event, i.e., addition of a monomer unit does not occur at the same moment on each growing radical. This broadens the distribution again (Figure 3.5). The point of inflection is the "memory" of the infinitely steep drop-off that was the original spike. This qualitative argument is verified by modeling complete kinetics (termination, transfer, propagation): point of inflection $\approx k_p$ (not exactly). The deviation from this is (usually) insensitive to the termination mechanism, etc. Under certain circumstances, the value of k_p may be better obtained from the molecular weight at the peak.

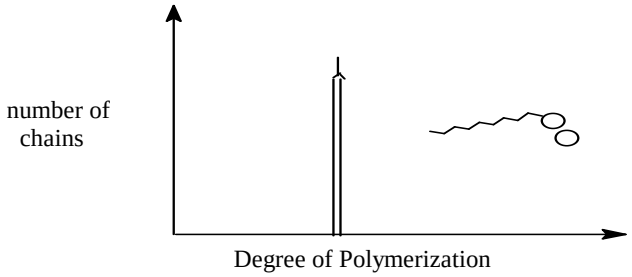

Figure 3.3 Spike distribution of chain lengths

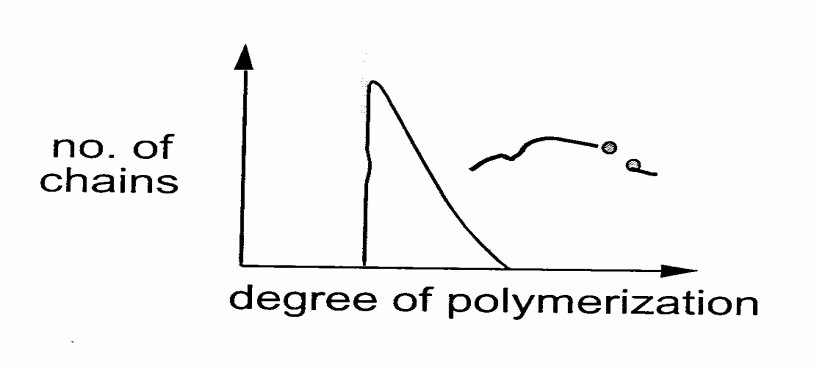

Figure 3.4 Termination in PLP not instantaneous

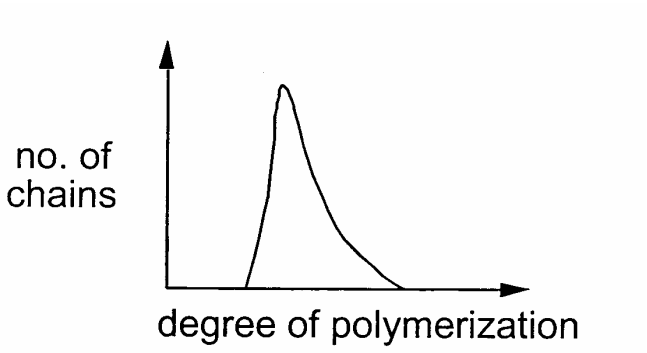

Figure 3.5 Stochastic broadening

CHAPTER 4

EXPERIMENTAL PROCEDURES

4.1 Material and Analytical Techniques

1,2,4-Trichlorobenzene of HPLC grade, methanol, toluene, chloroform, ethanol, cobalt acetate, α-furildioxome (H_2 afdo), dimethylglyoxime (H_2dmg) and etherated boron trifluoride (Fluka) were used as received. Monomers (Fluka) were freed from inhibitor by distillation. Liquid nitrogen was used to freeze the reaction mixture during degassing. Nitrogen gas (99.5% purity) was used to flush the reaction mixture. Apparatus used for characterization of catalysts and polymer, include Eager 200 elemental analyzer, Perkin-Elmer Lambda 5 spectrophotometer, Perkin-Elmer 16 FPC FT-IR and Jeol JNM-LA 500 NMR spectrometer. For determining molecular weights of polymers, Ubbelohde viscometers (from Cannon and Wescan Instruments Inc.) and WATERS GPC 150C. The brief instrumental conditions used for these analytical techniques are given below.

4.1.1 Gel permeation Chromatograph (GPC)

The samples of polymers were analyzed on WATERS GPC 150C plus. The solvent was 1,2,4-Trichlorobenzene with PL Gel 10 μm column from polymer laboratories. The flow rate was 1.0 ml min^{-1} and temperature was 150 ^{0}C. Polystyrene

standards were used for determining molecular weights and polydispersity of PMMA samples prepared in this study.

4.1.2 NMR Spectroscopic Measurements

4.1.2.1 ^{1}H NMR

The ^{1}H NMR spectra for PMMA samples with approximately 1.0 % concentration were recorded on Jeol JNM-LA 500 NMR spectrometer at the frequency of 500 MHz at 298 K in $CDCl_3$. The ^{1}H NMR spectra were recorded with the following instrumental conditions**:** No. of Points = 32,768, SW = 10,000.0 Hz, PD = 5.361 µsec, Resolution = 0.31 Hz, Scans = 16.

4.1.2.2 ^{13}C NMR

The ^{13}C spectra were obtained at 125.65 MHz with ^{1}H broad band decoupling with 45° pulse angle. Other instrumental conditions were: No. of Points = 8,192, SW = 33,003.0 Hz, PD = 12.1 µsec, Scans = 4200, Solvent = $CDCl_3$, Temperature = 299 K.

4.1.2.3 DEPT 135

The DEPT 135 of 1% PMMA was recorded at 500.0 MHz with the following instrumental conditions: No. of Points = 65,536, PD = 15.0 µsec, PW1= 7.80 sec, PW2 = 16.80 µsec, PW3 = 11.20 µsec, Temperature = 298 K. For DEPT 45, PW1= 7.80 sec, PW2 = 5.6 µsec, PW3 = 11.20 µsec were used.

4.1.3 FTIR and UV/Visible Spectroscopy

The solid state FTIR spectrum of the complexes were recorded in the range 3500-450 cm^{-1}on Perkin-Elmer 16 FPC FT-IR using KBr pellet with 8 scans and a resolution of 4. The UV/Vis spectra of the ligands and complexes in DMSO were recorded in the range 500-200 nm on Perkin-Elmer Lambda 5 spectrophotometer. The following instrumental conditions were used: slit width = 2 nm, scan speed = 60 nm min^{-1}, response = 0.2 sec, peak threshold = 0.02 A.

4.1.4 UV Excimer Laser

Lambda Physik Model EMG 203 MSC with XeCl Excimer giving 308 nm output at 10 Hz was used for pulsed laser polymerization (PLP). Laser energy was continuously monitored using a Molectron J-50 probe. The discharge voltage on the laser tube was increased in a controlled manner to maintain a constant energy output. The laser beam spot size was 10mm x 30mm which covered the volume of the sample cell. No focusing or beam expansion was needed in our experiments.

4.2. Preparation of Catalysts used as Chain Transfer Agent

4.2.1 Preparation of BF_2-bridged bis(dimethylglyoxime)cobalt(II) Complex

The catalyst [$Co(dmg\text{-}2H.BF_2)_2$] was prepared with slight modification of the procedure reported by Backac [84]. Initially 0.9887 g of dimethylglyoxime [H_2dmg] (8.514×10^{-3} moles) was dissolved in 100 ml of ether to which 0.9986 g (4.010×10^{-3} moles) of cobaltous acetate was added. After 45 minutes of stirring, 10.0 ml of etherated BF_3 was added and solution was refluxed for 24 hours. To the resulting suspension ice

cold water was added and the solution was filtered. The precipitates were washed with water, methanol and ether and dried under vacuum at room temperature. The UV/Visible spectrum of the complex is given in Figure 4.1, while results for elemental analysis are given in Table 4.1.

4.2.2 Preparation of BF_2-bridged bis(α-Furilglyoxime)cobalt(II) Complex

This catalyst was prepared by direct synthesis method rather than the two steps synthesis via Hydrogen-bonded precursor followed by cyclization reaction. To 101.0 mg (0.405 mmol) of cobaltous acetate tetrahydrate $Co(O_2CCH_3)_2.4H_2O$ dissolved in 100 ml of anhydrous ether, 191 mg (0.87 mmol) of α-Furilglyoxime was added. To this reaction mixture 5.0 ml of BF_3:Et_2O solution was added. The reaction mixture was refluxed at room temperature for 24 hours. The reddish brown product formed was precipitated by addition of distilled water to the reaction mixture, and filtered. It was repeatedly rinsed with distilled water and dried under vacuum at room temperature. The weight of the product was 110.0 mg and percent yield was 43.0%.

$$Co(CH_3CO_2)_2.4H_2O + 2H_2afdo + BF_3.Et_2O \xrightarrow[24\ hour]{anhydrous\ ether} [Co(afdo\text{-}2H)_2(BF_2)_2].2H_2O + 2CH_3COOH + 2H_2O \quad (4.1)$$

The UV/Visible spectrum of the complex is given in Figure 4.2 while for ligands are and results for elemental analysis are given in Table 4.1.

Table 4.1 Elemental Analysis for complexes used as Chain Transfer Agents

Complex	% C	%N	%H
$[Co(dmg\text{-}2H.BF_2)_2]$**	24.8	14.3	3.7
	(22.8)*	(13.3)	(3.8)
$[Co(afdo\text{-}2H.BF_2)_2]$**	36.6	8.4	2.4
	(38.2)	(8.9)	(2.5)
$[Co(dmg\text{-}2H)_2]$**	31.3	18.4	4.2
	(29.5)	(17.2)	(4.3)
$[Rh(afdo\text{-}2H.BF_2)_2]$** CH_3COO^-	38.2	8.3	3.2
	(36.0)	(7.6)	(2.6)

* These values were calculated using the respective formula weights of the complexes.

** The water molecules are shown.

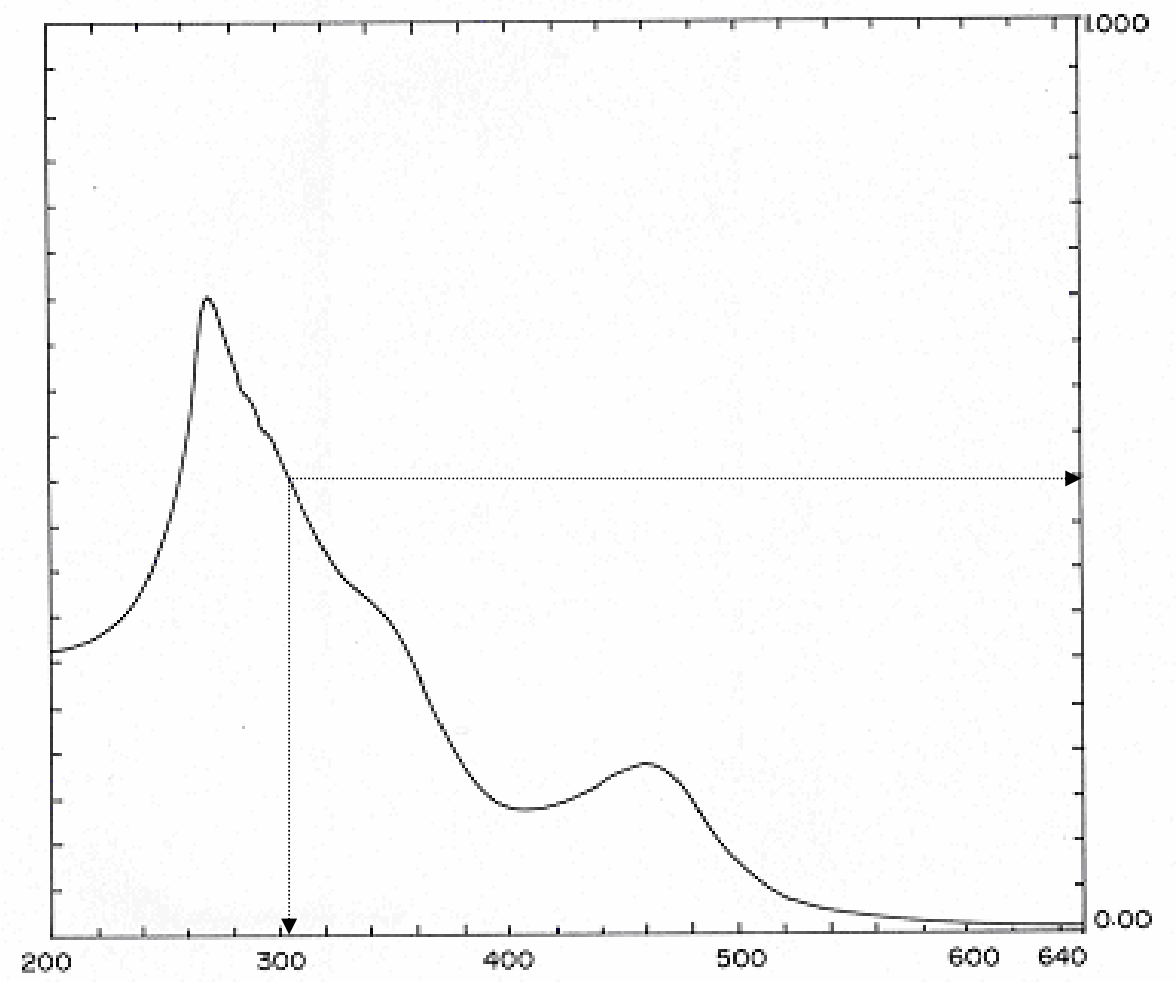

Figure 4.1 UV/Vis absorption spectrum of 9.9 x 10^{-5} M solution of [Co(dmg-2H.BF_2)$_2$] in DMSO.

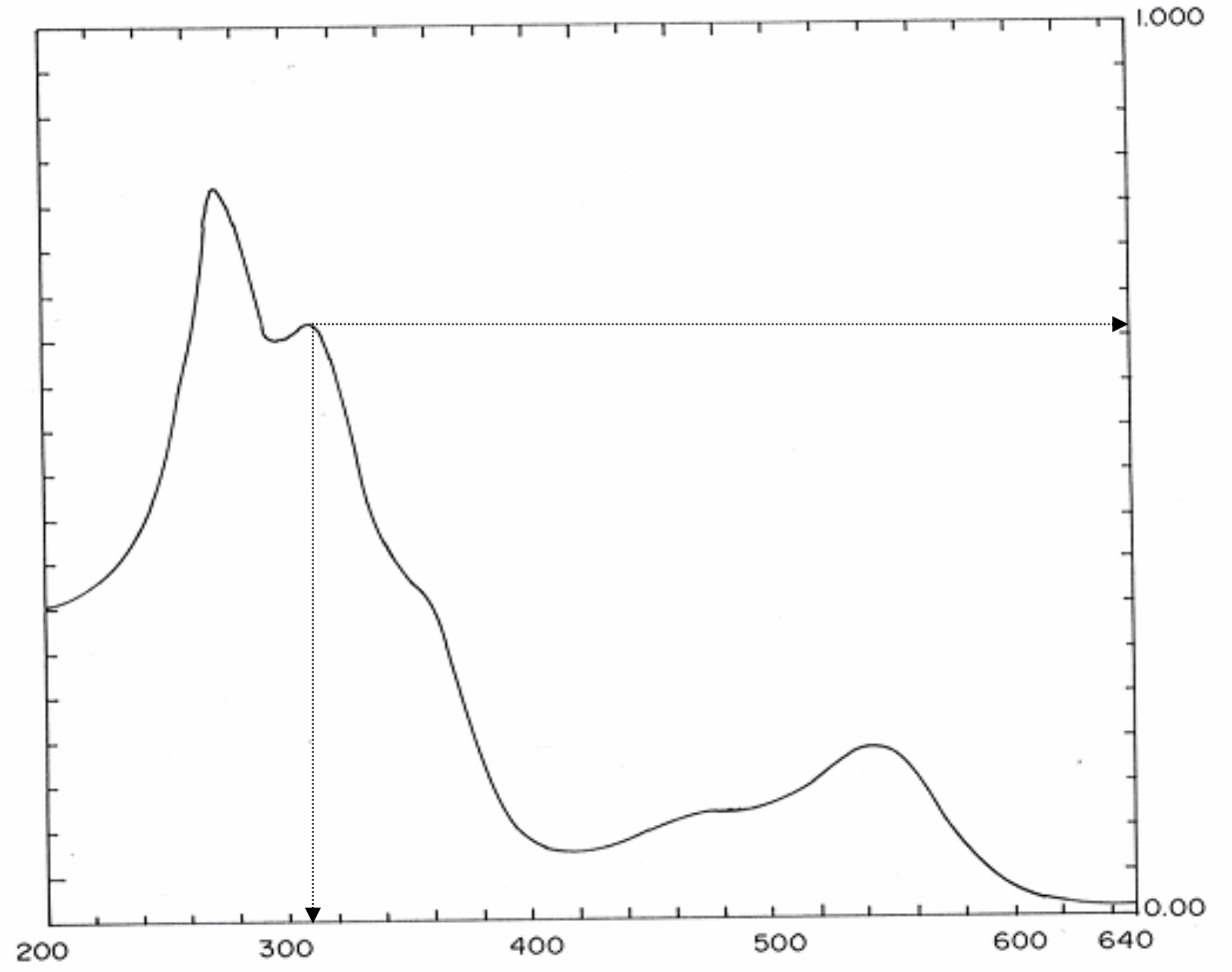

Figure 4.2 UV/Vis absorption spectrum of 2.73 x 10^{-5} M solution of [Co(afdo-2H.BF_2)$_2$] in DMSO.

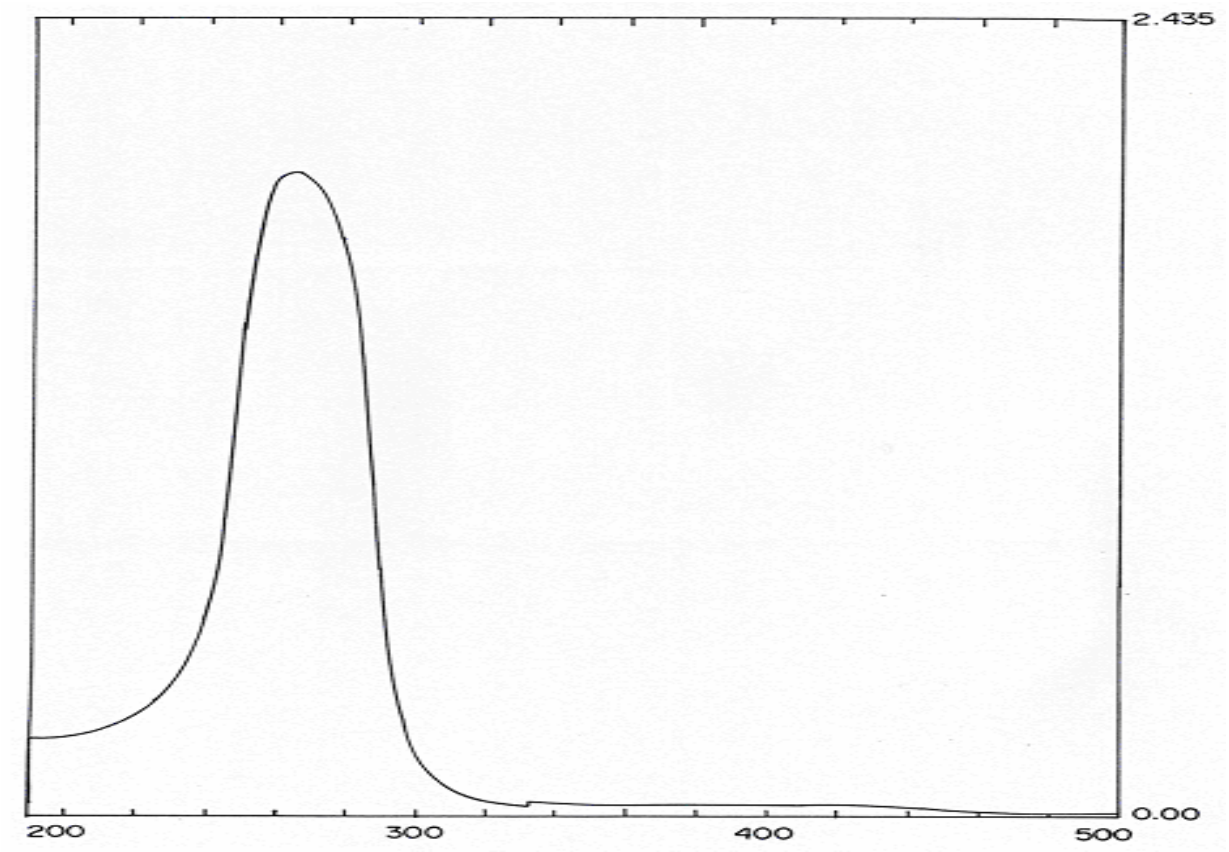

Figure 4.3 UV/Vis absorption spectrum of 7.5 x 10^{-4} M solution of alpha furilglyoxime ligand in DMSO.

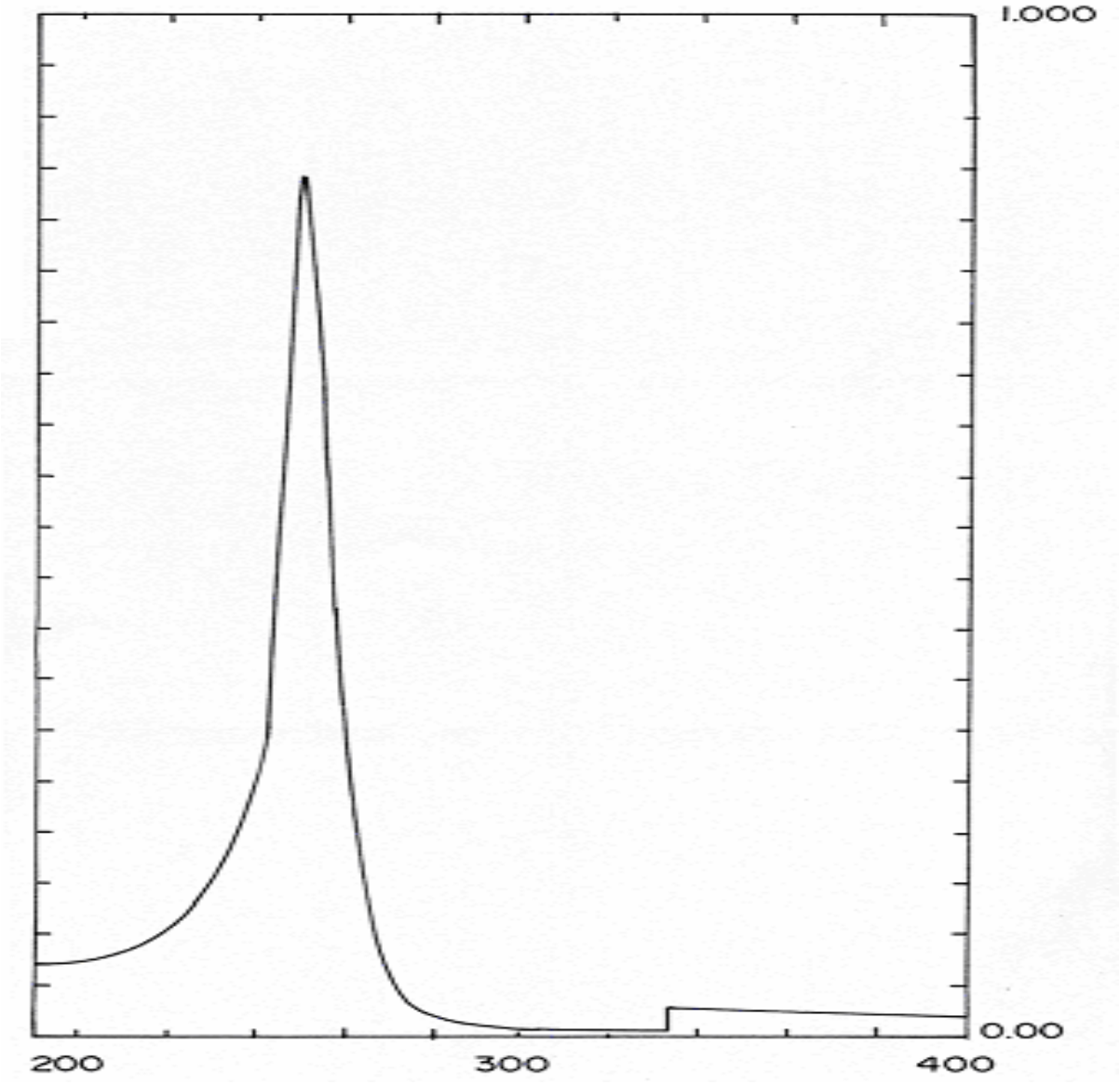

Figure 4.4 UV/Vis absorption spectrum of 7.5 x 10^{-4} M solution of dimethyl glyoxime ligand in DMSO

4.2.3 Preparation of [Co(dmg-H.$H_2O)_2$] Catalyst

Initially 0.2010 g of Co(II) acetate was dissolved in methanol and 0.2018 gram of dimethylglyoxime (H_2dmg) ligand was added. The solution was stirred for 1 hour. The resulting blackish red colored solution was evaporated and the final product was washed three times with excess of ether. Black crystalline product with 53.0 % yield was collected. The UV/Visible spectrum is given in Figure 4.5, while results for elemental analysis are given in Table 4.1.

4.2.4 Preparation of [Rh(afdo-2H.$BF_2)_2$] CH_3COO^- Complex

Initially 0.2047g (9.30×10^{-4} moles) of H_2afdo was dissolved in 50 ml of ethanol and 0.1004 g of Rh(II) acetate (4.54×10^{-4} moles) was added. After 24 hours of stirring the color of the solution changed from light green to orange black with some fine precipitate in the solution was also observed. After filtring, the precipitates were washed with ice cold water. The filtrate was yellow, which was gently heated to evaporate excess of water. Its color changed to orange yellow during the evaporation period. After addition of a small amount of acetone, the solution was kept in refrigerator for crystallization. The weight of the product was 0.1117 g with 39 % yield. The presence of an acetate group was confirmed by ^{1}H NMR. Overall quality of the ^{1}H NMR was not good, which is often observed in paramagnetic metal complexes. The results for elemental analysis are given in Table 4.1.

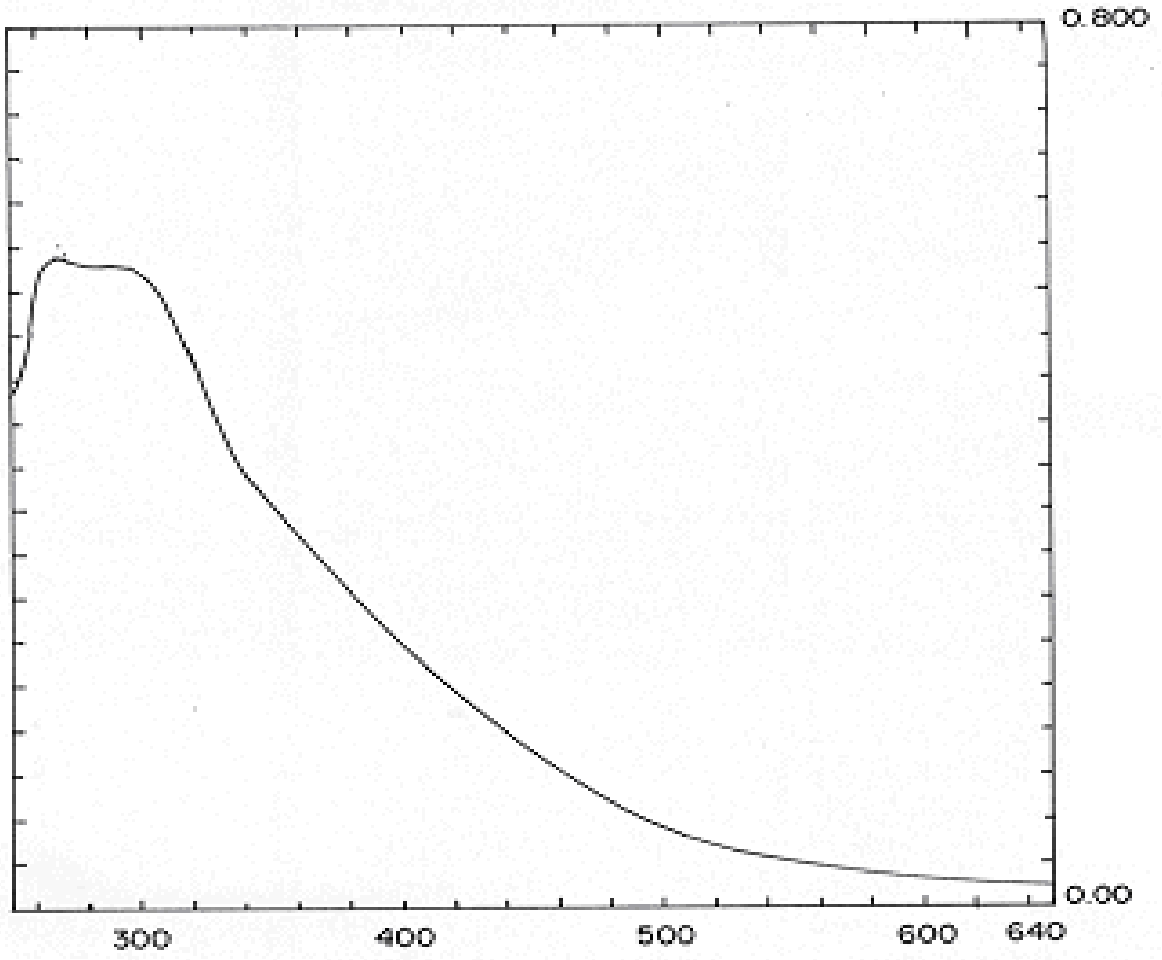

Figure 4.5 UV/Vis absorption spectrum of 6.15 x 10^{-5} M solution of [Co(dmg-2H.$H_2O)_2$] in DMSO

4.3 Polymerization Reactions

Bulk polymerization technique was employed for the investigation of catalysts as chain transfer agent. In general, for a successful study of catalytic chain transfer, the experiment should be designed in such a way that the chances of other chain transfer reactions occurring are either eliminated or minimized. Such chain transfer reactions may arise as a result of interactions between the propagating chain and a monomer molecule, which is called chain transfer to monomer. The propagating chain may also be transferred to a solvent molecule, initiator fragment, or to some impurity present in the reaction mixture. In bulk polymerization technique, only monomer, initiator and propagating chains are present at any stage in the reaction. Consequently, the choice of initiator is as important as the choice of the polymerization technique. The initiator chosen should offer minimum or no interference in the course of the experiment. That is, it should have a very low chain transfer constant.

2,2'-Azobis-(2-methylpropionitrile) [AIBN] was chosen as the initiator because it satisfies the condition stated above, with respect to the monomers to be studied (Table B2 Appendix B). Other reasons for its choice include availability, solubility, in a wide range of monomers and ease of handling. In designing the experiment, the effect of heat transfer on the kinetics of the reaction was not taken into consideration because monomer conversion was restricted at low level. At such low levels, the viscosity of the reaction mixture is not enough to cause any serious threat of explosion (due to heat transfer problem), or to impinge on the mobility of the molecules of the chain transfer agent. Similarly, the effect of increased rate of reaction(s), caused by local overheating is usually not significant at such conversion levels. The minimum temperature for

polymerization with heat was 50 °C, while for pulsed laser polymerization room temperature (25 °C) was opted. This was sufficient to decompose the initiator molecules into radicals, and at the same time, low enough to prevent high initiator rate, which may give rise to high conversion that will ultimately impinge on the mobility of the chain transfer agent molecules.

4.3.1 Purification of Monomers

The addition of certain substances suppresses the polymerization of monomers. These substances act by reacting with the initiating and propagating radicals and converting them either to non radical species or radical of reactivity too low to undergo propagation. Such polymerization suppressors are classified according to their effectiveness. Inhibitors stop every radical, and polymerization is completely halted until they are consumed. The inhibitor, usually an aromatic such as hydroquinone or t-butylpyrocatechol is present in Methyl methacrylate and styrene monomer and need to be removed prior to conducting any polymerization studies. The inhibitor was removed by washing the monomer with 10 % aqueous NaOH. Roughly equal parts of the basic solution and the monomer were placed in a separatory funnel and were mixed with regularly shaking. The heavier aqueous layer was drained off. The procedure was repeated at least twice until the liquid remains clear. The monomer was then washed with distilled water until litmus paper shows that all the base was removed. A drying agent such as anhydrous Na_2SO_4 was added to the monomer (100g/l). With occasional shaking, drying was complete in about an hour. The anhydrous monomer was stored in the refrigerator prior to distillation. A small amount of monomer was tested by adding to

methanol to ensure that no polymerization has taken place in the monomer. The MMA was distilled at 60 torr and 33-35 °C, while styrene was distilled at 20 torr and 40-43 °C [85].

4.3.2 Degassing The Monomer Solution

The tube [Figure 4.6] once charged with the monomer solution was degassed using a high efficiency vacuum pump. Each tube was degassed successively by several freeze-thaw cycles. The degassing process was carried out as follows. Each tube was conected to the vacuum line and immersed in a Dewar flask containing liquid nitrogen, with the vacuum pump switched off. The tubes were kept in the liquid nitrogen, until the contents were completely frozen. Next, the vacuum pump was switched on long enough to evacuate the air above the frozen solution. The vacuum pump was then switched off and the contents thawed by immersing the tubes in a beaker of water. Air bubbles trapped in the frozen solution were observed to escape to the evacuated surface as the frozen solution melted. Several freeze-thaw cycles were repeated until as much air as possible was removed from the solution. All the tubes in a particular run were subjected to the same number of freeze-thaw cycles. However, the relative number of these cycles differed from one monomer to another.

The following points are needed to be observed while degassing the samples.

- To get the maximum vacuum the oil of the pump should have the least amount of impurities and must be periodically changed.
- Before applying pencil mark grease, the female joint should be cleaned and dried. The grease must also be periodically changed.

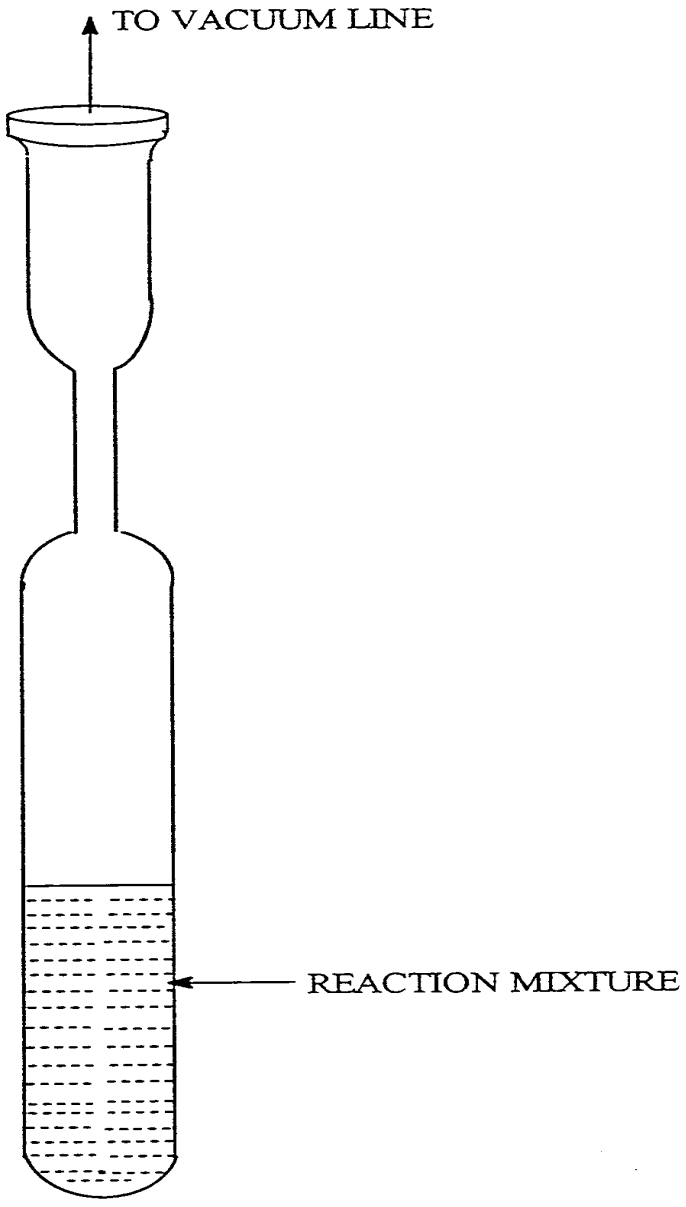

Figure 4.6 Test Tube used for removal of dissolved oxygen from the sample

- The beaker and other apparatus should be clean to watch the traces of bubbles.
- Use water at room temperature for thaw purpose, because higher time is required to melt the contents in cold water and chances of polymerization are also minimized while working at a reasonable speed at room temperature.

4.3.3. Thermal Polymerization

4.3.3.1 Polymerization in the Absence of Chain Transfer Agent at 70 and 80 °C using Benzoyl peroxide (BPO) as an Initiator

One stock solution was prepared by adding 70.0 mg of Benzoyl peroxide (BPO) in 70.0 ml of MMA. The test tubes after cleaning with acetone and drying in oven were charged with 5.0 ml of the stock solution. The tubes were degassed and sealed using the procedure outlined in section 4.3.2. Five of the test tubes were polymerized at 70 °C and another at 80 °C. The tubes were removed from the constant temperature bath at different time intervals and were promptly transferred into ice-cooled water. Then, the tubes were broken and the contents were added to 50 ml cold methanol with constant stirring. Initially methanol and un-reacted MMA were evaporated. *It is important to note that small size poly(methyl methacrylate) (PMMA) molecules are soluble in methanol. Therefore, it is advisable to evaporate methanol rather than decanting the solution.* The residual amount of MMA and methanol was removed by the following procedure. In a pre-weighed vial PMMA was dissolved in minimum amount of CH_2Cl_2. The vial was placed in beaker having hot water at 40-50 °C to increase the solubility of the polymer. The CH_2Cl_2 will also dissolve any un-reacted monomer. The methanol was added to this solution and the test tube was centrifuged. The methanol was drained off and this process

was repeated twice. Finally, the vial was placed in a beaker having hot water and nitrogen gas was passed. The vials were then decapped and wrapped with Al foils and a long thin wire was attached to its neck. Two tiny holes were made with the wire and were placed in round bottom flask. Rubber stopper with a central hole was fixed tightly and was connected to a vacuum pump. The outlet of the vacuum pump was placed in a fume hood. Before turning the vacuum pump on, it was ensured that the pressure releasing knob is lose enough. This knob was tightend gradually after turning the vacuum pump on. The bottom knob was gradually inspected for any drops of methanol collected. *The drops should be drained while the system is off*. Finally, the percent conversion was recorded and samples were analyzed by gel permeation chromatography (GPC) for determining the molecular weight and polydispersity index (PDI) values.

4.3.3.2 Polymerization in the pesence of Chain Transfer Agent

4.3.3.2.1 Polymerization of Styrene at 60, 70, and 80 °C

A stock solution of [Co(afdo-2H.BF_2)$_2$] catalyst was prepared by dissolving 2.0 mg of the catalyst in a minimum amount of acetone to which 11.0 ml of styrene containing 11.0 mg of AIBN was added. After gentle heating most of the acetone was evaporated. A second stock solution containing 15.0 mg of AIBN in 15.0 ml of styrene was prepared. To five clean test tubes 5.0, 4.0, 3.0, 2.0, and 1.0 ml from stock solution 2 was added and 0.0, 1.0, 2.0, 3.0, and 4.0 ml from stock solution 1 was added. The test tubes were degassed and polymerized at 60 °C. In the similar way ten more solutions of styrene were prepared using same amount of AIBN initiator but different concentration of [Co(afdo-2H.BF_2)$_2$]. These samples were polymerized at 70 and 80 °C.

4.3.3.2.2 Polymerization of Methyl methacrylate at 50 °C

A stock solution of [Co(afdo-2H.BF_2)$_2$] catalyst was prepared by dissolving 2.0 mg of catalyst in a minimum amount of acetone and then 10.0 ml of freshly distilled MMA was added. After slight heating acetone was evaporated. Exactly 2.0 ml of this solution was transferred to another beaker containing 10.0 ml of MMA and 8.0 mg of AIBN. This stock solution was 5.30 x 10^{-5} M. A second stock solution containing 23.0 mg of AIBN in 35.0 ml of MMA was prepared. To five clean test tubes 5.0, 4.0, 3.0, 2.0, and 1.0 ml from stock solution 2 and 0.0, 0.2, 0.4, 0.6, and 1.0 ml from stock solution 1 was added. The test tubes were degassed and placed in water bath at 50 °C with constant palpitation for a period of 60 minutes. Then, the test tubes were dowsed in ice-cooled water to cease the polymerization process. Finally, the polymer contents were precipitated out in cold methanol.

4.3.3.2.3 Polymerization of Methyl methacrylate at 60 °C in the presence of [Co(afdo-2H.BF_2)$_2$] Chain Transfer Agent

A stock solution of [Co(afdo-2H.BF_2)$_2$] catalyst was prepared by dissolving 2.2 mg of catalyst in 1.0 ml of acetone with subsequent addition of 10.0 ml freshly distilled MMA. Most of the acetone was evaporated with slight heat around 30-40 °C. This CTA solution was 3.785 x 10^{-4} M. Final stock solution of CTA was prepared by transferring exactly 2.0 ml from previous stock solution to 10.0 ml of MMA, which already contained 12.0 mg of AIBN initiator. This catalyst stock solution was labeled “A”. Initiator stock solution (6.17 x 10^{-3} M) was prepared by dissolving 33.0 mg AIBN in 35.0 ml of MMA.

Six reaction mixtures were prepared, each containing 5.0 ml of initiator solution and 0, 0.2, 0.4, 0.6, 0.8 and 1.0 ml of catalyst stock solution "A". The dissolved O_2 was removed by freeze-thaw operation and finally the test tubes were sealed.

4.3.3.2.4 Polymerization of Methyl methacrylate at 70 °C in the presence of [Co(afdo-2H.BF_2)$_2$] Chain Transfer Agent

The initiator stock solution (7.58×10^{-3} M) was prepared by dissolving 43.0 mg of AIBN in 35.0 ml of MMA. All other steps are similar as described in previous section.

4.3.3.2.5 Polymerization of Methyl methacrylate at 80 °C

The catalyst stock solution was exactly the same as described above in section 5.6.3.2.2. However, the initiator stock solution was prepared by dissolving 54.0 mg of AIBN (9.23×10^{-3} M) in 35.0 ml of MMA. The duration of polymerization was 10 minutes only.

4.3.3.2.6 Polymerization of Butyl methacrylate (BMA) at 60 °C in the presence of [Co(afdo-2H.BF_2)$_2$] Chain Transfer Agent

A stock solution of [Co(afdo-2H.BF_2)$_2$] catalyst was prepared by dissolving 1.2 mg of catalyst in 1.0 ml of acetone with subsequent addition of 10.0 ml freshly distilled MMA. Most of the acetone was evaporated with slight heating around 30-40 °C. This CTA solution was 3.47×10^{-4} M. Final stock solution of CTA was prepared by transferring exactly 2.0 ml from previous stock solution to 10.0 ml of MMA, which

contained 12.0 mg of AIBN initiator. This catalyst stock solution (5.78×10^{-5}) M was labeled "A". Initiator stock solution (6.17×10^{-3} M) was prepared by dissolving 33.0 mg AIBN in 35.0 ml of MMA. Six reaction mixtures were prepared, each containing 5.0 ml of initiator solution and 0, 0.2, 0.4, 0.6, 0.8 and 1.0 ml of catalyst stock solution "A". The dissolved O_2 was removed by freeze-thaw operation and finally the test tubes were sealed.

4.3.3.2.7 Polymerization of Butyl methacrylate at 70 and 80 °C

For polymerization of BMA at 70 °C 5.83×10^{-5} M and 7.67×10^{-3} M stock solutions of [Co(afdo-2H.BF_2)$_2$] catalyst and AIBN were prepared. Six samples were prepared according to procedure described in section 5.6.3.2.6 and were polymerized for a period of 40 minutes. For polymerization of BMA at 80 °C, 5.83×10^{-5} M and 9.37×10^{-3} M stock solutions of [Co(afdo-2H.BF_2)$_2$] catalyst and AIBN were prepared. Six samples were prepared according to the procedure described earlier and were polymerized for a period of 20 minutes.

4.3.3.2.8 Copolymerization of Methyl acrylate (MA) with Styrene at 70 °C

Before using the monomer, inhibitor was removed from MA with procedure outlined in 4.3.1 and later on distilled at 50 torr. A stock solution containing 11.0 mg of AIBN in 11.0 ml of styrene in addition to 3.0 mg of [Co(afdo-2H.BF_2)$_2$] catalyst was prepared. A second stock solution containing 16.0 mg of AIBN in 16.0 ml of MA was prepared. To the four clean test tubes 4.0, 3.0, 2.0, and 1.0 ml from stock solution 1 was

added and 1.0, 2.0, 3.0, and 4.0 ml of MA solution was added. The samples were polymerized at 70 °C.

4.3.3.2.9 Polymerization of Methyl methacrylate (MMA) and Styrene at 60 °C in the presence of [Rh(afdo-2H.BF_2)$_2$]Cl

A stock solution of [Rh(afdo-2H.BF_2)$_2$]Cl catalyst was prepared by dissolving 4.0 mg of catalyst in minimum amount of acetone. 10.0 ml of MMA containing10.0 mg of AIBN was added. After gentle heating acetone was evaporated. A second stock solution containing 15.0 mg of AIBN in 15.0 ml of MMA was also prepared. To five clean test tubes 5.0, 4.0, 3.0, 2.0, and 1.0 ml from stock solution 1 was added and 0.0, 1.0, 2.0, 3.0, and 4.0 ml from stock solution 2 was added. The test tubes were degassed and polymerized at 60 °C. After drying the polymer, molecular weights and PDI were determined by gel permeation chromatography (GPC).

4.4 Preparation of Samples for Pulsed Laser Polymerization

4.4.1 Polymerization of MMA and Styrene in the absence of CTA

First of all MMA was polymerized in the absence of both CTA and initiator to check the role of Excimer Laser. Then homopolymerization of MMA using 2.027×10^{-3} M AIBN was conducted using Excimer Laser with 10.0 Hz repetition rate.

Homo-polymerization of styrene was also investigated using 2.027×10^{-3} M AIBN and the same Laser. The typical set up used for Pulsed Laser Polymerization (PLP) process is shown in Figure 4.7.

4.4.2 Samples Preparation for the PLP in the presence of Chain Transfer Agent (CTA)

4.4.2.1 Polymerization of MMA in the presence of $[Co(dmg\text{-}2H.BF_2)_2]$ as CTA

A stock solution of $[Co(dmg\text{-}2H.BF_2)_2]$ catalyst was prepared by dissolving 1.0 mg of catalyst in 5.0 ml of freshly distilled MMA containing already 5.0 mg of AIBN. A second initiator stock solution was prepared by dissolving 35.0 mg AIBN (6.1×10^{-6} M) in 35.0 ml of MMA. Five reaction mixtures were prepared, each containing 6.0 ml of initiator solution and 0.1, 0.2, 0.3, 0.4, and 0.5 ml of catalyst stock solution. The dissolved O_2 was removed by freeze-pump-thaw operation and finally the test tubes were sealed. Then the solution of each test tube was transferred to 4.0 ml capacity quartz cell under dry nitrogen gas atmosphere. Lambda Physik Model EMG 203 MSC Excimer laser (XeCl) was used for irradiation (50 minutes for each of the sample). The laser wavelength was 308 nm. Typical laser energy per pulse was 150 mJ with repetition rate 10 Hz.

Figure 4.7 Schematic diagram of the experimental set up for Pulsed Laser Polymerization of MMA

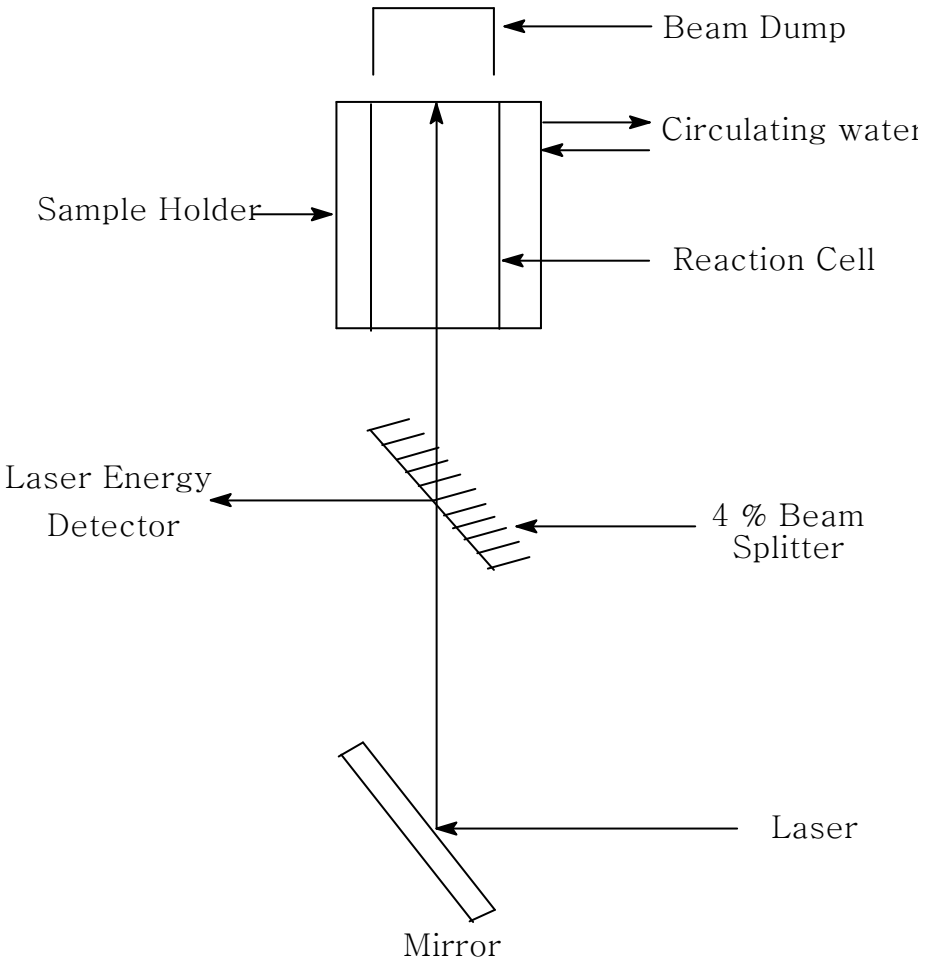

4.4.2.2 Polymerization of MMA in the presence of $[Co(afdo\text{-}2H.BF_2)_2]$ as CTA

A stock solution of $[Co(afdo\text{-}2H.BF_2)_2]$ catalyst was prepared by dissolving 1.0 mg of catalyst in 5.0 ml of freshly distilled MMA containing already 5.0 mg of AIBN. A second initiator stock solution was prepared by dissolving 35.0 mg AIBN in 35.0 ml of MMA. Five reaction mixture were prepared, each containing 6.0 ml of initiator solution and 0.1, 0.2, 0.3, 0.4, and 0.5 ml of catalyst stock solution. The dissolved O_2 was removed by freeze-pump-thaw operation. Finally, test tubes containing oxygen-free samples were sealed. Then the solution of each test tube was transferred to 4.0 ml capacity quartz cell under dry nitrogen gas atmosphere.

4.4.2.3 Polymerization of Styrene in the presence of $[Co(dmg\text{-}2H.BF_2)_2]$ as CTA

A stock solution of $[Co(dmg\text{-}2H.BF_2)_2]$ catalyst was prepared by dissolving 1.0 mg of catalyst in 10.0 ml of freshly distilled styrene containing already 10.0 mg of AIBN. A second initiator stock solution was prepared by dissolving 35.0 mg AIBN (6.1×10^{-6} M) in 35.0 ml of MMA. Five reaction mixtures were prepared, each containing 6.0 ml of initiator solution and 0, 0.2, 0.6, 0.8, 1.0 and 2.0 ml of catalyst stock solution. The dissolved O_2 was removed by freeze-pump-thaw operation and finally the test tubes were sealed. Then the solution of each test tube was transferred to 4.0 ml capacity quartz cell under dry nitrogen gas atmosphere.

4.4.2.4 Polymerization of Butyl methacrylate (BMA) in the presence of [Co(dmg-2H.BF_2)$_2$] as Chain Transfer Agent

A stock solution of [Co(dmg-2H.BF_2)$_2$] catalyst was prepared by dissolving 0.8 mg of catalyst in 20.0 ml of freshly distilled styrene containing already 20.0 mg of AIBN. A second initiator stock solution was prepared by dissolving 45.0 mg AIBN ($6.1x10^{-6}$ M) in 45.0 ml of MMA. Five reaction mixtures were prepared, each containing 6.0 ml of initiator solution and 0, 0.4, 0.8, 1.2, 1.6 and 2.0 ml of catalyst stock solution. The dissolved O_2 was removed by freeze-pump-thaw operation and finally the test tubes were sealed. Then the solution of each test tube was transferred to 4.0 ml capacity quartz cell under dry nitrogen gas.

4.4.2.5 Polymerization of Butyl methacrylate (BMA) in the presence of [Co(afdo-2H.BF_2)$_2$] Chain Transfer Agent

A stock solution of [Co(afdo-2H.BF_2)$_2$] catalyst was prepared by dissolving 1.0 mg of catalyst in minimum amount of acetone and transferred to 10.0 ml of freshly distilled butyl methacrylate containing already 10.0 mg of AIBN. A second initiator stock solution was prepared by dissolving 45.0 mg AIBN ($6.1x10^{-6}$M) in 45.0 ml of MMA. Five reaction mixtures were prepared, each containing 6.0 ml of initiator solution and 0, 0.4, 0.8, 1.2, 1.6, 2.0 and 3.5 ml of catalyst stock solution. The dissolved O_2 was removed by freeze-pump-thaw operation and finally the test tubes were sealed. Then the solution of each test tube was transferred to 4.0 ml capacity quartz cell under dry nitrogen gas atmosphere.

4.5 Polymerization of Methyl methacrylate (MMA) in the presence of Wilkinson's Catalyst

Wilkinson's catalyst (2.0 mg) was dissolved with slight warming in 10.0 ml of freshly distilled MMA. Then the solution was cooled down immediately. In each of four test tubes labeled as A, B, C, and D, 20.0 mg of AIBN was added. Test tube "A" contained 1 ml of Wilkinson's catalyst solution and 5.0 ml of MMA, test tube "B" contained 3.0 ml Wilkinson's catalyst solution and 3.0 ml MMA, test tube "C" contained 5.0 ml of Wilkinson's catalyst solution and 1.0 ml of MMA, while test tube "D" was the control sample as it contained only 6.0 ml of pure MMA (without any Wilkinson's catalyst). The dissolved O_2 was removed by freeze-pump-thaw operation. Finally test tubes containing oxygen free samples were sealed. Then the solution of each test tube was transferred to 4.0 ml capacity quartz cell under dry nitrogen gas atmosphere. Therefore each sample in quartz cell contained 13.8 mg of AIBN, but different concentrations of Wilkinson's catalyst. Lambda Physik Model EMG 203 MSC Excimer Laser (XeCl) was used for irradiation of samples (45 minutes for each of the sample). The wavelength of the Laser was at 308 nm. Typical laser energy per pulse was 150 mJ with repetition rate 10 Hz. The resulting polymer was added in 40 ml of methanol with constant stirring. Initially all methanol and residual MMA was evaporated. For any traces of the residual MMA, vacuum drying procedure was applied.

4.6 Polymer Characterization

The polymer samples obtained in the study were characterized by FTIR, UV/Vis and ^{1}H NMR spectroscopic techniques. Molecular weights were determined by dilute solution viscomety measurements and gel permeation chromatography techniques. The various characterization techniques employed are described below.

4.6.1 Electronic Spectroscopy of Polymer Samples

FTIR spectra can be used both for structure determination of the polymer and co-polymers. But, interpretation of these spectra is difficult because absorptions lie very close together and often overlap. Ploy(methyl acrylate) [86], PMMA [87-88] and Poly(styrene) PSTY [89-93] have been widely studied. For the FTIR analysis, samples were taken either in solid state, or as thin films of the polymer prepared in spectral grade chloroform. The spectra of Polystyrene and PMMA samples were taken in the solid state in the form of potassium bromide pellets. A Perkin Elmer FTIR Spectrophotometer was used in the region 400 to 4000 cm^{-1}.

The UV/Vis absorption spectroscopy yields information on multiple-bond and aromatic conjugation within macromolecules. The non-bonding electrons on oxygen atom may also be involved in extending the conjugation of multiple-bond systems in polymers. The UV/Vis spectra of PMMA samples were recorded below 300 nm because terminal double bond in PMMA appears around 250 nm.

4.6.2 ^{1}H NMR and ^{13}C NMR of Polymer Samples

^{1}H NMR and ^{13}C NMR of the polymer samples were recorded on a Jeol Lambda 500 MHz nuclear magnetic resonance spectrometer. In our study, we have used the double resonance technique to record the ^{13}C NMR. An appropriate quantity of the sample was weighed and dissolved in a vial in deuterated chloroform ($CDCl_3$) containing TMS as internal standard. The resulting polymer solution was filtered using cotton wool with the help of a dropper. The spectra recorded were compared to literature ^{13}C NMR of PMMA [94-95] and PSTY [96-99].

4.6.3 Dilute Solution Viscosity Measurements (DSV)

Viscosity measurements were conducted at 30 °C using two designs of the Ubbelohde viscometer. One of such designs from Wescan Instrument Inc; equipped with an automatic timing device and a thermostat water bath. All solvents used were reagent grade. Mark-Houwink constants were taken from Polymer Handbook [100]. The following general procedure was followed in the viscometry experiment on all samples. Stock solutions ranging from 0.5 to 1.0 g polymer per 100 ml toluene were prepared in all cases. The clean and dried viscometer was charged with pure solvent and time taken for the solvent to flow through points A and D was recorded. Next, 10.0 ml of the stock solution was transferred into the empty viscometer and was rinsed thoroughly and drained. Now fresh amount of same sample was taken in the viscometer and it was placed in thermostat for at least 10 minutes (to attain the temperature of the bath). The time taken for the solution to pass between the two points was recorded. At least three readings were taken for each sample. After suitable dilution of the sample solution of the

viscometer time of flow was noted by applying the same procedure outlined earlier. *Viscometer has to be mounted vertically because otherwise an additional error is introduced. Prior to measuring the viscosity of solution, filtration of dust is desirable in order to avoid irreproducibility of readings. Viscometer should be thermostated to ± 0.01 °C in order to measure the limiting viscosity number (intrinsic viscosity) with an accuracy of 1 %.* More details for appropriate use of the viscometer and its cleaning instructions are present in Lab Manual for Chemistry Lab 401 by Dr. Ashrof Ali [70].

4.7 Molecular Weight and Molecular Weight Distribution (MWD)

Two different methods were employed in characterizing the molecular weights of the polymer samples in this study. These methods produce molecular weight averages that are numerically different, because the techniques measure different properties of the polymer. The techniques are outlined below.

4.7.1 Gel Permeation Chromatography (GPC)

GPC is normally used as an analytical procedure for separating small molecules by their difference in size and to obtain molecular weight averages (Table 4.2) or information on the molecular weight distribution (MWD) of polymers. The molecular weight distribution, which represents breadth of the GPC curve is usually represented as ratio between weight-average molecular weight to number-average molecular weight. There is a drawback to SEC. In SEC, we're really not measuring mass so much as the *hydrodynamic volume* of the polymer molecules, that is, how much space a particular polymer molecule takes up when its in solution.

Table 4.2 Definitions of Molecular weights obtained from GPC

Name	Formula
Number-average molecular weight	$M_n = [\overline{\sum} N_i M_i / [\sum N_i]$
Weight-average molecular weight	$M_w = [\overline{\sum N_i M_i^2} / [\sum N_i M_i]$
Peak-average molecular weight	----------
Z-average molecular weight	$M_p = [\overline{\sum N_i M_i^3} / [\sum N_i M_i^2]$

We can approximate the molecular weight from SEC data because we know the exact relationship between molecular weight and hydrodynamic volume for polystyrene, and we use polystyrene as a standard. But the relationship between hydrodynamic volume and molecular weight isn't the same for all polymers, so we get only an approximate measurement. There is a new method that can measure molecular weight averages and molecular weight distributions very exactly. It is called matrix-assisted laser desorption/ionization mass spectrometry.

4.7.2 Viscosity Measurements

4.7.2.1 Viscosity Definitions

In dilute solutions the viscosity related terms as indicated in Table 4.3 are used. For Intrinsic Viscosity an extrapolation to infinite dilution requires measurements of the viscosity at several concentration (at least four concentrations, e.g. 0.05, 0.10, 0.15, and 0.20 g per 100 ml).The sample concentration should not be too large because additional effects may then arise from intermolecular forces and entanglements between chains (for very large molecular weights).

4.7.2.2 Viscosity-average Molecular Weight (M_v)

For polydisperse linear polymers the Viscosity-average molecular weight is given by Mark-Houwink-Sakurada Equation.

$$[\eta] = K\overline{M}_v^{a} \qquad (4.2)$$

Table 4.3 Definitions of different types of Viscosity

Official names	Common names	Quantity
Viscosity coefficient	Viscosity	η
Viscosity ratio	Relative viscosity	$\eta_{rel} = \eta/\eta_o$
	Specific viscosity	$\eta_{sp} = \eta_{rel} - 1$
Viscosity number	Reduced specific viscosity	$\eta_{red} = (\eta_{rel} - 1)/c$
Logarithemic viscosity number	Inherent viscosity	$\eta_{inh} = \ln \eta_{rel}/c$
Limiting Viscosity number	Intrinsic viscosity	$[\eta] = \lim_{C\to 0} (\eta_{sp}/c)$

The Viscosity-average molecular weight is defined as

$$\overline{M}_v = [\sum N_i M_i^{1+a} / [\sum N_i M_i]^{1/a} \qquad (4.3)$$

where "K" and "a" are constant for a given polymer at a given temperature in a given solvent. The viscosity-average molecular weight lies between the number-average and weight-average molecular weights.

$$\overline{M}_n < \overline{M}_v < \overline{M}_w$$

M_v lies closer to M_w than to M_n. The constant "a" usually varies within the range $0.5 < a < 0.8$. Higher values are sometimes obtained for stiff and/or short molecules.

4.7.2.3 Complications with Viscosity-average Molecular Weight (M_v)

- If a polymer sample used for measuring constants "K" and "a" has a broad molecular weight distribution, the values determined for "K" and "a" may have serious errors;
- If a polymer sample has the same M_w/M_n ratio, only the constant "a" will be correct, whereas the constant "K" will not;
- If log [η] is plotted versus log M_n, the constant "K" will be too high;
- If log [η] is plotted versus log M_w, the constant 'K" will be too low;

The application of viscosity measurements to obtain the viscosity-average molecular weight is additionally complicated [101-113] by the following factors:

- The influence of molecular weight distribution;
- The occurrence of branching;

- The existence of a compositional and sequential composition of segments in the case of stereospecific polymers and co-polymers;
- The existence of agglomerates;
- The solvation of macromolecules;
- Entanglements between chains;
- The drag effect;
- The Mark-Houwink equation is not valid for linear heterogeneous co-polymers.
- Physical factors such as

(a) adsorption of polymer molecules on wall capillaries,

(b) cleavage of chains by shearing,

(c) local heating due to viscous energy dissipation.

The capillary viscometers used for dilute solution measurements are made of glass. The flow time is related to the viscosity of the liquid and is determined by the driving pressure, using an equation known as Poiseulle's Law:

$$\eta = \pi R^4 P/8lQ = \pi R^4 Pt/8lV \qquad (4.4)$$

where,

R is the radius of the capillary,

P is the pressure driving the fluid through the capillary,

L is the length of the capillary

Q is volumetric flow rate,

V is the volume and t is the time of flow.

The Poisseulle equation (4.4) after corrections for the shear rate, shear stress, kinmatic energy and entrance correction, has the form,

$$\eta = A\rho t(1- B/At^2) \qquad (4.5)$$

where,

P is the liquid density,

A and B are constants for the particular viscometer used.

The relative viscosity for dilute solution now takes the final form,

$$\eta_{rel} = \eta/ \eta_o = t(1- B/At^2) / t_o(1- B/At_o^2) \qquad (4.6)$$

If the viscometer has an outflow time greater than 100 s for the pure solvent, the kinetic energy corrections B/At^2 are negligible compared to unity, and then

$$\eta_{rel} = t / t_o \qquad (4.7)$$

We have used this equation to calculate the relative viscosity of our polymer samples because t_o was greater than 100 s for our Ubbelohde Viscometer.

4.8 Determination of Chain Transfer Constant (C_s)

According to The Macromolecular Division of the International Union of Pure and Applied Chemistry [114], the chain transfer constant is represented as follows.

$$C_{tr} = k_{tr} / k_p \qquad (4.9)$$

However, in literature C_{tr} is also represented as C_s, and we have used C_s notation to represent the chain transfer constant value. By the appropriate choice of polymerization conditions one can determine the value of C_s [115] using Mayo equation: shown below;

$$\frac{1}{DP_n} = \frac{1}{DP_{n_0}} + Cs \frac{[S]}{[M]} \qquad (4.10)$$

where $1/DPn_0$ is the value of $1/DP_n$ in the absence of the chain transfer agent and k_{tr} and k_p represents transfer rate constant (to chain transfer agent) and propagation rate constant, respectively. Recently, [116-119] alternative to the Mayo plot has emerged from theoretical considerations of polymerization kinetics.

CHAPTER 5

RESULTS AND DISCUSSION

5.1.1 Characterization of the Ligands

The name oxime is a contraction of oxy-imine, C=NOH. The oxime group is amphiprotic with a slightly basic nitrogen atom and a mildely acidic hydroxyl group. It was Alfred Werner who, recognized [120-121] isomerism of oximes and attributed to " the different spatial arrangement" of the groups attached to the C=N moiety. The most significant early event in the area of transition metal chemistry of oximes took place in 1905 when a Russian chemist, Chugaev discovered [122] reaction between nickel (II) salts and dimethylglyoxime, which is the best example of a vicinal dioxime (henceforth abbreviated as vic-dioxime). The list of vic-dioximes and transition metals that can participate in complex formation was quickly augmented [123]. The analytical selectivity of vic-glyoximes is due partly to deprotonation and subsequent formation of strong hydrogen bond by OH group in the planar complexes.

In general, vic-glyoximes form complexes through nitrogen atoms and have similar bond distances for N-O and C=N regardless of the type or the size of the central metal atom. The N-O bond distance was observed to be shorter in case of the complex than the free ligands, while C=N bond is almost the same both for the complexes and the free

ligands. The C-N-O angle in vic-glyoximates is wider by about 10° compared to the corresponding angle in the free ligands [124].

Considering the importance of these ligands it is important to explore the structural details of these ligands and their complexes. In this connection ^{1}H NMR, ^{13}C NMR, ^{15}N NMR have been widely used to study the isomers and other structural details of oximes. In furfural oximes on the basis of ^{1}H-^{1}H spin spin coupling constants it was found that the E isomers have primarily an s-trans-conformation in polar dimethylsulfoxide, whereas the Z isomers, on the other hand, have an s-cis conformation. Liepin'sh and co-workers [125] on the basis of ^{1}H ,^{13}C and ^{15}N NMR spectra showed that the oximes of 5-X-2-acetylfurans (X = H, CH_3, Br, NO_2) have the E configuration exclusively or preferentially, depending on the method of production of the compound and the substituent X. For E-1-(2,4,6-trimethylphenyl)ethanone oxime it was found by X-ray analysis that the dihedral angle between the plane of aromatic ring and the oxime plane is 70.8°. This large angle precludes a significant π electron overlap between the oxime function and the benzene ring. The barrier to rotation about the aryl-oxime bond was estimated to be about 5.8 kcal/mol. Hussain and co-workers [126] have reported the spectroscopic data for α- furilglyoxime and various complexes of cobalt and rhodium. The data presented indicates that α- furilglyoxime has only one isomer.

In the present investigation we have recorded ^{1}H ,^{13}C and ^{15}N NMR spectra of both dimethlyglyoxime and α-furilglyoxime ligands on 500 MHz Jeol NMR and we believe that dimethlyglyoxime consists of one isomer while α-furilglyoxime consists of two isomers. Both alpha furilglyoxime (H_2afdo) and dimethylglyoxime (H_2dmg) ligands have been investigated by different analytical techniques.

The ^{1}H NMR (Figure 5.1) of H_2dmg indicates that it consists of only one isomer. The -CH_3 protons appear at 1.93 while –OH protons appear at 11.36 ppm. The solvent (DMSO-d_6) peak is at 2.50 ppm, while water (in DMSO-d_6) gives signal at 3.34 ppm. The ^{13}C for –CH_3 and =C appear at 9.36 and 153.15 ppm respectively. The H_2dmg produces only one sharp ^{15}N peak at 372.32 ppm, thus further validating the fact that this ligand consists of only one isomer. The broad peak in IR around 3200 cm^{-1} is due to O-H stretching peak, while weak C-H stretching peak appears around 2930 cm^{-1}. The N-O stretching vibration for H_2dmg in IR appears around 1145 cm^{-1}. Figures 5.2 and 5.3 represents IR spectra of H_2dmg and H_2afdo, respectively. All these vibrational bands are comparable to literature reported values [124,126]. Figures 5.4-5.5 for ^{1}H, ^{13}C and ^{15}N of H_2afdo indicate the complications associated with assigning accurate peak positions. One can easily infer that H_2afdo ligand consists of more than one structure. This observation is contrary to a previous observation [124], which describes only one isomer of H_2afdo.

However, careful inspection of peaks in ^{1}H NMR and ^{13}C NMR reveals that H_2afdo consists of two isomers, the expected structures of which is shown in Figure 5.6. In ^{1}H NMR the peaks at 12.24, 12.19 and 11.56 ppm corresponds to H_b, H_a and H_c protons with integration ratio 1:2:1 respectively.

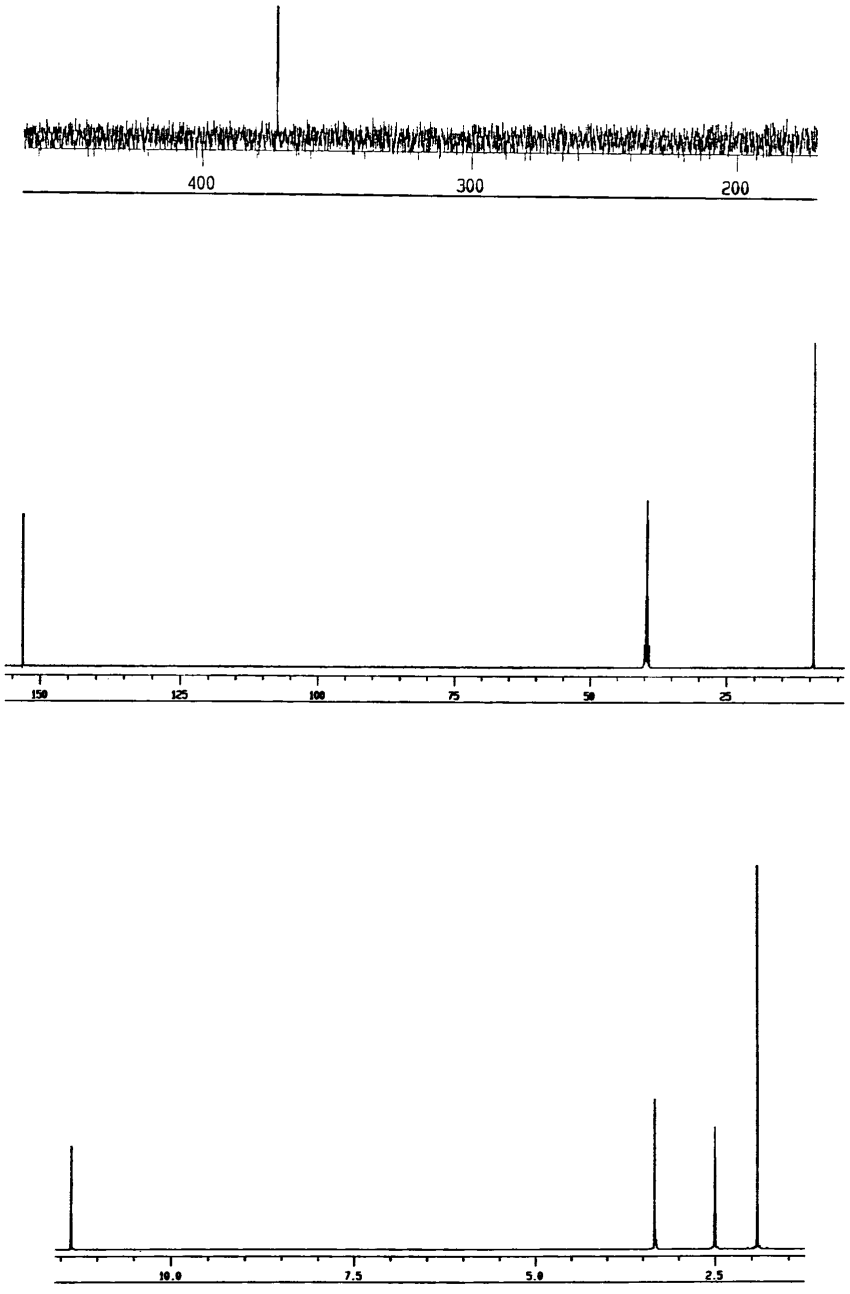

Figure 5.1 ^{15}N (Top), ^{13}C (Middle) and ^{1}H NMR (Bottom) of dimethylglyoxime in DMSO-d_6. The values are in δ (ppm)

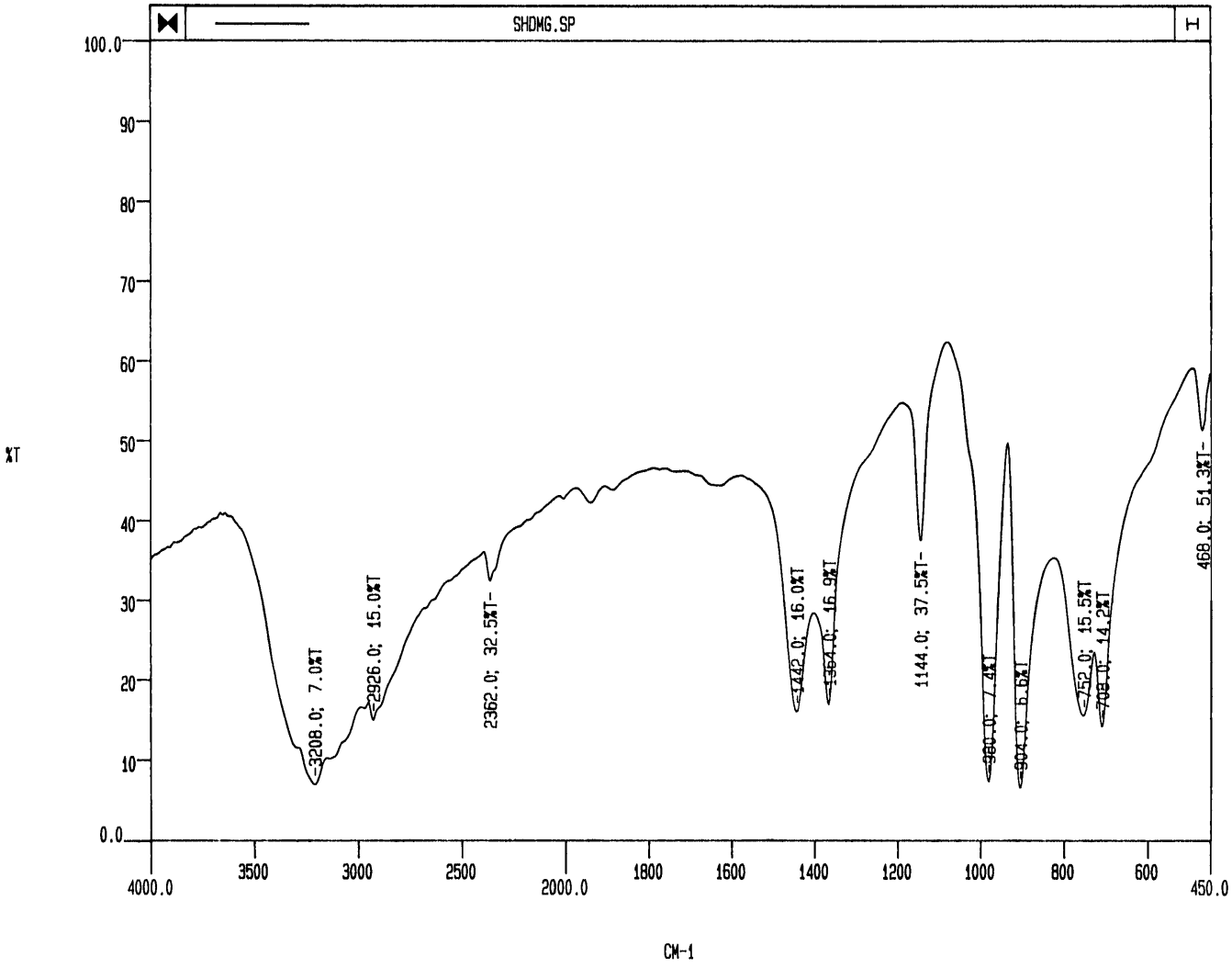

Figure 5.2 IR spectrum of dimethlyglyoxime

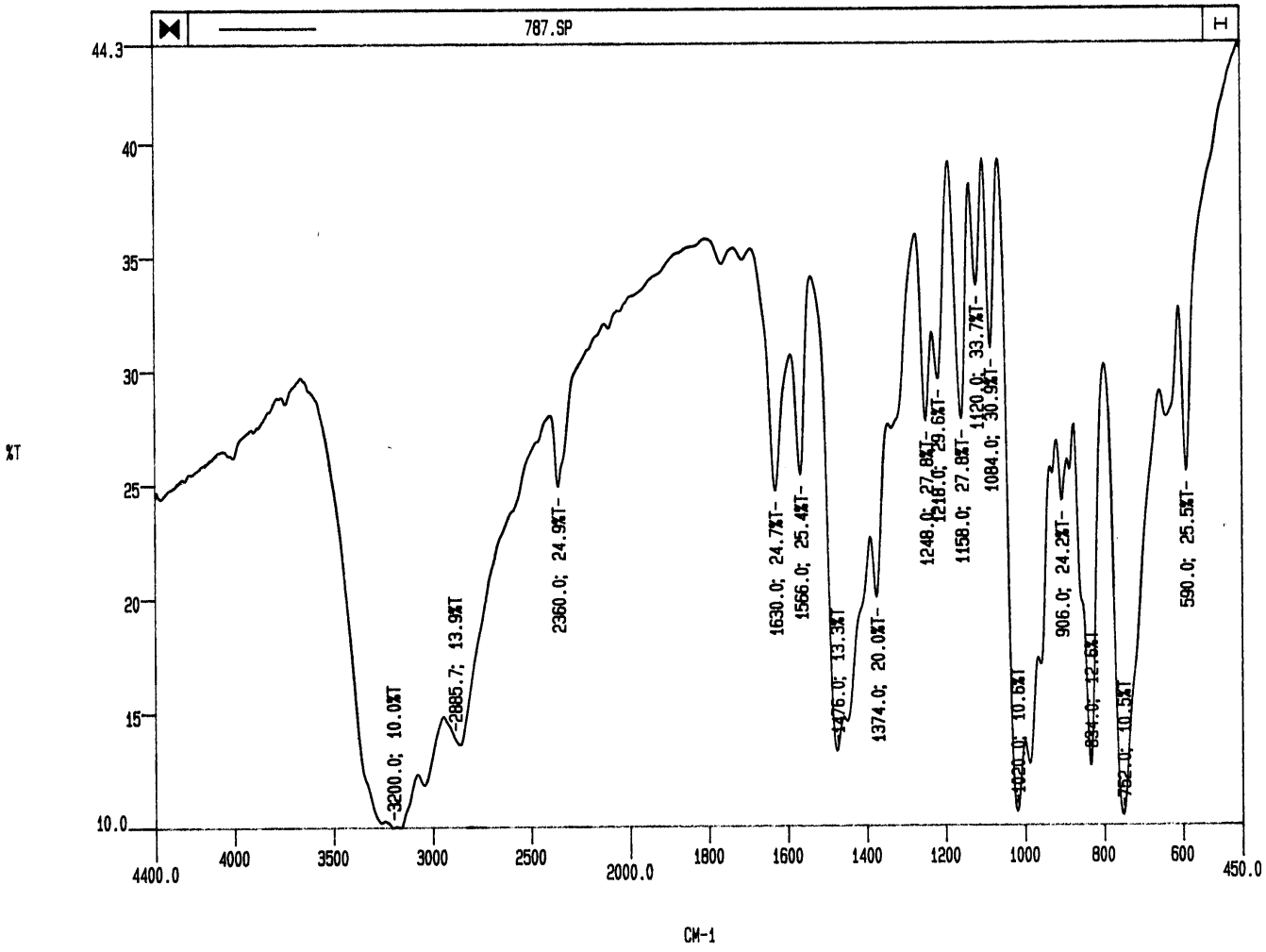

Figure 5.3 IR spectrum of α-furilglyoxime

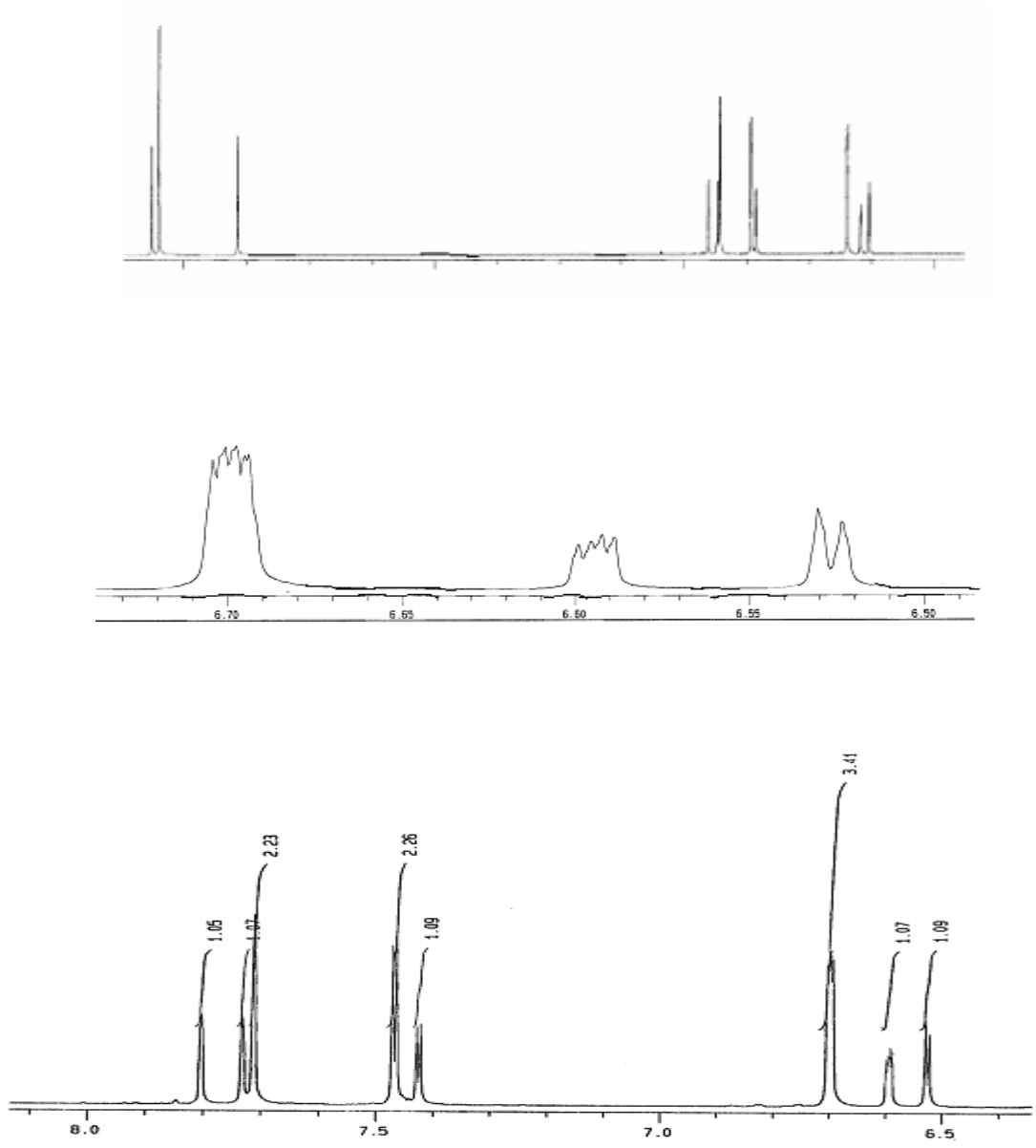

Figure 5.4 ^{1}H NMR of α-furiglyoxime. The middle figure showing two quartets of H_{12} (for more detail see Table 5.1 and Figure 5.6)

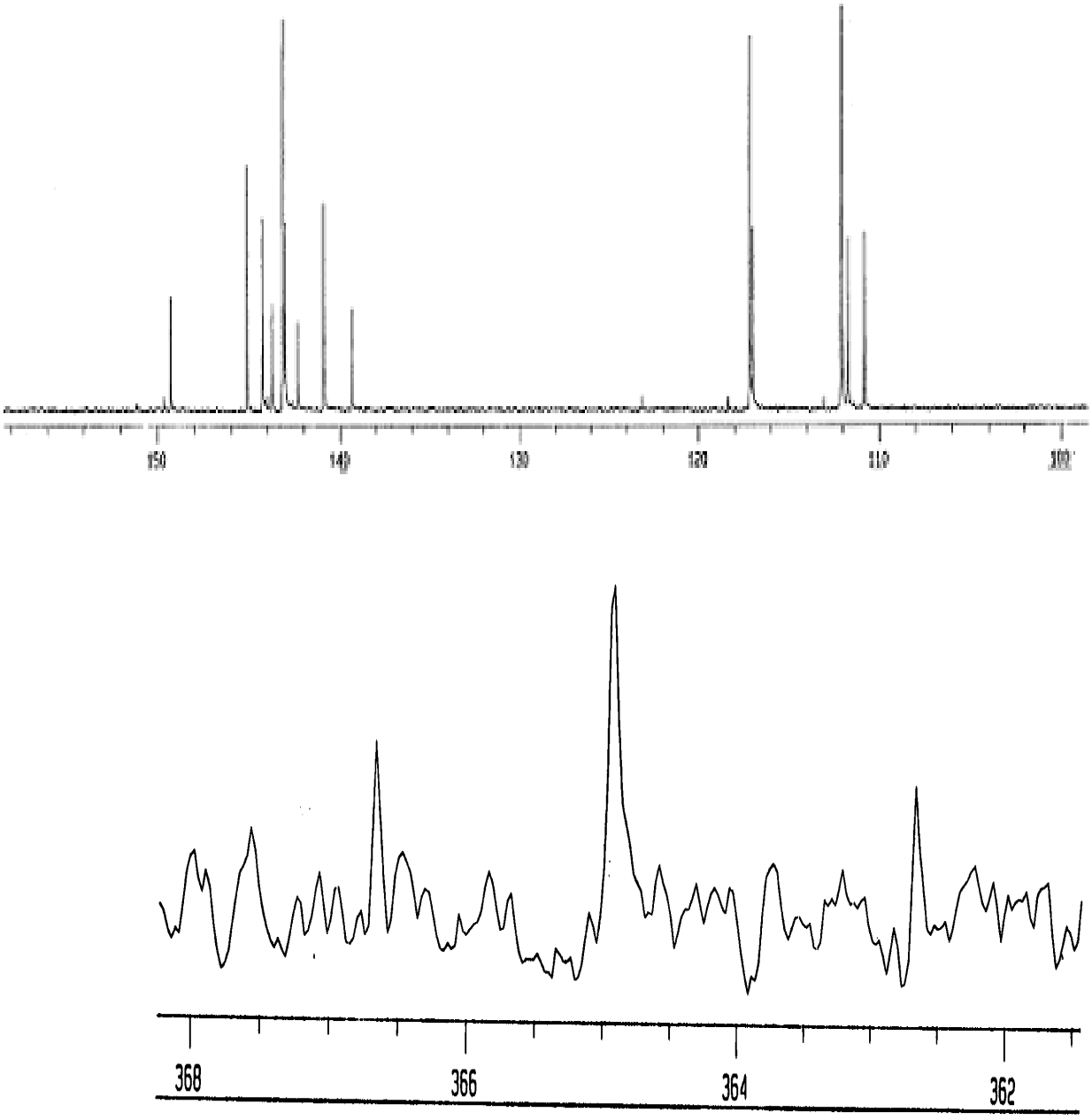

Figure 5.5 ^{13}C (Top) and ^{15}N (Bottom) NMR of α-furiglyoxime. $^{15}NH_4NO_3$ was used as reference for ^{15}N NMR

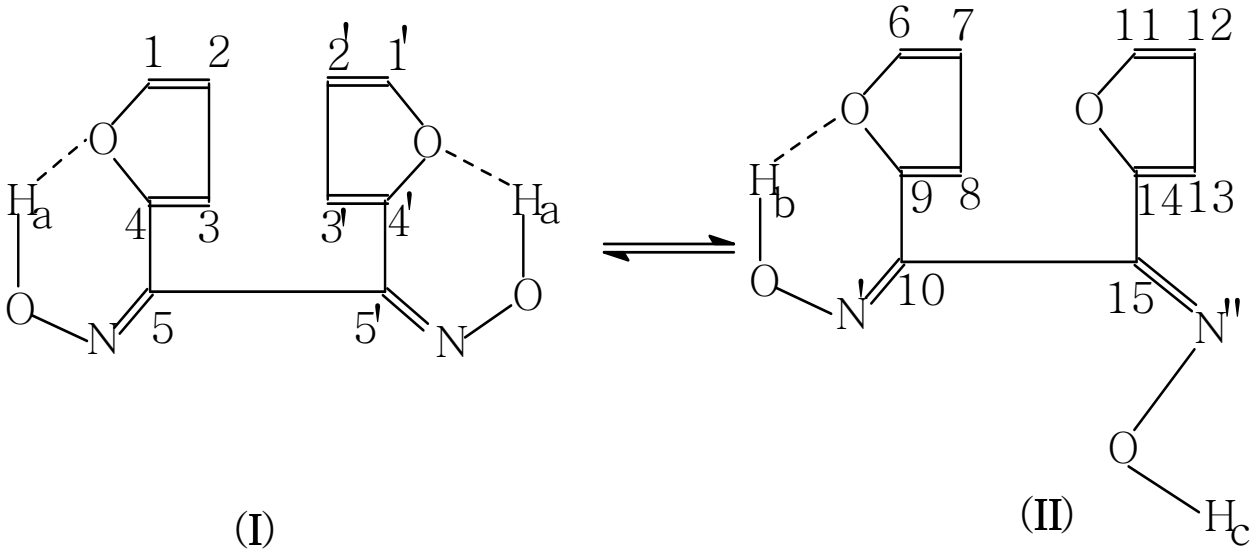

Figure 5.6 Isomers for α-furilglyoxime ligand

The ^{1}H NMR of H_2afdo taken with 1.0 sec pulse delay did not show any quartet. But the ^{1}H NMR spectrum recorded by changing the pulse delay to 5.36 sec was showing two quartet and six doublet peaks. These spectra then were subsequently used to assign the peaks of different kinds of protons in H_2afdo. The integration ratio indicates that three hydrogens are absorbing around 6.70 ppm. Initially this peak was assigned to H_2, H_2' and H_{12}, but after taking COSY spectrum, the H_{12} was replaced by H_7. From the COSY spectrum (Figure 5.7) the peak at 6.53 was assigned to H_{13}. The peaks assignments are shown in Table 5.1.

In ^{13}C NMR we can expect 15 peaks; 5 peaks for structure 1 and 10 peaks for structure 2. For structure 1 (Figure 5.6) the peak intensity should be higher than structure 2. Moreover, those carbon atoms, which are attached to hydrogen atoms are expected to have higher intensity. On the basis of these arguments and considering other electronic factors, the peaks at 112.50, 117.55 and 143.60 have been assigned to {C_2, C_2'}, {C_3,C_3'} and {C_1,C_1'}. The peak assignments are shown in Table 5.2. If we just consider the hydrogen bonding effects along with resonance and inductive effects then C_{15} should have been appeared downfield as compared to C_{10}, while C_9 should appear upfield than C_{14}. The peak assignments in Table 5.2 show that our prediction is valid only for C_9 and C_{14} case, while for C_{15} and C_{10} the order of assignment is reversed. Those carbons, which do not have hydrogen atom attached to them do not show any cross peaks in the spectrum. Therefore, the arrangement of various atoms in the structure of isomer is such that anisotropic effect due to C=N is probably shielding C_{15} more as compared to C_{10}. On the same basis C_6 appears upfield than C_{11}.

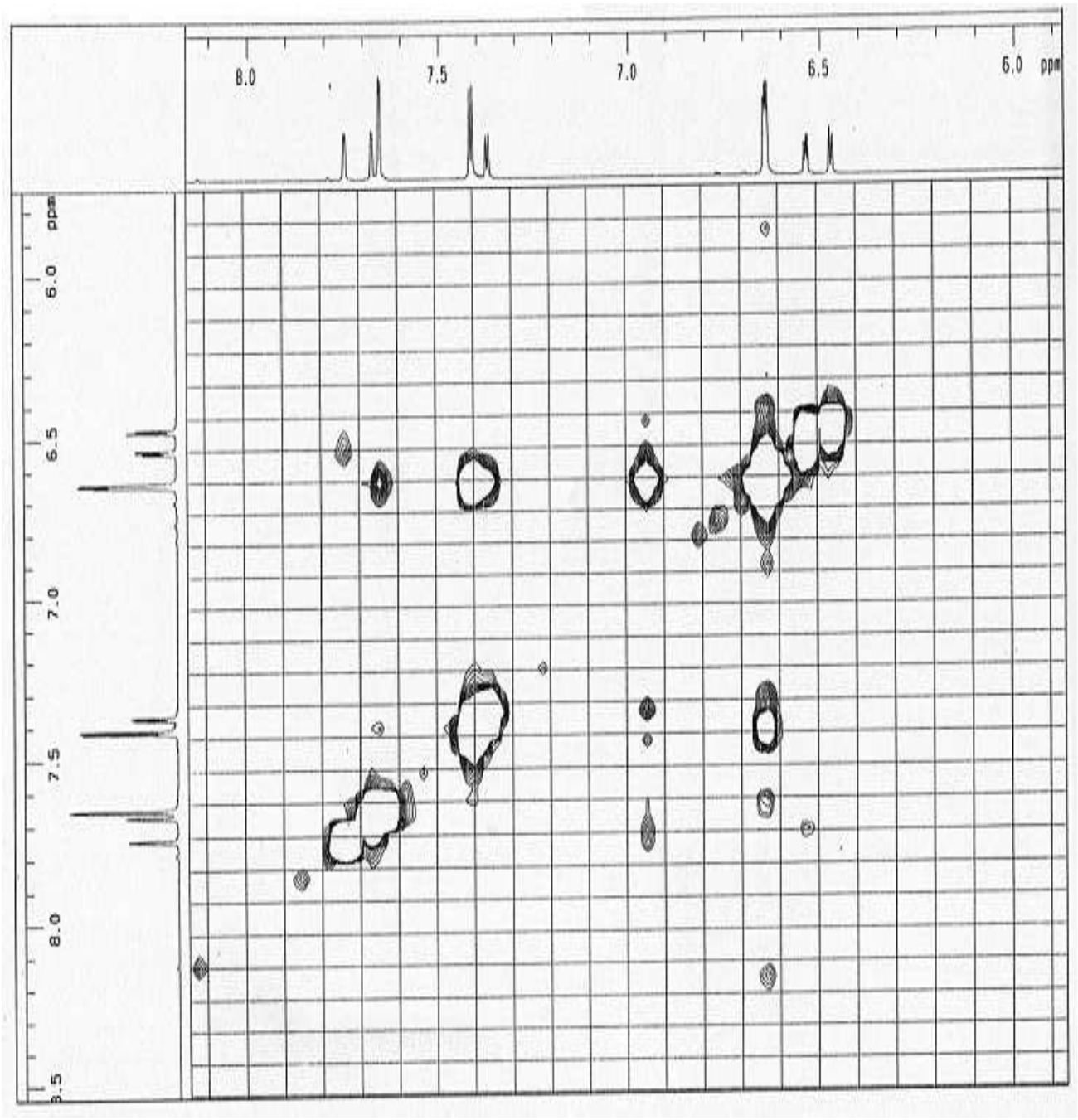

Figure 5.7 COSY spectrum for α-furilglyoxime

Table 5.1 ^{1}H NMR peak assignments for α-furilglyoxime in DMSO-d_6

Identity of Hydrogen	Peak Assignment in DMSO	Multiplicity	Integration Ratio
H_c	12.24	singlet	1.00
H_a	12.19	singlet	1.97
H_b	11.56	singlet	0.88
H_{11}	7.80 – 7.80	Doublet	1.05
H_6	7.73– 7.73	Doublet	1.07
H_1,H_1'	7.71 – 7.71	Doublet	2.23
H_8	7.42 – 7.43	Doublet	1.09
H_2,H_2' H_7	6.69 – 6.70	Quartet	3.41
H_{12}	6.59 – 6.60	Quartet	1.07
H_{13}	6.52 – 6.53	Doublet	1.09

Table 5.2 ^{13}C NMR resonance peak assignments for Carbon atom of ∝-furilglyoxime in DMSO-d_6

Identity of Carbon atom	Peak Position	Identity of Carbon atom	Peak Position
C_{13}	110.82	C_{10}	142.33
C_{12}	111.71	C_6	142.99
C_7, C_2, $C_{2'}$	112.07	C_1, $C_{1'}$	143.13
C_8	116.96	C_9	143.74
C_3, $C_{3'}$	117.13	C_{11}	144.23
C_{15}	139.34	C_4	145.08
C_5, $C_{5'}$	140.90	C_{14}	149.27

In the case of H_2dmg ligand =C appears at 153.2 ppm while C_5, C_{10}, and C_{15} in H_2afdo ligand appears comparatively upfield, which is contrary to electronic factors (-CH_3 is electron donating group and furil group is electron withdrawing group). We believe that due to bulky nature of two furil groups as compared to –CH_3 group rotation of H_2afdo molecule hampers and hydrogen bonding appears. Hence due to this fixing of various atoms in the H_2afdo molecule anisotropic effect appears resulting in shielding of C_5, C_{10}, and C_{15} in H_2afdo ligand and hence appear upfield. The labeling of the ^{13}C peaks is verified by HMBC as shown in Figure 5.8. In HMBC, which provides indirect connection of various atoms in a structure, it is clear that those carbon atoms, which are associated with hydrogen atoms are showing two peaks and the difference of these two peaks represents coupling constant J_{C-H}.

Those carbons, which are not attached with hydrogen show only one peak. A further verification for peak assignments as shown in Table 5.2 comes from HMQC (Figure 5.9), which gives direct connection between hydrogen and carbon atoms as shown in Figure 5.10. The –OH protons in symmetrical H_2afdo ligand appears at 11.36 ppm, indicating that these protons are deshielded due to anisotropic effect of C=N group. The –OH positions for H_2afdo are typical of intramolecular hydrogen bonded β-diketones [127]. These –OH proton appears downfield as compared to H_2dmg protons. This is because of strong intramolecular hydrogen bonding in case of H_2afdo ligand *i.e.* strong six membered intramolecular hydrogen bonding in one isomer, while comparatively weak intramolecular seven membered hydrogen bonding in second isomer. The peaks at 12.25, 12.20, and 11.57 ppm have been assigned to proton c, a, and b respectively. The position of “a” proton is also confirmed from integration ratio, as it was double for proton ‘a’ as

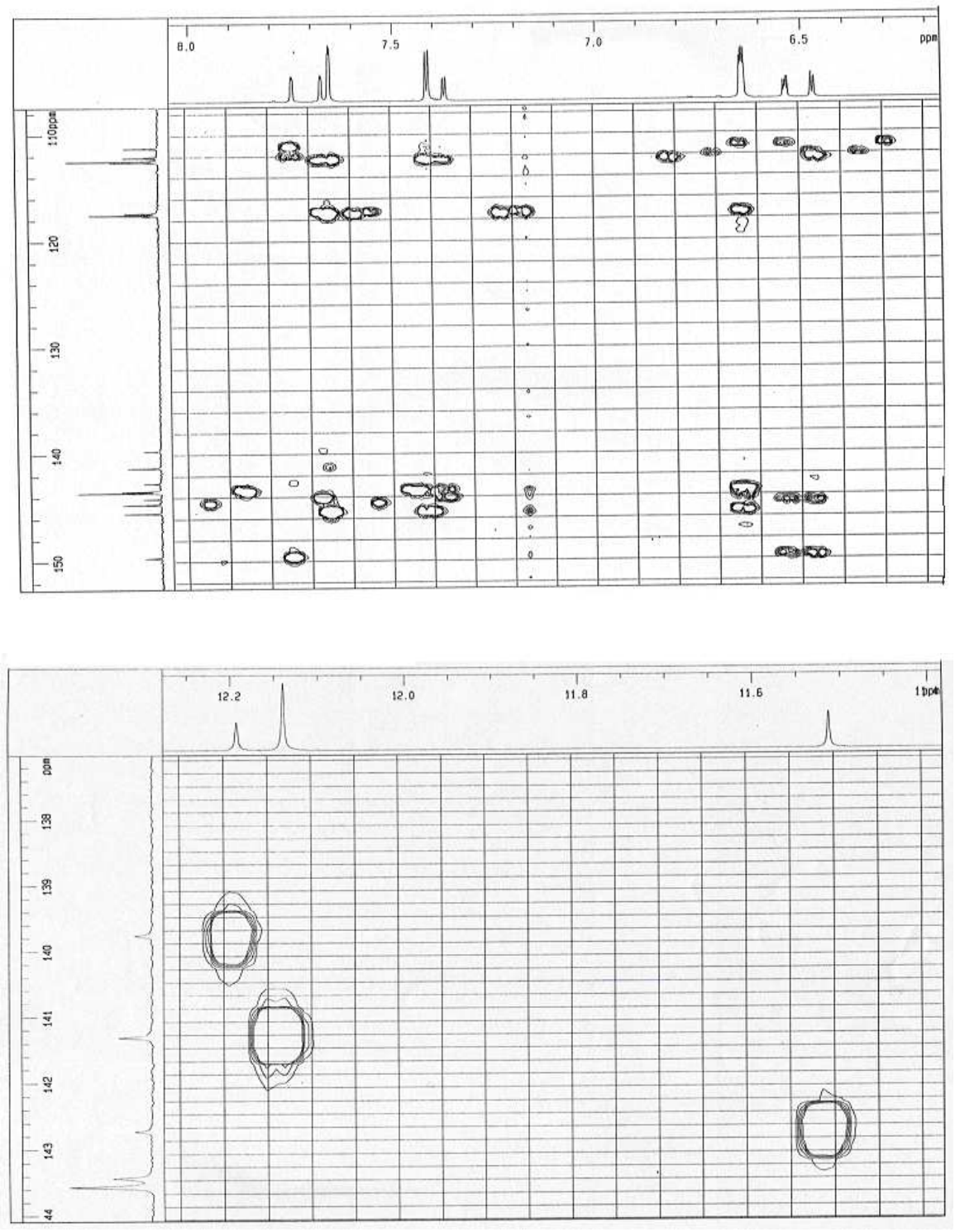

Figure 5.8 HMBC of α-furilglyoxime

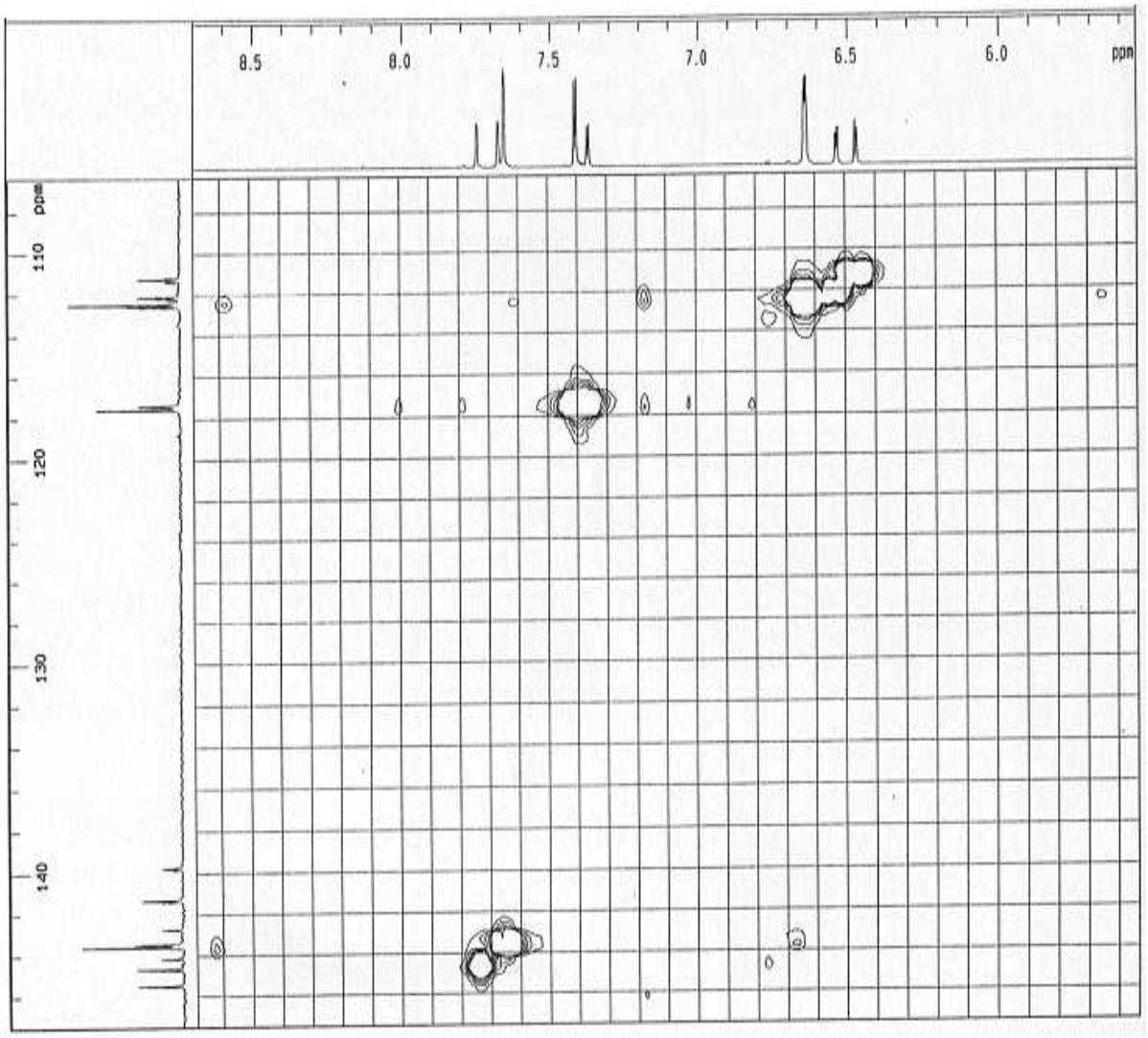

Figure 5.9 HMQC of α-furilglyoxime

compared to “b” and “c” protons, while protons “b” and “c” were assigned through HMBC. Finally, by inspection of integration ratio in ^{15}N NMR, signal at 365.0 has been assigned for nitrogen N in structure 1 of Figure 5.6, while, peaks at 362.5 and 366.5 ppm have been assigned to N’ and N’’ respectively.

5.1.2 Characterization of the Complexes

Proper characterization of the catalysts is also important to understand the electronic factors, which are the potential cause for higher chain transfer constant value (C_s) value of [Co(dmg-2H.BF_2)$_2$] catalyst (**I**) than [Co(afdo-2H.BF_2)$_2$] catalyst (**II**). The broad O-H stretching vibration at 3208 cm^{-1} for free dimethylglyoxime (H_2dmg) ligand is replaced by two sharp peaks at 3600 cm^{-1} and 3530 cm^{-1}, which are due to non hydrogen bonded water molecules at the axial positions of the catalyst. Absence of characteristic infrared bridging OHO hydrogen bonded bending vibration in the region 1680-1790 cm^{-1} [128-129] also indicates that catalyst is bridged with BF_2 at both its ends. The C=N peak at 1364 cm^{-1} for free H_2dmg ligand has shifted to 1386 cm^{-1}. Moreover, there is a significant d_π-$p_{\pi*}$ back bonding due to which C=N character increases with concomitant increase in C=N vibrational frequency. In case of [Co(afdo-2H.BF_2)$_2$] catalyst the two sharp peaks due to water molecules appeared at 3570 and 3628 cm^{-1} (Table 5.3), which indicates that σ-donation of electron from water molecule (ligand) is higher in this complex as compared to catalyst **(1)**. There is more back bonding in case of catalyst **(2)** as compared to catalyst **(1)**. Another indication of comparatively strong back bonding (d_π-$p_{\pi*}$) in catalyst **(2)** is appearance of Co-N stretching vibrations at higher wave

Table 5.3 Peak Assignment for Infrared spectra of ligands and catalyst used for both Thermal and Pulsed Laser Polymerization

Ligand/Catalyst	O-H cm^{-1}	C=N cm^{-1}	N-O cm^{-1}	B-O cm^{-1}	B-F cm^{-1}	Co-N cm^{-1}
H_2afdo	3200B	1566	1248	------	------	------
			1158			
H_2dmg	3208B	1364	1144	------	------	------
[Co(dmg-2H.BF_2)$_2$]	*3530s	1386	1250	1166	1008	464
			1166	820	944	502
	*3600s					
[Co(afdo-2H.BF_2)$_2$]	*3570s	1590	1220sh	1162	1012	504
	*3628s		1126	822	954	542

***** These absorptions peaks are due to water molecules at axial positions.

Table 5.4 Comparison of UV/Vis absorption spectra of [Co(dmg-2H.BF_2)$_2$] and [Co(afdo-2H.BF_2)$_2$] catalysts used for PLP of MMA using AIBN as an Initiator

		Peak 1		Peak 2		Peak 3		Peak 4	
Ligand or complex	Conc. (M)	λ^* (nm)	ε^* $cm^{-1}M^{-1}$	λ (nm)	ε $cm^{-1}M^{-1}$	λ (nm)	ε $cm^{-1}M^{-1}$	λ (nm)	ε $cm^{-1}M^{-1}$
H_2dmg[a]	1.12 x10^{-3}	250	756	-----	-----	-----	-----	-----	-----
H_2afdo[a]	7.49x10^{-4}	264	3250	-----	------	------	------	------	------
[Co(dmg-2H.BF_2)$_2$][a]	9.85x10^{-5}	270 288 (sh)	7310 6500	336 (sh) 310 (sh)	3550 5590	460	1910	------	------
[Co(afdo-2H.BF_2)$_2$][a]	2.73x10^{-5}	272	30040	310 356 (sh)	24400 13190	480	4400	544	7030
[Co(afdo-2H.BF_2)$_2$][b]	5.09x10^{-5}	250	53050	306 352	50100 27700	472	12850	523	17490

[*] These are λ_{max} and ε_{max} values.

[a] Solvent is DMSO.

[b] Solvent is acetone.

numbers (504 & 542 cm^{-1}) as compared to catalyst **(1)**, which appear at lower wave numbers (464 & 502 cm^{-1}) [130]. Table 5.3 incorporates summary of IR peaks. The π-π^* transitions of typical cobaloxime is observed at 250 and 264 nm in H_2dmg and H_2afdo free ligands.

From the data in Table 5.4 it is important to note that ligand to metal charge transfer transitions (LMCT) in both the complexes is almost at the same wavelength i.e. 270 nm. According to the selection rules, which are used to differentiate between charge transfer transition and ligand transfer transition (d-d transition) [131], we can assign transitions from 460-545 nm in both the complexes as metal to ligand charge transfer (MLCT) transitions. However, metal to ligand charge transfer (MLCT) transition in complex **(2)** takes place at lower energy and with more transition probability (ε value). This observation further substantiates the understanding that due to extensive conjugation in catalyst **(2)** there is strong d_{π}-p_{π^*} transition probability, resulting in less availability of unpaired electron in catalyst **(2)** and thus reducing its performance to act as a chain transfer agent. The results of UV/Vis absorptions are summarized in Table 5.4 and are in agreement with previously reported values for catalyst (1) and (2) [84,126].

5.2 Thermal Polymerization

5.2.1 Polymerization of MMA using Benzoyl Peroxide (BPO) as an Initiator at 70.0 and 80.0 °C

Using similar concentration of benzoyl peroxide, MMA was polymerized for different intervals of time. The results for polymerization at 70.0 °C are shown in Tables 5.5 – 5.6 and Figure 5.10. These Tables indicate that there is a propensity for increase in

Table 5.5 Polymerization of MMA at 70.0 °C (Run #1)

Time (min.)	Conversion (%)	M_n	M_w	PDI
15	3.06	212241	391235	1.84
30	7.50	190511	394988	2.07
45	10.13	181401	366422	2.02
60	11.86	202260	402942	1.99
75	13.39	98752	139832	1.42

Table 5.6 Polymerization of MMA at 70.0 °C (Run #2)

Time (min.)	Conversion (%)	M_n	M_w	PDI
15	3.11	126257	178899	1.42
30	4.99	168665	290796	1.72
45	8.50	205076	337107	1.64
60	9.09	219790	336063	1.53
75	17.13	204557	318441	1.56
90	27.63	179967	313671	1.74

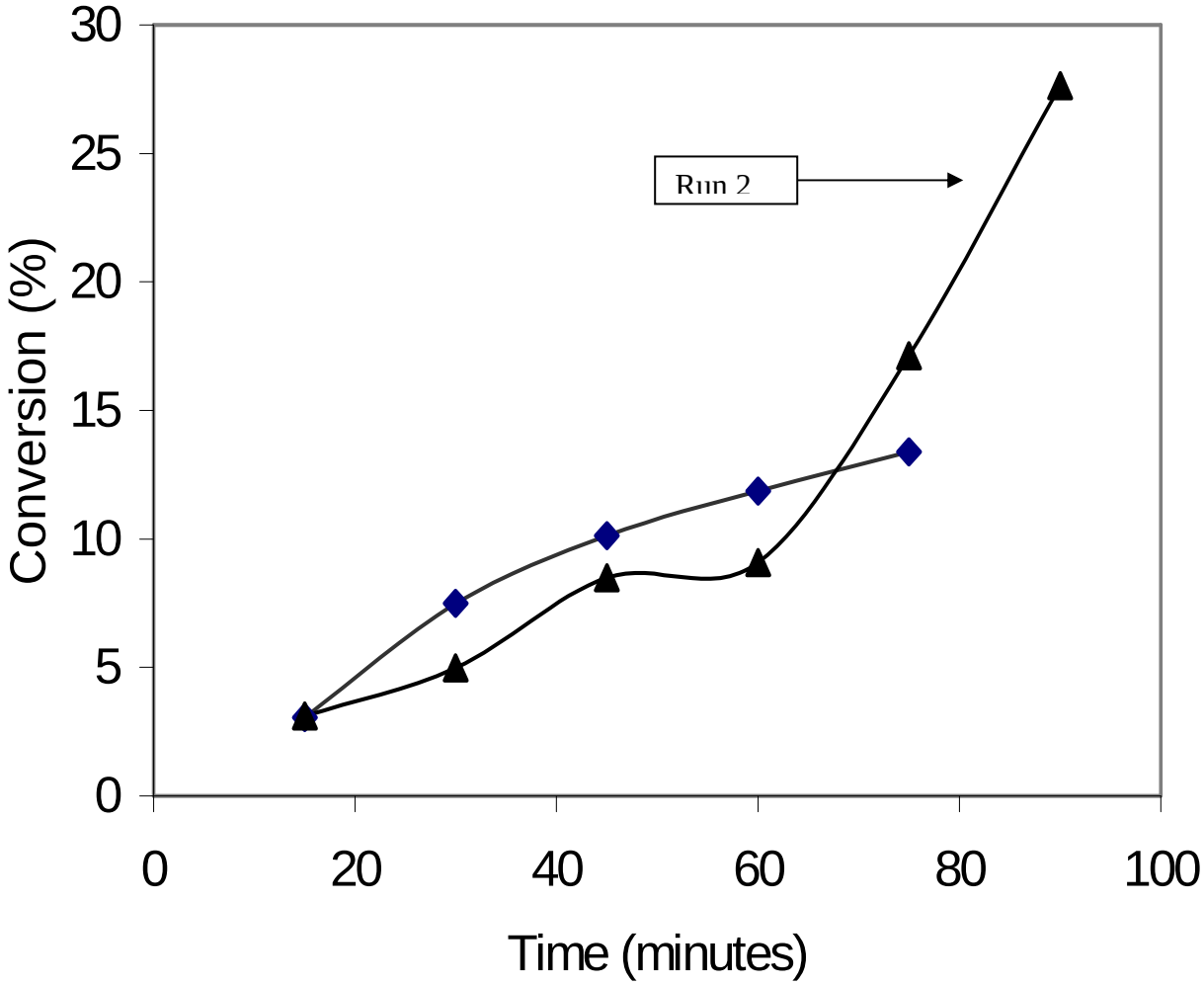

Figure 5.10 Graph between Percent Conversion and Time for Polymerization of MMA at 70 °C using BPO (4.13×10^{-3} M) as initiator

percent conversion with time for free-radical polymerization of MMA at 70 °C. As evident in This abrupt increase in percent conversion is more evident at 80 °C (Table 5.7), and is probably due to gel effect (Figure 5.11). An understanding of this behavior requires that termination is diffusion-controlled reaction best described as proceeding by three-step process [132-134] as discussed below.

1. Translational diffusion of two propagating radicals until they are in close proximity to each other:

$$M_n^{\bullet} + M_m^{\bullet} \underset{k_2}{\overset{k_1}{\rightleftharpoons}} [\, M_n^{\bullet} \text{-----} M_m^{\bullet} \,] \qquad (5.1)$$

2. Rearrangement of the two chains so that the two radical ends are sufficiently close for chemical reaction, which occurs by segmental diffusion of the chains.

$$[\, M_n^{\bullet} \text{-----} M_m^{\bullet} \,] \underset{k_4}{\overset{k_3}{\rightleftharpoons}} [\, M_n^{\bullet} / M_m^{\bullet} \,] \qquad (5.2)$$

3. Chemical reaction of two radical ends.

$$[\, M_n^{\bullet} / M_m^{\bullet} \,] \xrightarrow{k_c} \text{dead polymer} \qquad (5.3)$$

Table 5.7 Results for Polymerization of MMA with BPO at 80.0 °C

Time (min.)	Product (gram)	Conversion (%)	M_n	M_w	PDI
15	0.2888	6.17	178839	270323	1.51
30	0.6724	14.37	162379	259996	1.60
45	0.8476	18.11	172618	258909	1.50
60	1.9972	42.68	154304	242118	1.57
45 C*	0.1219	2.60	---------	---------	-----

- The sample having no initiator.

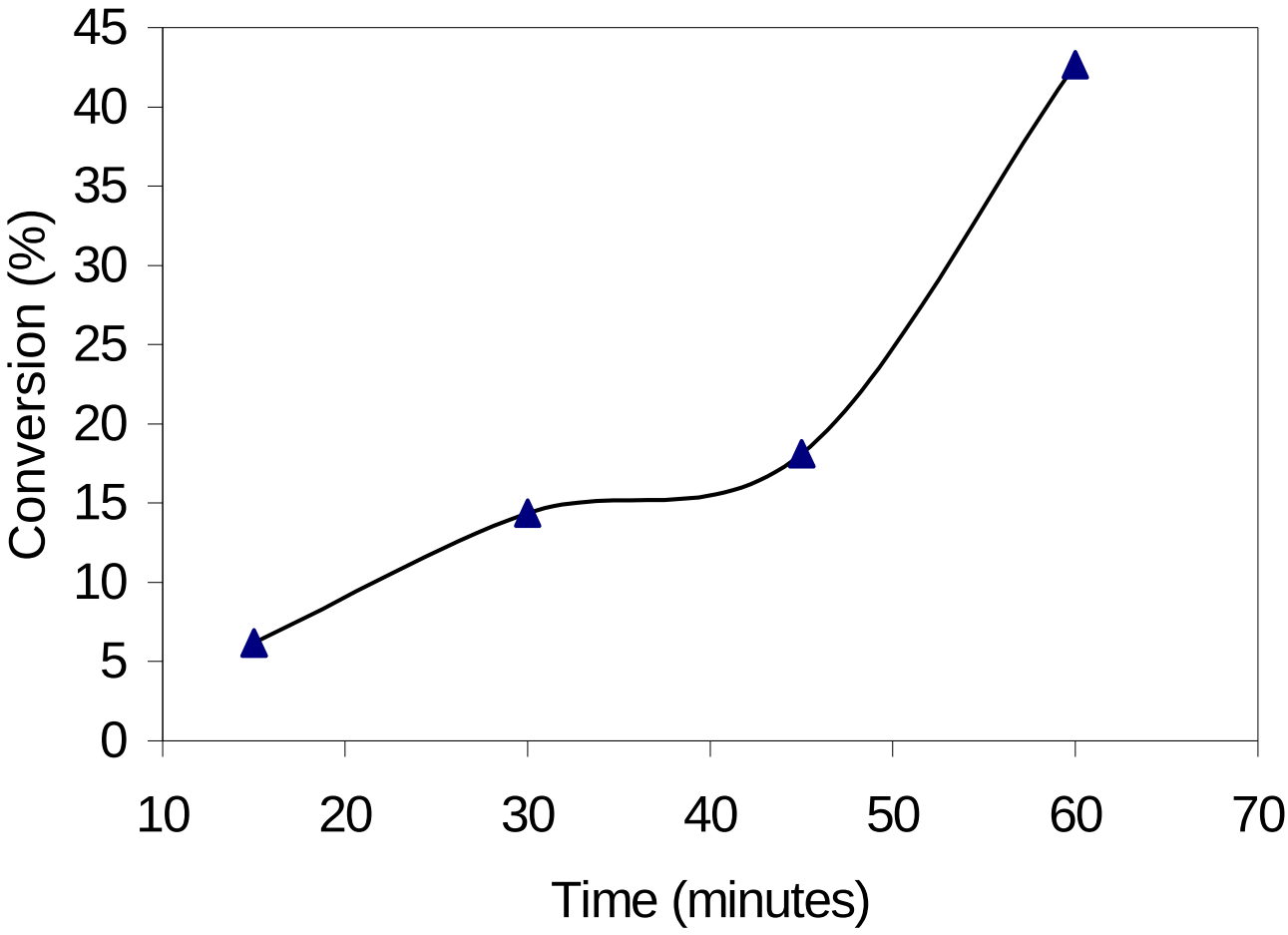

Figure 5.11 Polymerization of MMA at 80 °C using BPO (4.13×10^{-3} M) as initiator

Theoretical considerations indicate that k_c would be very large, about 8 x 10^9 liters/mole-sec, especially in bulk polymerization (where low viscosity prevails) for the reaction

$$R_t = \frac{k_1 k_3 [M^\bullet]^2}{k_2 + k_3} \qquad (5.4)$$

between two radicals. On the other hand experimentally determined k_t values for radical polymerizations are considerably lower, usually by two orders of magnitude or more. Thus diffusion is the rate determining process for termination, and under such conditions $k_c >> k_4$ one can obtains

For the case of slow translational diffusion, $k_3 >> k_2$, and

$$R_t = k_1 [M^\bullet]^2 \qquad (5.5)$$

For the case of slow segmental diffusion, $k_2 >> k_3$, and

$$R_t = \frac{k_1 k_3 [M^\bullet]^2}{k_2} \qquad (5.6)$$

Thus experimentally observed termination rate constant k_t corresponds to k_1 and $k_1 k_3/k_2$ respectively, for the two limiting situations.

With increasing conversion (Table 5.5 and Table 5.6) segmental diffusion of the radical end out of the coil to encounter another radical, is increased. Simultaneously, the increasing polymer conversion decreases translational diffusion as the reaction medium

becomes more viscous and, at sufficiently higher concentrations, the polymer radicals becomes more crowded and entangled with each other. Chain entanglement leads to a faster decrease in translational diffusion relative to the decrease with increasing viscosity. So as the polymerization proceeds the viscosity of the system increases with the subsequent chain entanglement and termination becomes increasingly slower. This is the cause of gel effect, which is noticeable in Figure 5.11 and to some extent in Run 2 Figure 5.10. Although propagation is also hindered, the effect is much smaller, since k_p values are smaller than k_t values by a factor of 10^4-10^5. Termination involves the reaction of two large polymer radicals, while propagation involves the reaction of small monomer molecules and only one large radical. High viscosity affects the former much more than the latter. Therefore, the quantity $k_p/k_t^{1/2}$ in equation 5.7 increases and the result in accordance to equation 5.7 ia an increase in R_p with conversion.

$$R_p = k_p [M] \left(R_i / 2k_t\right)^{1/2} \qquad (5.7)$$

Hayden and Melville [135] also reported that k_p is relatively unaffected until 50% conversion for polymerization of MMA, whereas, k_t has decreased by almost two orders of magnitude in the same span.

A second consequence of increase in percent conversion with increase in R_p is an increase in molecular weight as shown by equation 5.8.

$$\nu = R_p / R_t \qquad (5.8)$$

where ν is called kinetic chain length. Table 5.5 and 5.6 indicate that up to certain extent weight-average molecular weight M_w increases (as required by equation 5.8), and then surprisingly decreases (Figure 5.12). Actually, in Bulk polymerization local hot spots may occur (due to absence of any solvent, which can dissipate the heat of polymerization)-resulting in degradation of polymer and a broadened molecular-weight distribution due to chain transfer to polymer. However at 80 °C M_w is continuously decreasing with time as shown in Figure 5.12. This again indicates rise of some local

$$\ln \overline{X}_n = \ln \left[\frac{A_p}{(A_d A_t)^{1/2}} \right] + \ln \left[\frac{[M]}{(f[I]^{1/2})} \right] - \frac{E_{\overline{X}_n}}{RT} \qquad (5.9)$$

temperature (hot spots) resulting in degradation of polymer. By comparing Table 5.6 and Table 5.7 it is clear that at 80 °C both M_w and M_n are lower than at 70 °C. This is in accordance with equation 5.9.

where, X_n is degree of polymerization and E_{Xn} is overall activation energy for the degree of polymerization and has a value of about –60 kJ/mole and is sum of the following terms:

$$E_{\overline{X}n} = E_p - (E_d/2) - (E_t/2) \qquad (5.10)$$

where, E_p, E_d, and E_t are activation energies for propagation, initiator dissociation, and termination reactions, respectively. Equation 5.9 shows that degree of polymerization

(and thus the number average molecular weight M_n) decreases with increasing temperature. This is the reason that in our study for polymerization of MMA at 80 °C both M_w and M_n are lower than at 70 °C.

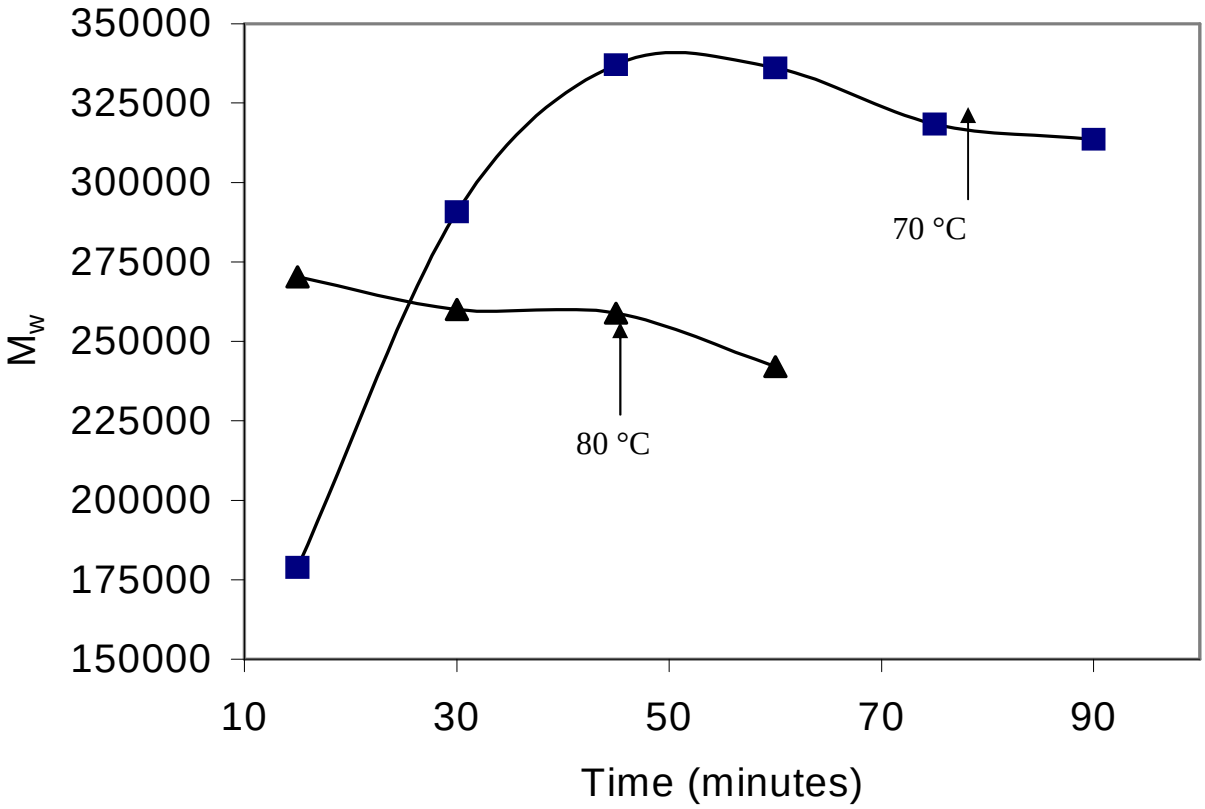

Figure 5.12 Comparison of M_w Values at 70 and 80 °C using BPO as Initiator

In Table 5.7 the control sample (without initiator) indicates 2.6 percent conversion even in the absence of initiator. This indicates self-initiated polymerization. The initiation and overall activation energies for a purely thermal self-initiated polymerization are approximately same as for initiation by the thermal decomposition (120-150 KJ/mole) of an initiator. However, purely thermal polymerizations proceed at very slow rates because of the low probability of initiation process values (10^4-10^5) of the frequency factor. Lingnau and Meyerhoff [136-137] proposed the initiation mechanism (Scheme 5.1) for self-initiated polymerization for methyl methacrylate and appears to involve the initial formation of a biradical by reaction of two monomer molecules followed by hydrogen transfer from some species in the reaction system to convert the biradical to a monomer radical. But Lehrle and Shortland [138] reported that most but not all of the previously reported self-initiated polymerization was caused by adventitious peroxides that were difficult to exclude by the usual purification techniques.

5.2.2 Copolymerization of Methyl acrylate and Styrene for 90 minutes at 70 ^{0}C

The purpose of this copolymerization without using chain transfer agent is just to get basic data and to develop the understanding for the copolymerization. The results are presented in Table 5.8. These results indicate that as moles percent of MA increases percent conversion increases. We can also note that both M_n and M_w also increase with increase in moles of MA. The last sample, which does not contain styrene monomer, has shown a very high percent conversion (89 %). Thus these results indicate that rate of polymerization increases with increase in moles percent of MA.

Scheme 5.1 Mechanism for Self-initiated polymerization in MMA

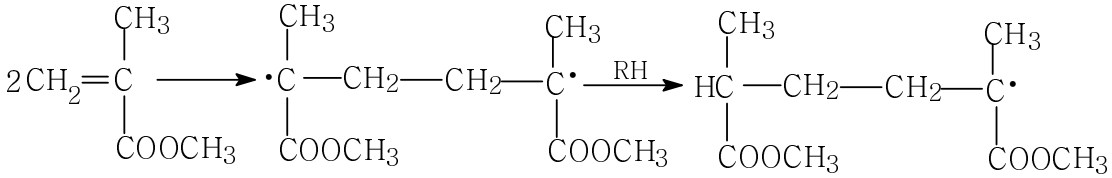

Table 5.8 Results for the Copolymerization of Styrene and Methyl acrylate at 70 °C using AIBN as an Initiator

STY (Moles) x 10^{-2}	MA (Moles) x 10^{-2}	Conver. (%)	M_n	M_w	PDI
3.49	1.11	10.47	101285	167130	1.6501
2.62	2.22	14.97	104341	186321	1.7857
1.74	3.33	17.77	117118	192372	1.7498
0.0872	4.45	22.42	135909	231963	1.7067
-------	5.56	88.60	--------	---------	------

5.2.3 Copolymerization of Methyl methacrylate and Methyl acrylate in the presence of [Rh(afdo-2H.BF_2)$_2$]Cl using AIBN as an Initiator

This copolymerization was conducted at 60 °C for a total duration of 90 minutes. The composition of the monomers in the feed is shown in Table 5.9 and results are shown in Table 5.10 From the results it is clear that there is a regular trend of increase in the molecular weight with the composition variation of the monomers. As percent composition of the Methyl acrylate monomer increases in the feed copolymer composition, molecular weight also increases. The increasing trend in molecular weights with increase in molar ratio of MA is even more clear in peak molecular weight (M_p) [Figure 5.13] than number average molecular weight (M_n). However, we have already noted for the polymerization of MMA (section 5.2.5) that polydispersity index values are lower in the presence of Wilkinson's catalyst indicating living polymerization. In the copolymerization, the same trend has been observed. Therefore, living polymerization takes place in the presence of [Rh(afdo-2H.BF_2)$_2$]Cl catalyst. Thus, [Rh(afdo-2H.BF_2)$_2$]Cl catalyst increases the living polymerization characters and the mode of action, probably is similar to Wilkinson's catalyst. Kameda and co-workers [139] reported the polymerization of MMA in the presence of $RhCl(CO)(PPh_3)_2$ and dihydrido (1,3 diphenyltriazeno) bis triphenylphosphine) rhodium(III) complexes. However, the monomer conversion never exceeded 25%, and the recovered polymer was poorly analyzed.

Table 5.9 Different molar ratios of Monomers for the Copolymerization of Methyl methacrylate and Methyl acrylate at 60 °C

Sample #	MMA (ml)	MA (ml)	MMA (moles)	MA (moles)	Molar ratio (MA/MMA)	catalyst (ppm)
1	5.0	0.0	0.0468	0	0	200
2	4.5	0.5	0.0421	0.0048	0.114	180
3	4.0	1.0	0.0374	0.0096	0.257	160
4	3.0	2.0	0.0281	0.0191	0.680	120
5	2.0	3.0	0.0187	0.0287	1.535	80
6	1.0	3.0	0.0094	0.0287	3.053	50

Table.5.10 Molecular weight distribution for the Copolymerization of Methyl methacrylate and Methyl acrylate at 60 °C

Sample #	M_p	M_n	M_w	M_z	M_{z+1}	PDI
1	149825	96777	150984	193480	226402	1.56
2	163228	120126	133151	146242	157988	1.11
3	172824	120461	158342	199100	248041	1.31
5	177831	121417	162379	213892	278718	1.34
6	190992	122541	169603	214120	255521	1.38

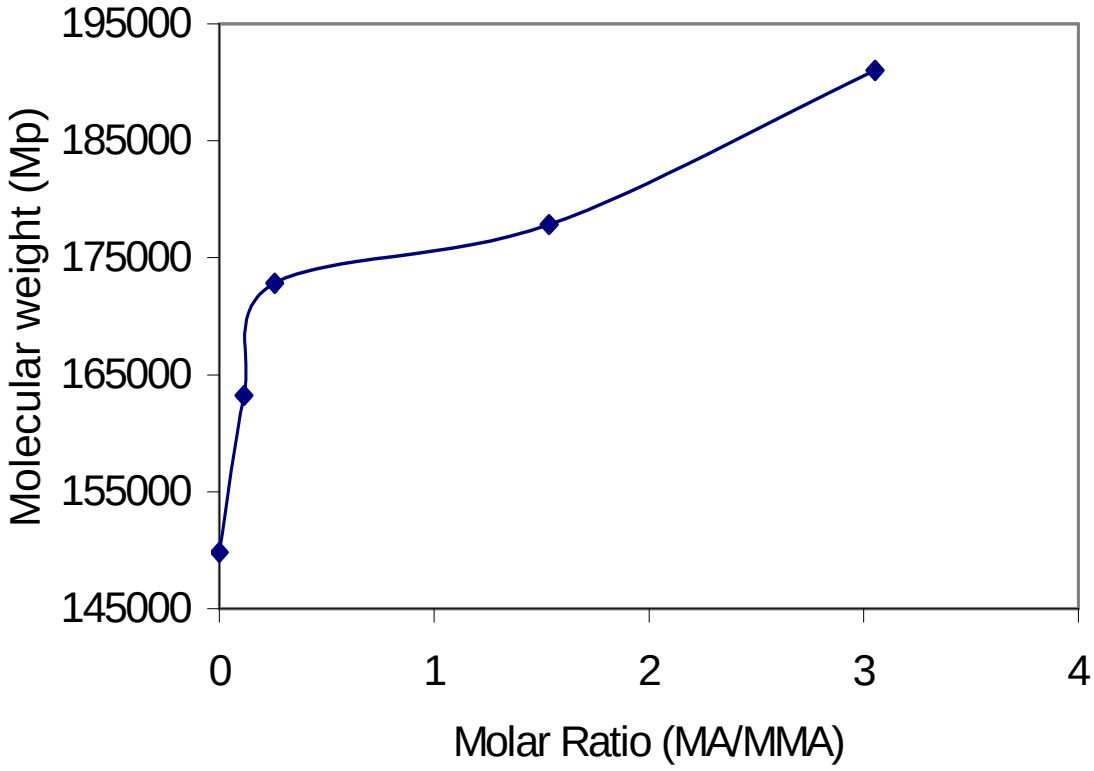

Figure 5.13 Graph between Molar Ratio of MA/MMA and Peak Molecular Weight for copolymerization of MA and MMA at 60 °C

5.2.4 Polymerization of MMA at 60 °C for 75 minutes in presence of [Rh(afdo-2H.BF_2)$_2$] Cl Catalyst and AIBN as an Initiator

Results of polymerization at 60 ºC are given in Table 5.11. The results are erratic but overall there is increase in molecular weight with increase in concentration of the catalyst. Therefore, like other reported rhodium complexes [139] in literature, our [Rh(afdo-2H.BF_2)$_2$]Cl catalyst also promotes the polymerization process.

5.2.5 Polymerization of Methyl methacrylate at 60 °C in the presence of Wilkinson's catalyst [Rh(PPh_3)$_3$Cl] and AIBN as an Initiator

Before starting the results and discussion for the polymerization, a very brief literature review about polymerization reactions in the presence of rhodium complexes is given here to help in understanding the results for polymerization of Methyl methacrylate in the presence of Wilkinson's catalyst. Sawamoto et al [140-141] were the first to report on controlled radical polymerization of vinyl monomers on the basis of Kharasch addition reaction. They coined the name "atom- transfer radical polymerization" [ATRP] for the mechanism of this polymerization. In the 1970s Kameda and co-workers [139] reported on the polymerization of MMA in the presence of some rhodium complexes. Wilkinson's catalyst [RhCl(PPh_3)$_3$] is known to be active in the Kharasch addition reaction i.e by ATRP. Percec et al [142] previously reported the styrene polymerization by ATRP using Wilkinson's catalyst.

Table 5.11 Results for the Polymerization of MMA in the presence of [Rh(afdo-2H.BF_2)$_2$] Cl catalyst

catalyst (ppm)	M_n	M_w	PDI
0	169692	312710	1.84
80	178626	352018	1.97
160	171605	345913	2.01
240	201057	368200	1.83
320	184767	353508	1.91

This group indicated that both Polydispersity Index value (M_w/M_n) and the rate of polymerization decreases with the increase in catalyst concentration. The results for percent conversion as a function of catalyst concentration in our investigation is presented in Table 5.12, which indicates that both percent conversion and molecular weights for polymerization of MMA increases with the catalyst concentration. Therefore, Wilkinson's catalyst behaves oppositely to chain transfer agents (which decreases the percent conversion) and we can say that this [$RhCl(PPh_3)_3$] catalyst acts as promoter for polymerization of Methyl methacrylate.

The data in Table 5.12 also incorporates different molecular weights determined by GPC. Like Percec [142], our results also indicates that in the absence of Wilkinson's catalyst PDI value is 1.98, while with addition of 0.60 ppm of catalyst PDI value dropped to 1.26. Even for all other samples this value of PDI stayed around 1.5, and is well below 1.98. Figure 5.14 indicates (overall) linearity of plot of Molecular weight versus percent conversion, which indicates lack of transfer reactions. It should be noted that Methyl methacrylate shows living free-radical polymerization, which is evident from low polydispersity index values. This observation is in accordance with previous findings of Moineau and co-workers [143]. This research group concluded that, "although the Wilkinson's catalyst is less efficient than the Sawamoto and Matyjaszewski systems in terms of polymerization kinetics, it allows MMA to be polymerized in a living manner at a temperature as low as 60 °C and in the absence of any Lewis acid".

Table 5.12 Data for Molecular weights and Polydispersity index values for the Polymerization of MMA in the presence of Wilkinson's Catalyst at 60 °C for 90 minutes

Wilkinson's catalyst (ppm)	Conver. %	M_w	M_n	M_z	M_p	PDI
0	5.50	226222	114151	336799	260777	1.98
0.60	5.68	202680	161390	241621	239020	1.26
1.15	6.14	209701	129634	272479	246063	1.62
2.14	6.56	221304	142980	281666	280413	1.55
5.02	6.77	258070	168803	377606	225533	1.53
144.44	-----	324021	242192	410933	278385	1.34

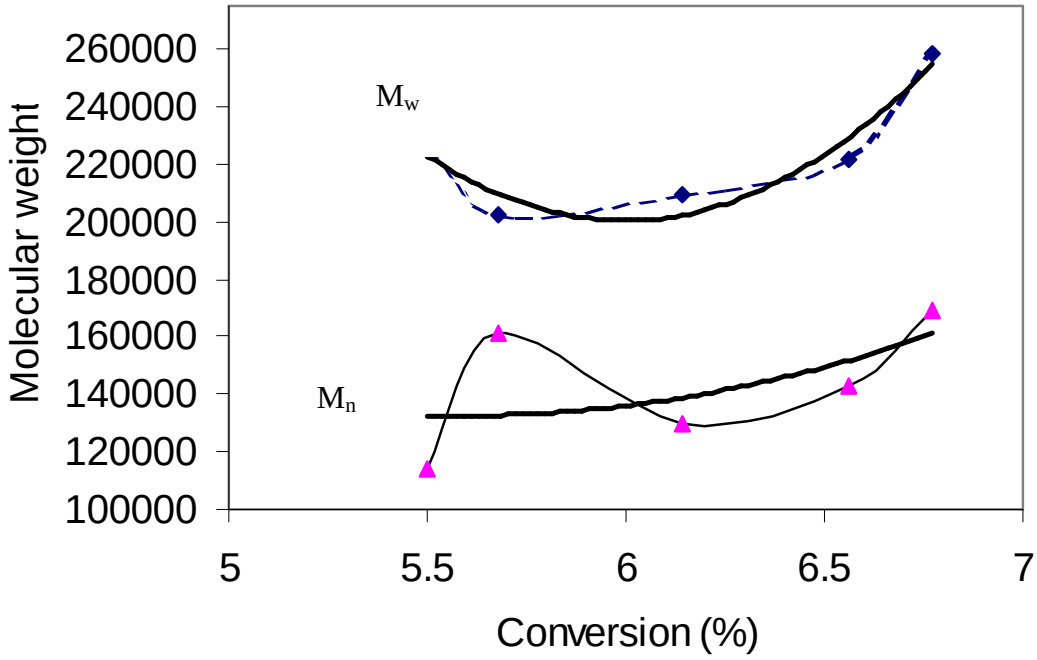

Figure 5.14. Graph between percent conversion and molecular weight for the Polymerization of MMA using Wilkinson's Catalyst at 60 ^{o}C

It is important to note that Moineau and co-workers investigated the effect of Wilkinson's catalyst by using 2,2'- dicholoroacetophenon in the presence of the Wilkinson's catalyst (plus 7 equivalent of PPh_3) in THF (as solvent) at 60 °C.

In contrast, we have not used any solvent and moreover, we have used AIBN as initiator too. ^{1}H NMR results indicate that the polymerization mechanism in the presence of Wilkinson's catalyst is free-radical in nature since the PMMA tacticity (typically rr:rm:mm = 64:32:4) is equivalent to the tacticity known for a radical-polymerization i.e. atactic polymer has formed. For more discussion on ^{1}H NMR results see under PLP in the presence of Wilkinson's catalyst (section 5.7.2). We propose the Scheme 5.2 for living–radical polymerization in the presence of Wilkinson's catalyst. There is also possibility for dissociation of one of the ligand from the Wilkinson's catalyst and then the bond formation process between the growing polymer chain and the Wilkinson's catalyst. However, we believe that this bond formation between Rh-R_n is not stable enough to help β-elimination to produce the dead polymer chain. Instead this bond formation is reversible and thus indicates living free–radical polymerization.

5.2.6 Polymerization of Styrene at 60 °C in the presence of [Co(dmg-2H.BF_2)$_2$] Chain Transfer Agent

The total duration of polymerization for each sample was 150 minutes and results are presented in Figure 5.15 and Table 5.13. Figure 5.15 indicates that there is propensity for decrease in percent conversion with increase in [Co(dmg-2H.BF_2)$_2$] chain transfer agent.

Scheme 5.2 Proposed Living Free-radical Polymerization of MMA at 60 °C in the presence of Wilkinson's Catalyst

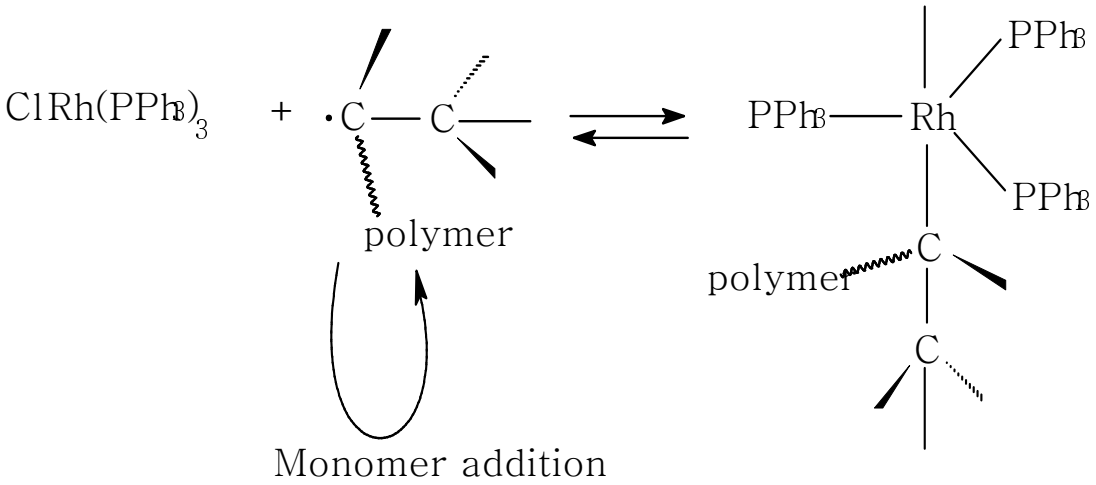

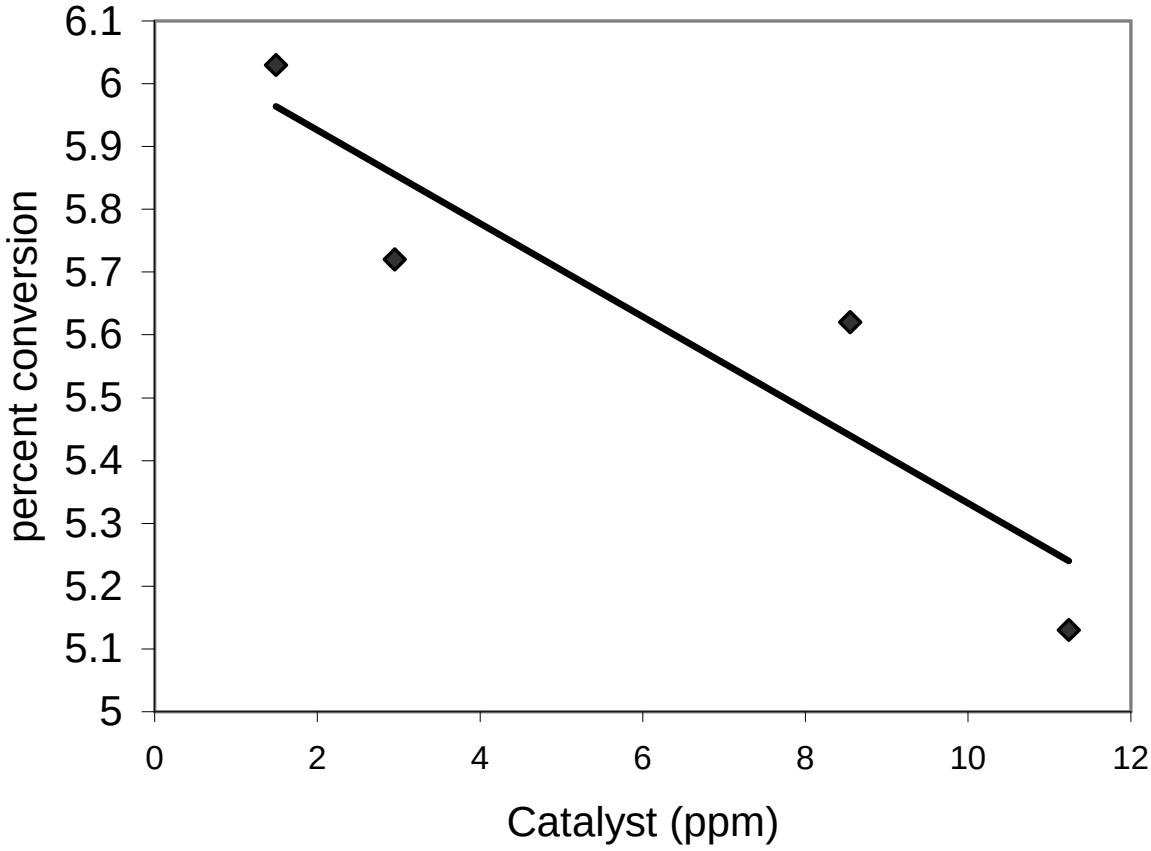

Figure 5.15 Graph indicating dependence of percent conversion on catalyst concentration for Polymerization of Styrene at 60 °C using [Co(dmg-2H.BF_2)$_2$] as Chain Transfer Agent

Table 5.13 Different parameters used to calculate the value of Chain Transfer Constant from Mayo plot using M_v values

[catalyst] x 10^6	[catalyst]/[monomer] x 10^7	M_v	DP_v	$1/DP_v$ x 10^4
3.53	4.10	138300	1329.8	7.52
7.01	8.15	120900	1162.5	8.60
20.3	16.0	93100	895.2	11.17
26.7	23.6	88100	847.1	11.81

Table 5.13 indicates that when catalyst concentration is increased from 3.53 ppm to 7.01 ppm it's viscosity average molecular weight decreases from 138,300 to 120,900. Chain transfer constant value was calculated by using Mayo plot and this value comes out to be 230, which is an order of three lower than reported in literature. This C_s value however, is more reliable when calculated from GPC. This lower value of C_s for styrene in general is due to the absence of β-protons required for β-elimination needed to complete the transfer process.

5.2.7 Polymerization of Styrene at Higher Temperatures using [Co(afdo-2H.BF_2)$_2$] as Chain Transfer Agent

Styrene was polymerized at 60, 70, and 80 °C using AIBN as initiator and [Co(afdo-2H.BF_2)$_2$] as chain transfer agent. The results for polymerization at 60 °C are shown in Table 5.14 indicating that both Run 1 and Run 2 have comparable results. The M_n decreases sharply with catalyst concentration initially but above 80 ppm the decrease is much slower. M_w also shows the same propensity. In both Run 1 and Run 2 Polydispersity index (PDI) values first increase and then there is a decrease in the values. The increase in PDI values probably indicates dominant chain transfer catalysis. The decrease in PDI values may be due to decrease of solution viscosity of the polymer resulting in increase of chain transfer ($k_{tr's}$) to catalyst. Table 5.15 indicates that the decrease in both M_n and M_w at 70 and 80 °C is not significant compared with the behavior at 60 °C.

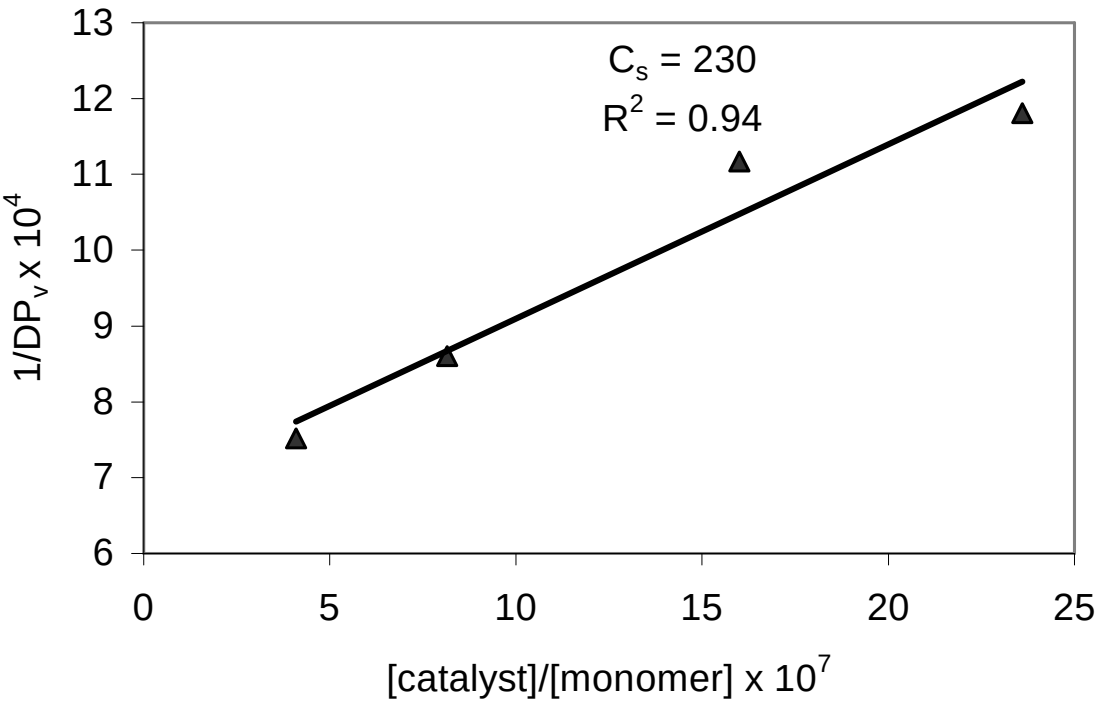

Figure 5.16 Mayo plot for the Polymerization of Styrene at 60 °C using [Co(dmg-2H.BF_2)$_2$] as a Chain Transfer Agent

Table 5.14 Data from GPC for Polymerization of Styrene at 60 ^{o}C (for 150 minutes) using AIBN (6.1 x 10^{-3} M) as Initiator and [Co(afdo-2H.BF_2)$_2$] as Chain Transfer Agent

catalyst (ppm)	Conversion (%)		M_n		M_w		PDI	
	Run 1	Run 2	Run 1	Run 2	Run 1	Run 2	Run1	Run 2
0	5.58	5.92	106698	114651	199101	208882	1.87	1.82
40	5.15	5.23	33289	23607	101665	101013	3.05	4.28
80	4.80	4.85	11382	12861	79390	54370	6.98	4.23
120	4.25	4.17	10141	8399	66334	25697	6.54	3.06
160	3.98	---*	9767	---	57568	---	5.89	---

*For Run # 2 polymerization with catalyst concentration of 160 ppm was not performed

Table 5.15 Molecular Weight Distribution data (from GPC) for Polymerization of Styrene in the presence of [Co(afdo-2H.BF_2)$_2$] catalyst at 70 and 80 ºC using AIBN (6.1 x 10^{-3} M) as Initiator

catalyst	M_n		M_w		PDI	
(ppm)	70 °C	80 °C	70 °C	80 °C	70 °C	80 °C
0	87937	55035	152209	217681	1.73	3.96
40	68811	34472	128006	132532	1.86	3.84
80	34388	58892	76863	126146	2.24	2.14
120	47918	49955	120654	124457	2.52	2.49
160	47775	71880	107902	120633	2.26	1.67

The PDI values are also comparable but the sample without catalyst has lower PDI value than others. The percent conversion has decreased from 14 % for sample having no CTA to 9 % for sample having 160 ppm of the catalyst. Table 5.15 also reveals that M_n values at 80 °C are erratic (may be due to baseline corrections) and do not show any regular trend, but on the other hand M_w values behave systematically. The PDI value at 80 °C is higher for the sample polymerized in the absence of catalyst, and is contrary to polymerization both at 60 and 70 °C.

Table 5.16 indicates that there is higher tendency for decrease in M_n values than M_w values. Point to point calculated C_s values at different temperatures are shown in Table 5.17. For both run 1 and run 2 at 60 °C average point to point chain transfer constant value of C_s is not comparable. C_s value has also been determined from slope of the curve by using Mayo equation, and was found to be 390 and 510 for run 1 and run 2, respectively (Figure 5.17). The chain transfer constant C_s at 70 °C (Figure 5.17) is 50 only. The values can also be calculated from M_w as shown in Figure 5.18. The value at 70 and 80 °C from Mayo plot is 220 and 44, respectively. It could be concluded that it is better to use M_w values to calculate C_s as compared to M_n values. This conclusion is based on the fact that at 80 °C we are unable to calculate the C_s value due to erratic nature of M_n data, but still at this temperature we are able to calculate the C_s value from M_w data. A C_s value (from M_n data) of 50 at 70 °C is still almost 2 times higher than C_s value of n-butyl mercaptan. Since degree of polymerization DP_n in the presence of catalyst is lower at 60 °C, hence C_s value is higher at this temperature. More than 10% decrease in catalyst efficiency at 70 °C as compared to 60 °C is probably due to increase in percent conversion at higher temperature.

Table 5.16 The percent difference among the Molecular weights for the Polymerization of Styrene using [Co(afdo-2H.BF_2)$_2$] as CTA

Temperature 60 °C	M_w % difference	M_n % difference
Run #1	49	69
	22	66
	16	11
	13	4
Run #2	52	79
	46	46
	53	35

Table 5.17 Point to point C_s value for the Polymerization of Styrene using AIBN as initiator and [Co(afdo-2H.BF_2)$_2$] as Chain Transfer Agent

[S]/[M] x 10^6 (60 ºC)	[S]/[M] x 10^6 (70 ºC)	$1/DP_n$-1/DPn(o)			C_s		
		60 ºC Run 1 x 10^3	60 ºC Run 2 x 10^3	70 ºC x 10^3	60 ºC Run 1	60 ºC Run 2	70 ºC
3.47	5.47	2.149	3.498	0.328	620	480	45
6.95	10.94	8.166	7.177	1.841	850	490	125
10.40	16.41	9.282	11.469	0.987	1120	390	45
13.90	21.88	9.675	--------	0.994	1440	----	34
				Average	1005	450	63

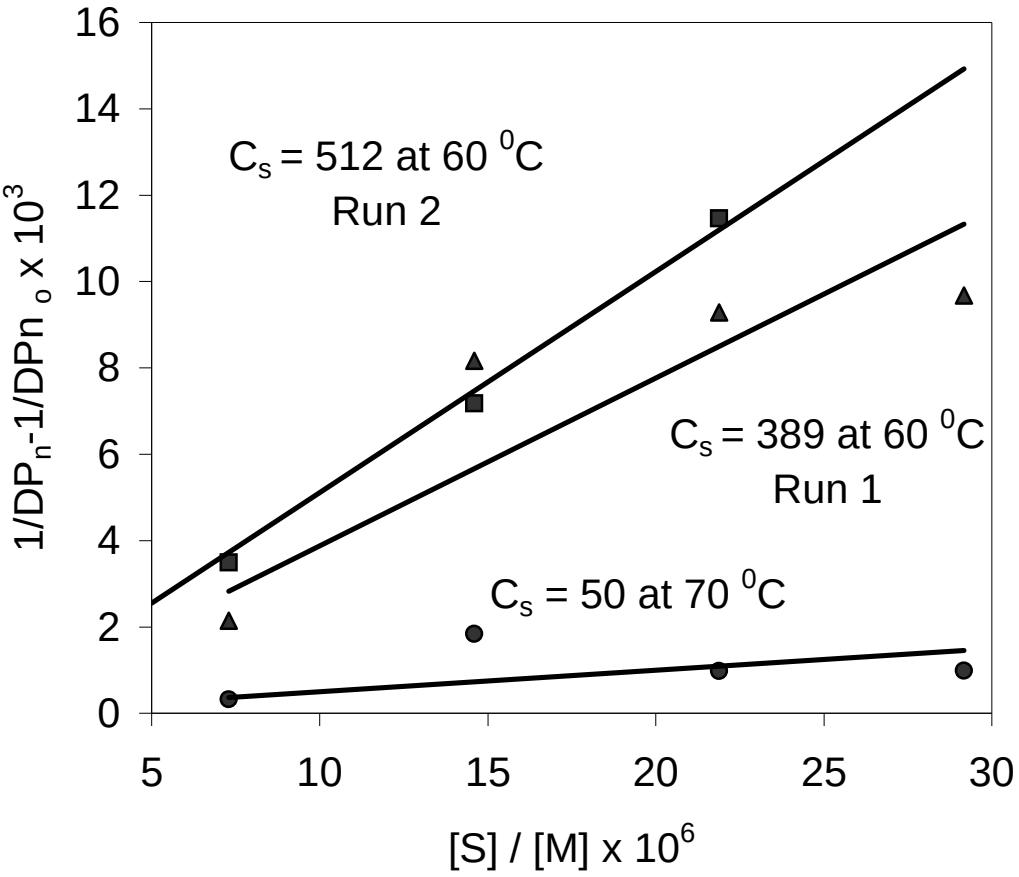

Figure 5.17 Mayo Plots for the Polymerization of Styrene at 60 and 70 °C using [Co(afdo-2H.BF_2)$_2$] as CTA

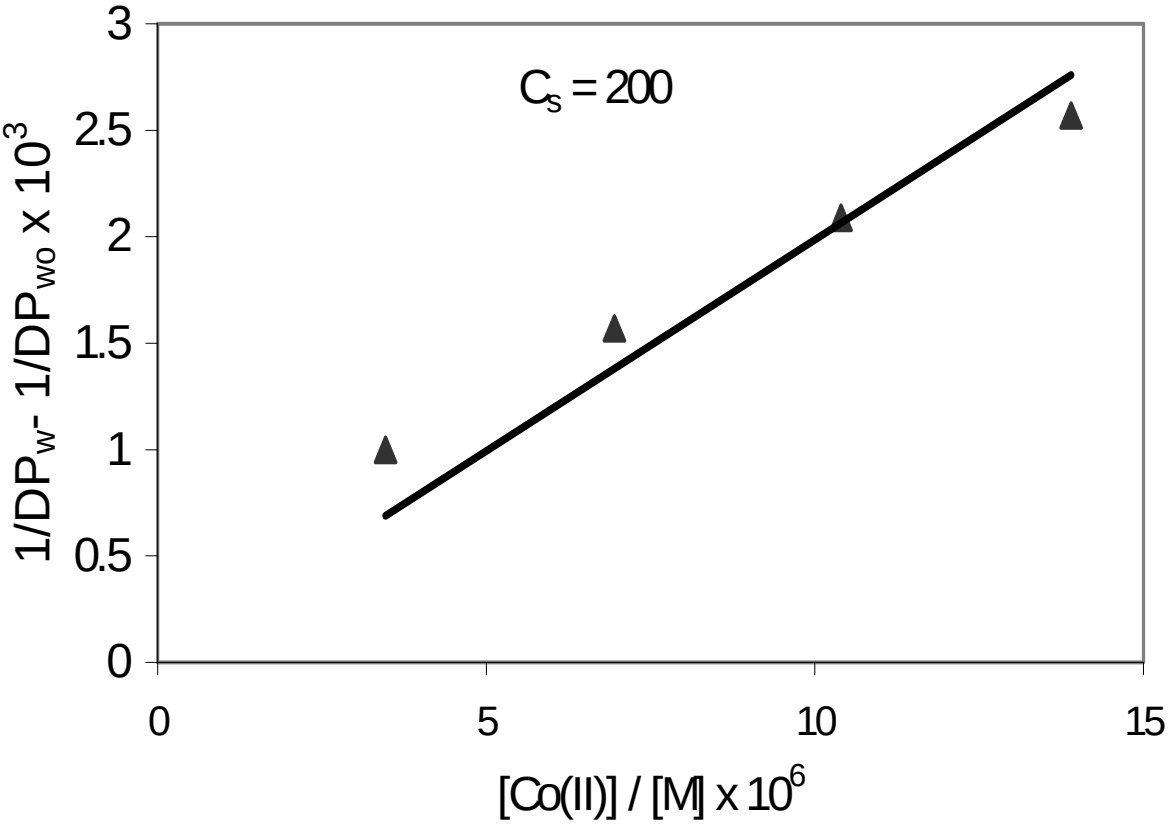

Figure 5.18 Mayo plot for the calculation of C_s value from M_w at 60 °C

The overall C_s value for the polymerization of styrene is less than the C_s value for the polymerization of MMA. This lowering in C_s value for the polymerization of styrene is mainly attributed to lack of β-hydrogen atoms. Secondly, it is known that the strength of the Co-R_n bond is also responsible for the increase or decrease of the catalytic activity. Since polymer radical of MMA is more electron acceptor than polymer radical of styrene, the C_s value for styrene is less as compared to MMA. Gridnev [45] pointed out that Co-R_n is a side reaction and that the radical pair [LCo + R_n) is the true intermediate in the hydrogen abstraction reaction by the sterically hindered porphyrin. He ascribed a special role for the methyl group of MMA in the three centered intermediate as compared to two centered intermediate for styrene. The methyl group in the poly(Methyl methacylate) radical can reach the cobalt in a deep pocket of sterically crowded porphyrin, as shown in Scheme 5.3, whereas the methylene radical of the polystyrene radical most likely cannot. We believe that Gridenev approach can be extended to cobaloximes and their derivatives along with other factors for showing less C_s value for styrene. However, it is not possible to calculate the C_s value from the number-average molecular weight "M_n" at 80 °C owing to erratic behavior of "M_n" values.

By using equation 5.9, a plot between 1/T and ln DP_n can be constructed and from the slope of this plot Composite or Overall Activation Energy for the degree of polymerization of styrene at higher temperatures was found to be –35.8 KJ/mol. By inserting literature value of E_t and E_d in equation 5.10, propagation activation energy (E_p) was found to be 29.9 KJ/mole. This E_p value is comparable to literature value of 26.0 and 32.0 KJ/mol [100].

Scheme 5.3 Comparative Mechanism of Hydride ion abstraction by Styrene and MMA

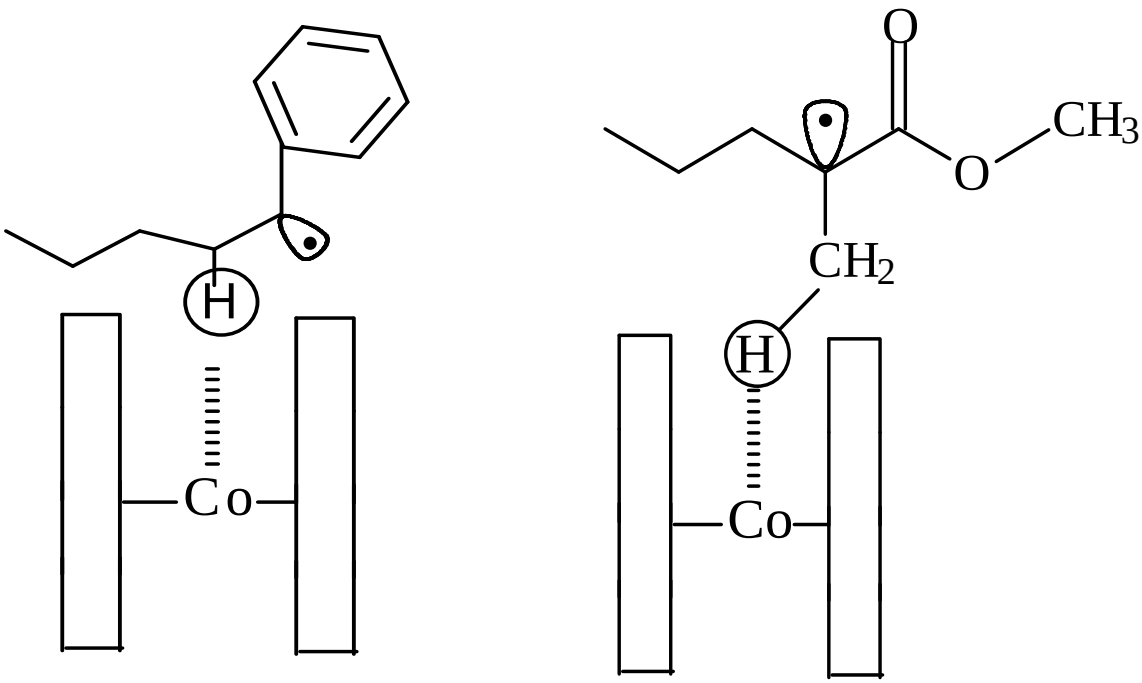

5.2.8 Polymerization of Methyl methacrylate at 50, 60, 70 and 80 °C using [Co(afdo-2H.BF_2)$_2$] as a Chain Transfer Agent

The results for molecular weights for the polymerization of MMA at 50 to 80 °C are shown in Table 5.18 - 5.21, respectively. For the polymerization at 60 °C, it is noted that with the addition of 1.53 ppm of chain transfer agent [Co(afdo-2H.BF_2)$_2$], number-average molecular weight (M_n) reduced to 12,260 from 106,750, which indicates more than 8 times decrease in M_n. However, the rate of decrease in molecular weight reduces with further increase in CTA concentration. The decrease in M_w is also comparable with M_n, as upon addition of 1.53 ppm of CTA M_w decreases to 20,960 from 151,330. The decrease in molecular weights at 70 °C (Table 5.21) is also comparable with polymerization at 60 °C. The results presented in Tables 5.18 to 5.21 also reveal that as temperature increases both number-average and weight-average molecular weights decrease. For the sample having no chain transfer agent, M_n = 34,100 at 80 °C, which is significantly lower than the M_n value of = 121,140 at 50 °C. However, the PDI values are noted to be somewhat higher at higher temperatures e.g. at 50 °C PDI values are between between 1.47 to 1.77, while at 70 °C the PDI values lie between 1.77 to 2.27. Figures 5.19 and 5.20 indicate that as CTA concentration increases percent conversion decreases. Both at 50 and 60 °C percent conversion was kept below 6 % as this range was noted to be most suitable for evaluation of the C_s value.

Table 5.18 Molecular weights distribution for the Polymerization of MMA at 50 ^{0}C for 60 minutes

Sample #	M_n	M_w	M_z	M_p	PDI
1	121140	171730	215440	204240	1.42
2	24800	42930	59340	50130	1.73
3	13790	13180	34490	22110	1.68
4	12450	21390	28750	18360	1.72
5	10640	18670	22380	15980	1.75
6	8510	13750	17180	13680	1.62

Table 5.19 Molecular weight distribution for the Polymerization of MMA at 60 ^{0}C for 45 minutes

Sample #	M_w	M_n	M_p	PDI
1	171330	106750	147980	1.60
2	20960	12260	18140	1.71
3	18160	11290	21390	1.61
4	15760	9020	14950	1.75
5	12480	7380	13520	1.69
6	11010	6210	12320	1.77

Table 5.20 Molecular weight distribution for the Polymerization of MMA at 70 ^{0}C for 30 minutes

Sample #	M_w	M_n	M_p	PDI
1	121470	71740	115160	1.69
2	24090	12600	21700	1.91
3	14640	8280	15720	1.77
4	15830	7100	12230	2.23
5	11830	6320	13920	1.71
6	11340	5010	9120	2.27

Table 5.21 Molecular weight distribution for the Polymerization of MMA at 80 ^{0}C for 10 minutes

Sample #	M_n	M_w	M_z	M_p	PDI
1	34100	63980	88850	79320	1.88
2	18450	33890	54650	32590	1.84
3	14130	23610	34720	22260	1.67
4	10970	12940	18530	13110	1.58
5	8770	13850	16390	12570	1.58
6	7430	11360	13190	9940	1.53

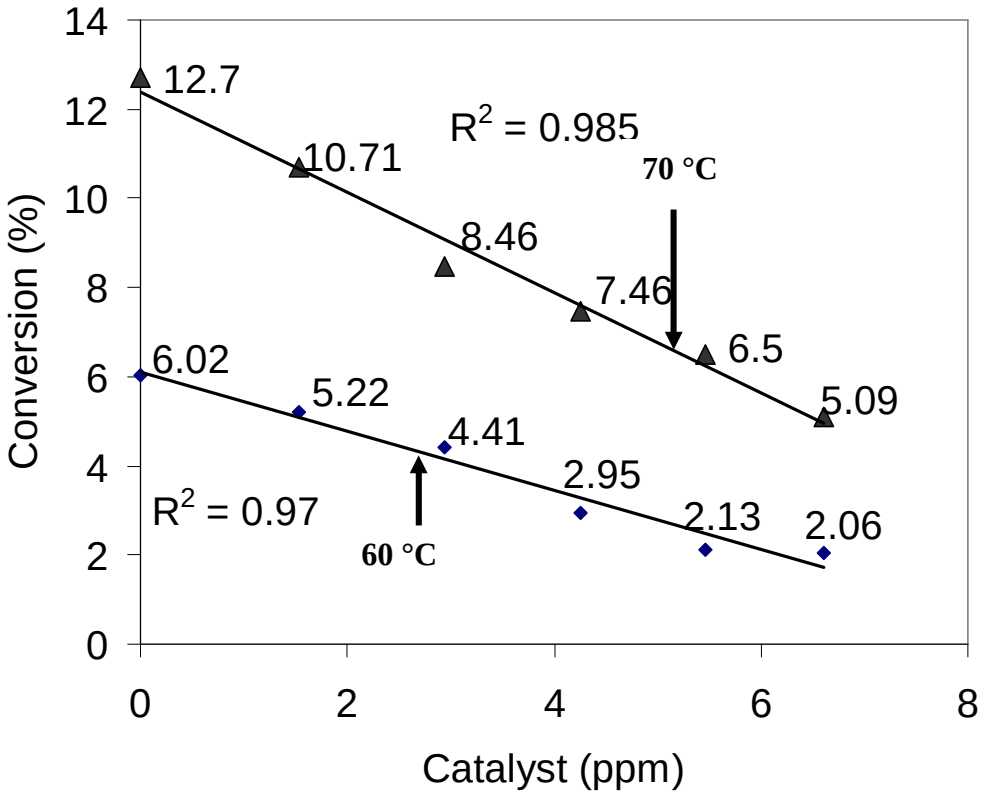

Figure 5.19 Dependence of percent conversion on the concentration of [Co(afdo-2H.BF_2)$_2$] CTA used for the Polymerization of MMA at 60 (for 45 minutes and [AIBN] = 0.00617 M) and 70 ^{o}C (for 30 minutes and [AIBN] = 0.00760 M)

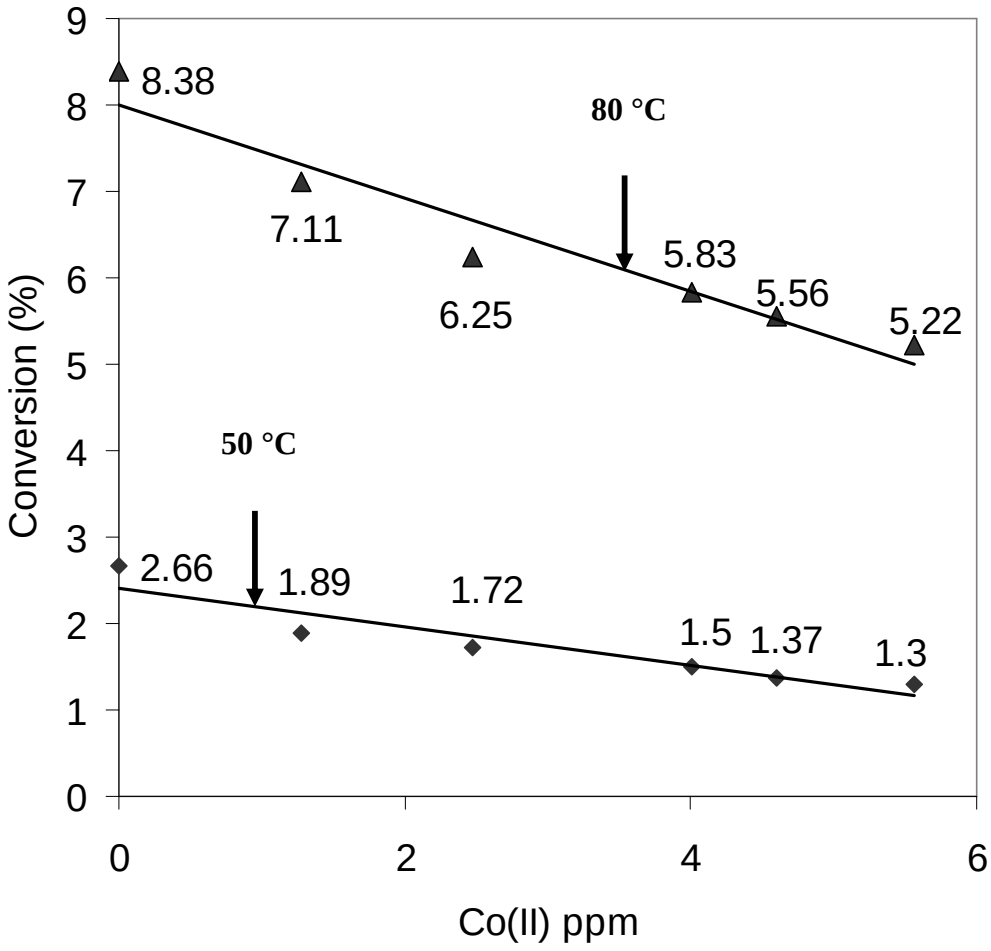

Figure 5.20 Dependence of percent conversion on the concentration of [Co(afdo-2H.BF_2)$_2$] Chain Transfer Agent used for the Polymerization of MMA at 50 (for 60 minutes and [AIBN] = 0.00401 M) and 80 ^{o}C (for 10 minutes and [AIBN] = 0.00923 M)

C_s value. However, higher percent conversions are also reported in literature e.g. Sanayei and O'Driscoll [144] have calculated C_s value for the polymerization of MMA using [Co(dmg-2H.BF_2)$_2$] CTA at 60 °C and reported percent conversion from 12.2 to 5.04. The Mayo Plots for the evaluation of C_s value are shown in Figures 5.21 to 5.22. For the polymerization of MMA at 80 °C, viscosity-average molecular weight (Table 5.23) has also been calculated from viscosity measurements technique (Table 5.24). Since DP_{n0} value is higher, hence $1/DP_n$ can be assumed ≈ 0. At 60 °C average point to point C_s value is lower (16,580) than the average point to point C_s value found at 70 °C (18,930). From Mayo plot the C_s value at 50 °C is calculated to be 12,230, and thus it is justifiable to conclude that with the increase in temperature, the C_s value increases (Table 5.24). This observation is contrary to the case of polymerization of styrene at 60, 70 and 80 °C, where the C_s value was found to be temperature dependent and founded to be 1000, 220 and 45, respectively.

Probably, a longer polymerization time of 150 minutes at 60, 70 and 80 °C for styrene polymerization deterioated the catalyst. In the present case, MMA was polymerized for a period of 45 and 30 minutes at 60 and 70 °C, respectively. Analysis of results in Patent literature [145] using [Co(dmg-2H)$_2$] CTA with MMA indicate that, C_s generally increases with temperature (60, 70, and 80 °C), but Sanayei and O'Driscoll [144] reported a decrease in chain transfer activity with increasing temperature (60, 70, 80 and 90 °C) resulting in a small, negative, activation energy. Two separate patents, from Dupont [146-147] and CSIRO reported a decrease in C_s value on increasing temperature for polymerization of MMA using [Co(dmg-2H.BF_2)$_2$] as CTA.

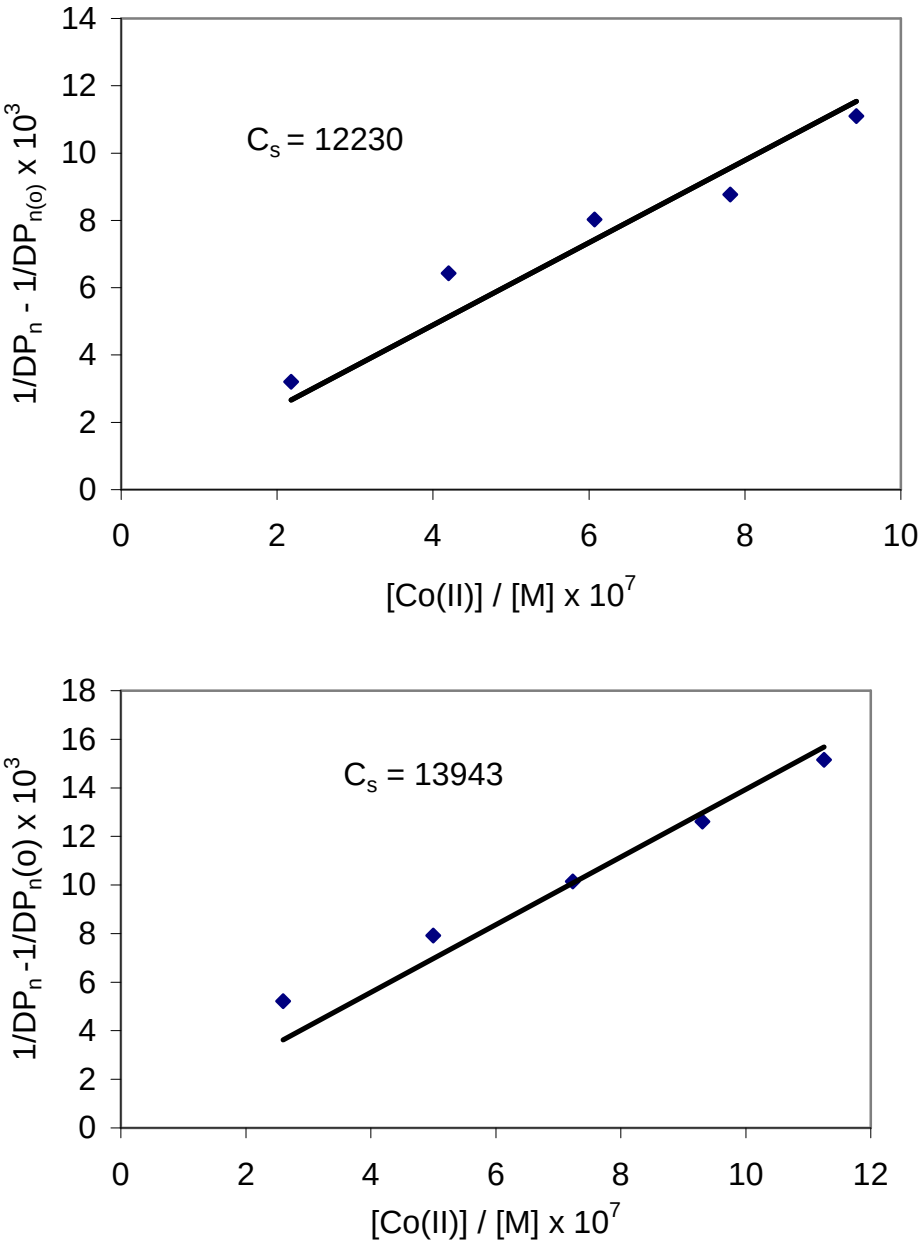

Figure 5.21 Mayo plots for the Polymerization of MMA at 50 (Top) and 60 °C (Lower) using [Co(afdo-2H.BF_2)$_2$] as CTA

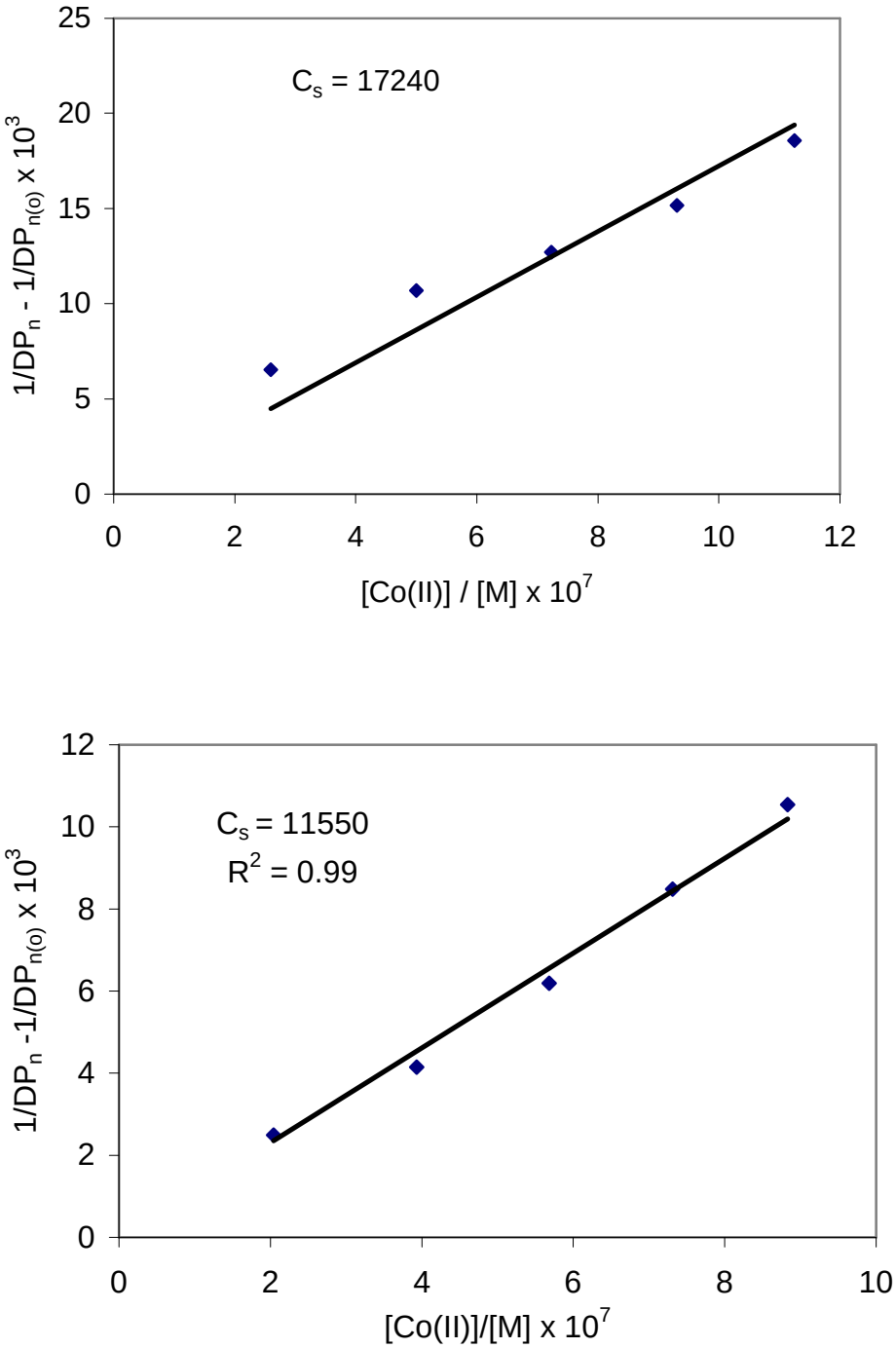

Figure 5.22 Mayo plots for Polymerization of MMA at 70 (Top) and 80 °C (Lower) using [Co(afdo-2H.BF_2)$_2$] as CTA

Table 5.22 Viscosity data for the Polymerization of MMA at 80 °C

Sample #		Conc. g/100g	t_{av} (sec)	$\eta_{rel} = t_{av}/t_o$	$\eta_{sp} = \eta_{rel} - 1$	$\eta_{red} = \eta_{sp}/c$	$[\eta]$
1	(i)	1.1547	180.2	1.4509	0.4509	0.3905	0.5248
	(ii)	0.7035	164.6	1.3253	0.3253	0.4624	
	(iii)	0.4116	148.9	1.1989	0.1989	0.4832	
	(iv)	0.2128	137.2	1.1047	0.1047	0.4920	
2	(i)	1.2093	151.0	1.2158	0.2158	0.1785	0.2118
	(ii)	0.7384	141.4	1.1385	0.1385	0.1876	
	(iii)	0.4523	135.2	1.0886	0.0886	0.1959	
	(iv)	0.2837	131.5	1.0588	0.0588	0.12073	
3	(i)	1.3276	140.6	1.1320	0.1320	0.1092	0.1192
	(ii)	0.8049	134.1	1.07957	0.07957	0.1070	
	(iii)	0.4854	128.4	1.03392	0.03392	0.1078	
	(iv)	0.2769	126.6	1.01855	0.01855	0.1018	
4	(i)	1.3004	137.5	1.1071	1.1709	0.08236	0.0675
	(ii)	0.7683	131.8	1.06119	0.06119	0.07965	
	(iii)	0.4859	128.8	1.03704	0.03704	0.07623	
	(iv)	0.1451	125.4	1.00966	0.009662	0.06658	
5	(i)	1.1515	135.5	1.0998	0.09098	0.07901	0.0716
	(ii)	0.6757	130.6	1.05146	0.05146	0.07745	
	(iii)	0.3881	128.2	1.03201	0.03201	0.07469	
	(iv)	0.2322	126.6	1.01933	0.01933	0.07627	

Table 5.23 Viscosity-average molecular weight data required to construct Mayo plot

$[Co(II)]/[S] \times 10^7$	M_v	DP_v	$1/DP_{v(o)} \times 10^3$	$1/DP_v - 1/DP_{v(o)} \times 10^3$
0	286810	2868.10	0.3487	-----
2.04	79905	799.05	1.2515	0.9028
3.93	27920	279.20	3.5817	3.5817
5.68	15960	159.60	6.2657	5.9170
7.31	13850	138.5	7.2219	6.8732

Table 5.24 Comparison of C_s value for the Polymerization of MMA using [Co(afdo-2H.BF_2)$_2$] as Chain Transfer Agent

T(ºC)	Point to Point "C_s"	Mayo Plot "C_s"	k_p* L/mol.sec	$k_{tr's}$ L/mol.sec
50	13,240	12,230	649	7.94×10^6
60	16,940	13,940	833	1.16×10^7
70	19,390	17,240	1054	1.82×10^7
80	10,860	11,550	-----	-------

*Taken from reference [148].

Recently, Heuts and co-workers [148] have reported, a virtually constant C_s value for polymerization of MMA, EMA, BMA at 40, 50, 60 and 70 °C using [Co(dmg-2H.BF_2)$_2$] and [Co(dpgo-2H.BF_2)$_2$] as chain transfer agents. In our investigations for polymerization of MMA using [Co(afdo-2H.BF_2)$_2$] as a CTA there is an increase in chain transfer activity with increase in temperature.

By using equation 5.9 a graph (Figure 5.23) for 1/T vs ln DP_n was plotted. From the slope of the graph, Overall Activation Energy for the Degree of Polymerization (E_{xn}) was calculated to be –39.5 KJ/mol and consequently, using equation 5.10 Activation Energy for the Propagation Reactions (E_p) is 28.1 KJ/mol. Equation 5.11 is used to calculate Overall Activation Energy for the Transfer reactions ($E_{tr's}$).

$$\ln 1/C_S = \ln \frac{A_p}{(A_{tr's})} - \frac{E\overline{X}_n}{RT} \qquad (5.11)$$

where, E_{xn} (= $E_{tr's}$ - E_p) is Overall Activation Energy for Degree of Polymerization in the presence of a chain transfer agent, and $A_{tr's}$ is frequency factor for chain transfer reactions. A graph (not shown) was constructed between 1/T against ln $1/C_s$ and from the line of the curve $E_{tr's}$ was found to be 42.1 KJ/mol. This value is 15.74 KJ/mol higher than the Activation Energy for the Propagation reactions (E_p). Probably, this is the cause for the increases in chain transfer constant value with the increase in temperature. From Table 5.23 it should be noted that with the increase of temperature, there is concomitant increase both in propagation (k_p) and transfer rate constant ($k_{tr's}$) values, but this increase is dominant for transfer rate constant as there is 46 % increase in it's value at 60 ºC compared with 50 ºC.

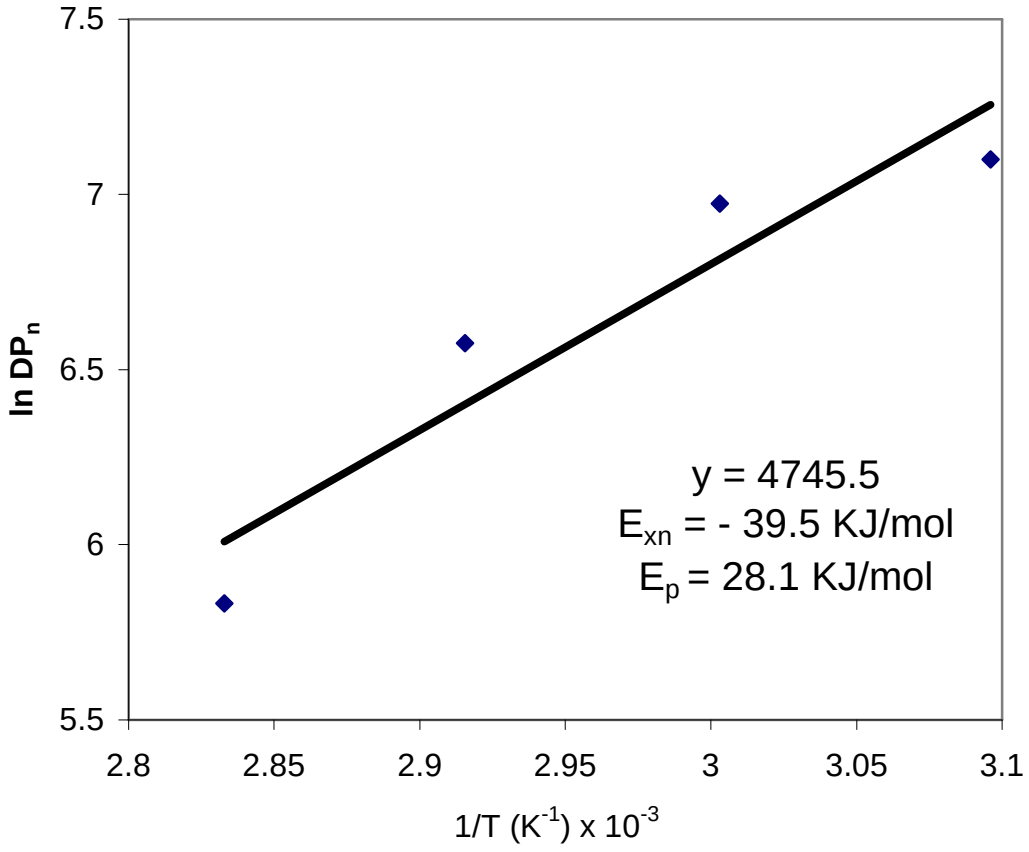

Figure 5.23 Composite or Overall activation Energy for the Degree of Polymerization of MMA

On the other hand there is only 28 % increase in propagation rate constant value at 60 ºC compared with 50 ºC. Similarly, at 70 ºC there is further 36 % and 26 % increase in $k_{tr's}$ and k_p, respectively. Owing to these observations, it was concluded that C_s value increases at higher temperatures because of increase in transfer rate constant values. The transfer rate constant value $\approx 10^7$ indicates diffusion-controlled nature of transfer reactions. The higher frequency factor for transfer reactions ($A_{tr's} = 3.7 \times 10^{12}$) is of typical bimolecular reactions and thus further validates our conclusion of diffusion-controlled bimolecular transfer reactions.

5.2.9 Polymerization of Butyl methacrylate at 60, 70 and 80 °C using [Co(afdo-2H.BF_2)$_2$] as a Chain Transfer Agent

Previously, we determined C_s values of around 1000 and 14,000 for the polymerization of styrene and MMA at 60 °C using [Co(afdo-2H.BF_2)$_2$] as a CTA. Lower C_s value for styrene was mainly attributed to absence of β-hydrogen in styrene. In the polymerization of Butyl methacrylate (BMA) at 60 °C, effect of ester chain length was explored, as both BMA and MMA have β-hydrogen atoms available for transfer process. Results for the polymerization of BMA at 60 to 80 °C are given in Tables 5.25 to 5.27. The results in these Tables indicate that the PDI values are around 2, which indicates dominant chain transfer catalysis. For the polymerization at 60 °C, with the addition of 1.40 ppm of [Co(afdo-2H.BF_2)$_2$] as the chain transfer agent, M_n reduces to 40,844 from 80,925. It is worthwile to note that for the polymerization of BMA, both M_n and M_w values at higher temperature are lower than the values recorded for the

Table 5.25 Molecular weight distribution for the Polymerization of Butyl methacrylate at 60 °C for 60 minutes using [Co(afdo-2H.BF_2)$_2$] complex as a CTA

catalyst ppm	M_w	M_n	M_p	PDI
0.00	152748	80925	175734	1.89
1.40	81940	40844	90914	2.01
2.69	49225	27243	58309	1.81
3.90	38405	20458	40755	1.88
5.02	36768	18856	233829	1.95
6.06	36518	16685	47033	2.19

Table 5.26 Molecular weight distribution for the Polymerization of Butyl methacrylate for 40 minutes at 70 °C using [Co(afdo-2H.BF_2)$_2$] complex as a CTA

catalyst ppm	M_w	M_n	M_p	M_z	PDI
0.00	60330	29610	70850	84430	2.04
1.41	23730	11120	27320	35060	2.13
2.72	11000	4600	21690	39820	2.39
3.93	10340	3980	18770	21400	2.59
5.06	8720	3460	18230	15560	2.53
6.11	5870	2570	14370	23710	2.28

Table 5.27 Molecular weight distribution for the Polymerization of Butyl methacrylate for 20 minutes at 80 °C using [Co(afdo-2H.BF_2)$_2$] as a CTA

catalyst ppm	M_w	M_n	M_p	M_z	PDI
1.54	16640	7560	18140	26720	2.20
2.96	13260	5060	13580	23250	2.61
4.29	7910	3650	8310	18780	2.17
5.52	6620	2520	6290	12560	2.62
6.67	5230	2160	4610	9480	2.42
7.80	4920	1940	4020	9230	2.54

polymerization of MMA at the corresponding higher temperatures. For the calculation of C_s values for the polymerization at different temperatures Mayo plots were constructed and are shown in Figures 5.24-5.25. Polymerization at 60 °C produces an average point to point C_s value of 5430, while from Mayo plot (Figure 5.24) this value is noted to be 5590 and thus both values are in agreement with each other. The C_s value of 5430 for the polymerization of BMA at 60 ºC, is almost three times less than the C_s value of 14,400 recorded for the polymerization of MMA at the same temperature. This indicates that with increase in size of ester chain length C_s value decreases. This observation is in accord with the work of Mironychev et al [149], who found that the chain transfer constant C_s of cobalt(II) porphyrin in the catalytic chain transfer polymerization of alkyl methacrylate decreases with increasing size of the ester group. These workers ascribed the reduction in chain transfer constant mainly to an increasing steric hindrance from the bulky ester side chains and an enhanced stability of the complex upon axial ligation of the monomer with the Co(II) center. Heuts et al [148] estimated a value of 10^{10} dm^3 $mole^{-1}$ sec^{-1} for pre-exponential factor "$A_{tr's}$" and concluded that such a high value is indicative of unusual chain transfer mechanism i.e. β-elimination of a hydrogen atom from a radical coordinated to the cobalt center.

For the polymerization of BMA at different temperatures, $k_{tr's}$ (recall that $C_s = k_{tr's}/k_p$) was found to be 6.1 x 10^6 dm^3 $mole^{-1}$ sec^{-1} . The value of k_p required to calculate $k_{tr's}$ has been taken from reference 148. The chain transfer rate coefficients, $k_{tr's}$ ($\approx 10^7$ dm^3 $mole^{-1}$ sec^{-1}) are similar to the rate coefficients obtained for bimolecular termination reactions in free radical polymerizations and are known to be diffusion controlled.

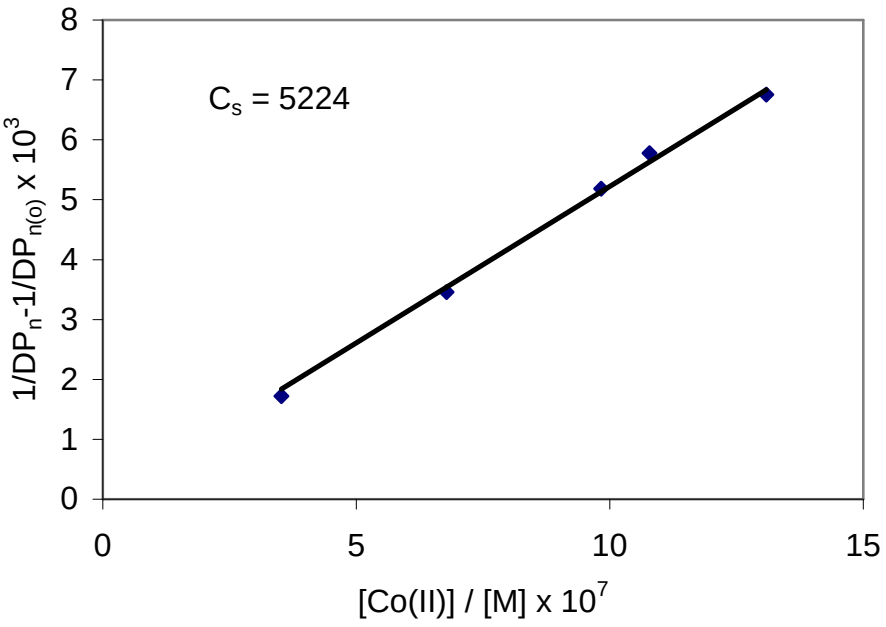

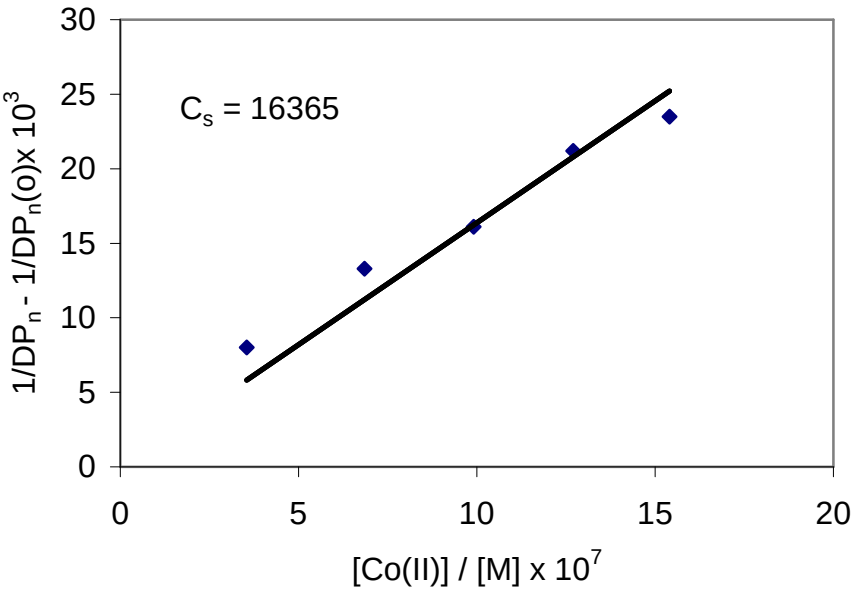

Figure 5.24 Mayo plots for the Polymerization of Butyl methacrylate at 60 and 70 ºC using [Co(afdo-2H.BF_2)$_2$] as a CTA

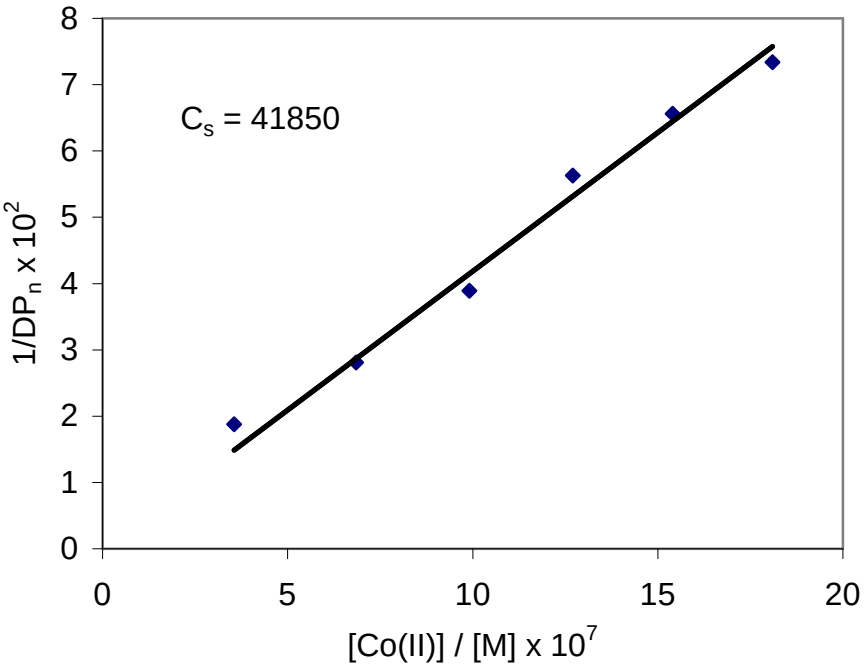

Figure 5.25 Mayo plot for the Polymerization of Butyl methacrylate at 80 °C using [Co(afdo-2H.BF_2)$_2$] as a CTA

For the polymerization of MMA at 70 ºC using [Co(afdo-2H.BF_2)$_2$] as a CTA, $k_{tr's}$ has been found to be 1.4 x 10^7 dm^3 $mole^{-1}$ sec^{-1}, which is lower than $k_{tr's}$ value of 2.20 x 10^7 for the polymerization of BMA at the same temperature (Table 5.28). However, for both cases $k_{tr's}$ value is $\approx 10^7$ dm^3 $mole^{-1}$ sec^{-1} at 70 ºC and thus chain transfer process for the polymerization of BMA is also diffusion controlled. Table 5.28 also reveals that as temperature increases C_s value for the polymerization of Butyl methacrylate increases sharply. There is significant increase in transfer rate constant value with increase in temperature. Overall Activation Energy for the Degree of Polymerization of BMA in the presence of [Co(afdo-2H.BF_2)$_2$] as a CTA has been calculated from the slope of the line (Figure not shown) by using equation 5.11. This value is -105.6 KJ/mol compared with the value -15.75 KJ/mole for the polymerization of MMA.

The decrease in C_s value for the polymerization of BMA at 60 ºC compared with polymerization of MMA at the same temperature can only be partially explained by an increasing propagation rate coefficient of 1085 dm^3 $mole^{-1}$ sec^{-1} for BMA compared with 833 dm^3 $mole^{-1}$ sec^{-1} for the polymerization of MMA at 60 °C [150]. It is also important to note that absolute viscosity [148] of MMA and BMA at 60 °C is 0.37 and 0.55 centipoise (Table 5.29) respectively. Therefore, this further supports the argument that chain transfer constant should be lower for BMA.

The comparision of PDI values for MMA and BMA in the absence of chain transfer agent at different temperatures is given in Figure 5.26. It was observed for both the cases that as temperature increases PDI values increase. This is probably due to an increase of termination reactions by disproportionation.

Table 5.28 Comparison of C_s value for the Polymerization of BMA using [Co(afdo-2H.BF_2)$_2$] as a CTA

T(ºC)	Point to Point "C_s"	Mayo Plot "C_s"	k_p* L/mol.sec	$k_{tr's}$ L/mol.sec
60	5,180	5,220	1085	5.67×10^6
70	18,030	16,365	1347	2.20×10^7
80	37,835	41,850	-----**	**---------

- *Values taken from reference 148
- **Value not available

Table 5.29 Absolute viscosity of MMA and BMA at Higher Temperatures

Temperature	Absolute viscosity (centi poise)	
(°C)	MMA	BMA
40	0.45	0.70
50	0.40	0.62
60	0.37	0.55
70	0.33	0.49

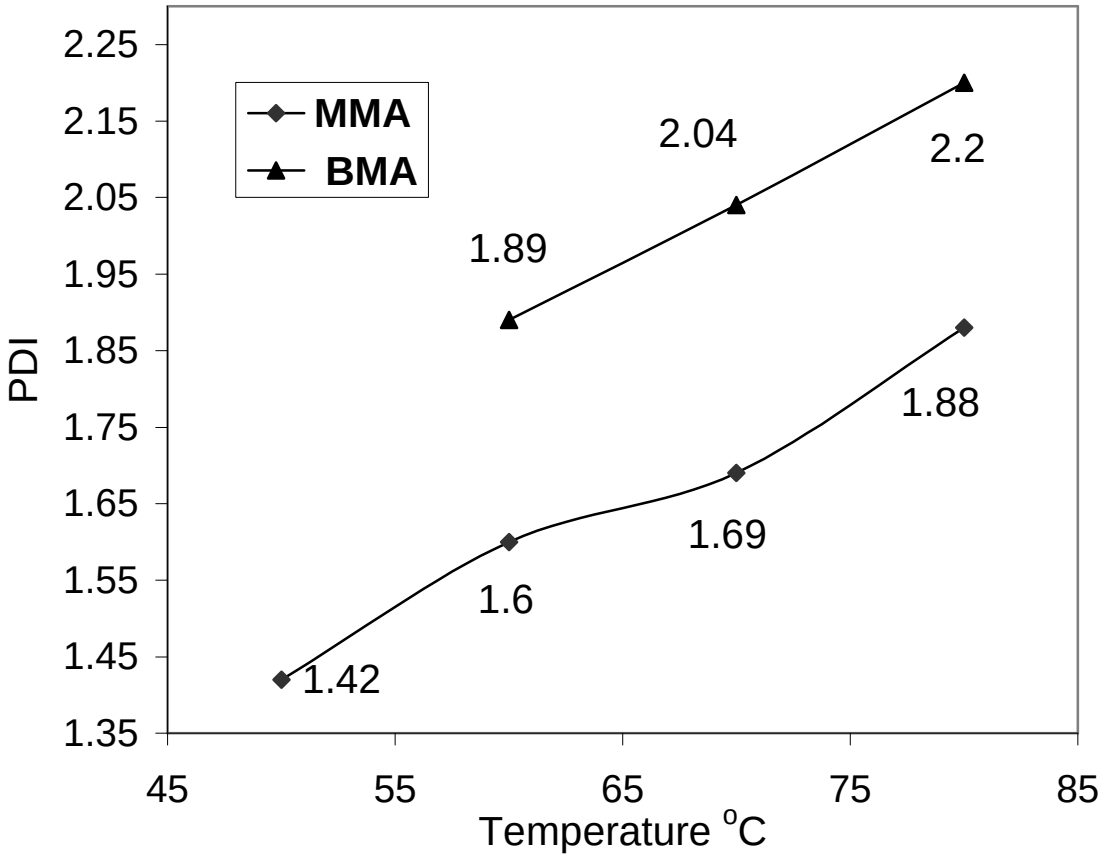

Figure 5.26 Comparasion of PDI values for the Polymerization of MMA and BMA

The disproportionation termination characters are higher for BMA as compared to MMA. In general, the relative amount of disproportionation in a given series of radicals increases [151] by:

- increasing the number of β-hydrogen atoms, both MMA and BMA have the same no of β-hydrogen atoms;
- increasing degree of substitution at the radical center: tertiary radicals tend to give more disproportionation than secondary radicals;
- increasing the bulkiness of β-substituents: bulky substituent on either the β- and/or γ- positions can slow down both combination and disproportionation significantly. Combination is, however, somewhat more sensitive towards bulky β-substituents than disproportionation (BMA has bulky substituent than MMA);
- increasing polarity of the solvent: it has been proposed that disproportionation has a more polar transition state;
- decreasing delocalization of the unpaired electron by α-substituents: as disproportionation requires overlap of the unpaired electron orbital and breaking C-H bond, delocalization of the unpaired electron will diminsh the amount of disproportionation. However, a decreasing radical density at the α-carbon atom can also lead to slower combination reactions;
- increasing temperature: the effects are small and appear to be opposite for small radicals as compared to large macroradicals (for the former the amount of disproportionation seems to decrease with increasing temperature);
- increasing viscosity: this effect, however, depends upon the structure and rotational freedom of the radicals involved. A hindered rotation can promote

disproportionation reactions. The viscosity of MMA and BMA at different temperatures [148] is given in Table 5.29. From the table it is clear that viscosity of BMA is higher than MMA, therefore, disproportionation characters should be higher in former and indeed this has been observed experimentally (Figure 5.26).

5.3 Pulsed Laser Polymerization

5.3.1 Pulsed Laser Polymerization of MMA without using Chain Transfer Agent

Results of the experiments on MMA without using AIBN as photoinitiator are presented in Table 5.30. These results show that some minimum irradiation time of Excimer laser is required for the significant amount of the polymer to be formed and detected. Further, the sample with dissolved oxygen did not show any product for a total irradiation time of 30 minutes. Thus, it is also clear that dissolved O_2 at room temperature does not act as initiator. The results of PLP of MMA with AIBN are shown in Table 5.30. Comparison of Table 5.30 with Table 5.31 reflects that for irradiation of 45 minutes, percent conversion of PMMA is 31 %, while the sample of MMA irradiated for 50 minutes without using AIBN produced only 0.566 % of PMMA. This idicates that the laser mainly interacts with the initiator AIBN rather than the MMA. By comparing the results of Table 5.31 with Table 5.32 it is clear that percent conversion for polystyrene is much lower as compared to percent conversion of PMMA irradiated for comparable time.

Table 5.29 Homopolymerization of MMA without using AIBN

Time (minutes)	Conversion (%)
20	0.00
30	0.00
40	0.41
50	0.57
30*	0.00

*The dissolved O_2 was not removed from this sample.

Table 5.31 Homopolymerization of MMA using 2.03 x 10^{-3} M AIBN and 10.0 Hz repetition rate of the Excimer Laser

Time (minutes)	Transmitted Energy (mJ)	Conversion (%)
15	37.0	6.28
25	32.0	14.54
35	37.0	21.29
45	22.5	30.85

Table 5.32 Pulsed Laser Homopolymerization of Styrene using 2.03 x 10^{-3} M AIBN and 10.0 Hz repetition rate of the Excimer Laser

Time (minutes)	E (mJ)	Conversion (%)
25	100	0.298
35	98	0.389
45	105	0.471
55	110	0.543
65	103	0.692
75	97	0.628

It indicates that propagation rate (k_p) for PLP of styrene is lower than PLP of MMA. This is consistent with the findings of Olaj and co-workers [59-60] who reported at 25 °C, k_p values of 80 and 299 L mol^{-1} sec^{-1} for the polymerization of styrene and MMA, respectively.

The values of different molecular weights of polystyrene are given in Table 5.33. The results in Table 5.33 signifies that polydispersity index value of polystyrene (PSTY) increases with molecular weight of PSTY. High PDI values for PSTY samples also indicate that there is probability for the formation of branched polmer. Table 5.34 lists some of the values of k_p determined at 25 ^{0}C and other reported values in literature for the PLP of styrene. The values reported in references 59-60 were calculated at 25 °C by taking value of log Mol.Wt. of first derivative spectra of MWD curve (Figure 5.27). Our calculated values in last column suggests that it is an accurate method to calculate the value of L_0 at the point where cumulative % curve crosses the MWD curve on low molecular weight side of the MWD curve. Similarly modification of equation $L_o = k_p [M] t_f$ gives the results presented in column 4 of Table 5.34. The new modified equation 5.12 in addition to L_0 also incorporates polydispersity. Therefore, this modified equation 5.12 presented by us, is quite appropriate to determine the L_0 at a point where a horizontal line from 50 percent conversion crosses on the lower molecular weight side of MWD curve of highly polydisperse polystyrene.

Table 5.33 Molecular weight distribution for the PLP of Styrene

Time (minutes)	M_w Trial 1	M_w Trial 2	M_n Trial 1	M_n Trial 2	PDI Trial 1	PDI Trial 2	M_p Trial 1	M_p Trial 2
25	102038	103204	20469	18294	4.99	5.64	25542	28266
35	118680	138112	16278	18559	7.29	7.44	24296	24903
45	128018	140398	15489	17190	8.27	8.17	12084	14692

Note: Theoretically, the molecular weight of polystyrene can also be calculated by using equation 5.12.

$$M_n^{calc.} = \frac{[M]}{[AIBN]} \times \frac{MW_{STY} \times Conversion\ (\%)}{100} \qquad (5.11)$$

Table 5.34 Values of k_p for the PLP of Styrene

Time (minutes)	*k_p	*k_p	*k_p	k_p[a]	k_p[b]	k_p[c]
----	80	78±6	74	----	----	----
25	----	----	----	57	70	81
35	----	----	----	58	78	78
45	----	----	----	54	78	76

* Taken from references 59-60.

a. These values were calculated at 50 conversion (%) on the lower molecular weight side of MWD curve by using equation $L_o = k_p [M] t_f$ and $L_o = M_n / M_o$, where, M_n is the number average molecular weight of the polymer and M_o is the molar mass of the monomer.

b. These values were calculated by using equation 5.12.

$$k_p = \frac{L_0}{[M]\, t_f} + (PDI)^{3/2} \qquad (5.12)$$

c. These values were calculated by taking log Molecular weight value at the point where cumulative % curve crosses the MWD curve on low molecular weight side. The procedure is same as described in “a”.

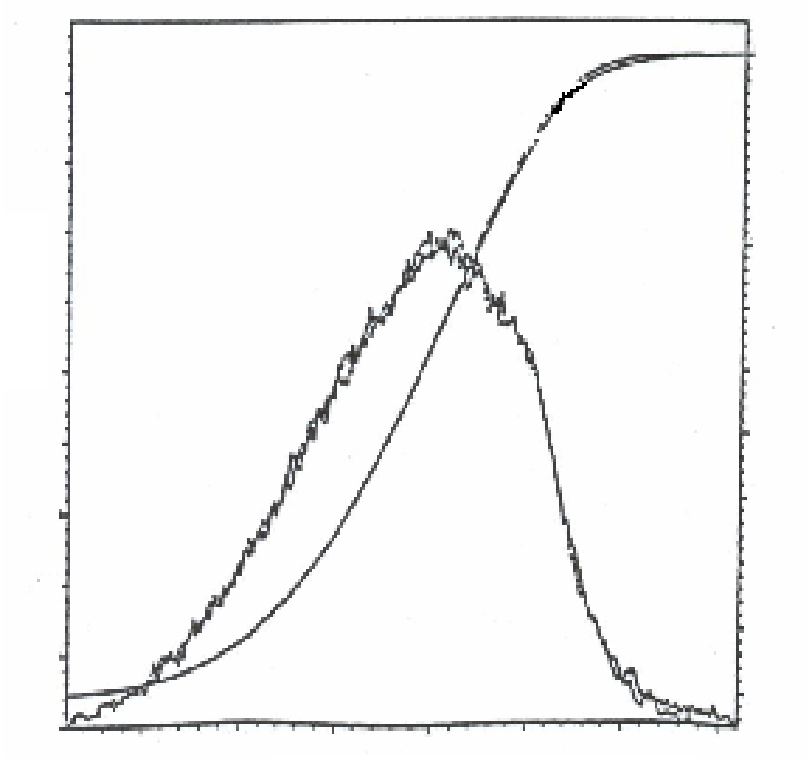

Figure 5.27 A representative GPC chromatogram

5.3.2 Pulsed Laser Polymerization of Methyl methacrylate in the presence of Wilkinson's Catalyst

Pulsed Laser Polymerization (PLP) MMA in the presence as well as absence of 2,2-Azobis-(2-methyl isobutyronitrile) [AIBN] with tris(triphenylphosphane)rhodium(I) chloride $[(C_6H_5)_3P]_3RhCl$ (Wilkinson's catalyst) was investigated. The polymerization was carried out at room temperature (25 ^oC) as compared to high temperature required for homo-polymerization of MMA. Lambda Physik Model EMG 203 MSC was used for excimer laser (XeCl) irradiation (45 minutes for each of the samples). The laser emits UV light of wavelength at the rate of 308 nm. Typical laser energy per pulse was 150 mJ with repetition rate of 10 Hz. The laser beam spot size was 10mm x 30mm which covered most of the volume of the sample cell. No focusing or beam expansion was needed in this system. Laser energy was continuously monitored using a Molectron J-50 probe with the output displayed on an oscillioscope. The discharge voltage on the laser tube was increased in a controlled manner to maintain a constant energy output.

Initially, both AIBN and Wilkinson's catalyst were used on the assumption that the latter will act as chain transfer agent and restrict further growth of polymer chains. The results are shown in Table 5.35, which indicates that polydispersity of PMMA samples is less than 2. This is possibly due to the termination process, which under the prevailing conditions is mainly by combination (especially when PDI is around 1.5). There is decrease of PDI values from 1.89 to 1.52 in the presence of 0.0361 milli molar (mM) solution of Wilkinson's catalyst. On the other hand Polydispersity Index (PDI) increases for sample B and sample C. Apparently, this contradicts the previous statement,

Table 5.35 Effect of the concentration of Wilkinson's Catalyst on the Molecular weight distribution for PMMA using 2.03 x 10^{-2} M AIBN as an Initiator in PLP of MMA

Entry	Time (minutes)	[Catalyst] milli molar	Conversion (%)	M_n	M_w	PDI
Control	45	0	12.72	14032	26565	1.89
A	45	0.036	15.05	6333	9826	1.52
B	45	0.108	15.71	10494	16347	1.56
C	45	0.181	17.26	13152	24291	1.85

but in reality one must know that usually PDI and molecular weights increases with the increase of percent conversion of MMA. It appears that autoacceleration due to the gel effect is probably operating to some extent. Actually the polymer weight depends on the ratio $[M]/[I]^{1/2}$.

In normal cicumstances initiator concentration [I] decreases faster than [M] and the molecular weight of the polymer produced at any instant increases with conversion. As a result, molecular weight distribution also increases with percent conversion. The sample C in which 0.181 mM Wilkinson's catalyst was used is still less (1.85 with percent conversion of 17.26 %) as compared to control sample for which PDI is 1.89 with percent conversion of 12.72 %. Although Wilkinson's catalyst does not inhibit the polymerization process (rather promotes it), it still narrows the molecular weight distribution curve. The corresponding GPC chromatograms are shown in Figure 5.28. It is clear from the chromatograms that the shape of chromatogram C is comparable to reference sample in which no Wilkinson's catalyst was added. The difference between chromatogram A and reference samples indicate that there is some change in the termination process in the presence of Wilkinson's catalyst. Since the amount of AIBN is constant in each sample, therefore it is concluded that Wilkinson's catalyst is responsible for the increase of percent conversion of PMMA.

In order to verify that Wilkinson's catalyst can act as a mild photoinitiator, a set of additional experiments was performed. The results are presented in Table 5.36. The control experiment (having no Wilkinson's catalyst) which was irradiated by the laser for 35 minutes, the percent conversion was noted to be 0.107 %, while for sample having

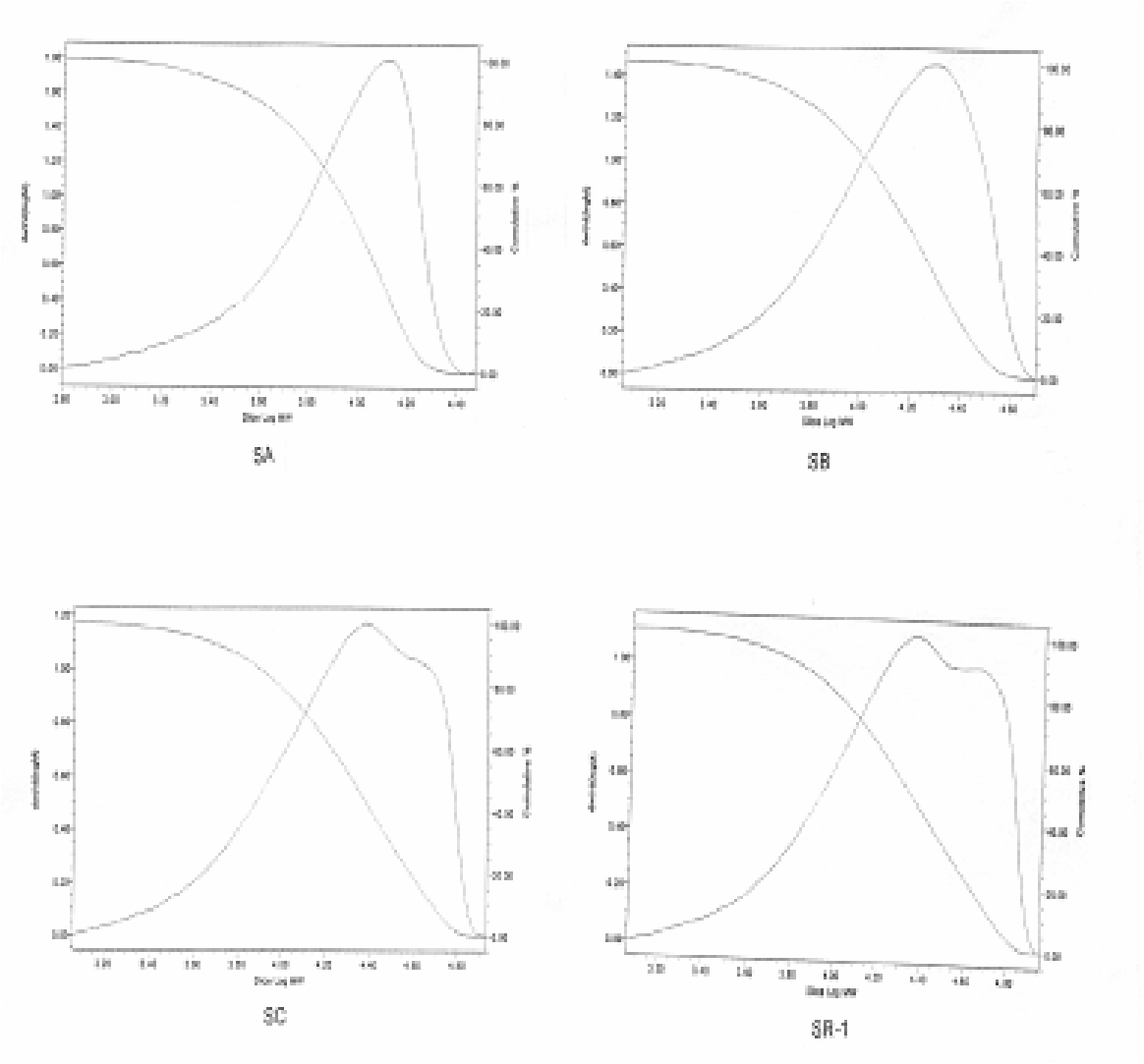

Figure 5.28 Molecular Weight Distribution Curves for different samples determined by GPC. SA, SB, SC and SR-1 have the same meaning as in Table 5.35

Table 5.36 Effect of the irradiation time on Pulsed Laser Polymerization of MMA at constant concentration (1.3 mM) of Wilkinson's Catalyst without using AIBN

entry	Time (min.)	Conversion (%)
1	25	0.122
2	35	0.565
3	45	0.710
Control	35	0.107

Wilkinson's catalyst with same duration of laser irradiation, the percent conversion is higher (0.565 %). UV/Vis spectrum for Wilkinson's catalyst indicates strong absorption bands at 276 nm, 268 nm, and 260 nm. There is also significant absorption around 308 nm for Wilkinson's catalyst, while for AIBN and MMA there is no significant absorption at this wavelength. All these observations suggest that Wilkinson's catalyst either dissociate itself to give free radicals, which in turn produce free radicals of MMA directly or enhance the total number of free radicals of AIBN when this is present. In this case photochemical activation has accelerated the ligand dissociation from Wilkinson's catalyst. Absorption of uv photon of the proper wavelength can excite an electron due to which a strong δ- anti-bonding effect would favor the loss of the more strongly δ-donating ligand [152]. In the present case PPh_3 is comparatively strong sigma donating ligand [153] than Cl^-, therefore Rh-PPh_3 bond has most probably broken [Scheme 5.4]. Additionally, by the dissociation of PPh_3 ligand steric interactions around Rh(I) will also decrease.

Another possibility is that Wilkinson's catalyst absorbs energy and moves to an excited state and from this excited state it loses it's extra energy to AIBN or directly to MMA monomer, and thus helps to form free radicals as indicated in equation 5.13. Therefore, Wilkinson's catalyst behaves like a photoinitiator or photosensitizer under excime laser irradiation.

$$D \xrightarrow{hv} D^* \xrightarrow{A} (D, A) \longrightarrow (\dot{D}^+, \dot{A}^-)^* \longrightarrow \text{radicals} \quad (5.13)$$

Scheme 5.4 Dissociation of Wilkinson's Catalyst in the presence of Ultra violet light

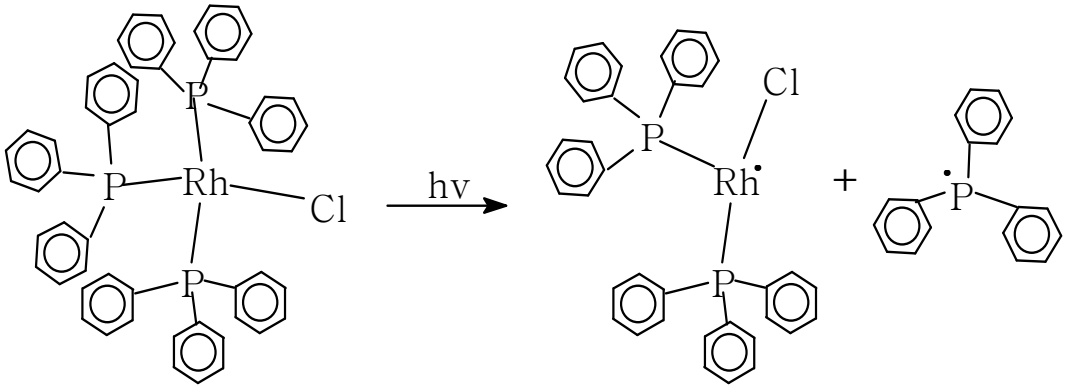

The ^{1}H NMR spectrum of PMMA of different tacticity [154] is shown in Figure 5.29. The ^{1}H NMR spectrum of PMMA formed in the presence of Wilkinson's catalyst is shown in Figure 5.30. The peaks around 3.60 ppm are due to OCH_3. The peak around 3.76 ppm is either from unreacted residual monomer or due to the terminal ester group, which is adjacent to a chlorine atom [143].

Three types of signals appear for methylene (CH_2) protons of PMMA. Owing to different environment of methylene protons in isotactic portion of atactic PMMA polymer, two separate peaks for methylene CH_2 protons appear. The doublet signal appearing around 2.3 ppm (downfield) corresponds to *erythreo* (Figure 5.31) methylene protons (these are trans to ester group). On the other hand *threo* protons produce double around 1.5 ppm. Unfortunately signals for *erythreo* and *threo* methylene protons (CH_2) can no longer be analyzed unambiguously. The methylene protons for syndiotactic PMMA appear as single moiety and gives comparatively strong signal around 2.0 ppm. Figure 5.29 suggests that in all cases in our experimental work the atactic PMMA was formed *i.e.* polymer incorporates simultaneously both type of C-CH_3 groups i.e. syndiotactic and isotactic. Both C-CH_3 and O-CH_3 peaks for the samples C, B, and A are shifted to some extent with respect to C-CH_3 and OCH_3 peaks of reference sample. For the analysis of atactic ^{1}H NMR spectrum, we must include in our discussion not only the nearest, but also the next nearest neighbors, i.e. we usually need to look at the triad, tetrad sequences [Figure 5.31] as compared to diad sequence [154]. In atactic PMMA formed in this work (Figure 5.30), like other atactic PMMA, C-CH_3 groups produce three signals of very different intensities in the region 0.80-1.18 ppm.

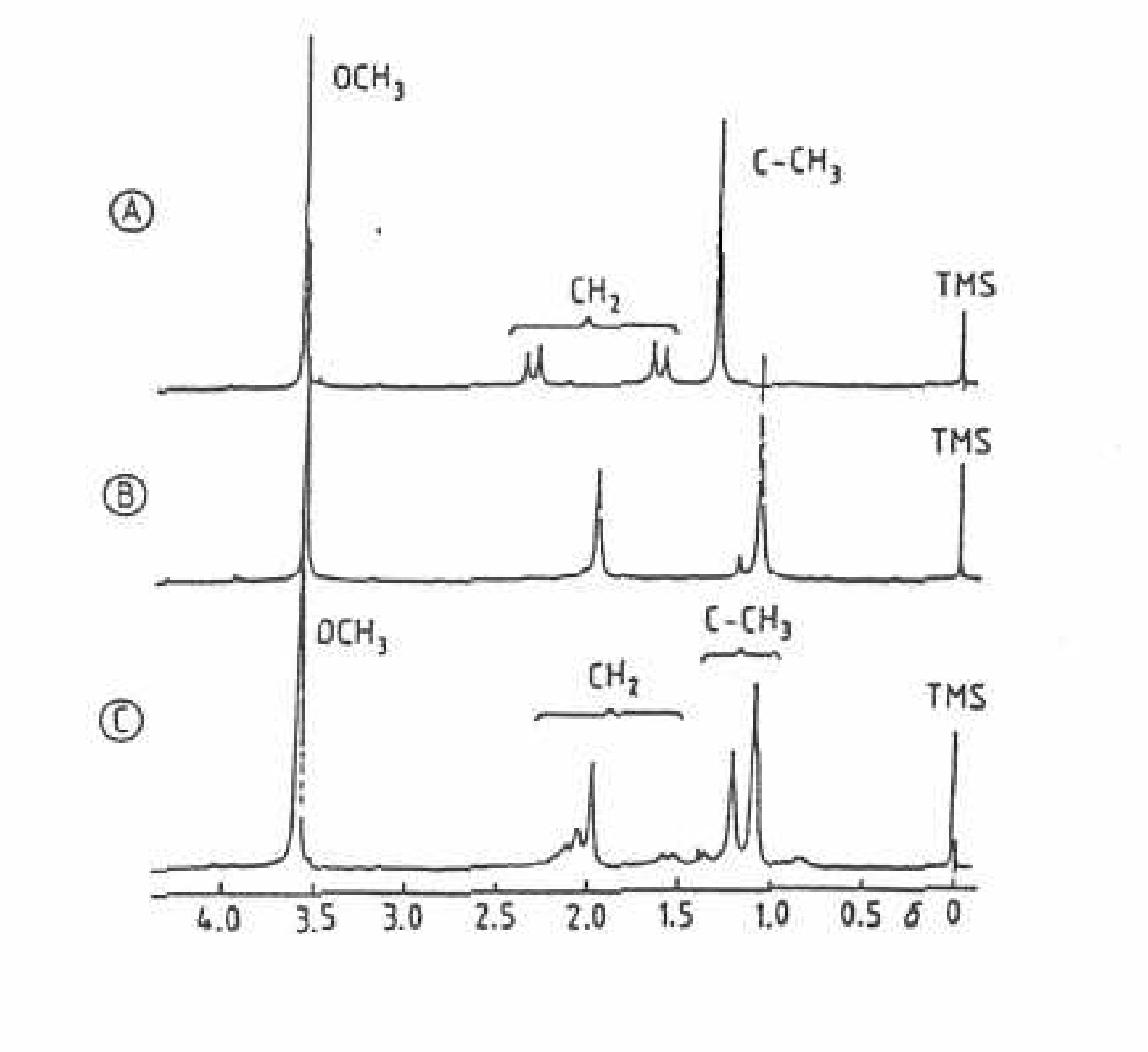

Figure 5.29 220 MHz ^{1}H NMR spectra of PMMA samples of different tacticities in o-dicholorobenzene at 100 °C. A: isotactic; B: syndiotactic; C: atactic.

Taken from reference 154

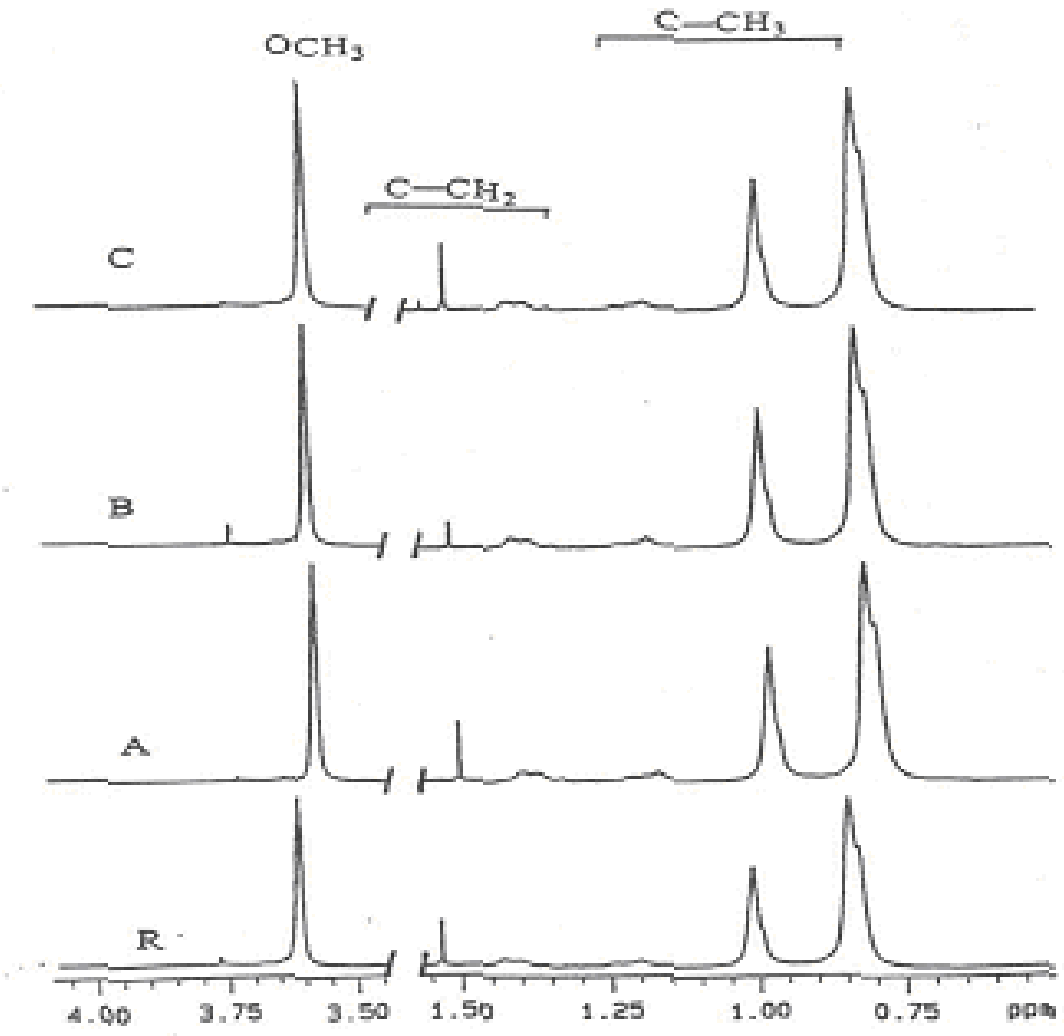

Figure 5.30 500 MHz ^{1}H NMR spectra of PMMA samples in $CDCl_3$ at 298 K. The spectrum "R" indicate PMMA sample prepared in the absence of Wilkinson's Catalyst

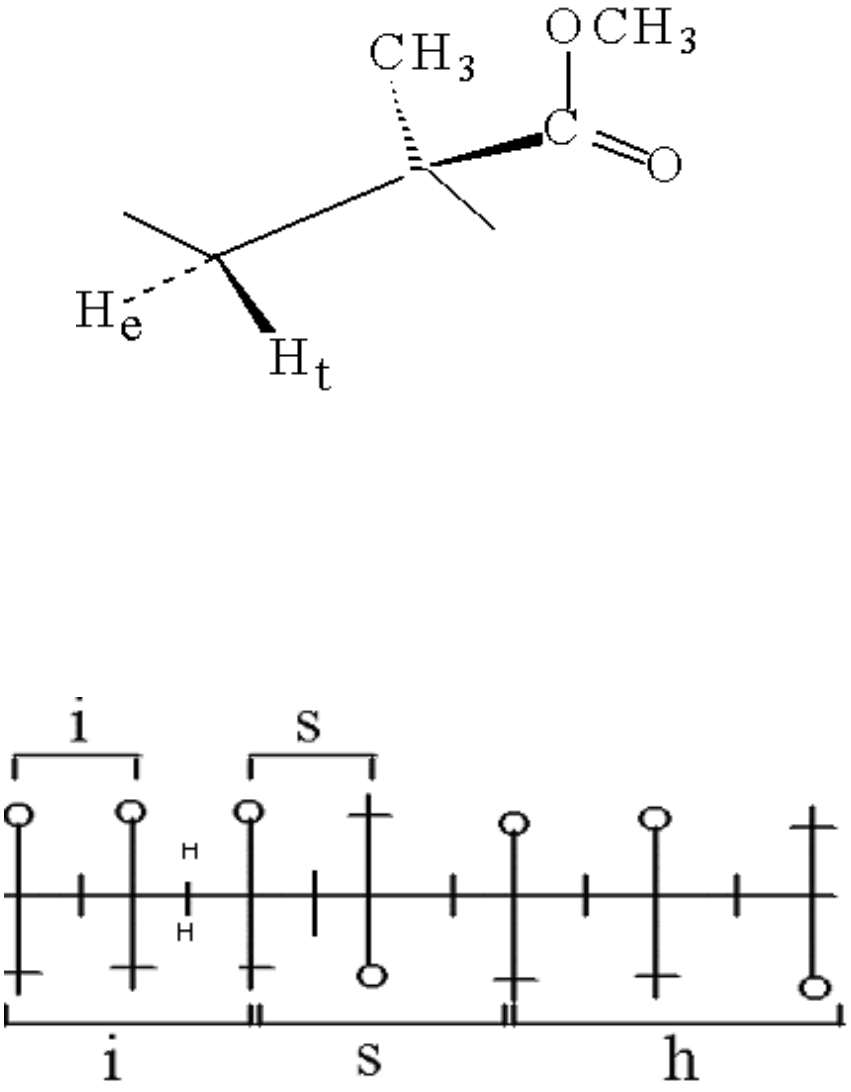

Figure 5.31 **(Top)** The conformation indicating non-equivalent methylene protons (**Bottom**) Diagram indicating diads and triads. † and 0 indicate CH_3 and $–COOCH_3$ group in MMA, respectively. Taken from reference 154

The signal at 0.80 ppm indicates syndiotactic arrangement of C-CH_3 groups in the atactic PMMA sample, while signal around 0.98 ppm corresponds to isotactic arrangement of C-CH_3 groups in the same atactic PMMA sample. The signal at 1.18 ppm belongs to methyl groups at changeover positions between isotactic and syndiotactic C-CH_3 groups in the atactic PMMA sample. Integration ratios for syndiotactic to isotactic C-CH_3 groups are shown in Table 5.37.

5.3.3 Pulsed Laser Polymerization of Methyl methacrylate in the presence of [Co(afdo-2H.BF_2)$_2$] as Chain Transfer Agent

The results for percent conversion of this polymerization are presented in Table 5.38. The percent conversion for pulsed laser polymerization of MMA decreased to almost 50 % with the addition of 33.3 ppm of [Co(afdo-2H.BF_2)$_2$] chain transfer agent. When concentration of this agent was raised to 55.6 ppm no dectecable polymer was observed. Then the remaining two samples having 83.3 and 111.1 ppm of CTA were polymerized at 60 °C (no laser present) for a duration of 40 minutes but again no detectable amount of polymer was noted. Results of Table 5.38 also reveal that as concentration of [Co(afdo-2H.BF_2)$_2$], transmitted energy decreases, e.g. sample having no CTA transmits 23.3 mJ enegy, while sample with 33.3 ppm of CTA only transmits 6.0 mJ energy. The point to point C_s values for the first two samples polymerized with excimer laser was calculated and noted to be 15,040. The PDI value for the sample with 4.42 x 10^{-5} M CTA concentration in Table 5.39 is greater than two and thus indicates dominant chain transfer catalysis.

Table 5.37 Intensity ratios of syndiotactic to isotactic C-CH_3 groups in ^{1}H NMR of atactic PMMA

Entry	**Intensity ratio**
Ref.	2.4951
A	2.5215
B	2.4738
C	2.4156

Table 5.38 PLP of MMA using [Co(afdo-2H.BF_2)$_2$] as a Chain Transfer Agent

[Co(II)] ppm	Time (minutes)	Trans.Ene.(mJ)	Conversion (%)
0.0	30	23.3	5.02
33.3	40	6.0	2.57
55.6	40	5.4	-----*
83.3	40**	-----	-----**
111.1	40**	-----	-----**

* No solid PMMA was detected in methanol.

** These samples were subjected to heat at 60 °C without using Laser.

Table 5.39 Results for the Molecular weight distribution for the PLP of MMA using [Co(afdo-2H.BF_2)$_2$] as a Chain Transfer Agent

[Co(II)] catalyst x 10^5	M_n	M_w	*M_p	PDI
0	5964	7125	7693	1.20
4.42	1140	2540	2381	2.23

*Peak molecular weight is determined at the point where detector response is maximum

5.3.4 Pulsed Laser Polymerization of Methyl methacrylate in the presence of [Co(afdo-2H.BF_2)$_2$] and [Co(dmg-2H.BF_2)$_2$] Chain Transfer Agents

The results for the polymerization of Methyl methacylate in the presence [Co(dmg-2H.BF_2)$_2$] and [Co(afdo-2H.BF_2)$_2$] catalysts are given in Table 5.40 and Table 5.40, respectively. The present percent conversion was kept under 8% for PLP of MMA using [Co(afdo-2H.BF_2)$_2$] catalyst and below 16% for PLP of MMA by [Co(dmg-2H.BF_2)$_2$]. This was required because quartz cell capacity was only 4.0 ml and a reasonable amount of the product was needed for all the analysis to be performed. This is well known that chain transfer phenomenon is usually studied below the percent conversions we obtained. Like other reported Co(II) chain transfer agents, the catalysts reported here, are quite effective at ppm level. Figure 5.32 indicate that there is a propensity for the decrease in percent conversion with an increase in catalyst concentration. Initially number average molecular weight (M_n) was calculated with the help of ^{1}H NMR (Table 5.42). Previously [144,155] this technique was used to calculate the M_n for macronomers and it was found that results were quite comparable to M_n values calculated from GPC. But, for the polymers, the peak heights, although easily measured, are not a reliable measure of relative intensities [156] since peak widths, being proportional to T_2^{-1}, will in general differ for different protons.

Comparison of results in Table 5.40 and Table 5.41 show that the MMA monomer samples having [Co(dmg-2H.BF_2)$_2$] as a CTA have higher values of

Table 5.40 Pulsed Laser Polymerization of MMA in the presence of [Co(dmg-2H.$BF_2)_2$] Chain Transfer Agent using AIBN as an Initiator

Run#	Voltage (kV)	Transmitted Energy (mJ)	Catalyst ppm	Conversion (%)
1	17.4	478	0	16.19 (16.16)*
2	17.7	476	1.0081	14.59 (14.56)
3	17.9	470	2.8409	13.08 (13.07)
4	17.8	465	3.6765	12.77 (12.75)
5	17.8	470	4.4643	12.29 (12.16)
6	17.8	460	9.6155	11.62 (11.50)

* The values in brakets have been calculated by subtracting the contribution of unreacted residual MMA monomer in the sample. This substraction was performed by using ^{1}H NMR spectrum of the respective samplees.

Table 5.41 Pulsed Laser Polymerization of MMA in the presence of [Co(afdo-2H. $BF_2)_2$] Catalyst using AIBN as Initiator. Duration of laser irradiation for each sample is 50 minutes

Run #	**Voltage (KV)**	**Transmitted Energy(mV)**	**Conversion (%)**	**M_n***	**M_w***	**PDI**
1	18.0	116-97	7.55	6200	7400	1.19
2	18.1	97-90	7.50	5500	7000	1.27
3	18.2	93-87	7.02	5000	6900	1.38
4	18.0	86-66	6.26	4800	6400	1.33
5	18.0	72-55	5.80	4700	6200	1.32

*The values are rounded to the nearest hundred

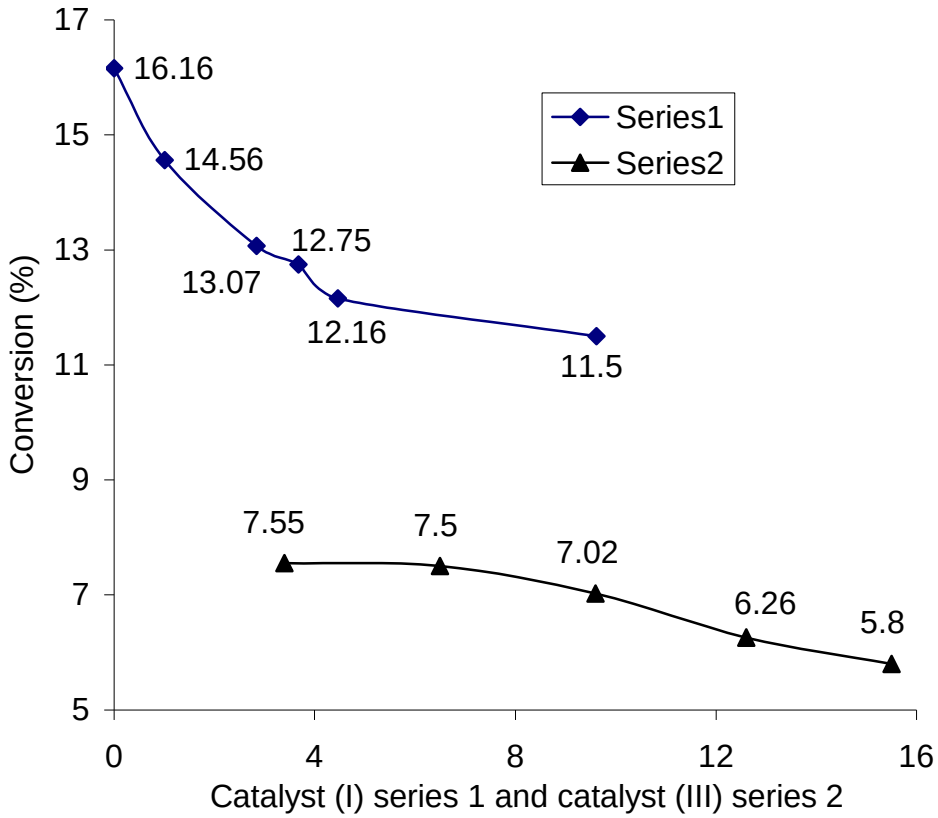

Figure 5.32 Graph indicating effect of [Co(dmg-2H.BF_2)$_2$] (series 1) and [Co(afdo-2H.BF_2)$_2$] (series 2) catalyst on percent conversion for PLP of MMA

Table 5.42 ^{1}H NMR results for Molecular weight and "C_s" value calculation for PLP of MMA in the presence of [$Co(dmg\text{-}2H.BF_2)_2$] catalyst

Run#	$^{*}M_n^{NMR}$	[Catalyst] x 10^6	DP_n	$1/DP_n - 1/DP_{n(o)}$ x 10^3	$[S]/[M]^{**}$ x 10^7
1	45200	0.000	452	-----	-----
2	19200	2.387	192	2.996	2.554
3	12800	6.727	128	5.601	7.199
4	8100	8.706	81	10.134	9.316
5	5900	10.574	59	14.737	11.315
6	3800	22.769	38	24.104	24.365

* The number-average molecular weight calculated from the ^{1}H NMR data. The procedure is similar as reported in reference [144].

** [M] indicates [MMA] i.e moles per liter of MMA

transmitted enegy (between 460-478 mJ), while the samples with [Co(afdo-2H.BF_2)$_2$] CTA have significantly transmitted energy (between 55-116 mJ). This is probably due to α-furilglyoxime ligand, which has extensive conjugation and thus absorbs more excimer laser at 308 nm. It is also noted that (Table 5.41) towards the end of polymerization, amount of transmitted enrgy decreses.

The M_n values calculated by ^{1}H NMR in the present work are summarized in Table 5.42 while Table 5.43 incorporates molecular weights obtained from GPC and other parameters needed to calculate the "C_s" value. There is gradual decrease both on M_n and M_w values with an increase in catalyst concentration. Mayo plot for polymerization of MMA in the presence of [Co(afdo-2H.BF_2)$_2$] chain transfer agent is shown in Figure 5.33 and yields a C_s value of 2530. The necessary data required to calculate C_s value is shown in Table 5.44. A linear regression (Figure 5.34 and Figure 5.35) was performed on the experimental data in the form of $1/DP_n$ against [catalyst]/[MMA] to evaluate the C_s value for the PLP of MMA in presence of [Co(dmg-2H.BF_2)$_2$] chain transfer agent. The slope of these lines passing through the origin equates to the chain transfer constant 10,342 and 13,400 for (number average molecular weights obtained from) ^{1}H NMR and GPC techniques, respectively.

For PLP of MMA by [Co(afdo-2H.BF_2)$_2$] catalyst the "C_s" value is four orders of magnitude lower than the value found for [Co(dmg-2H.BF_2)$_2$] chain transfer agent**.** Actually, cobalt (II) complexes [157-159] belong mainly to two types. The unpaired electron in both types of paramagnetic complexes is believed to lie in the dz^2 orbital [68,160-161].

Table 5.43 GPC results for Molecular weight distribution for PLP of MMA in the presence of [Co(dmg-2H.BF_2)$_2$] as Chain Transfer Agent

Run#	M_n	M_w	M_p	PDI	DP_n	$1/DP_n-1/DP_{n(o)}$ x 10^3
1	9582	19205	21152	2.00	95.66	-----
2	6820	11816	12913	1.73	68.09	4.24
3	4974	7457	7599	1.50	49.66	9.69
4	4058	5802	5155	1.43	40.52	14.23
5	4180	5984	5597	1.43	41.73	13.51
6	3179	4094	2896	1.29	31.74	21.06

Table 5.44 Summary of experimental results for the determination of the chain transfer constant at 25 °C for PLP of MMA in the presence of [Co(afdo-2H.BF_2)$_2$] as Chain Transfer Agent

Run	[catalyst] x 10^6	[Catalyst]/[MMA] x 10^6	DP_n	$1/DP_n x10^2$
1	5.21	0.5566	62.00	1.613
2	10.26	1.0962	55.00	1.818
3	15.14	1.6175	50.00	2.000
4	19.87	2.1229	48.00	2.083
5	24.46	2.6132	47.00	2.128

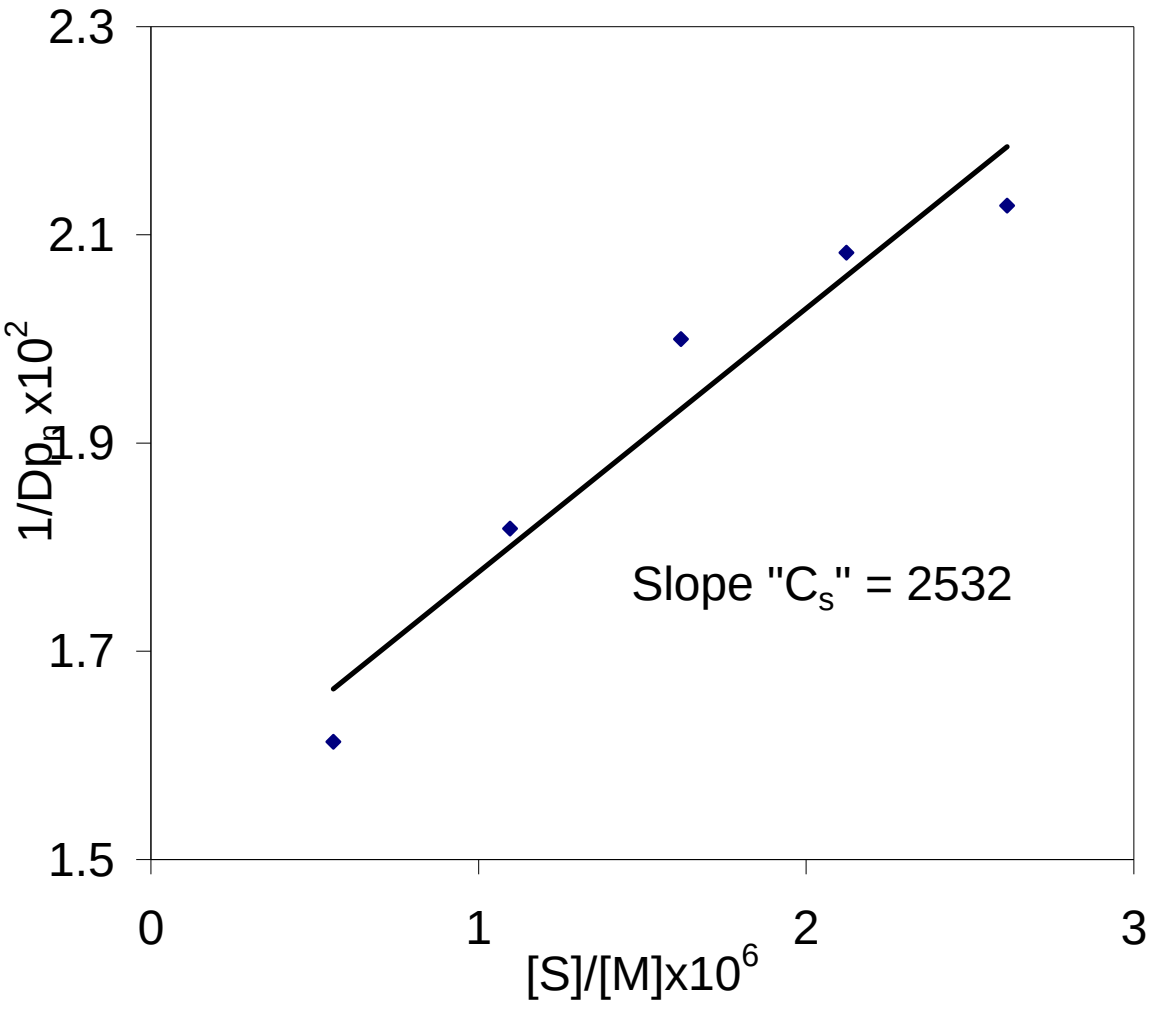

Figure 5.33 Mayo plot for Pulsed Laser Polymerization of MMA using [Co(afdo-2H.BF_2)$_2$] as a Chain Transfer Agent

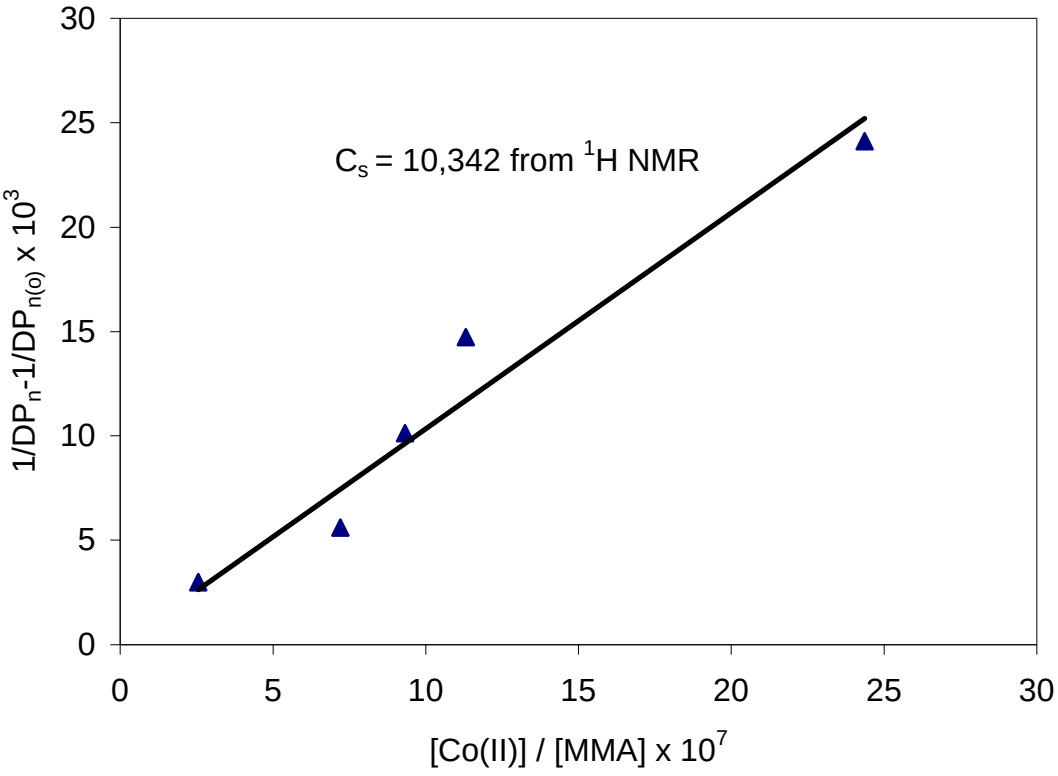

Figure 5.34 Mayo plot for Pulsed Laser Polymerization of MMA using [Co(dmg-2H.BF_2)$_2$] as a Chain Transfer Agent. Data from ^{1}H NMR was used

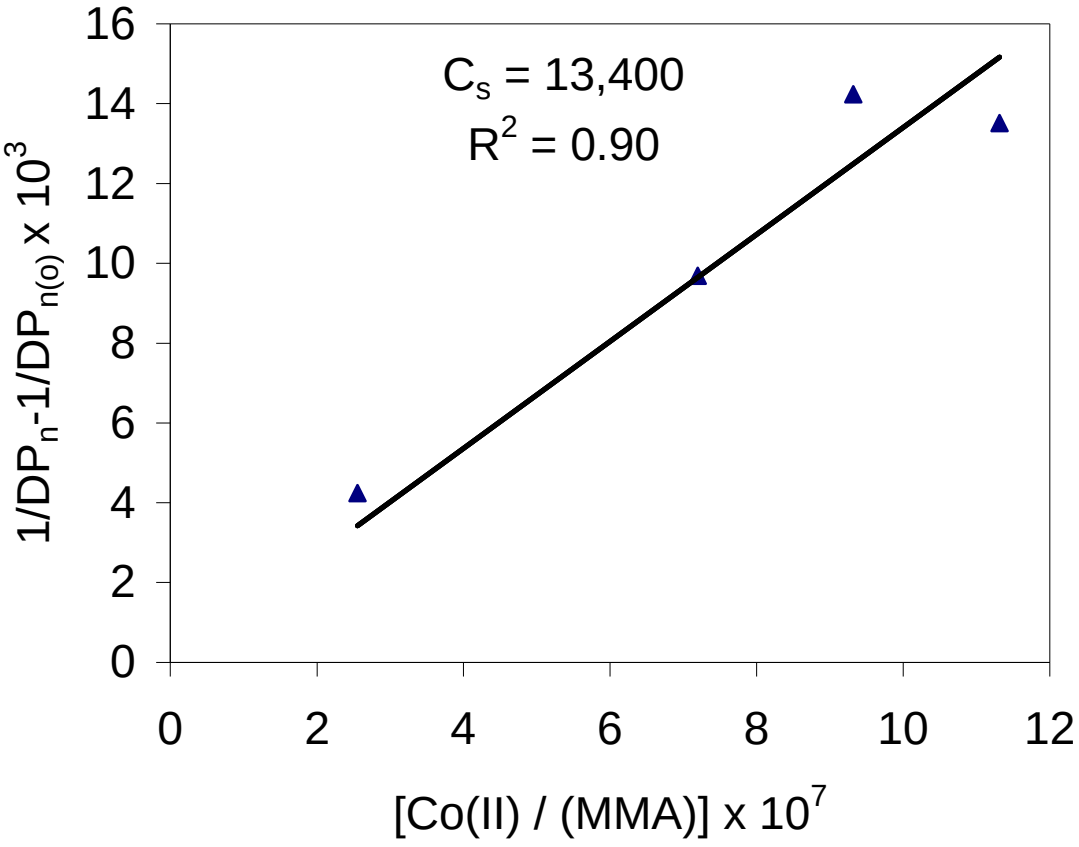

Figure 5.35 Mayo plot for Pulsed Laser Polymerization of MMA using [Co(dmg-2H.BF_2)$_2$] as a Chain Transfer Agent. Data from GPC technique was used

At this stage it is fruitful to recall that, for [Co(afdo-2H.BF_2)$_2$] there is a significant d_π-p_{π^*} back bonding due to which C=N characters increase with concomitant increase in C=N vibrational frequency. In case of [Co(afdo-2H.BF_2)$_2$] catalyst the two sharp peaks in FTIR due to water molecules appeared at 3570 and 3628 cm^{-1}, which is an indication that σ-donation of electron from water molecule (ligand) is higher in this complex compared to [Co(dmg-2H.BF_2)$_2$]. There is more back bonding in case of [Co(afdo-2H.BF_2)$_2$] catalyst compared to [Co(afdo-2H.BF_2)$_2$] catalyst. Another indication of comparatively strong back bonding (d_π-p_{π^*}) in [Co(afdo-2H.BF_2)$_2$] catalyst is appearance of Co-N stretching vibrations (Table 5.3) at higher wave numbers (504 & 542 cm^{-1}) compared to [Co(dmg-2H.BF_2)$_2$] catalyst, which appear at lower wave numbers (464 & 502 cm^{-1}) [130]. Table 5.3 incorporates summary of IR peaks for both free ligands and Co(II) complexes used as chain transfer agents. The π-π* transitions of typical cobaloxime is observed at 250 and 264 nm in H_2dmg and H_2afdo free ligands. From the data in Table 5.4 we can assign transitions from 460-545 nm in both the complexes as metal to ligand charge transfer (MLCT) transitions. However, metal to ligand charge transfer (MLCT) transition in [Co(afdo-2H.BF_2)$_2$] catalyst takes place at lower energy and with more transition probability (ε value). This observation further substantiates the fact that due to extensive conjugation in [Co(afdo-2H.BF_2)$_2$] catalyst, there is a strong d_π-p_{π^*} transition probability, thus resulting in less availability of unpaired electron in [Co(afdo-2H.BF_2)$_2$] catalyst and thus reducing its performance to act as a chain transfer agent. On the basis of "C_s" values for [Co(dmg-2H.BF_2)$_2$] and [Co(afdo-2H.BF_2)$_2$] chain transfer agents, it is justifiable to believe that the former is more nucleophilic in nature than the later. This is also supported from the spectroscopic data highlighted earlier.

It is noted that polydispersity index (PDI) values for polymers formed with Pulsed Laser Polymerization of MMA in the presence of Co(II) complexes as chain transfer agents [Figure 5.36] are remarkably lower than 2, especially with [Co(afdo-2H.BF_2)$_2$] catalyst [Figure 5.37]. For [Co(dmg-2H.BF_2)$_2$] catalyst there is gradual decrease in PDI values with concentration of catalyst. This probably indicates that Pulsed Laser Polymerization with [Co(afdo-2H.BF_2)$_2$] catalyst is "living polymerization" in nature. Therefore, we believe that the formation of the Co-C bond with catalyst (III) is reversible **(Scheme 2.1-2.4)** [28], which is in accordance with free-radical polymerization of acrylates.

Since in the present investigation irradiating excimer laser wavelength is 308 nm, therefore, it is also beneficial to note the effect of the amount of absorbed light on the Co-C bond breaking process. It has been noted (Table 5.4) that for the [Co(afdo-2H.BF_2)$_2$] catalyst molar absorptivity (24,400 L mol^{-1} cm^{-1}) is four orders of magnitude higher than [Co(dmg-2H.BF_2)$_2$] catalyst (5,590 L mol^{-1} cm^{-1}), which can also be the reason for hampering the Co-C bond formation or facile Co-C bond dissociation in [Co(afdo-2H.BF_2)$_2$] catalyst compared to [Co(dmg-2H.BF_2)$_2$] catalyst.

The literature data [68,160-161] suggest that for Co(II) square planar complexes (as we assume the same structure in bulk PLP of MMA due to highly labile water molecules) the unpaired electron occupies the dz^2 orbital, which perturb the growing free radical polymer chain and produce new Co-C bond by interacting with unpaired electron in the sp^2 orbital of the growing oligomer or polymer chain (R_n). From Co(III)-Rn

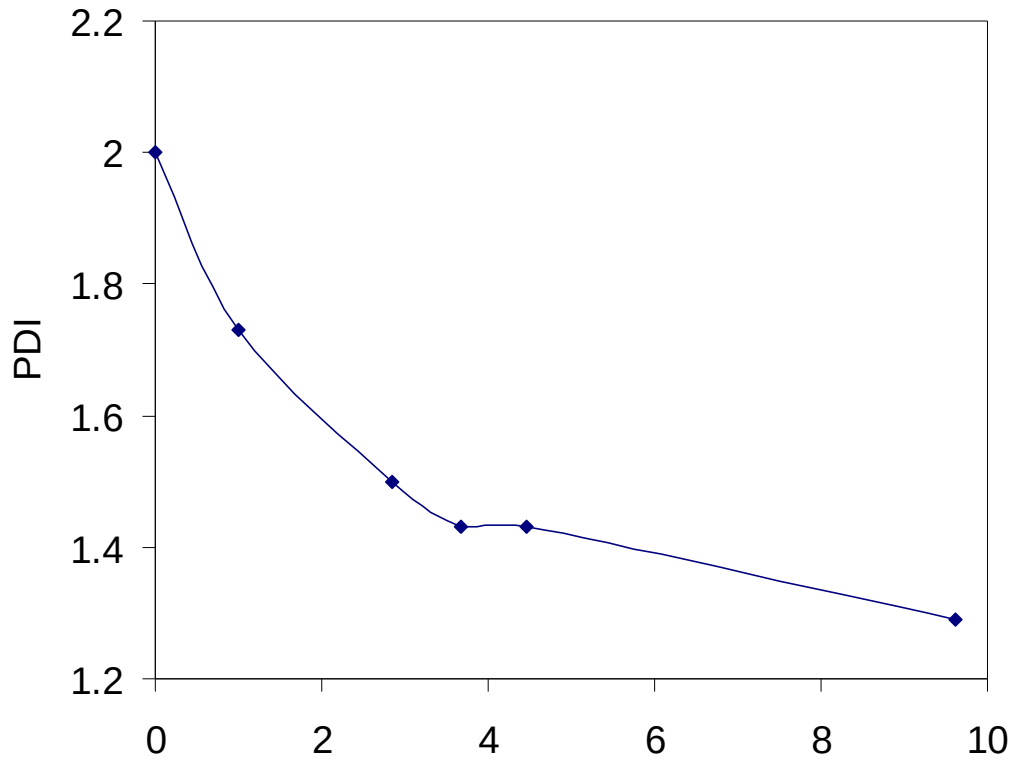

Figure 5.36 Dependece of PDI values on concentration of [Co(dmg-2H.BF_2)$_2$] catalyst for the Pulsed Laser Polymerization of MMA at 25 ºC

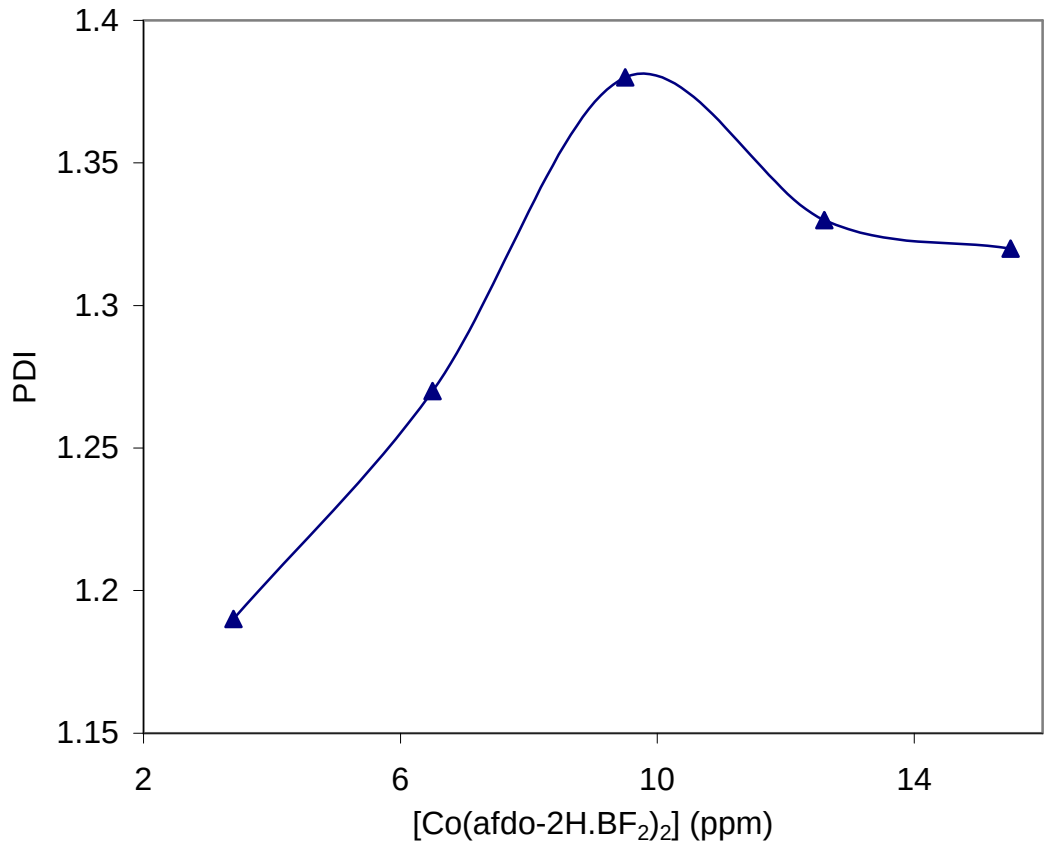

Figure 5.37 Dependece of PDI values on concentration of [Co(afdo-2H.BF_2)$_2$] for the Pulsed Laser Polymerization of MMA at 25 ºC

intermediate, β-elimination of hydrogen takes place thereby producing a dead polymer chain "P_n" and "LCo(III)H" cobalt hydride [Scheme 2.2]. It is important to note that both Co(III) ions and H^{-1} (hydride ion) are soft acid and base respectively.

The overlap of "dz^2" with "s" orbital of hydride ion (which is of comparable size as I^-) is better than "dz^2" with "sp^2"orbital of growing polymer chain. In [Co(dmg-2H.BF_2)$_2$] chain transfer agent, dz^2 orbital is at higher energy state, because of the presence of four elctron donating groups (–CH_3 groups) in stead of four electron withdrawing groups (furil groups) in [Co(afdo-2H.BF_2)$_2$] catalyst. This results in higher energy and size of the dz^2 orbital and thus increasing its ability to intercept the growing polymer chain. This is shown in Figure 5.38.

In atactic PMMA formed in this work, like other atactic PMMA [151,161-162], C-CH_3 groups produce three signals of very different intensities (as discussed earlier) in the region 0.85-1.20 ppm [Figure 5.39]. In this Figure, the area between 5.4 to 6.2 ppm has been blown up and this is the area where vinyl protons of both residual monomer and polymer are absorbed. In Figure 5.39 we can see that the these vinyl protons of monmer and polymer are not equal. Results for ^{13}C NMR spectra of PMMA samples polymerized in the presence of [Co(dmg-2H)$_2$(BF_2)$_2$] chain transfer agent is shown in Table 5.45, while DEPT spectra is shown in Figure 5.40. The signal of ^{13}C for "rr" arrangement of α-CH_3 in PMMA appears around 16.50 ppm, while signal for "mr" arrangement appears around 18.70 ppm. The intensity of peak is noted to be higher for the former arrangement as compared to later one. The signal for isotactic arrangement (mm) of ^{13}C is very weak thereby indicating less probability of isotactic portion of PMMA in atactic PMMA. A similar trend has been noted for the three signals of quaternary carbon atoms between

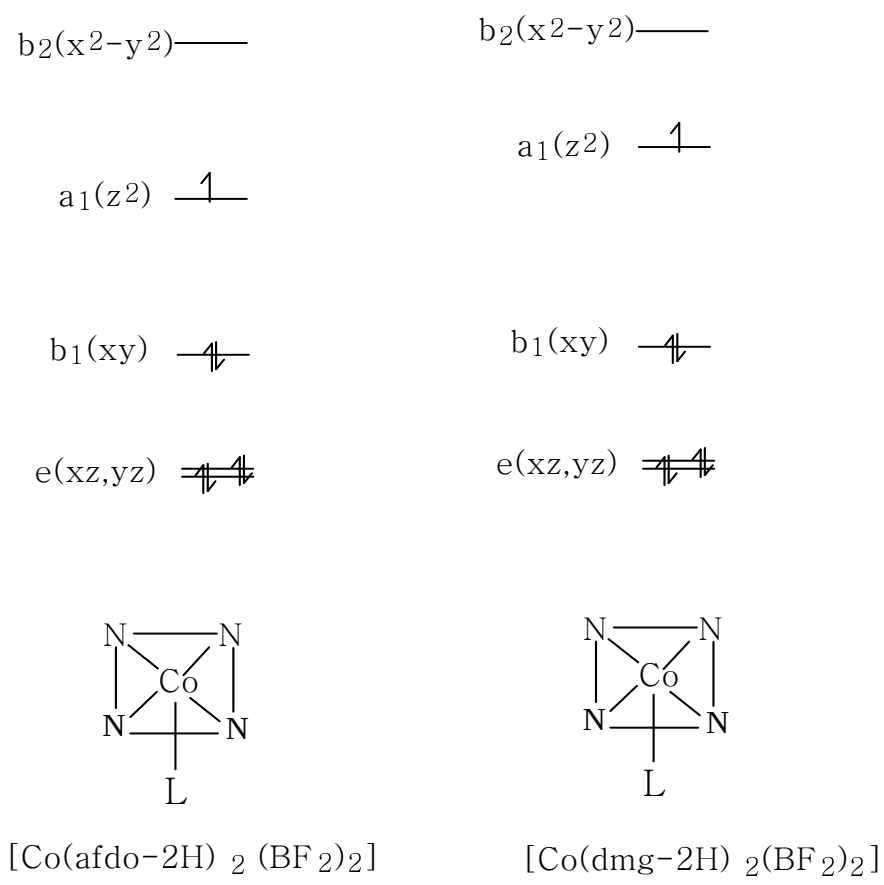

Figure 5.38 A qualitative molecular orbital scheme for the energy levels of Co(II) catalysts (1 and 2) used as Chain Transfer Agent in PLP of MMA. Ligand (L) indicates H_2O molecule at pyramidal position

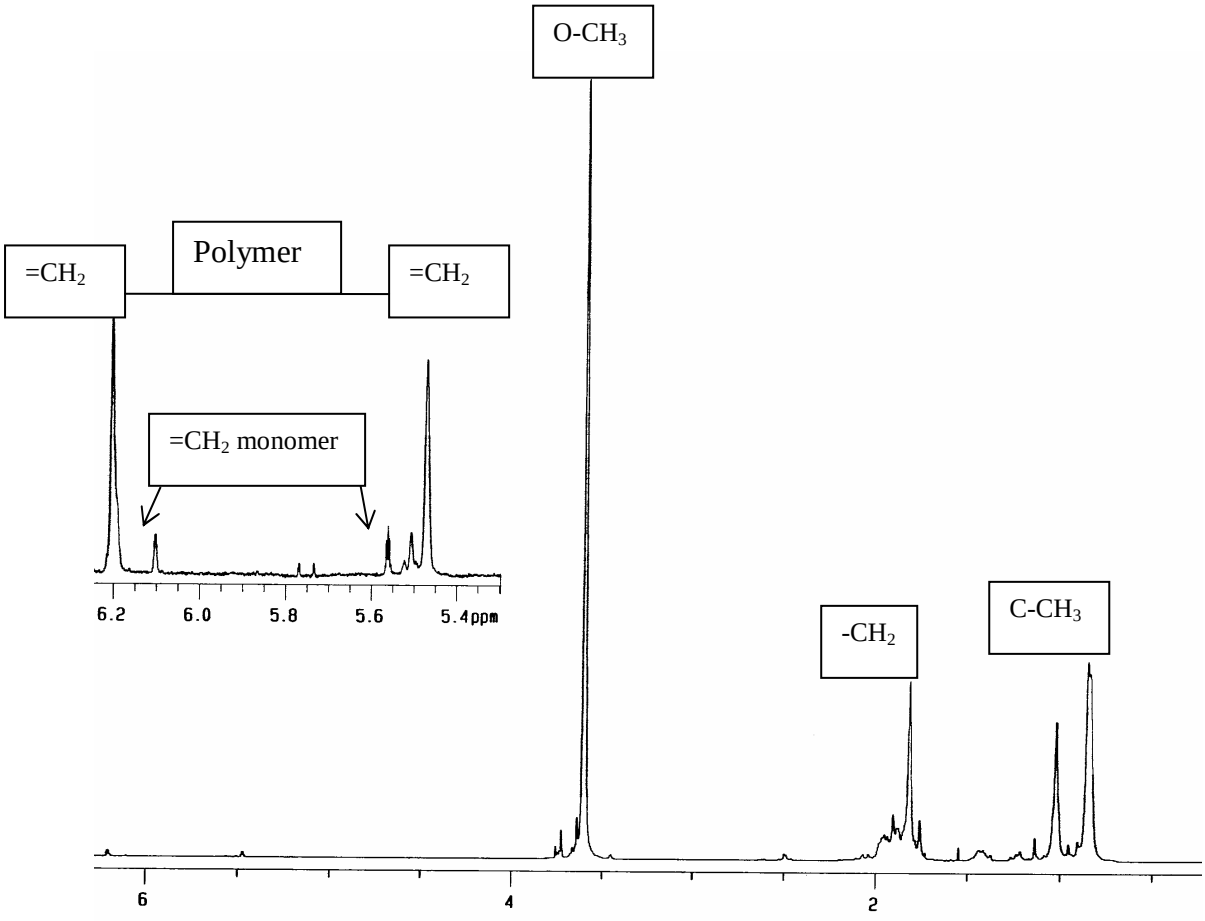

Figure 5.39 ^{I}H NMR spectrum of PMMA (sample 4) with blown up from 5.4 to 6.2 ppm

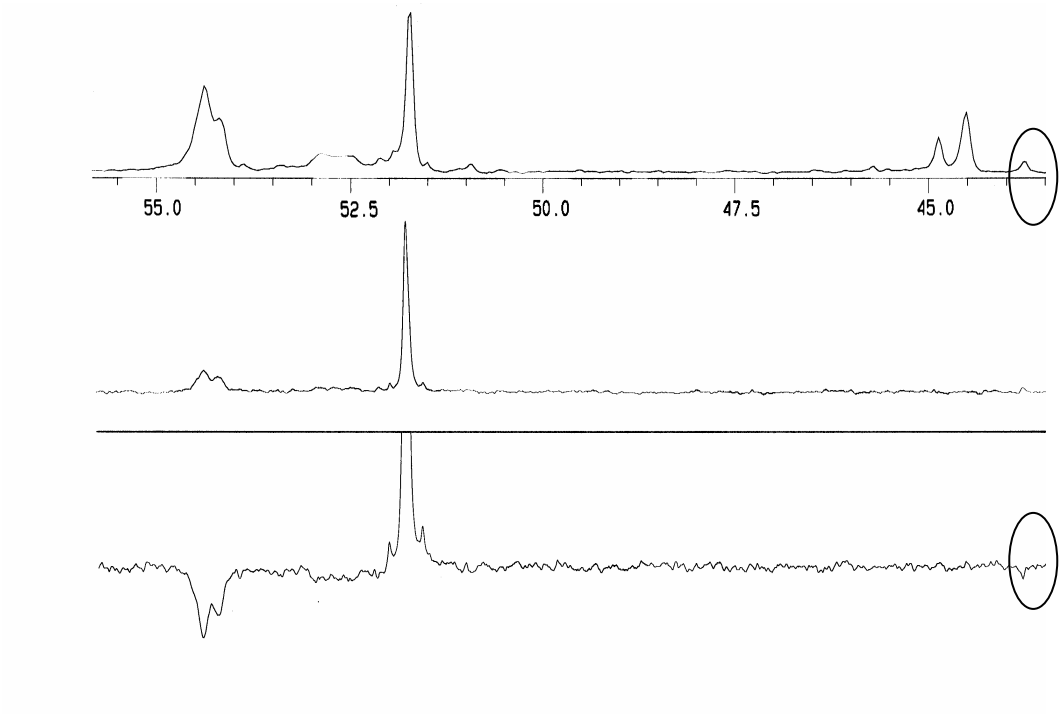

Figure 5.40 ^{13}C with DEPT 45 and 135 spectrum of PMMA sample 6 in Table 5.44

Table 5.45 Results for ^{13}C NMR spectra of PMMA samples using [Co(dmg-2H.BF_2)$_2$] at 25 ºC

Peak Identity	Stereo-sequence	Sample 1 δ = ppm	Sample 2 δ = ppm	Sample 3 δ = ppm	Sample 4 δ = ppm	Sample 5 δ = ppm	Sample 6 δ = ppm
α-CH_3	rr	16.49	16.53	16.50	16.46	16.46	16.46
	mr	18.70	18.74	18.74	18.70	18.70	18.70
	mm	21.04W	21.10W	21.09W	21.16W	20.94W	21.07W
		22.06W	22.36W	22.33W	22.25W	22.29W	22.38W
C-Q	rr	44.52	44.59	44.56	44.52	44.52	44.52
	mr	44.87	44.91	44.91	44.87	44.87	44.87
	mm	45.10W	45.13W	45.08W	45.12W	45.13W	45.10W
OCH_3		51.76	51.80	51.80	51.76	51.73	50.92,
		54.16	54.20	54.20	54.16	54.16	51.73
		52.62B	52.70B	52.66B	52.62B	52.65B	52.88B
-CH_2		54.38	54.43	54.43	54.62	54.38	54.16 54.38
=CH_2		----	----	----	128.45	128.36	128.45
C=O	mm	175.54W	175.62W	175.56W	175.55W	175.60W	175.62W
	rm	176.91	176.95	176.95	176.91	176.88	176.88
	rr	177.75	177.79	177.79	177.7	177.75	177.75

44.5 to 45.1 ppm. Terminal vinylic $^{13}CH_2$ signal appears around 128.5 ppm. In case of ^{13}C for carbonyl signals, trend is somewhat different as “mm” signal appears before “rr” signal. However, signal for “mm” arrangement is still weaker as compared to “rm” and “rr” signals. DEPT 45 and DEPT 135 indicate that signal around 54.4 ppm is due to methylene carbon atoms instead of ester carbon atoms.

5.3.5 Pulsed Laser Polymerization of Butyl methacrylate in the presence [Co(dmg-2H.BF_2)$_2$] Chain Transfer Agent

The results for PLP of Butyl methacrylate are presented in Table 5.46. It was noted that with the addition of 2.50 ppm of [Co(dmg-2H.BF_2)$_2$] catalyst, weight average molecular weight (M_w) decreased from 27,637 to 12,096. This corresponds to a difference of 15,540, which represents more than 100 % decrease in molecular weight. With the addition of 4.7 ppm catalyst, a decrease of 5,120 molecular weight was observed, which again represents more than 100 % decrease in molecular weight. After this there is no significant decrease in weight average molecular weight with [Co(dmg-2H.BF_2)$_2$] catalyst concentration. There is an erratic behavior both for Polydispersity Index (PDI) values, ranging from 13.05 to 4.21, and Peak Molecular Weight (M_p). This is probably due to instrumental error since detector response is known to be maximum for peak molecular weight. The lack of any regularity in number-average molecular weight (M_n) further validates our assumption about instrumental error. High PDI values can also be due to chain transfer to polymer. Davis and co-workers [46] used tetramer of MMA as chain transfer agent for free-radical polymerization of Butyl methacrylate. They found

Table 5.46 Data for Pulsed Laser Polymerization of BMA using [Co(dmg-2H.BF_2)$_2$] as a Chain Transfer Agent

catalyst (ppm)	M_n	M_w	M_p	PDI
0	2117	27637	1199	13.05
2.50	2661	12096	2594	4.55
4.70	823	6976	455	8.47
6.67	643	7776	276	12.10
8.42	1287	6065	1278	4.71
10.00	1462	6157	1633	4.21

that tetramer of MMA indeed acts as a chain transfer agent. Keeping this in mind we can predict that not only [Co(dmg-2H.BF_2)$_2$] is acting as chain transfer agent but also resulting small chain molecules of MMA are acting as chain transfer agent. Therefore, both these factors (especially chain transfer to polymer) are responsible for high polydispersity index values. Odian [34] has also stated that, "Excessive molecular-weight broadening occurs when branched polymers are produced by chain transfer to polymer. Chain transfer to polymer can lead to M_w/M_n ratios as high as 20-50".

Since it is well known that for low molecular weight polymers M_n are not reliable due to the base line corrections, therefore, it is advisable to use weight-average molecular weight (M_w) values under such circumstances. In Table 5.47 degree of polymerization was calculated from M_w values and Mayo plot (not shown) produced a C_s value of 11,080. High value of chain transfer coefficient certainly indicates that [Co(dmg-2H.BF_2)$_2$] CTA acts as a good chain transfer agent for pulsed laser polymerization of Butyl methacrylate.

5.3.6 Pulsed Laser Polymerization of Butyl methacrylate in the presence of [Co(afdo-2H.BF_2)$_2$] Chain Transfer Agent

Results of Pulsed Laser Polymerization of Butyl methacrylate (BMA) in the presence of [Co(afdo-2H.BF_2)$_2$] complex are shown in Table 5.48. These results again indicate that either the detector response is not good or chain transfer to polymer has taken place. It is important to note that with the addition of catalyst there is remarkable decrease in polydispersity index (PDI) values [Figure 5.41].

Table 5.47 Data for Mayo Plots for Pulsed Laser Polymerization of BMA using $[Co(dmg\text{-}2H.BF_2)_2]$ as Chain Transfer Agent

[catalyst] x 10^6	[catalyst]/[M] x 10^7	DP_n	$1/DP_n$ x 10^2	DP_w	$1/DP_w$ x 10^2	$1/DP_w$-$1/DP_{w(o)}$ x 10^2
0.00	0.00	-----	----	97.31	1.03	----
5.94	9.41	18.74	5.34	42.60	2.35	1.32
11.20	17.7	5.80	17.24	24.56	4.07	3.04
15.80	25.0	4.53	22.08	27.38	3.65	2.62
20.00	31.7	9.06	11.04	21.36	4.68	3.65
23.80	37.7	10.30	9.71	21.68	4.61	3.58
			*C_s = 6770			*C_s = 11080

* These C_s values calculated from slope of the lines of corresponding Mayo Plots

Table 5.48 Pulsed Laser Polymerization of Butyl methacrylate in the presence $[Co(afdo\text{-}2H.BF_2)_2]$ as Chain Transfer Agent

catalyst (ppm)	M_n	M_w	M_p	PDI
0.00	1798	22888	969	12.73
6.25	674	7912	----	11.73
11.76	668	7604	----	11.39
16.67	534	4133	----	7.37
25.00	547	4566	----	8.34
38.90	460	2222	161	4.83

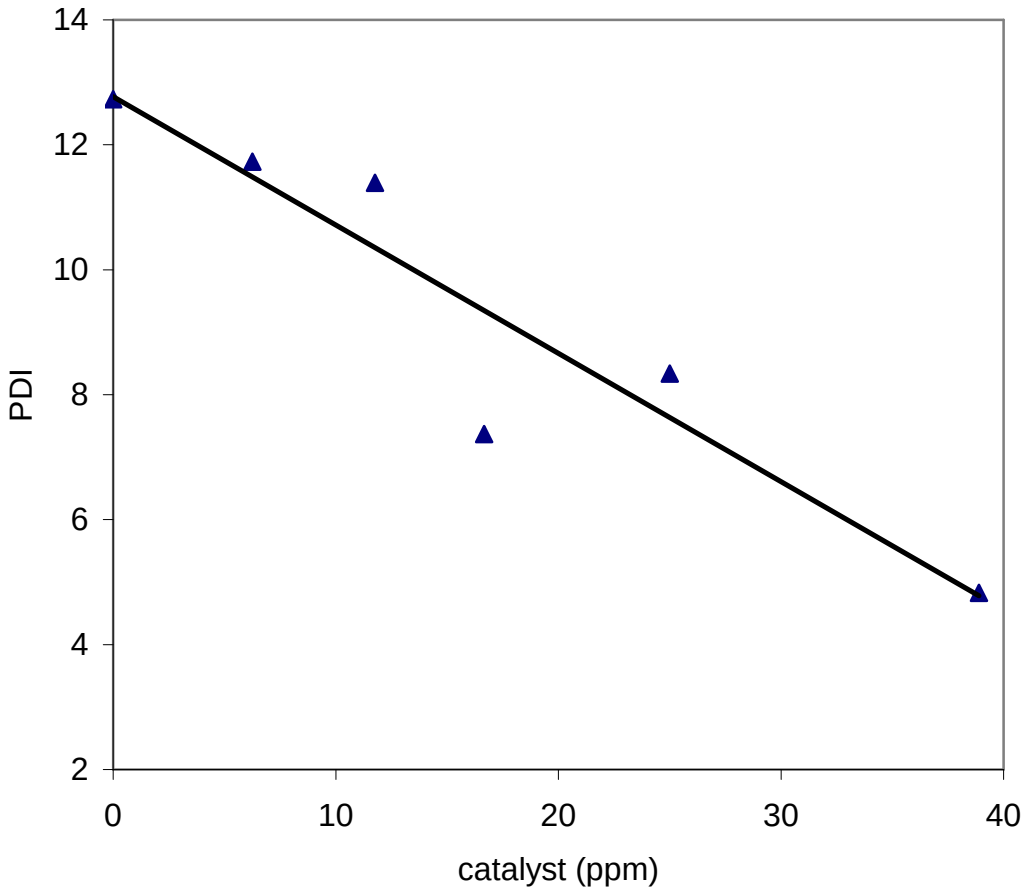

Figure 5.41 Graph between Polydispersity index and [Co(afdo-2H.BF_2)$_2$] concentration (ppm) for the PLP of BMA at 25 ºC

This trend signifies that there is a gradual decrease of chain transfer to polymer with the increase in catalyst concentration. Table 5.48 indicates that with the addition of ≈ 40 ppm of catalyst PDI values decrease from 12.73 to 4.83. Moreover, this also indicates that with the addition of 6.25 ppm of [Co(afdo-2H.BF_2)$_2$] catalyst, the M_n decreases from 1800 to 674. Similarly, M_w also decreases from 22,888 to 7,912. Data in Table 5.49 was used to construct Mayo plot and thus to calculate the C_s value. The C_s value calculated from M_n is around 39,000 while with a better regression value the C_s is 22,000 (calculated from M_w). Both these values are higher than those calculated for [Co(dmg-2H.BF_2)$_2$] complex. It appears that, perhaps due to free rotation of four methyl groups in [Co(dmg-2H.BF_2)$_2$] complex, steric interactions are higher and dominant. It is also important to note that BMA is bulky monomer compared to MMA therefore, steric interactions are expected to play a major role for the stability of Co-R_n bond. The X-ray structure of [Co(afdo-2H.BF_2)$_2$] catalyst indicates that the furil groups are fixed in position and thus expected to create less steric hindrance and stable Co-R_n bond formation, thus increasing its ability to act as a better chain transfer agent compared to [Co(dmg-2H.BF_2)$_2$] catalyst.

Table 5.49 Pulsed Laser Polymerization of Butyl methacrylate in the presence [Co(afdo-2H.BF_2)$_2$] as Chain Transfer Agent

[catalyst] x 10^5	[catalyst] / [M] x 10^6	DP_n	$1/DP_n$ x 10^2	1/DPn-$1/DP_{n(o)}$ x 10^2	DP_w	$1/DP_w$ x 10^2	1/DPw-$1/DP_{w(o)}$x 10^2
0	0	12.66	7.90	0	80.59	1.241	0
0.994	1.575	4.75	21.07	13.17	27.86	3.589	2.348
1.870	2.964	4.70	21.26	13.36	26.77	3.736	2.495
2.650	4.200	3.76	26.59	18.69	14.55	6.873	5.632
3.347	5.304	3.85	25.96	18.06	16.08	6.219	4.978
3.975	6.300	3.23	30.87	22.97	7.82	12.790	11.550

CONCLUSIONS

Following conclusions are drawn from the present research work:

1. Our investigation indicates that α-furilglyoxime ligand consists of two isomers and dimethylglyoxime ligand consists of only one isomer.
2. Polymerization of MMA with BPO at 70 ºC indicates that Degree of Polymerization first increases and then decreases.
3. For Polymerization of MMA using Benzoyl Peroxide (BPO) as initiator, percent conversion increases with the increase of temperature from 70 to 80 ºC but degree of polymerization decreases.
4. Polymerization of Styrene at 60 °C using AIBN as initiator is well regulated by [Co(afdo-2H.BF_2)$_2$] chain transfer agent and its C_s value is 500, which is approximately 25 times more than the best mercaptans.
5. For Polymerization of Styrene "C_s" Value for [Co(afdo-2H.BF_2)$_2$] CTA decreases with temperature increase.
6. Polymerization of MMA at 60 °C in the presence of Rh(III) catalyst indicates that both Conversion (%) and Degree of Polymerization increase as catalyst concentration increases, therefore Rh(III) does not behave as chain transfer agent.
7. With Laser irradiation time, percent conversion of both MMA and Styrene increases but this increase is more significant in MMA.
8. Propagation rate constant "82" L/mol.sec is in reasonable agreement with IUPAC accepted value "84" for Pulsed Laser Polymerization of styrene at 25 ºC.

9. Polymerization of both MMA and BMA at higher temperatures indicate increase in chain transfer constant value with temperature. Various kinetics parameters for these polymerization reactions have been determined successfully.
10. Wilkinson's catalyst promotes living free-radical polymerization for the Pulsed Laser Polymerization of MMA and thus can act as photoinitiator.
11. For Pulsed Laser Polymerization (PLP) of MMA, [Co(dmg-2H.BF_2)$_2$] acts as a better CTA with 13,400 C_s value as compared to [Co(afdo-2H.BF_2)$_2$] CTA with 10,140 C_s value.
12. Living free-radical polymerization is dominant with [Co(afdo-2H.BF_2)$_2$] for PLP of MMA, thus indicating weaker Co-C bond formation between this CTA and growing polymer chain.
13. For PLP of BMA, [Co(afdo-2H.BF_2)$_2$] acts as a better chain transfer agent with C_s = 22,000 as compared to [Co(dmg-2H.BF_2)$_2$] with a C_s value of 11,100. For this polymerization process steric factors are probably dominant over electronic factors.
14. In all experiments on polymerization of MMA, atactic PMMA was formed, which indicates free-radical polymerization.
15. Laser is a better clean source used for polymerization process at room temperature.

Future Prospects

- New Derivatives of the Chain Transfer Agents [(Coafdo-2H.BF_2)$_2$] and [(Codmg-2H.BF_2)$_2$] are needed to be prepared. These Derivatives could be used for the Catalytic Chain Transfer Polymerization [CCTP] (both Bulk & Emulsion Polymerization) by Heat and Laser.
- Mechanism involving Co-R_n bond formation is required to be investigated in length. For this purpose experiments involving esr technique should be conducted.
- In our current investigation Excimer Laser (λ = 308 nm) was used for PLP experiments. The energy associated with this wavelength corresponds to 387 KJ/mol (= 92.6 K cal/mol). The bond dissociation energy of C-C bonds is usually between 80-90 KJ/mol. Therefore, the CTA's used in our study should also be tested with Nd:YAG Laser (λ = 352 nm and E = 339 KJ/mol or 81 Kcal/mol).
- In our investigation of PLP in presence of CTA's some change of color of solution was recorded. This probably indicates catalyst degradation. This area of research, is still needed to be explored in detail.
- Photopolymerization at different temperatures using Chain Transfer Agents with Excimer Laser must also be investigated.

REFERENCES

[1] T. Otsu, M. Yoshida, Makromol. Chem., Rapid Commun. **3**, 127 (1982).

[2] D. H. Solomon, E. Rizzardo, P. Cacioli, Eur. Pat. Appl. EP 135280 (1985).

[3] M. Kato, M. Kamigaito, M. Sawamoto, T. Higashimura, Macromolecules, **28 (5)**, 1721 (1995).

[4] J. S. Wang, K. Matyjaszewski, Macromolecules, **28**, 7901 (1995).

[5] J. Chiefari, Y. K. Chong, F. Ercole, J. Krstina, J. Jeffery, P. T. Le Tam, R. T. A. Mayadunne, G. F. Meijs, C. L. Moad, G. Moad, S. H. Thang, Macromolecules, **31**, 5559 (1998).

[6] T. R. Darling, T. P. Davis, M. Fryed, A. A. Gridnev, D. M. Haddleton, S. D. Ittel, R. R. Matheson, G. Moad, E. Rizzardo, Journal of Polymer Science: Part A: Polymer Chemistry, **38(10)**, 1706 (2000).

[7] D. Colombani, Prog. Polym Sci, **22(8)**, 1649 (1997).

[8] G. Moad, D. H. Solomon, The Chemistry of Free Radical Polymerization, Oxford, p315 (1995).

[9] B. R. Smirnov, I. S. Morozova, A. P. Marchenko, M. A. Markevich, L. M. Pushchaeva, N. S. Enikolopyan, Doklady Chemistry, **253(4)**, 891 (1980).

[10] N. S. Enikolopyan, B. R. Smirnov, G. V. Ponomarev, I. M. Belgovskii, J. Polym. Sci. Polym. Chem. Ed. **19**, 879 (1981).

[11] G. M. Carlson, K. J. Abbey, US Patent 4526945 (1985).

[12] L. R. Melby, A. H. Janowicz, S. D. Ittel, Eur. Pat. Appl. EP Patent 199436 (1987).

[13] M. Nomura, Y. Minamino, K. Fujita, M. Harada, Journal of Polymer Science, Polymer Chemistry Edition, **20(5)**, 1261 (1982).

[14] A. Martchenko, T. Bremner, K. F. O'Driscoll, F. Kenneth, European Polymer Journal, **33(5)**, 713, (1997).

[15] I. Barudio, J. Guillot, G. Fevotte, Journal of Polymer Science, Polymer Chemistry Edition, **36(1)**, 157 (1998).

[16] H. C. Lee, G. W. Poehlein, Polymer Process Engineering, **5(1)**, 37 (1987).

[17] H. Ludovic, T. Pith, H. Guo-Hua, M. Lambla, Journal of Applied Polymer Science, **52(8)**, 1105, (1994).

[18] V. Smigol, F. Svec, Journal of Applied Polymer Science, **48(11)**, 2033 (1993).

[19] M. Fernandez-Garcia, E. L. Madruga, Journal of Polymer Science, Polymer Chemistry Edition, **35(10)**, 1961 (1997).

[20] N. K. Vail, J. W. Barlow, J. J. Beaman, H. L. Marcus, D. L. Bourell, Journal of Applied Polymer Science, **52(6)**, 789 (1994).

[21] G. F. Meijs, E. Rizzardo, Polymer Bulletin (Berlin), **26(3)**, 291 (1991).

[22] C. S. Chern, Y. C. Chen, Journal of Macromolecular Science-Pure and Applied Chemistry, **A35(6)**, 965 (1998).

[23] G. P. Scott, C. C. Soong, W. S. Huang, J. L. Reynolds, J. Org. Chem. **29(1)**, 83 (1964).

[24] J. Brandrup, E. H. Immergut, Polymer Handbook, Second Edition, Wiley Interscience, NY. (1975).

[25] C. Walling, J. Am. Chem. Soc. **70**, 2561 (1955).

[26] J. L. O'Brien, F. Gornick, J. Am. Chem. Soc. **77**, 4757 (1955).

[27] (a) W. V. Smith, J. Am. Chem. Soc. **68**, 2069 (1946);

(b) W. V. Smith, J. Am. Chem. Soc. **68**, 2064 (1946).

[28] G. P. Scott, J. C. Wang, C. James, J. Org. Chem. **28**, 1314 (1963).

[29] L. A. Wall, D. W. Brown, J. Polymer Sci. **14**, 513 (1954).

[30] (a) V. A. Dinaburg, A. A. Vansheidt, J. Gen. Chem. USSR (Eng. Trans.), **24**, 839 (1954);
(b) V. A. Dinaburg, A. A. Vansheidt, J. Gen. Chem. USSR (Eng. Trans.), **24**, 840 (1954).

[31] E. J. Meehan, I. M. Kolthoff, P. R. Sinha, J. Polymer Sci. **16**, 471(1955).

[32] S. T. Eckersley, A. Rudin, Progress in Organic Coatings, **23(4)**, 387 (1994).

[33] M. K. Shanmuganada, G. Kannan, K. Kaushal, Polymer, **37(24)**, 5541 (1996).

[34] G. Odian, Principles of Polymerization, third edition, (1991).

[35] M. Nodono, T. Tokimitsu, S. Tone, A. Yanagase, Polymer Preprints **39(1)**, 286 (1998)

[36] D. Ed. Dolphin, B12; Wiley: (1982).

[37] J. Halpern, Science, **227**, 4689 (1985).

[38] T. P. Davis, D. M. Haddleton, S. N. Richards, J. Macromol. Sci., Rev. Macromol. Chem. Phys. **C34(2)**, 243 (1994).

[39] D. I. Pashchenko, E. K. Vinogradova, I. M. Bel'govskii, G. V. Ponomarev, N. S. Enikolopyan, Dokl Chem **265(4)**, 889 (1982).

[40] E. K. Vinogradova, A. B. Davydova, G. G. Aleksanyan, A. S. Shustov, S. V. Sheberstov, I. M. Bel'govskii, N. S. Enikolopyan, Khim Fiz. **4(4)**, 518 (1985).

[41] L. V. Karmilova, G. V. Ponomarev, B. R. Smirnov, I. M. Bel'govskii, Russ Chem Rev, **53(2)**, 223 (1984).

[42] N. S. Enikolopov, I. M. Bel'govskii, A. A. Gridnev, A. P. Marchenko, B. R. Smirnov, Russ. Patent 940,487, (1987).

[43] A. A. Gridnev, Polym Sci. **31(10)**, 2153 (1989).

[44] A. F. Burczyk, K. F. O'Driscoll, G. L. Rempel, J. Polym. Sci; Polm. Chem. Ed. **22(11)**, 3255 (1984).

[45] A. A. Gridnev, J. Polym. Sci. Part A: Polym. Chem. **38(10)**, 1753 (2000).

[46] T. P. Davis, D. Kukulj, D. M. Haddleton, D. R. Maloney, Trends in Polymer Science, **3(11)**, 365 (1995).

[47] K. C. Berger, G. Brandrup, in 'Polymer Handbook', 3 rd Edition' (Eds. Brandrup, J.; Immergut, E.H.), Wiley: p. II/109 (1989).

[48] G. Moad, D. H. Solomon, The Chemistry of Free Radical Polymerization, Ist Ed., Pergamon, Oxford: (1995).

[49] J. P. A. Heuts, T. P. Davis, G. T. Russell, Macromolecules, **32(19)**, 6019 (1999).

[50] B. R. Smirnov, L. M. Pushchaeva, V. D. Plotnikov, Polymer Science USSR, **31(11)**, 2607 (1989).

[51] J. P. A. Heuts, D. J. Forster, T. P. Davis, B. Yamada, H. Yamazoe, M. Azukizawa, Macromolecules, **32(8)**, 2511 (1999).

[52] D. Kukulj, T. P. Davis, Macromol. Chem. Phys. **199(8)**, 1697 (1998).

[53] D. M. Haddleton, D. R. Maloney, K. G. Suddaby, A. V. G. Muir, S. N. Richards, Macromol. Symp. **111**, 37 (1996).

[54] R. A. Sanayei, K. F. O'Driscoll, J. Macromol. Sci. Chem; **A26(8**), 1137, (1989).

[55] K. G. Suddaby, D. R. Maloney, D. M. Haddleton, Macromolecules, **30(4)**, 702 (1997).

[56] D. J. Forster, J. P. A. Heuts, T. P. Davis, Polymer **41(4)**, 1385 (1999).

[57] G. Ayrey, M. J. Humphrey, R. C. Poller, Polymer, **18(8)**, 840 (1977).

[58] C. H. Bamford, "Radical Polymerization," pp. 708-867 in "Encyclopedia of Polymer Science and Engineering," **Vol.13**, H. F. Mark, N. M. Bikales, C. G. Overberger, Menges Eds; Wiley-Interscience, New York, (1988).

[59] O. F. Olaj, J. W. Breitenbach, K. J. Parth, N. Philippovich, J. Macromol. Sci. Chem. **A11(7)**, 1319 (1977).

[60] O. F. Olaj, H. F. Kaufmann, J. W. Breitenbach, Makromol. Chem. **178(9)**, 2707, (1977).

[61] P. A. Small, Adv. Polym. Sci. **18**, 1 (1975).

[62] A. A. Gridnev, Polym. Sci. USSR, **31(10)**, 2153 (1989).

[63] A. A. Gridnev, S. D. Ittel, M. Fryd, B. B. Wayland, Organometallics, **12(12)**, 4871 (1993).

[64] A. A. Gridnev, S. D. Ittel, B. B. Wayland, M. Fryd, Organometallics, **15(1)**, 5116 (1996).

[65] A. A. Gridnev, S. D. Ittel, M. Fryd, B. B. Wayland, Organometallics, **15**, 222 (1996).

[66] D. M. Haddleton, D. R. Maloney, K. G. Suddaby, A. V. G. Muir, S. N. Richards, Macromol. Symp. **111**, 37 (1996).

[67] (a) N. S. Enikolopov, G. V. Korolev, A. P. Marchenko, G. V. Ponomarev, B. R. Smirnov, V. I. Titov, Russ. Patent 664,434, (1980); (b) B. R. Smirnov, I. M. Bel'govskii, G. V. Ponomarev, A. P. Marchenko, N. S. Enikolopyan, Dokl Chem. **254(1)**, 127 (1980); (c) B. R. Smirnov, V. D. Plotnikov, B. V. Ozerkovskii, Roschupkin, N. S. Enikkolopyan, Polym. Sci. USSR, **23(11)**, 2588 (1981).

[68] A. F. Cotton, G. Wilkinson, Advanced Inorganic Chemistry, Fourth Edition, A Wiley-Interscience Publication, 772 (1980).

[69] (a) A. A. Gridnev, Y. D. Lampeka, B. R. Smirnov, K. B. Yatsimirskii, Theor Exp Chem. **23(3)**, 317 (1987); (b) A. V. Goncharov, A. A. Gridnev, Y. D. Lampeka, S. P. Gavrish, Theor Exp Chem. **25(6)**, 698 (1989).

[70] S. A. Ali, Experiments in Polymer Science: Theory and Practice, (2002).

[71] S. P. Pappas, H. F. Mark, N. M. Bikales, C. G. Overberger, M. G. Ed; "Photopolymerization," **11**, p.186 (1988); in " Encyclopedia of Polymer Science and Engineering," Wiley-Interscience, New York.

[72] J. Pelgrims, J. Oil & Color Chemists Assoc. **61(4)**, 114 (1978).

[73] O. F. Olaj, I. Bitai, G. Gleixner, Makromol. Chem. **186(12)**, 2569 (1985).

[74] O. F. Olaj, I. Bitai, F. Hinkelmann, Makromol. Chem. **188(7)**, 1689 (1987).

[75] M. D. Zammit, T. P. Davis, Macromolecules, **31(6)**, 1763 (1998).

[76] M. L. Coote, M. D. Zammit, T. P. Davis, G. D. Willett, Macromolecules, **30(26)**, 8182 (1997).

[77] D. Kukulj, T. P. Davis, Macromolecules, **31(17)**, 5668 (1998).

[78] M. Kato, M. Kamigaito, M. Sawamoto, T. Higashimura, Macromolecules, **28(5)**, 1995 (1721).

[79] T. Ando, M. Kamigaito, M. Sawamoto, Macromolecules, **30(16)**, 4507 (1997).

[80] H. Uegaki, Y. Kotani, M. Kamigaito, M. Sawamoto, Macromolecules, **30(8)**, 2249 (1997).

[81] V. Percec, B. Barboiu, A. Neumann, J. C. Ronda, Macromolecules, **29(10)**, 3665 (1996).

[82] G. Moineau, C. Granel, Ph. Dubois, R. Jerome, Ph. Teyssie, Macromolecules, **31(2)**, 542 (1998).

[83] D. J. Forster, J. P. A. Heuts, T. P. Davis, Polymer, **41(4)**, 1385 (2000).

[84] A. Bakac, M. E. Brynildson, J. H. Espenson, Inorg. Chem. **25(23)**, 4108 (1986).

[85] F. W. Billmeyer, E. A. Collins, J. Bares, Experiments in Polymer Science, John Wiley & Sons, 1973.

[86] J. K. Haken, R. L. Werner, Brit. Polym. J. **3(6)**, 263 (1971).

[87] U. Baumann, H. Schreiber, K. Tessmar, Makromol. Chem. **36**, 81 (1959).

[88] H. A. Pohl, R. Bacskai, W. P. Purcell, J. Phys. Chem. **64**, 1701 (1960).

[89] C. Y. Liang, S. Krimm, J. Polym. Sci. **27**, 241 (1958).

[90] K. Ogura, S. Kawamura, H. Sobue, Macromolecules, **4(1)**, 79 (1971).

[91] H. Tadokoro, H. Nagai, S. Seki, I. Nitta, Bull. Chem. Soc. Japan J. **34**, 1504 (1961).

[92] H. Tadokoro, N. Nishiyama, S. Nozakura, S. Murahashi, J. Polym. Sci. **36**, 553 (1959).

[93] L. M. Wolinski, Makromol. Chem. **176(7)**, 2079 (1975).

[94] L. F. Johnson, F. Heatley, F. A. Bovey, Macromolecules, **3(2)**, 175 (1970).

[95] F. A. Bovey, High Resolution NMR of Macromolecules, Academic Press Inc. New York, (1972).

[96] Y. Inoue, A. Nishioka, R. Chujo, Makromol. Chem. **156**, 207 (1972).

[97] F. Laupretre, C. Noel, L. Monnerie, J. Polym. Sci. A2, **15(12)**, 2127 (1977).

[98] K. Matsuzaki, T. Uryu, T. Seki, K. Osada, T. Kawamura, Makromol. Chem. **176(10)**, 3051 (1975).

[99] J. C. Randall, J. Polym. Sci. A2, **13(5)**, 889 (1975).

[100] J. Brandrup, E. H. Immergut, E. A. Grulke, Polymer Handbook, Fourth Edition, (1999).

[101] S. M. Aharoni, J. Appl. Polym. Sci. **21(5)**, 1323 (1977).

[102] T. Jr. Altares, D. P. Wyman, V. R. Allen, K. Meyersen, J. Polym. Sci. A, **3(12)**, 4131 (1964).

[103] M. R. Ambler, D. Mclntyre, L. J. Fetters, Macromolecules, **11(2)**, 300 (1978).

[104] B. Baysal, A. V. Tobolsky, J. Polym. Sci. **9**, 171 (1952).

[105] G. C. Berry, T. G. Fox, J. Amer. Chem. Sco. **86(17)**, 3540 (1964).

[106] W. F. H. Borman, J. Appl. Polym. Sci. **22(8)**, 2119 (1978).

[107] A. J. Bur, L. J. Fetters, Macromolecules, **6(6)**, 874 (1973).

[108] F. Cane, T. Capaccioli, European Polymer Journal, **14**, 185 (1978).

[109] N. Doddi, W. C. Forsman, C. C. Price, J. Polym. Sci. A2, **12(7)**, 1395 (1974).

[110] A. Dondos, Polymer, **18**, 1250 (1977).

[111] A. Dondos, H. Benoit, Makromol. Chem. **176(11)**, 3441 (1975).

[112] A. Donades, Benoit H. Polymer, **18**, 1161 (1977).

[113] S. Enomoto, J. Polym. Sci. **55**, 95 (1961).

[114] S. Penczek, J. Polym Sci A: Polym Chem. **40**, 1665 (2002).

[115] R. A. Gregg, F. R. Mayo, J. Am. Chem. Soc; **70**, 2373 (1948).

[116] R. G. Gilbert, Emulsion Polymerization: A Mechanistic Approach; Academic Press: New York, 1995.

[117] R. G. Gilbert. Trends Polym. Sci. **3(7)**, 222 (1995).

[118] P. A. Clay, R. G. Gilbert, Macromolecules, **28(2)**, 552 (1995).

[119] D. I. Christie, R. G. Gilbert, Macrol. Chem. Phys. **197(1)**, 403 (1996).

[120] A. Hantzsch, A. Werner, Chem. Ber; **23**, 11 (1890).

[121] G. B. Kauffman, J. Chem. Educ; **43(3),** 155 (1966).

[122] L. Tschugaeff, Chem. Ber; **39**, 3382 (1907).

[123] L. Tschugaeff, J. Chem. Soc; London, **105**, 2187 (1914).

[124] A. Chakravorty, Coordin. Chem. Rev; **13(1)**, 1 (1974).

[125] E. E. Liepinsh, N. Saldabol, J. Org. Chem. USSR (Engl. Transl.), **17(3)**, 521 (1981).

[126] M. S. Hussain, H. M. Al-Mohdhar, Al-Arfaj. J. Coord. Chem. **18(4)**, 339 (1988).

[127] R. M. Silverstein, G. C. Bassler, T. C. Morrill, Spectrometric Identification of Organic Compounds, Fifth Edition, John Wiley and Sons Inc. (1991).

[128] E. Emsely, Chem. Soc. Rev. 91, 1981.

[129] G. De Alti, V. Galasso, A. Bigotto, Inorganica Chim. Acta, **4(2)**, 267 (1970).

[130] G. N. Schrauzer, R. J. Windgassen, J. Am. Chem. Soc. **88(16)**, 3738 (1966).

[131] D. F. Shriver, P. W. Atkins, C. H. Langford, Inorganic Chemistry, Second Edition, (1994).

[132] H. K. Mahabadi, K. F. O'Driscoll, J. Polym. Sci. Chem. Ed; **15(2)**, 283 (1977).

[133] H. K. Mahabadi, K. F. O'Driscoll, Macomolecules, **10(1)**, 55 (1977).

[134] A. M. North, "The Influence of Chain Structure on the Free Radical Termination Reaction," Chapter 5 in "Reactivity, Mechanism and Structure in Polymer Chemistry," A. D. Jenkins, A. Eds. Ledwith; Wiley-Interscience, New york, (1974).

[135] P. Hayden, H. Melville, J. Polym. Sci. Chem. Ed; **43**, 201 (1960).

[136] J. Lingnau, G. Meyerhoff, Macromolecules, **17(4)**, 941 (1984).

[137] J. Lingnau, G. Meyerhoff, Makromol. Chem; **185(3)**, 587 (1984).

[138] R. S. Lehrle, A. Shortland, European Polymer Journal, **24(5)**, 425 (1988).

[139] a) N. Kameda, N. Itagaki, N. Bull. Chem. Soc. Jpn; **46(8)**, 2597 (1973); b) N. Kameda, E. Ishii, Makromol. Chem. **184(9)**, 1901 (1983); c) N. Kameda, E. Ishii, Nippon Kagaku Kaishi. **8**, 1196 (1983); d) N. Kameda, M. Hattori, Kobunshi Ronbunshu, **41(11)**, 679 (1984); e) N. Kameda, M. Hattori, Kobunshi Ronbunshu; Chem. **42(8)**, 485 (1985).

[140] M. Kato, M. Kamigaito, M. Sawamoto, T. Higashimura, Macromolecules, **28(5)**, 1721 (1995).

[141] T. Ando, M. Kamigaito, M. Sawamoto, Macromolecules, **30(16)**, 4507 (1997).

[142] V. Percec, B. Barboiu, A. Neumann, J. C. Ronda, M. Zhao. Macromolecules, **29(10)**, 3665 (1996).

[143] G. Moineau, C. Granel, Ph. Dubois, R. Jerome, Ph. Teyssie, Macromolecules, **31**, 542 (1998).

[144] K. G. Suddaby, R. M. Sanayei, A. Rudin, K. F. O'Driscoll, J. Applied Polymer Science, **43(8)**, 1565 (1991).

[145] G. M. Carlson, K. J. Abbey, US Patent US 4,526,945 (1985).

[146] L. R. Melby, A. H. Janowicz, S. D. Ittel, European Patent, EP 196783 (1986).

[147] D. G. Hawthorne, WO Patent 8703605 (1987).

[148] J. P. A. Heuts, D. J. Forster, T. P. Davis, Macromolecules, **32(12)**, 3907 (1999).

[149] V. E. Mironychev, M. M. Mogilevich, B. R. Smirnov, Y. E. Shapiro, I. V. Golikov, Polym. Sci. USSR, **28(9)**, 1891 (1986).

[150] M. D. Zammit, M. L. Coote, T. P. Davis, G. D. Willet, Macromolecules, **31(4)**, 955 (1998).

[151] J. B. Lidwien de Kock, PhD Dissertation, Chain- Length Dependent Bimolecular Termination in Free-Radical polymerization, (1999).

[152] C. M. Lukehart, Fundamental Transition Metal Organometallic Chemistry, Brooks/ Cole Publishing Company, California, 67 (1985).

[153] G. L Miesseler, D. A. Tarr, Inorganic Chemistry, Second Edition, Prentice- Hall, Inc. 408 (1999).

[154] Friebolin, H. Basic One and Two – Dimensional NMR Spectroscopy, New York : VCH, 305 (1991).

[155] H. D. Choi, S. Oh Joon, Europeon Polymer Journal, **38,** 1559 (2002).

[156] F. A. Bovey, High Resolution NMR of Macromolecules, Academic Press Inc. New York,1972.

[157] A. G. Sharpe, D. B. Wakefield, J. Chem. Soc. London. 281 (1957).

[158] G. N. Schrauzer, Inorganic Synthesis, **11**, 61 (1968).

[159] G. N. Schrauzer, R. J. Windgassen. Chem. Ber. **99**, 602 (1966).

[160] G. N. Schrauzer, L. P. Lee, J. Am. Chem. Soc. **90(23)**, 6541 (1968).

[161] L. M. Engelhardt, M. Green, J. Chem. Soc. Dalton Trans; (6), 724 (1972).

APPENDIX A

METHYL METACRYLATE

CAS/DOT IDENTIFICATION #: 80-62-6/UN1247

Synonyms: methacrylate monomer, methyl ester of methacrylic acid, methyl-2-methyl-2-propenoate, 2-methyl-2-propenoic acid methyl ester.

Physical Properties: colorless liquid; acrid, fruity odor; soluble in acetone; very slightly soluble in water; MP (-48 °C); BP (100°C); DN (0.936 g/ml at 20 °C).

Chemical Properties: may polymerize if exposed to heat, oxidizers, or ultraviolet light; usually contains an inhibitor such as hydroquinone; reacts with strong acids, alkalies, nitrates, oxidizers, peroxides and moisture; FP (10 °C).

Explosion and Fire Concern: flammable liquid; very dangerous fire hazard; NFPA rating Health 2, flammability 3; Reactivity 2; explodes on evaporation at 60 °C; ignites on contact with benzoyl peroxide, liquid floats on water and may travel to ignition source and flash back; use carbon dioxide, dry chemical, foam, or water spray for firefighting purposes.

Health Symptoms: inhalation (sleep effects, excitement, anorexia, decrease in blood pressure, nausea, vomiting, headache, dizziness, unconsciousness); contact (burning sensation, dermatitis).

First Aid: wash eyes immediately with large amounts of water; flush skin promptly with large amounts of water; provide oxygen and respiratory support.

Human Toxicity Data: inhalation-human TCLo 125 ppm; toxic effect: central nervous system; inhalation-human TCLo 60 mg/m^3; toxic effect: central nervous system, cardiovascular system.

Chronic Health Risks: cardiovascular disorders; lesions of the kidney and liver; effects on the nasal cavity; sleeping disturbances; dermatitis.

Other Comments: use as a monomer in the manufacture of PMMA resins and plastics; used as a component of bone cement and molding/extrusion powder; used in the manufacture of plumbing and bathroom fixtures, lighting fixture, sky lights etc.

Reference: J. M. Spero, B. devito, L. Theodore, Regulatory Chemicals Handbook, Marcel Dekker, Inc. (2000), Switzerland.

Styrene

CAS/DOT IDENTIFICATION #: 100-42-5/UN2055

Synonyms: cinnamene, ethylbenzene, phenylethene, phenylethylene, styrene monomer, styrol, vinylbenzene.

Physical Properties: colorless to light yellow, oily liquid; viscous liquid, sweet floral odor at low concentrations; soluble in carbon disufide, alcohol, ether, methanol, ethanol, toluene, carbon tetrachloride and heptane; soluble in all proportions in benzene and petroleum ether; slightly soluble in water; MP(-31 °C); BP (145°C); DN (0.9074 g/ml at 20 °C).

Chemical Properties: slowly undergoes polymerization and oxidation with formation of peroxides on exposure to light and air; corrodes copper and copper alloys; usually contains apolymer inhibitor such as ter-butylcatechol; reacts vigorously with oxidizers, peroxides, strong acids, aluminum chloride, and catalyst for vinyl polymer; FP (31 °C).

Explosion and Fire Concern: flammable liquid; NFPA rating Health 2, flammability 3; Reactivity 2; containers may explode violently when heated; storage hazard above 32 °C. very dangerous fire hazard; use water spray, dry chemical, foam, or carbon dioxide for firefighting purposes.

Health Symptoms: inhalation (eye and olfactory changes, irrition and violent itching of the eyes, lacrimation, anesthetic or narcotic effect); contact (defatting dermatitis).

First Aid: wash eyes immediately with large amounts of water; flush skin promptly with large amounts of water; provide oxygen and respiratory support.

Human Toxicity Data: inhalation-human LCLo 10,000 ppm/30M; inhalation-human TCLo 600 ppm; toxic effect: nose, eye; inhalation-human TCLo 20ug/m^3; toxic effect: eye.

Chronic Health Risks: effects on central nervous system; weakness; fatigue; depression, headache; possible liver damage, reproductive effects, possible human carcinogen; increased risk of leukemia, effects on blood.

Other Comments: used in the manufacture of plastics and synthetic rubber; used as insulating agent; used in the manufacture of styrenated polyester; used as a synthetic flavoring substance, e.g. for ice cream and candy; also used to make paints.

Reference: J. M. Spero, B. devito, L. Theodore, Regulatory Chemicals Handbook, Marcel Dekker, Inc. (2000), Switzerland.

APPENDIX B

Table B1 Monomer Chain Transfer Constant at 60 °C.

Monomer	$C_M \times 10^4$
Methyl methacrylate	0.07-0.25
Styrene	0.30-0.60
Vinyl chloride	10.8-16.0
Vinyl acetate	1.75-2.80
Acrylamide	0.6, 0.12 (at 40 °C)
Acrylonitrile	0.26-0.30
Ethylene	0.40-4.20
Methyl acrylate	0.036-0.325

Table B2 Initiator Chain Transfer Constants at 60 °C.

Chain Transfer agent	C_I for MMA	C_I for Styrene
AIBN	0.02	0.091-0.14
Benzoyl Peroxide	0.02	0.048-0.10
Cumyl hydroperoxide	0.33	0.063
Lauroyl peroxide	----	0.024
Cumyl peroxide	----	0.01
t-Butyl hydrperoxide	----	0.035
t-Butyl peroxide	----	0.00076-0.00092

Curriculum Vitae

I was born in Aroop (Gujranwala, Pakistan) on October 10, 1967. After obtaining first position from my school in secondary school examination, I got higher education from prestigeous institute Govt. College Lahore, Pakistan. In my MSc exam, held in 1990, I secured first position in college and overall second position in Punjab University Lahore, Pakistan. I completed M. Phil Degree in 1994 from Quaid-i-Azam University Islamabad. Later I joined one of the prestigious organizations in Pakistan and worked there, till september 1997. I joined KFUPM in September 27, 1997.

s/o Haji Nazir Ahmad Awan

village & post office Aroop

Tehsil and District **Gujranwala**

Punjab

Pakistan

shafiqueawan2003@yahoo.com